ACTIVE NEGATIVE GROUP DELAY CIRCUITS AND APPLICATIONS

by

THOMAS THATAPUDI

A thesis submitted to the University of Birmingham for the degree of
DOCTOR OF PHILOSOPHY

Department of Electronic Electrical and Systems Engineering
School of Engineering
College of Engineering and Physical Science
The University of Birmingham
September 2020

ABSTRACT

The design of a low profile antenna operating over wide bandwidth with enhanced radiation performance is the objective of this work. The methods to improve the operational bandwidth, reduce the size and enhance the radiation properties such as directivity and gain, while minimising the beam squint for an antenna are presented. Two antennas are designed: an electrically small antenna (ESA) integrated with an active circulator for simultaneous signal transmission and reception (duplex operation) operating over a wide bandwidth and a Fabry-Perot cavity antenna having high directivity and gain with reduced beam squint.

A negative group delay (NGD) concept is used in lumped element implementation and in frequency selective surface implementation for achieving the objectives of this work. A detailed study is carried out on the filter based NGD network design. The NGD network impact is clearly demonstrated: in adjusting the impedance characteristics for the design of an ESA; in achieving wideband signal cancellation for the active circulator and in optimising the phase characteristics of a high impedance surface (HIS) for the design of a wideband Fabry-Perot cavity antenna with reduced beam squint.

A low profile ESA is designed using a NGD matching network. The passive NGD network offers wide bandwidth impedance matching for an antenna over the frequency band, far lower than the quarter wavelength resonance frequency associated with the physical length of the antenna. The inevitable transmission loss of the NGD based matching network is compensated using an active circulator. This enables the ESA to be used in duplex mode. An active quasi-circulator operating over a wide bandwidth, working on a signal cancellation principle is designed using NGD networks. The employment of the NGD network achieved signal cancellation over a wide bandwidth. This network also offered extra design flexibility in terms of optimisation and selection of gain blocks. The ESA is integrated with an active

circulator of 14% bandwidth operating at 1.8GHz. The average 5dB gains in the transmission and reception paths are used to compensate the losses of the matching network. This novel antenna is suitable for duplex operation over a wide bandwidth.

The prototypes of the ESA and the active circulator are fabricated and tested separately. An ESA operating at 1.08GHz ($=0.98\lambda/2\pi$) of 50% bandwidth with a physical length of 43mm is designed and tested. This method is more stable and effective than those that are reported in the literature. The performance parameters of the ESA are discussed in detail. A three-port active circulator (clockwise: transmitter, antenna, receiver) operating at 1.5GHz with 200MHz (14%) bandwidth offering 20dB isolation between the transmitter and the receiver is fabricated and tested. Between any pair of ports the average gain in the clockwise direction is 5dB and the isolation in the anti-clockwise direction is greater than 20dB. The noise figure is less than 5dB from the antenna to the receiver. Using the proposed method the bandwidth of the circulator is improved almost 30 times compared to a similar design reported in the literature.

A Fabry-Perot cavity antenna operating at 10GHz is designed with a partially reflective surface (PRS) and a high impedance negative group delay surface. The HIS with NGD characteristics enabled the establishment of the resonance phase condition over a 0.75GHz bandwidth resulting in a wideband cavity antenna with reduced beam squint. The signal absorption along the HIS and the possible loss compensation techniques are also discussed. A lossy design has exhibited only 0.2^0 per 100MHz beam squint over 1.5GHz bandwidth with degraded directivity and gain. A loss compensated model has exhibited 1.3^0 per 100MHz beam squint over 0.75GHz with improved directivity and gain of 19dBi and 5.6dBi respectively.

ACKNOWLEDGEMENTS

Firstly my thanks should go to Prof. Peter Gardner for offering a place in his research group as a PhD student. Without his initial support all of this research work would have been impossible.

I would like to thank the University of Birmingham, UK for awarding me a School of Engineering Scholarship and the Social Welfare Department of Andhra Pradesh, India for awarding an Ambedkar Overseas Vidya Nidhi Scholarship - enabling me to undertake my PhD studies.

In addition, I express my gratitude to the Wireless Communications Research Group and the Metamaterials Engineering Laboratory of the University of Birmingham UK for providing the facilities needed to carry out this research; as well as the wider university PGR support team.

I am very grateful for the invaluable support and guidance given by my supervisors Prof. Peter Gardner and Dr. Alexandros Feresidis. My supervisors have demonstrated throughout my PhD studies a perfect combination of kindness, support and professionalism. I have been greatly helped by their vast knowledge of the subject area, deeper understanding of research methods, many years of experience and overall expertise in their respective research fields. I believe that one cannot hope for better supervisors than mine.

I would also like to thank Professor Costas Constantinou for giving valuable suggestions and comments on my work in review meetings. I hugely benefitted from his immense experience and wide range of subject knowledge.

My office mates and colleagues J Churm, M S Rabbani, A A M Almahroug, A A A Abdelrehim, D Kampouridou, A Christodoulides, E Vassos, I Gerafentis, P Kihogo and L Shen have also provided a supportive working environment, allowing for thoughtful

discussion. In addition they have shared their expertise, for which I am thankful. I would also like to thank Andy, Alan, Lily, Mandy and the other office staff for giving timely help and supporting me in the various tasks that needed to be undertaken.

I would like to thank Andrew and Janelle Mullan and family for their great hospitality and kindness they showed by offering a place in their home and in their family, which I will never forget. Also my roommates Lalit, Emmanuel and Nick for their huge support as well as Satish and Raj who supported me immensely. I would like to thank too the believers at Hope Chapel and Slade Evangelical Church for their continuing moral and spiritual support as well as their practical help.

I express my love and gratitude to my family in the UK and India for their remarkable support in so many ways throughout my journey to complete my PhD. My special thanks should go to my mother Grace Thatapudi for supporting me in a countless number of ways.

My wife, Sarah Ruth Thatapudi (Jenkins) has been a wonderful support. I am complete as a person having my own family and I will always recognise the great contribution of my wife in making this a reality. Since finding my wife I have felt a new sense of meaning and direction to life. I am greatly inspired by her many virtues, discipline and remarkable character. Completion of my studies would have been impossible without my wife's ongoing encouragement and support both practically and emotionally. Most of all I am thankful for the gift of my daughter Abigail Grace Thatapudi who has been a cheerful motivation to complete this work.

I strongly believe that God is the source and provider of wisdom and knowledge. I express my eternal thanks for the great help, which is beyond my understanding, that I received daily from my Saviour and Lord, Jesus Christ. These acknowledgements would not be complete

without mentioning the positive influence of the teachings of the Lord Jesus Christ from the Holy Bible on my life, all honour and glory be unto Him.

Table of contents

List of Tables

List of Figures

ABBREVIATIONS

Ant	Antenna
ACW	Anti- Clockwise
AMC	Artificial Magnetic Conductor
AWR-MO	AWR Microwave Office
BW	Bandwidth
CW	Clockwise
CST-MS	CST Microwave Studio
ESA	Electrically Small Antenna
FPC	Fabry-Perot Cavity Antenna
FSS	Frequency Selective Surfaces
GHz	Giga hertz
HIS	High Impedance Surface
Meas	Measurement
MHz	Mega Hertz
MMIC	Monolithic Microwave Integrated Circuit
mW	Milli Watt
NA	Not Applicable
NGD	Negative Group Delay
PDK	Process Design Kit
PRS	Partially Reflective Surface
PEC	Perfect Electric Conductor
RLC	Resistor Inductor Capacitor
Rx	Receiver
Sim	Simulation
Tx	Transmitter

LIST OF PUBLICATIONS

T. Thatapudi, P. Gardner and A. Feresidis, "*Engineered group delay transmission lines based on novel negative group delay networks,*" Loughborough Antennas & Propagation Conference (LAPC 2017), Loughborough, 2017, pp. 1-2.

T. Thatapudi, P. Gardner and A. Feresidis, "*Enhancing bandwidth of an electrically small antenna using a negative group delay network,*" Loughborough Antennas & Propagation Conference (LAPC 2018), Loughborough, 2018, pp. 1-2.

T. Thatapudi, P. Gardner and A. Feresidis, "*The antenna impedance matching circuit using negative group delay network: Design and analysis*," Antennas and Propagation Conference 2019 (APC-2019), Birmingham, UK, 2019, pp. 1-4.

Manuscript under preparation

T. Thatapudi, P. Gardner and A. Feresidis, "*An NGD based electrically small antenna integrated with an active circulator for duplex operation over wide bandwidth,*" IEEE trans, 2020, pp. 1-11.

Chapter 1: Introduction

The successful establishment of wireless communication technologies for use in commercial and public services changed day to day life. There is a demand for techniques and methods for achieving stable wideband operation in electronic circuits in order for the wireless communication systems to provide better services. The inherent characteristics of electronic components, the limitation of physical laws, the tolerance of fabrication facilities, the inter dependency of sub-systems and many other issues have made the design of a wideband system challenging.

Different types of antennas have certain operational bandwidth limitations. For example, a dipole antenna generally operates over 10% bandwidth, whereas a patch antenna has an smaller operational bandwidth. An electrically small antenna operating over a wide bandwidth of 20% is even more complicated to design [1]. The impedance matching of an antenna over a wide bandwidth is a design challenge. By using a single antenna for both transmission and reception, portable devices such as wireless communication devices and radar systems can be made more compact. Circulators can be used to achieve this duplex operation. A compact circulator with an integrated antenna, operating over a wide bandwidth and offering enough electrical isolation between the transmitter and receiver is another design challenge. Meta-material based surfaces are useful in designing compact directional antennas. Achieving the adaptive phase characteristics for a meta-surface would improve the performance of frequency selective surface antennas. Even though there are many techniques in use and many other techniques have been proposed in literature, any further work to improve these processes will be of benefit. This is because the quality of these processes has a large effect on the overall system performance.

Any passive nondispersive two terminal reactance that exhibits negative slope with frequency is called a non-Foster element [2, 3]. A negative inductor or a negative capacitor is an example of a non-Foster element. These non-Foster elements are implemented as active networks and are very effective in addressing some of the above design challenges [4-7].

Negative group delay (NGD) means a negative delay in propagation. The NGD network makes the peak of a RF pulse envelope appear to lead the input peak. However, due to causality at the start and stop points of a wave, the input peak will be leading the peak of a RF pulse envelope. The NGD networks can be implemented using passive elements [8]. The non-Foster behaviour can be implemented using the NGD passive networks and these are more stable than active implementations. These networks act as a negative reactance element and can be used to compensate the antenna reactance to achieve impedance matching over a wide bandwidth.

In addition to the techniques that are presented in literature, in this thesis an investigation has been carried out to find out the impact of the NGD network in establishing an effective process to achieve wideband functionality in various scenarios. The extent to which the NGD network would be able to overcome the bandwidth and stability limitations that are presented in literature is also investigated. Compatibility with MMIC technology is also verified to ensure that the proposed concepts are suitable for low profile applications.

1.1 Motivation

The overall operational bandwidth of an electronic device depends on the performance and bandwidth of the internal circuit. In most electronic systems this restricts their operation to narrow bandwidth. In the majority of cases the impedance matching and signal cancellation over wideband depend on optimising the reactance of an electronic component or a microstrip line. The conventional method to compensate the capacitive reactance with an inductive

counterpart or the inductive reactance with a capacitive counterpart is possible at a single frequency or over a very narrowband, according to the broadband matching theory developed by Bode, Fano and Youla [9-11]. With the use of the negative capacitor or negative inductor, the positive capacitive reactance or the positive inductive reactance of an antenna can be compensated respectively and impedance matching can be achieved over a wide frequency range. The NGD networks behave as negative passive elements and have a profound impact on the resonance characteristics of an antenna or a microstrip line. The NGD network can be implemented in different forms such as lumped, distributed and MMIC technology. These networks can be designed and fabricated at different parts of the frequency spectrum.

A filter based NGD network is used as an impedance matching network, for signal cancellation over wide bandwidth and for designing a frequency selective surface with adaptive phase response. Filter design by the insertion loss method is used to design the NGD network and the filter theory is useful in the analysis of these networks [12, 13]. This approach also guarantees a design with precise specifications and the desired functionality. Different possible realisations of the filter extend the scope of the NGD network to different design environments and different parts of the frequency spectrum. The best impact of a NGD network can be seen by selecting a suitable realisation depending on the application and specifications. A firm foundation for the theoretical analysis of NGD networks that are used in this work is guaranteed by adopting a filter-based design approach. The NGD networks are realised in the form of lumped element networks and frequency selective surfaces. The circuits are designed to operate in the L, S (1-3GHz) and X (10GHz) bands for feasibility and simplicity of prototypes to validate the proposed concepts. With appropriate implementation the proposed concepts can be used at higher frequencies. Availability of gain blocks is another factor to consider when designing prototypes at a higher frequency.

1.1.1 NGD based Electrically Small Antenna

The footprint of an antenna needs to be as small as possible in handheld and low profile applications, but the size of an antenna is inversely proportional to the operating frequency. The limitations and design issues of an electrically small antenna (ESA) are discussed by Wheeler and Chu [14, 15]. The ESA's are observed to have the following issues: high Q-factor due to low input impedance and high reactance, relatively small gain-bandwidth product and degraded efficiency.

The antenna impedance matching can be achieved using NGD networks [16]. By acting as a negative reactance The NGD network compensates the antenna reactance resulting in impedance matching over a wide bandwidth. Moreover, with the use of a NGD network an antenna can be impedance matched at frequencies far lower than the resonance frequency associated with the quarter wavelength of the antenna. The optimisable impedance characteristics of the NGD network provides necessary real and imaginary parts to impedance match the antenna at the desired frequencies. Instead of an active network, in this work a passive NGD network is used as a matching network. However, the inevitable insertion loss of a NGD network has to be compensated by using an amplifier. By using a unilateral amplifier the loss can be compensated, but the duplex operation cannot be achieved. The bidirectional amplifier can be used, but these designs are complex and more susceptible to stability problems.

1.1.2 NGD Based Active Circulator

A low profile, lightweight wideband active circulator integrated with an electrically small antenna is desired in wireless self-powered devices like handheld devices and radar systems. Though the stable passive bulky ferrite based circulators are the first model for the circulator concept, accommodating these is always challenging. To overcome the limitations of

conventional Ferrite-based circulators, many alternative models designed based on transistors, op-amps, phase shifters, transmission lines, dividers and combiners and couplers have been published in literature[17-19]. The designs presented in literature suffer with narrow bandwidth and/or instability. The majority of the designs published are implemented using Monolithic Microwave Integrated Circuit (MMIC) technology, leaving very little scope to customise the models for different environments. Power handling capability is another parameter that needs to be addressed. Part of the presented work in this thesis is motivated by the need for a wide bandwidth active circulator operation in mobile communication devices and radar systems.

A NGD based wideband active circulator working on signal cancellation phenomena is designed and tested in this work. In a hybrid ring configuration, a path from transmitter to receiver is formed in an anti-clockwise (ACW) direction to counteract the signal coming from a clockwise (CW) direction at the receiver junction. The NGD network has been incorporated in both CW and ACW paths of a circulator to achieve wideband signal cancellation at the junction of the receiver port. In an active circulator the receiver to transmitter isolation can be achieved when the two signals, arriving in CW and ACW directions at the receiver port, have equal magnitude and 180^0 anti-phase. The ability of the NGD network to adjust its phase characteristics plays a crucial role, along with the amplifier, in establishing the signal cancellation condition over a wide bandwidth.

1.1.3 NGD Based ESA Integrated with An Active Circulator

An electrically small antenna integrated with an active circulator suitable for duplex operation operating over wide bandwidth is desirable. Most often while designing an active circulator a 50Ω load will be replaced by an antenna. However in practice the impedance characteristics of an antenna will deviate from the ideal 50Ω load with the change in frequency. In such designs

the performance of the active circulator will change considerably when a practical antenna is connected. An active circulator with an integrated antenna with duplex operation working over a narrow bandwidth is reported in [17]. In some circulator designs the antenna works either in transmit mode or in receive mode, but not both [20]. More designs from the literature are discussed in the next chapter.

In this work a NGD based electrically small antenna is integrated with an active circulator. The active circulator is designed with sufficient gains in the transmission and reception paths to compensate the loss due to the matching NGD network. This will enable the ESA to be used in duplex mode over a wide bandwidth. It is observed that the proposed concept is valid for different types of antenna.

1.1.4 NGD Based Cavity Antenna

The concept of cavity antennas was well established and proved to be efficient in designing the antenna with high directivity and gain. A cavity antenna designed using the Partially Reflective Surface (PRS) and High Impedance Surface (HIS) is presented in literature as a high gain and highly directive antenna, yet the bandwidth has always been narrow [21-24]. Despite the advantages of a cavity antenna, in the conventional designs the resonance phase condition between the HIS and the PRS can be established only over a very narrow bandwidth. This limits the operating bandwidth and could lead to beam squinting. Establishing the phase condition over a wide bandwidth would eventually produce a wideband high gain highly directive cavity antenna with reduced beam squint.

In the design presented in this thesis the negative group delay HIS has played a prominent role in designing a wideband cavity antenna with reduced beam squint. The wideband high directional cavity antenna has been designed by achieving a satisfactory phase condition

between the PRS and the NGD based HIS over a wide bandwidth. The concept has been verified by full wave simulation.

1.2 Structure of the Thesis

The arrangement of the thesis is discussed in the following and is shown in Fig.1.1.

- The design aspects and literature in connection with the concepts that are used in the thesis are discussed in chapter 2. The NGD network design approaches and characterisation, as well as the advantages and disadvantages of the techniques that are used in the proposed models in comparison with literature are presented. The design constraints and various approaches to the design of circulators are presented. The literature on ESA and Fabry-Perot cavity antennas is also discussed in chapter 2.
- Filter based NGD network analysis, design, prototyping, advantages and disadvantages are discussed in chapter 3.
- ESA design aspects, specifications, and the use of a NGD network to achieve impedance matching, including the operating principle and noise figure analysis are presented in chapter 4, see Fig 1.2(a). The non-Foster matching principle is shown in Fig. 1.3.
- Achieving signal cancellation by using a NGD network for designing a wideband active circulator is presented in chapter 5, see Fig. 1.2(b). Integration of an ESA with the active circulator to demonstrate the duplex communication model is also presented. The gain needed to compensate the loss introduced by the matching NGD network is provided by the active circulator in transmission and reception mode, Fig. 1.2(c). The operating principle, analysis, fabrication issues and measurement results are discussed in detail in this chapter.
- The use of a negative group delay high impedance surface to design a wideband highly directive cavity antenna with reduced beam squint is presented in chapter 6, see Fig. 1.2(d).

Theoretical analysis, realisation of the concept to fabricate the prototype and the results are discussed.

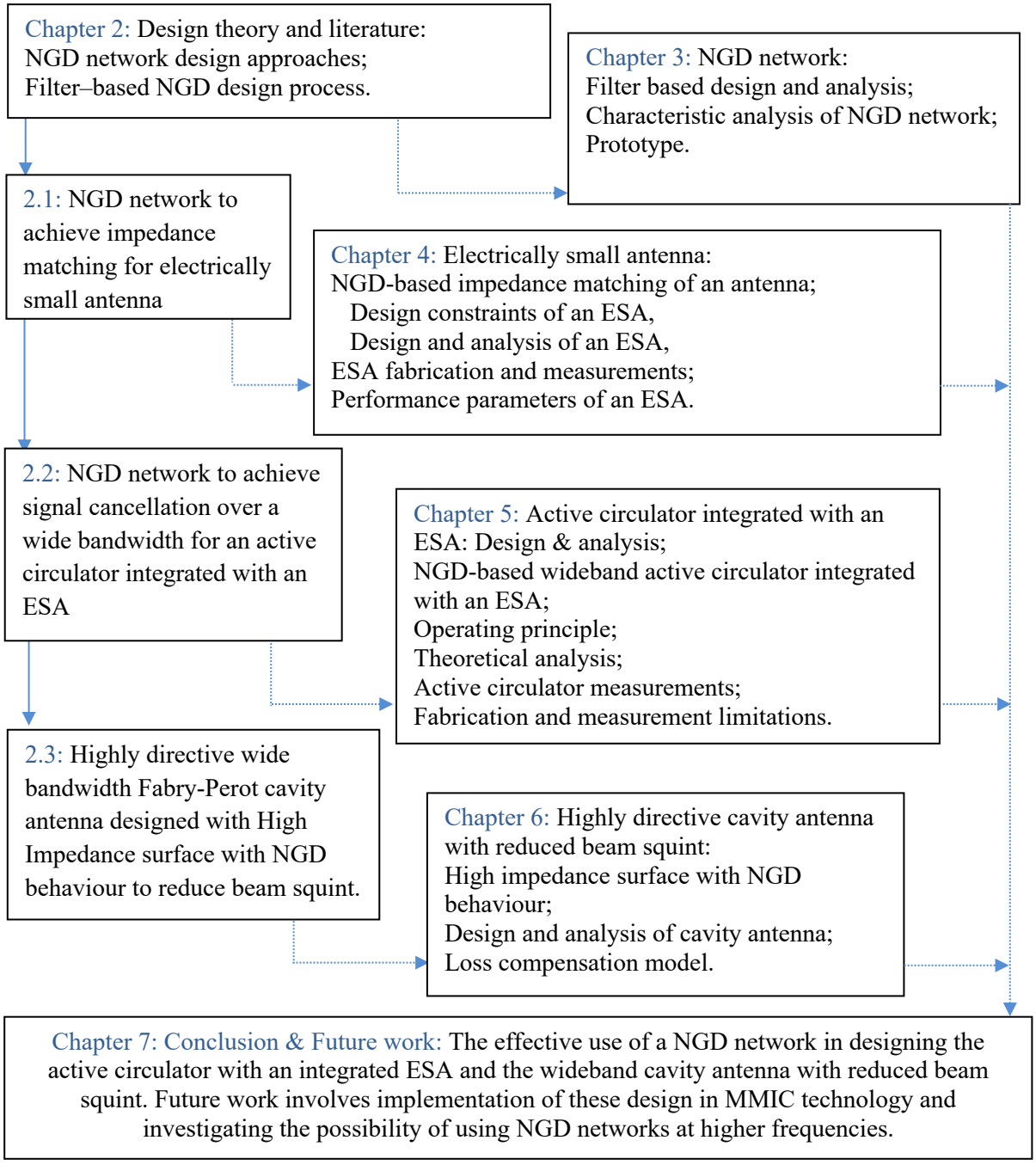

Fig. 1.1 The structure of thesis

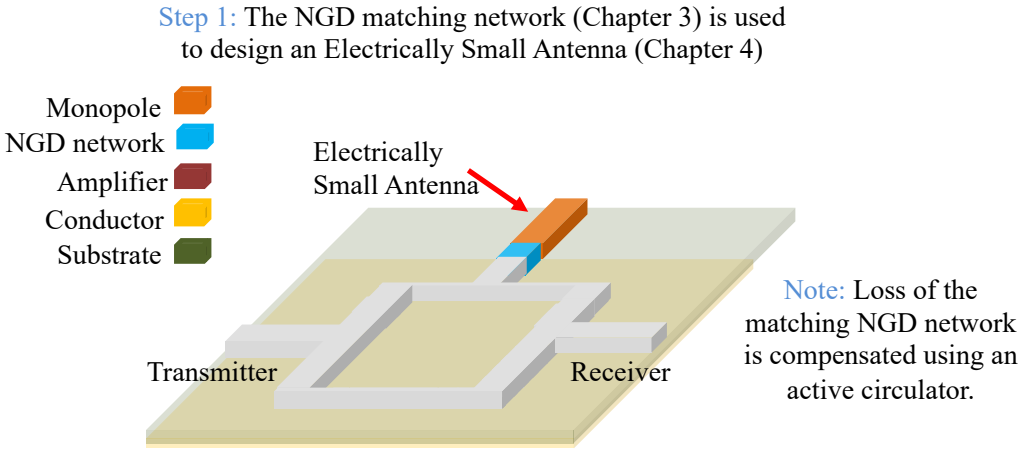

(a) Design of an electrically small antenna using a NGD network

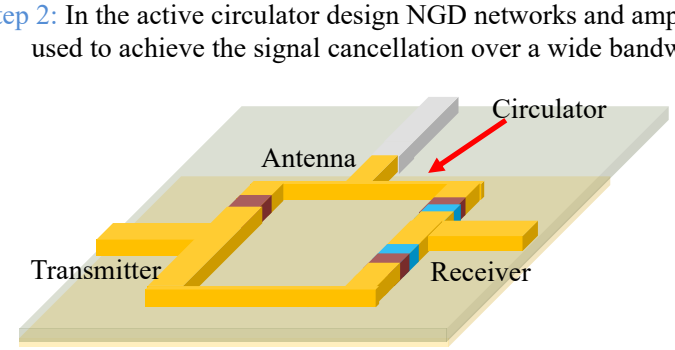

(b) Design of an active circulator using a NGD network

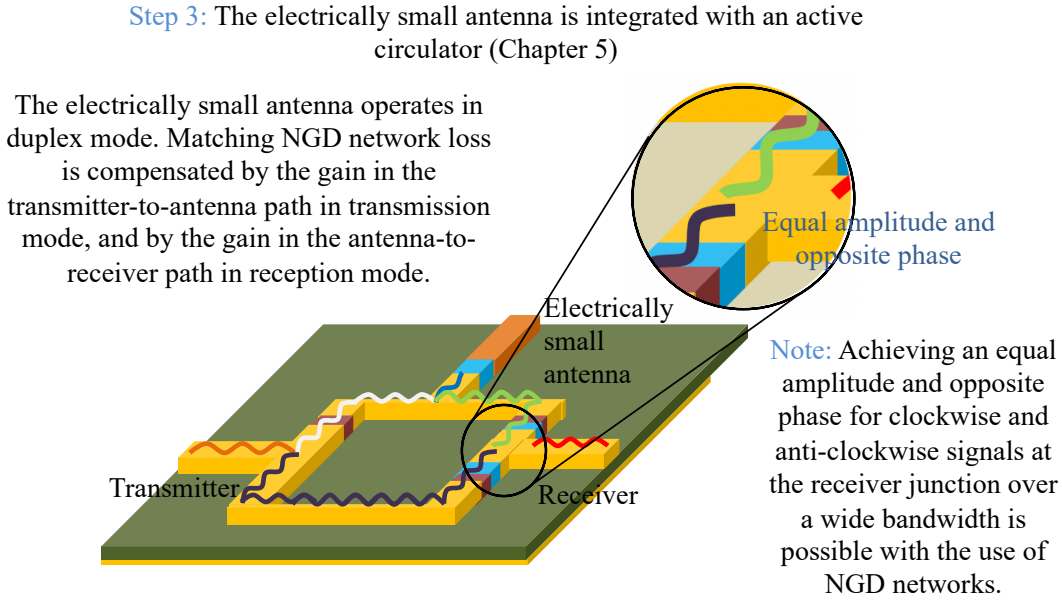

(c) An active circulator with an integrated electrically small antenna

Fig. 1.2 The overview of the work presented in the thesis (continues to next page)

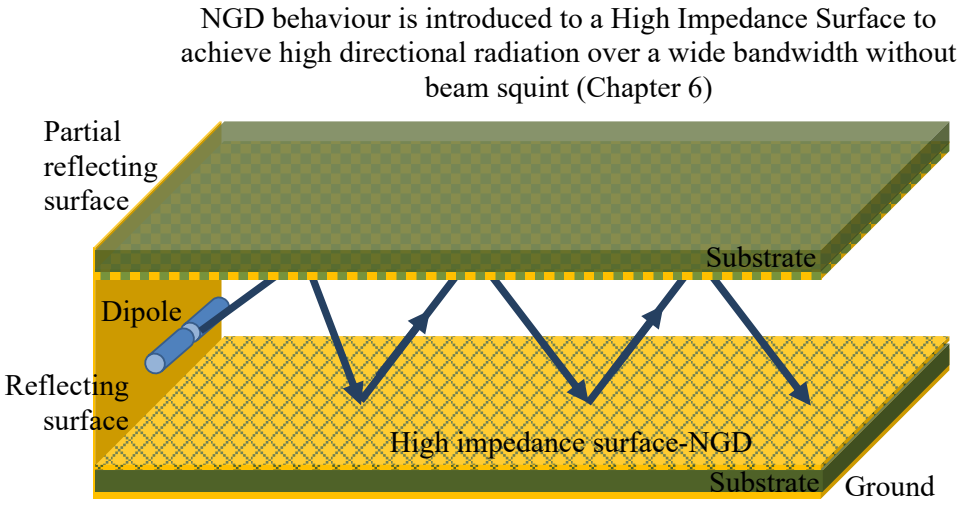

(d) A Fabry-Perot cavity antenna with reduced beam squint

Fig. 1.2 The overview of the work presented in the thesis

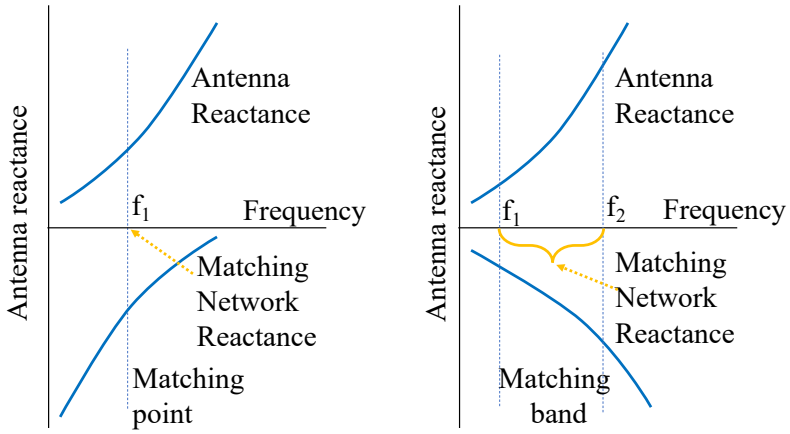

Fig. 1.3 Non-Foster network based antenna impedance matching

List of References

[1] C. A. Balanis, "Antenna Theory: Analysis and Design," *John Wiley & Sons, INC, New York,* 1989.

[2] R. M. Foster, "A reactance theorem," *Bell Syst. Tech,* vol. 3, pp. 259-267, 1924.

[3] O. J. Zobel, "Theory and design of uniform and composite electric wave-filters," *The Bell System Technical Journal,* vol. 2, no. 1, pp. 1-46, 1923.

[4] S. E. Sussman-Fort and R. M. Rudish, "Non-Foster Impedance Matching for Transmit Applications," in *IEEE International Workshop on Antenna Technology Small Antennas and Novel Metamaterials, 2006.*, 6-8 March 2006, pp. 53-56.

[5] S. E. Sussman-Fort and R. M. Rudish, "Non-Foster Impedance Matching of Electrically-Small Antennas," *IEEE Transactions on Antennas and Propagation,* vol. 57, no. 8, pp. 2230-2241, 2009.

[6] D. J. Gregoire, C. R. White, and J. S. Colburn, "Wideband Artificial Magnetic Conductors Loaded With Non-Foster Negative Inductors," *IEEE Antennas and Wireless Propagation Letters,* vol. 10, pp. 1586-1589, 2011.

[7] C. R. White, J. W. May, and J. S. Colburn, "A Variable Negative-Inductance Integrated Circuit at UHF Frequencies," *IEEE Microwave and Wireless Components Letters,* vol. 22, no. 1, pp. 35-37, 2012.

[8] H. Mirzaei, R. Islam, and G. V. Eleftheriades, "Anomalous Negative Group Velocity in Coupled Positive-Index/Negative-Index Guides Supporting Complex Modes," *IEEE Transactions on Antennas and Propagation,* vol. 59, no. 9, pp. 3412-3420, 2011.

[9] H. W. Bode, "Network Analysis and Feedback Amplifier Design," *New York: Van Nostrand,* 1945.

[10] R. M. Fano, "Theoretical limitations on the broadband matching of an arbitrary impedance," *J. Franklin Inst.,* vol. 249, pp. 57-98, February 1950.

[11] D. C. Youla, "A new theory of broadband matching," *IEEE Trans. Circuit theory,* vol. 11, pp. 30-50, Mar. 1964.

[12] J. D. Rhodes, "Thoery of electrical filters," *London: Wiley,* 1976.

[13] D. M. Pozar, "Microwave and RF Design of Wireless System," *John Wiley & Sons, INC, New York,* 2001.

[14] H. A. Wheeler, "Fundamental limitations of small antennas," *Proceedings of IRE,* vol. 35, pp. 1479–1484, 1947.

[15] L. J. Chu, "Physical limitations in omni directional antennas," *J. Appl. Phys,* vol. 19, pp. 1163-1175, 1948.

[16] H. Mirzaei and G. V. Eleftheriades, "Realizing Non-Foster Reactive Elements Using Negative-Group-Delay Networks," *IEEE Transactions on Microwave Theory and Techniques,* vol. 61, no. 12, pp. 4322-4332, 2013.

[17] C. Kalialakis, M. J. Cryan, P. S. Hall and P. Gardner , "Analysis and design of integrated active circulator antennas " *IEEE Transactions on Microwave Theory and Techniques,* vol. 48, no. 6, pp. 1017-1023, 2000.

[18] G. Carchon. and B. Nanwelaers , "Power and noise limitations of active circulators," *IEEE Transactions on Microwave Theory and Techniques,* vol. 48, no. 2, pp. 316-319, Feb. 2000.

[19] S. W. Y. Mung and W. S. Chan, "The Challenge of Active Circulators: Design and Optimization in Future Wireless Communication," *IEEE Microwave Magazine,* vol. 20, no. 7, pp. 55-66, 2019.

[20] Ziad El-Khatib, Leonard MacEachern and Samy A. Mahmoud , , "A fully-integrated linearized CMOS bidirectional distributed amplifier as UWB active circulator," *International Conference on Microelectronics,* pp. 106-109, 2008.

[21] A. P. Feresidis and J. C. Vardaxoglou, "High gain planar antenna using optimised partially reflective surfaces," *IEE Proceedings - Microwaves, Antennas and Propagation,* vol. 148, no. 6, pp. 345-350, 2001.

[22] A. P. Feresidis, G. Goussetis, W. Shenhong, and J. C. Vardaxoglou, "Artificial magnetic conductor surfaces and their application to low-profile high-gain planar antennas," *IEEE Transactions on Antennas and Propagation,* vol. 53, no. 1, pp. 209-215, 2005.

[23] Y. E. Erdemli, K. Sertel, R. A. Gilbert, D. E. Wright, and J. L. Volakis, "Frequency-selective surfaces to enhance performance of broad-band reconfigurable arrays," *IEEE Transactions on Antennas and Propagation,* vol. 50, no. 12, pp. 1716-1724, 2002.

[24] T. Akalin, J. Danglot, O. Vanbesien, and D. Lippens, "A highly directive dipole antenna embedded in a Fabry-Perot type cavity," *IEEE Microwave and Wireless Components Letters,* vol. 12, no. 2, pp. 48-50, 2002.

Chapter 2: Design Theory and Literature

The objective in this thesis is to study the possibility of using the NGD concept to address the issues such as antenna matching, signal cancellation and reduction of beam squint. In this chapter various techniques and methods from literature to address these issues are discussed. Different approaches to design and implement NGD networks are also presented.

Any passive non-dispersive two terminal reactance that exhibits negative slope with frequency is called a non-Foster element. The non-Foster elements are implemented using active circuits. Non-Foster networks are a very effective solution for wide bandwidth matching of an antenna and modifying the signal characteristics. In literature, non-Foster network implementation is reported using negative impedance convertors[1-3]. Being active designs, they suffer from stability issues. Active components such as amplifiers are the core of a negative impedance convertor design. Any variation in biasing of the amplifier would lead to degraded performance and the network may not exhibit non-Foster behaviour. NGD networks however also exhibit non-Foster behaviour and these can be implemented as passive designs, resulting in stable operation. Though amplifiers need to be used for loss compensation with a NGD network, the overall design is more stable than the negative impedance convertors. This is because the actual NGD behaviour is achieved by a passive network and the amplifiers are employed as gain blocks. This gives freedom for stable amplifier design resulting in improved stability of the overall system.

The negative group delay is defined in the study of Sommerfeld and Brillouin [4] on the propagation of light in a dispersive medium. They defined the group velocity as the pulse envelope propagation speed and the front velocity as the abrupt disturbance (initial transient period, when signal is turned-on suddenly) propagation speed, which are used to characterise

the narrow-band pulse. They successfully demonstrated the fact that within an absorption line in the region of abnormal dispersion, the group velocity would be greater than c (the speed of light in vacuum). Whereas, the front velocity is always positive and equal to light velocity in all circumstances. However, the peak of the pulse always lags the front, and the Einstein causality is still satisfied. In fact the superluminal (faster than light velocity) group velocities will be well exhibited in a dispersive medium in a specific segment of the spectrum while satisfying the causality [5]. Negative group velocity, negative phase velocity [6], negative refractive index [7] and superluminal velocities [8] are part of an irregular wave propagation phenomena. The negative group delay is the consequence of negative group velocity. The scenario where the output peak of a pulse precedes the input peak, characterises the medium with negative group delay behaviour. All physically realisable causal linear systems obey the Kramers-Kronig relations, however the absorption is inevitable in such media [5].

Numerous NGD network designs are reported in the literature. Each method has its own advantages and limitations. The most relevant design approaches from literature are discussed in this section. Implementation of the concept and experimental verifications depend on the application environment and the availability of relevant technologies. In the academic setting most of the electronic principles and concepts in microwave frequency are realised using active elements, passive lumped elements, microstrip lines and in MMIC technology. Each of these implementations have different degrees of fabrication accuracy.

2.1 Negative Group Delay Network Design Approaches

An NGD network has been modelled by linear resistor-capacitor (RC) and resistor-inductor (RL) networks along with canonical transfer function and optimal bandwidth prediction formulas, as reported in [9]. A broadband NGD network implemented using distributed

transmission lines technique was presented in [10]. A method of reducing the signal loss in a conventional NGD network was reported using a hybrid coupler along with resistors and transmission lines and the possibility of efficiency enhancement was demonstrated [11]. An optimisation method to reduce the number of resonators compared to that of conventional designs, to achieve the required group delay was reported in [12]. A flat NGD frequency response was demonstrated using multi-section asymmetric directional couplers accompanied with distributed amplifiers [13]. The method to design a NGD network with a predefined group delay value was reported, where the network was designed using RLC-resonators [14]. A NGD network design was reported using low-pass, high-pass, band-pass, band-stop active topologies [15, 16]. NGD network designs with periodical transmission lines which have an effective negative refractive index were reported in [17].

For more NGD several stages of basic building blocks should be used, this increases the complexity and footprint of the circuit. Most of the NGD circuits found in the literature can be classified as designs with lumped/distributed lossy structures, parallel stubs or left-handed metamaterial based periodical transmission lines having an effective negative refractive index. The lumped element based design is simple but the parasitic effects of passive elements and other structures on the PCB board will affect the phase response of the design. An accurate modelling of lumped elements is required. The distributed structures will be a help to accurately design the required values of passive elements. However, scaling of the design to work at different frequencies is not easy and sometimes not practical. The metamaterial based implementation is effective in reducing the size of the overall design and even scaling the structure to operate at different frequencies is easy. Fabrication of these structures is challenging. Table 2.1 summarises the various reported design approaches for NGD networks.

Table 2.1: Design approaches of NGD networks

	Active	Passive
Lumped lossy structures	• low-pass, high-pass, band-pass and stop-band active topologies [15, 16]	• RL-RC cells for first order low pass NGD [9]
Distributed lossy structures	• Multi section asymmetric directional couplers accompanied with distributed amplifier [18]	• Parallel stubs, distributed transmission lines techniques [10] • Hybrid coupler along with resistors and transmission lines [11] • Half wavelength resonators [12] • J-inverter with series and parallel RLC-resonators[14]
Metamaterial concept		• Periodical transmission lines with an effective negative refractive index [17]

Linear filter based NGD topologies were introduced in [19] and [20]. The majority of the topologies were developed by low-pass and band-pass designs [18, 21-23]. The band stop filter synthesis is used to design the NGD network. In this design a low pass filter is transformed into a band-stop filter for the NGD network [24]. Optimised resistors inserted in the resonators could give the desired values of NGD. These designs turn out to be the RLC resonators.

NGD Network: Design and Analysis

For the Butterworth low-pass filter of N[th] order shown in Fig. 2.1(a) element values can be obtained using Equ. 2.1 [25].

$$g_k = 2\sin\frac{(2k-1)\pi}{2N}, \qquad k = 1,2,N \tag{2.1}$$

The resistive elements are added to design the NGD network as shown in Fig. 2.1(b).

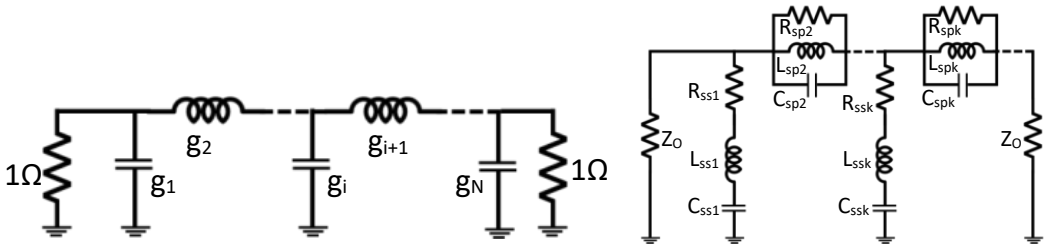

(a) Low-pass filter topology (b) NGD network

Fig. 2.1 A low-pass filter transformed into the NGD network

To determine the element values of the above network a frequency transformation from low pass to band stop given in Equ. 2.2 should be applied [25]. Assume ω_0 be the centre frequency, ω' be cut-off frequency and ω operating frequency.

$$\frac{1}{\omega'} \leftarrow \Delta\left(\frac{\omega}{\omega_o} - \frac{\omega_o}{\omega}\right) \tag{2.2}$$

where Δ is the FBW(3dB-fractional-bandwidth) of the proposed network.

The values for the parallel inductor and capacitor in the series branch (L_{ssk}, C_{ssk}) can be found using the following equations.

$$L_{ssk} = \frac{Z_o}{g_k \Delta \omega_o} \tag{2.3a}$$

$$C_{ssk} = \frac{g_k \Delta}{Z_o \omega_o} \tag{2.3b}$$

where Z_0 = port impedance, g_i = i-th prototype element value and ω_0 = centre frequency of the NGD network. Likewise, the values for the series inductor and capacitor of the parallel branch (L_{spk}, C_{spk}) can be evaluated using Equ. 2.4.

$$L_{spk} = \frac{g_k \Delta Z_o}{\omega_o} \tag{2.4a}$$

$$C_{spk} = \frac{1}{Z_o \omega_o g_k \Delta} \tag{2.4b}$$

The NGD will be obtained by adding resistors to the shunt and series resonators. To get a certain value of group delay τ, the resistor values can be calculated using the inductor and capacitor values in the respective resonators [26]. Each resonator produces slightly more group delay than what is obtain by the equation, so a correction factor α is used in Equ. 2.5 and 2.6 for accuracy. This is to compensate the extra group delay contributed by each resonator particularly in the higher order filters. The shunt resistor in a series branch (R_{ssk}) is given by:

$$R_{ssk} = \frac{\frac{-Z_o}{2} + \sqrt{\left(\frac{Z_o}{2}\right)^2 - \frac{4 Z_o L_{ssk}}{\alpha \tau}}}{2} \tag{2.5}$$

Similarly, the series resistor in a shunt branch (R_{spk}) is given by:

$$R_{spk} = \frac{\frac{-\alpha\tau}{C_{spk}} + \sqrt{\left(\frac{-\alpha\tau}{C_{spk}}\right)^2 - \frac{4\alpha\tau}{C_{spk}} Z_o}}{2} \tag{2.6}$$

With this procedure a NGD network can be designed for required group delay value. Due to the added loss the signal attenuation is inevitable in the NGD networks. The smaller the magnitude

of S21, the higher will be the signal attenuation. The amplifier can be used to compensate these losses, however, complexity and stability concerns for the network will increase. Adding the amplifier for loss compensation of NGD networks, makes them unidirectional and/or susceptible to stability issues. Either avoiding the use of an amplifier or limiting the use of number of stages is recommended. In practice there is a trade-off between the signal attenuation and the group delay value. The resistors in the NGD network can be optimised to balance these two parameters.

The resonator based NGD networks have a narrow operational bandwidth. Therefore, if a wideband network is needed multiple stages should be used. One possible solution is to design the NGD network with cascaded resonators of closely spaced centre frequencies [27] and cross-coupling between resonators [28]. For the NGD network the transmission coefficient, S21, magnitude is a function of frequency. More often in applications where a flat magnitude is expected this is a problem. However, the loss of a NGD network does not have to be compensated in every application. For example, the NGD networks can still be used for the signal cancellation application as discussed in the following chapters.

2.2 NGD Network To Achieve Impedance Matching For Electrically Small Antenna

For an antenna to be called electrically small, its physical length should be smaller than $\lambda/2\pi$ (λ operating-wavelength). Chu-Harington theoretically determined the limitations on the operational bandwidth and efficiency of electrically small antennas (ESA) [29]. Many active matching networks for designing a wide bandwidth ESA are reported in the literature. A wide bandwidth ESA with Linvill's negative impedance converter as a matching network is reported. These non-Foster networks have proved to be very effective in cancelling the capacitive reactance of the antenna and offering impedance matching [30]. A negative impedance

convertor is reported as an impedance matching network of an antenna in [31]. However, these active implementations have serious stability problems at microwave frequencies [32, 33]. As an alternative matching network a negative capacitor designed using digital-to-analog and analog-to-digital convertors supported by digital signal processing has been reported to overcome the stability problems [34]. A non-Foster negative inductor implemented using transistors is presented as a matching network [35]. For wireless communication systems a highly directional low profile Huygens-source ESA is reported in [36]. A reflection mode NGD network is used to match the antenna [37]. The designs reported above have stability issues and/or are not suitable for duplex communication. An ESA designed with a stable matching network suitable for duplex communication operating over a wide bandwidth is still a design challenge.

2.3 The Need Of Wideband Signal Cancellation For The Active Circulator

The necessity of isolated transmitters and receivers in communication systems and radar systems for duplex action led to the invention of the circulator. The size and weight advantages of the active circulator over that of the Ferrite-based were demonstrated [38, 39]. The first active circulator using transistors in a delay ring configuration is presented in [40, 41]. Active devices have been employed in order to achieve the required decoupling between receiver and transmitter for duplex operation. Compatibility of these techniques with monolithic microwave integrated circuit (MMIC) technology is an added advantage. Two possible designs of circulator are “three way” and “quasi”. Designs that offer full rotational symmetry are three way circulators. A lossy implementation of a three way circulator offers stable operation. An active quasi-circulator connects the transmitter to the antenna and the antenna to the receiver, but isolates the receiver from the transmitter. It can be implemented with gains on transmit and receive ports [42].

The aim is to find an active circulator with an integrated antenna which operates over a wide bandwidth. The following is such a design, but with some limitations. An active circulator implemented using amplifiers and ring configuration operating at 3.75GHz is reported in literature. An antenna is also integrated with this circulator, enabling full duplex communication. The CW and ACW paths were created to establish signal cancellation at the receiver junction. The operating bandwidth and power handling capacity are to be improved for this design [43, 44].

There are various models published that have addressed different issues related to circulators. Though some designs have a wide bandwidth there are some performance limitations. In some designs either the antenna is not integrated or a unidirectional antenna is employed as discussed below. Table 2.2 and 2.3 present the classification and summary of the following designs.

A fully integrated linearised CMOS 4-port circulator operating around 5.5GHz has been designed using bidirectional distributed amplifiers. An unity gain bandwidth of 11.5 GHz has been reported, however in each tuning state the isolation is good over a narrow bandwidth and the antenna operates in only one mode: either transmission or reception [45]. The stability and insertion loss characteristics are yet to be studied for this design. A CMOS multi-port active circulator designed with Bridged-T networks has a bandwidth of 8.4-11GHz. However a ~55.8mW power dissipation, a large chip area, the power-handling capability and noise performance of the three-port active circulator are its limitations [46]. Branch line couplers and bidirectional constructive wave amplifiers are used for the design of a circulator. This reconfigurable circulator operates over the 62-75GHz bandwidth, but the feedback network has degraded the performance and there is a shift in the frequency of operation [47]. A wave guide circulator designed using waveguide-couplers and FET-amplifiers operating over 17-21.5GHz has been reported [48]. The design is limited to wave-guide based applications, hence the size

of the design is a limitation. In addition above 21.5GHz this design can't operate as a circulator because the gain of the FET decreases. Another MMIC circulator uses the signal cancellation phenomena and operates at 24GHz. This model has the disadvantages of higher insertion losses and a very narrow operational bandwidth [49]. None of the above designs met the need for a wideband circulator integrated with an antenna for duplex operation.

A narrow band active circulator working by current reuse technology was presented. However the poor isolation between the antenna port and the transmitter port due to common gate configuration is yet to be addressed [50]. A CMOS wide bandwidth(1.5 to 9.6GHz) active circulator with high insertion losses(6dB) and high noise figure(15dB average) was reported in [51]. In a hybrid active circulator the phase compensation technique was used with a complementing phase shifter to achieve duplex action. A passive filter has been involved in this design [52], but the circulator stability analysis is yet to be done. Also the performance of this circulator with an integrated wide bandwidth antenna is yet to be studied. An active circulator operating on out-of-phase cancellation technique was implemented by using two common source buffers for improved isolation [53], but suffers from high insertion losses. Another active circulator designed with an in-phase current combiner and a balun which consists of operational transconductance amplifiers was reported [54]. This design is very compact and has good isolation characteristics, but the performance of this design with an integrated antenna is yet to be studied. A hybrid active circulator operating over 0.2 to 2.5GHz was reported [55]. This design suffers from insertion loss and assumes a 50Ω load, so the performance might change when an antenna is attached to this circulator. A passive distributed tunable active circulator for high isolation with tunable capacitive effect was presented. Though the tunable range is wide at any particular case the operating bandwidth is only ~0.3GHz and this model has 20dB noise figure in the antenna to receiver path [56]. An active circulator consisting of an Op-amp

based differential amplifier and voltage divider made of a chip-resistor is reported. The Op-amp input impedance mismatch resulted in poor isolation and high insertion loss [57]. An integrated reconfigurable CMOS quasi-active circulator operating over 2.3 to 2.4 GHz bandwidth was accompanied by a reconfigurable antenna impedance matching circuit. This had good receiver gain, but had 4dB transmitter to antenna insertion loss [58]. An active circulator with an integrated antenna operating over a wide bandwidth with a small footprint is yet a design challenge. Table 2.2 summarises the above review and shows a classification of circulators.

Table 2.2: Different types of circulator designs and implementations

Circulator type [42]	3-Way		Quasi	
	Active	Passive	Active	Passive
NGD network based phase cancellation			Proposed work	
Transistor based gain blocks	[59, 60]		[38, 40, 41, 43, 44]	
Bridge T network			[46]	
Couplers	[47]			
Op-amp			[57]	
FET- waveguide-type	[48]			
Distributed amplifiers	[45]		[49, 56]	
Signal cancellation-transistor			[50, 51]	
Phase compensation: Phase shifter, FET			[52] [53]	
Operational transconductance amplifiers			[54] [55]	

Table 2.3 lists various circulator designs in the literature that are discussed above. Most of the designs reported here are implemented in MMIC technology. The design presented in this thesis is also compatible with MMIC technology.

Table 2.3: Various circulator designs reported in literature

Ref	Type	Dimension	Application	Made up of	Operating frequency, bandwidth and parameters	Limitations
[44]	Hybrid Ring-type 3-port	Total 50X40 mm^2 Antenna 20X12 mm^2	To isolate the transmitter from the receiver in communication equipment.	Gain blocks & Microstrip lines	Fc = 3.75GHz BW = 7MHz Isolation 26.9dB Gain-Tx 10dBi Gain-Rx 4dBi	Bandwidth is low
[45]	Fully-Integrated Linearized CMOS 4-port	Total 1.89 X 0.8 mm^2 Antenna 280X220 μm^2	Communication systems over fibre. Ultra-wideband and highly linear.	Bi-directional Distributed Amplifier	Unity gain BW 11.5 GHz, 5.5 GHz Isolation -26dB	The stability of the design is yet to be studied. Insertion losses should be analysed. Antenna is unidirectional.
[46]	CMOS Ring-type 3-port & n-port possible	RF 0.81mm^2 & DC probes 0.72 mm^2	For testing the reflection coefficient of an antenna and tx-line integrity in the field using an extremely small reflection test instrument. Also for short-range radar.	Bridged-T Networks (BTNs)	8.4 to 11.1 GHz Power consumption 18.2 mW Isolation 25dB Transmission ratio 18.3dB	Large chip area and a power dissipation of ~55.8-mW. Low power threshold and high noise figure of a 3-port active circulator.

Ref	Type	Dimension	Application	Made up of	Operating frequency, bandwidth and parameters	Limitations
[47]	Re-configurable 3-port	1.13 X1.10 mm^2	Multi-band radar, built-in self-test and vector network analyser on-a-chip system	Branch line couplers & Bidirectional constructive wave amplifiers	62-75 GHz Insertion losses 7.4dB Isolation 18dB	Feedback networks resulted in performance degradation and a shift in operating frequency.
[48]	Waveguide-type 4-port	In cm's	Waveguide circuit	FET amplifiers & fine-line circuits & waveguide-type directional couplers	17-21.5 GHz Isolations 40dB Forward Insertion loss 0.1dB	Over 21.5GHz, this circuit can't operate as a circulator because the gain of the FET decreases.
[49]	Monolithic Circuit 3-port	0.55 x 0. 64 mm2	In transceiver systems, to be integrated into monolithic circuits	FETs	Insertion losses |S32| 9dB |S2I| 8.5dB isolation |S31| 30 dB, DC power consumption 9.12 mW	The isolation |S23| is poor from the receiver to the antenna. Insertion losses are high.
[50]	Integrated CMOS circulator	820x750 um^2	Low power applications	FET based current reuse method	2.4GHz Isolation 68dB	Narrow bandwidth. High insertion losses.
[51]	CMOS active circulator	0.72x0.57 mm^2	NA	FET's	1.5 to 9.6 GHz Isolation 18dB	Noise figure (15dB). High insertion losses (6dB). Stability analysis is needed.

Ref	Type	Dimension	Application	Made up of	Operating frequency bandwidth and parameters	Limitations
[52]	Hybrid active circulator	NA	RF/Microwave portable devices	FET distributed amplifier and T-network phase shifters	0.8-2.2GHz 15dB Isolation 0dB insertion loss	Stability analysis is needed.
[53]	MMIC	NA	Radio system	FET's	30GHz, Isolation 12dB. Insertion loss 7.9dB. P_{com} 1.5mW	High insertion losses (7.5dB)
[54]	Active MMIC circulator	0.25mm^2	NA	Operational trans-conductance amplifier	1.5 to 2.7GHz Isolation 26dB	Insertion loss ~3dB
[55]	Hybrid active circulator	NA	Network analyser	Differential amplifiers and lossy broadband combiner	0.2- 2.5GHz	Isolation is only 15dB over 0.2 to 1.7 GHz band. 4 dB insertion loss.
[56]	Distributed Active Circulator	1.67 X 0.97 mm^2	Radio system	Distributed amplifiers	5.3 ~ 7.3GHz tuning range Isolation 30dB	Noise figure 20dB Insertion loss 5dB
[57]	Op-Amp type 3-port	4 X 4 cm^2	Suitable for low frequency lumped element system implementation	An Op Amp based differential amplifier and voltage divider using chip-resistors	0.5GHz insertion loss flatness within +/-0.8 Isolation 20dB	Poor isolation, high insertion loss and degraded performance.

2.4 Optimised High Impedance Negative Group Delay Surface For Cavity Antenna

High directivity, low profile, high efficiency antennas are preferable for wireless communications. Beam steering technologies benefit from these types of antennas. A planar design with high gain-bandwidth product and efficiency is possible using a patch array antenna. However unfortunately feeding mechanisms are complex and this limits the achievable gain bandwidth product and degrades the efficiency [61, 62]. Metamaterial based antennas, such as Fabry-Perot-type resonant cavity antenna (FP-Cavity antenna), proved to be highly directive, low profile antennas compared to the Horn antenna or other conventional high directivity antennas [63, 64]. A Fabry-Perot resonant cavity antenna comprises of passive structures: a partially reflective surface, ground plane and high impedance surface. These structures create a cavity with a primary radiator such as a dipole. Fig 2.2 shows the Fabry-Perot cavity antenna evolution for high gain, high directivity, and wide operational bandwidth.

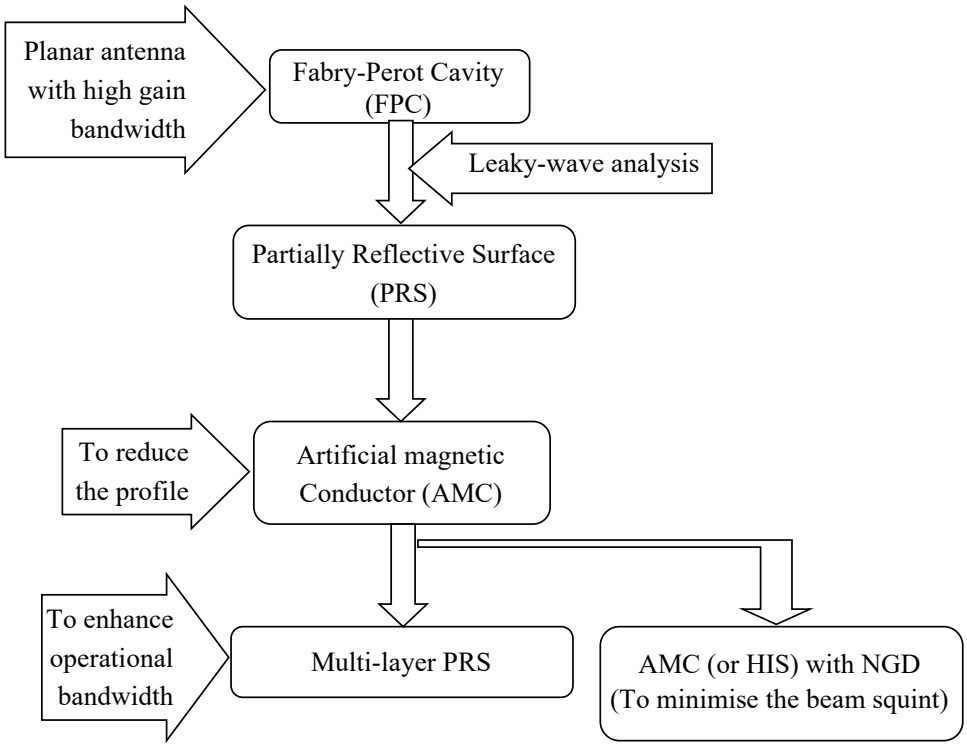

Fig: 2.2 Development of Fabry-Perot Cavity antenna

The combined efforts of Trentini [65] and James [66] unveiled a new concept, partially reflective surface (PRS), as an alternative to patch arrays to design high gain planar antennas. The distance and reflecting wave characteristics between PRS and ground plane determines the gain and bandwidth. When placed in front of a grounded waveguide aperture, PRS produces leaky wave and beam forming effects. Using structures such as superimposed dichroic microstrip antenna arrays [67], waveguides with partially reflecting walls [68, 69] and frequency selective surfaces (FSS) leaky wave phenomenon can be produced. The frequency selective surfaces are either an aperture in a conducting plane or an array of conducting elements (patches). Both the apertures and conducting elements can be designed in different shapes[70]. Due to the structure of FSS it acts as an electromagnetic wave filter. At the resonance frequency apertures allow the electromagnetic transmission and patches perform total reflection. However adjacent to resonance frequency, FSS acts as a partially reflecting surface [63].

The PRS consists of passive arrays of conducting elements printed on a substrate. The shape of these conducting elements can be arbitrary, but usually patches and dipoles are in use [63, 65, 71, 72]. With the right height between the ground plane and the PRS a Fabry-Perot resonance cavity can be designed for enhancing the gain and directivity of the primary antenna. The design and analysis of a Fabry-Perot Cavity antenna using leaky-wave approach has been successfully demonstrated [73-79]. The use of a planar artificial magnetic conductor (AMC) ground plane has further reduced the profile of the FP-Cavity antenna to sub-wavelength values [80-84].

An inherently narrow operational bandwidth has always been a limitation of FP-Cavity antennas. The multi-layer PRS in a FP-Cavity antenna demonstrated significant improvement in bandwidth. Examples of this type of cavity antenna are: a double layer array of square metallic patch arrays with non-uniform conductor dimensions [85]; a double-layer square-ring

defected structure with increased phase [86]; a dielectric substrate with dipoles printed on both sides for a positive phase gradient [87] and a multi-layer PRS in [88].

The multiple sources and multiple electromagnetic band gap (EBG) structures proved to improve the directivity [83, 89-91]. The phase agile cells were used to demonstrate the reconfigurable FP-Cavity antenna in [92]. And the dual band FP-Cavity antenna with high directivity has been reported in [93].

A wideband antenna with non-Foster behaviour in a PRS is reported in [94]. For enhancing the operational bandwidth of a FP-Cavity antenna a non-foster cavity boundary has been presented in [95]. According to this, the desired reflection phase characteristics can be obtained by replacing the Perfect Electric Conductor (PEC) ground with a ground that has the non-Foster behaviour.

2.5 Observations From Literature And Proposed Solutions

It is observed from the literature that designing an ESA for duplex communication over a wide bandwidth for low profile applications is still a design challenge. In the following section a novel approach to achieve this desired antenna is presented.

2.5.1 The Proposed Filter Based Negative Group Delay Circuit Design Approach

The proposed NGD network design flow is shown in Fig. 2.3. The proposed work involves investigation of the change in NGD network behaviour with filter types such as Butterworth, Bessel, Chebyshev 1 & 2 and Elliptic. The impact of filter order on group delay value and signal attenuation is also studied.

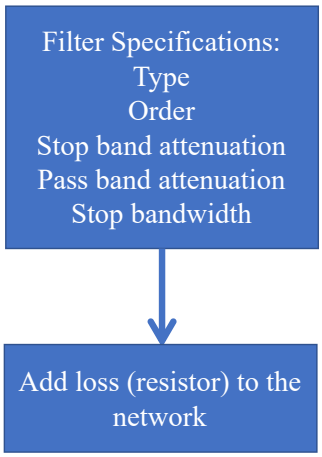

Fig. 2.3 Proposed NGD network design approach

Using this procedure, the NGD network will be used for matching the antenna to design an ESA. NGD networks are also designed for the active circulator to achieve the signal cancellation over a wide bandwidth.

2.5.2 Proposed NGD Based Electrically Small Antenna

The low profile antennas are desirable to operate at low frequencies in wireless applications. In the proposed design the NGD network is used as an impedance matching network. The non-Foster behaviour is achieved by the NGD network resulting in a negative inductor or negative capacitor effect for wide bandwidth matching. The optimisable resistor values help to impedance match the radiating element at frequencies far lower than the resonance frequency associated with the quarter wavelength of the antenna, as shown in Fig. 2.4. The validity of the proposed matching method with different types of antennas will be studied in chapter 3. The wide bandwidth and dual band matching possibilities will also be studied.

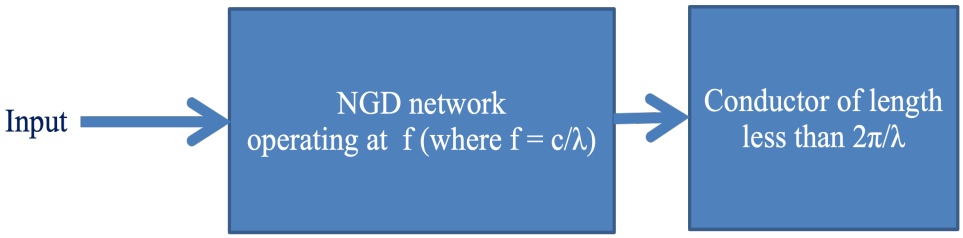

Fig. 2.4 Proposed NGD based electrically small antenna design flow

The losses of the matching NGD network will be compensated by the gains in the transmission and reception modes of an active circulator. This enables the proposed ESA to be suitable for duplex communication over a wide bandwidth.

2.5.3 Proposed Active Circulator Using NGD Network

The proposed active circulator works on signal cancellation phenomena. As shown in Fig. 2.5, equal amplitude and opposite phase is the necessary condition needed for signal cancellation to achieve isolation between the transmitter and the receiver. The quasi active circulator operation has been established by maintaining gains and isolations between respective ports. The NGD network will be used to achieve wide bandwidth signal cancellation. In addition the design method allows the amplifiers used in this design to be optimised for stable operation as shown in Fig.2.6. The MMIC compatibility of the proposed design makes it suitable for low profile applications.

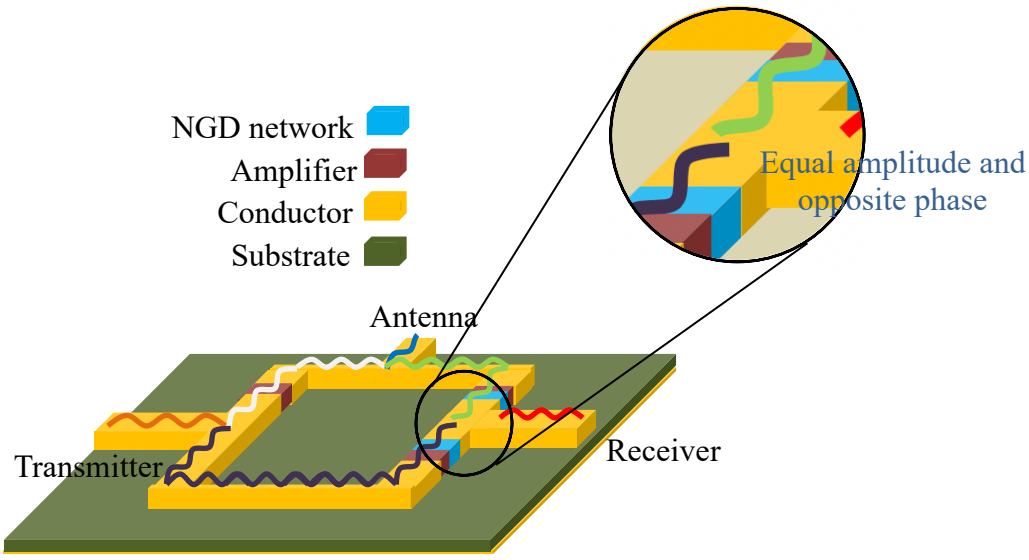

Fig. 2.5 Proposed NGD based active circulator

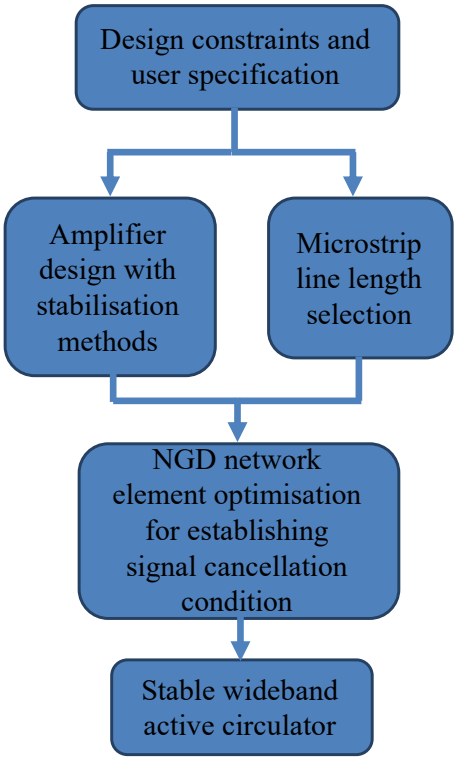

Fig. 2.6 Proposed NGD based active circulator design flow

2.5.4 Proposed NGD Based Cavity Antenna with Reduced Beam Squint

A low profile antenna with high directivity and gain and minimum beam squint over a wide bandwidth is still a design challenge. The Fabry-Perot cavity antenna formed by frequency selective surfaces has demonstrated an improved directivity and gain. In the proposed design the beam squint problem of the Fabry-Perot cavity antenna will be addressed. In conventional design the necessary phase condition between two surfaces of the cavity can be achieved only over a very narrow bandwidth. By introducing NGD behaviour in the high impedance surface the phase condition will be established over a wide bandwidth, leading to minimum beam squint, see Fig. 2.7.

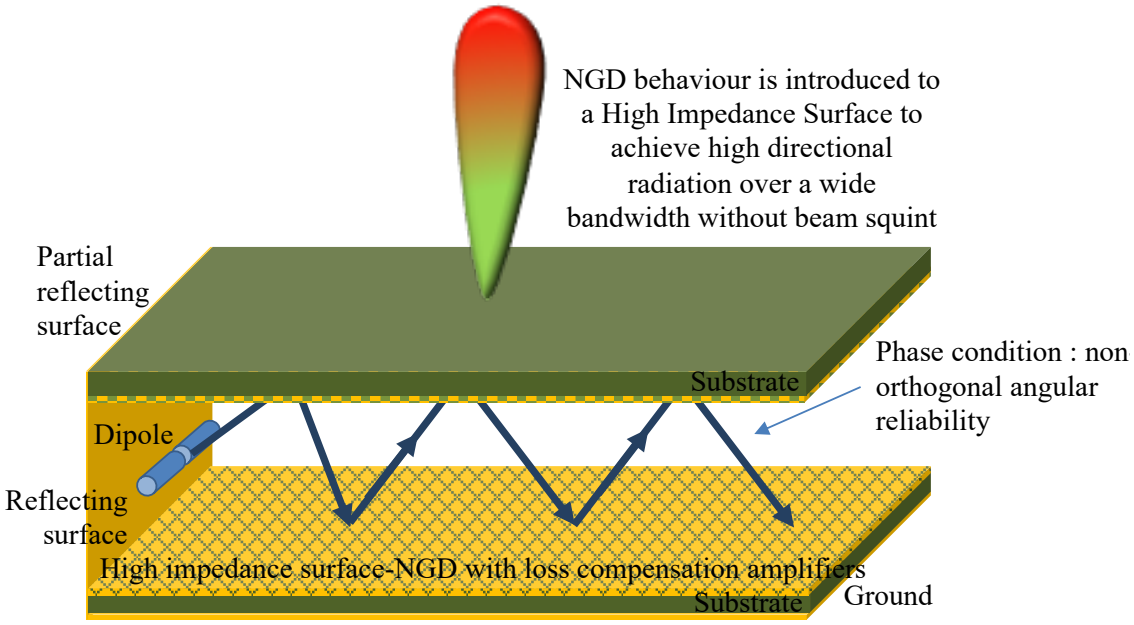

Fig. 2.7 Proposed NGD based Fabry-Perot cavity antenna design

References

[1] R. L. Brennan, T. R. Viswanathan, and J. V. Hanson, "The CMOS negative impedance converter," *IEEE Journal of Solid-State Circuits,* vol. 23, no. 5, pp. 1272-1275, 1988.

[2] E. Yuce, "Negative Impedance Converter With Reduced Nonideal Gain and Parasitic Impedance Effects," *IEEE Transactions on Circuits and Systems I: Regular Papers,* vol. 55, no. 1, pp. 276-283, 2008.

[3] P. V. Ananda Mohan, "On Actively Compensated Amplifiers Using Negative Impedance Converters," *IEEE Transactions on Circuits and Systems II: Express Briefs,* vol. 67, no. 4, pp. 640-644, 2020.

[4] L. Brillouin, "Wave propagation and group velocity," *Academic Press, New York,* 1960.

[5] E. L. Bolda, R. Y. Chiao, and J. C. Garrison, "Two theorems for the group velocity in dispersive media," *Physical Review A,* vol. 48, no. 5, pp. 3890-3894, 11/01/ 1993.

[6] I. A. Ibraheem, J. Schoebel, and M. Koch, "Group delay characteristics in coplanar waveguide left-handed media," *Journal of Applied Physics,* vol. 103, no. 2, Jan 15 2008.

[7] Y. Z. Wang, Y. W. Zhang, L. He, F. Q. Liu, H. Q. Li, and H. Chen, "Direct observation of negative phase velocity and positive group velocity in time domain for composite right/left-handed transmission lines," *Journal of Applied Physics,* vol. 100, no. 11, Dec 1 2006.

[8] M. Mojahedi, E. Schamiloglu, F. Hegeler, and K. J. Malloy, "Time-domain detection of superluminal group velocity for single microwave pulses," *Phys Rev E Stat Phys Plasmas Fluids Relat Interdiscip Topics,* vol. 62, no. 4 Pt B, pp. 5758-66, Oct 2000.

[9] B. Ravelo, "High-Pass Negative Group Delay RC-Network Impedance," *IEEE Transactions on Circuits and Systems II: Express Briefs,* vol. 64, no. 9, pp. 1052-1056, 2017.

[10] C. D. Broomfield and J. K. A. Everard, "Broadband negative group delay networks for compensation of microwave oscillators and filters," *Electronics Letters,* vol. 36, no. 23, pp. 1931-1933, 2000.

[11] G. Chaudhary and Y. Jeong, "Distributed Transmission Line Negative Group Delay Circuit With Improved Signal Attenuation," *IEEE Microwave and Wireless Components Letters,* vol. 24, no. 1, pp. 20-22, 2014.

[12] R. Das, Q. Zhang, A. Kandwal, and J. Mukherjee, "General synthesis method for negative group delay response: A filter base approach," in *2017 47th European Microwave Conference (EuMC)*, 10-12, pp. 424-427, 2017.

[13] C. T. M. Wu and T. Itoh, "Maximally Flat Negative Group-Delay Circuit: A Microwave Transversal Filter Approach," *Ieee Transactions on Microwave Theory and Techniques,* vol. 62, no. 6, pp. 1330-1342, Jun 2014.

[14] G. Chaudhary, Y. Jeong, and J. Lim, "Microstrip Line Negative Group Delay Filters for Microwave Circuits," *IEEE Transactions on Microwave Theory and Techniques,* vol. 62, no. 2, pp. 234-243, 2014.

[15] F. Wan, N. Li, B. Ravelo, Q. Ji, B. Li, and J. Ge, "The Design Method of the Active Negative Group Delay Circuits Based on a Microwave Amplifier and an RL-Series Network," *IEEE Access,* vol. 6, pp. 33849-33858, 2018.

[16] B. Ravelo, A. PÉrennec, M. L. Roy, and Y. G. Boucher, "Active Microwave Circuit With Negative Group Delay," *IEEE Microwave and Wireless Components Letters,* vol. 17, no. 12, pp. 861-863, 2007.

[17] J. Woodley and M. Mojahedi, "Negative group velocity in left-handed materials," in *IEEE Antennas and Propagation Society International Symposium. Digest. Held in conjunction with: USNC/CNC/URSI North American Radio Sci. Meeting (Cat. No.03CH37450)*, 22-27, vol. 4, pp. 643-646, June 2003.

[18] C. M. Wu and T. Itoh, "Maximally Flat Negative Group-Delay Circuit: A Microwave Transversal Filter Approach," *IEEE Transactions on Microwave Theory and Techniques,* vol. 62, no. 6, pp. 1330-1342, 2014.

[19] B. Ravelo, "Similitude between the NGD function and filter gain behaviours," *Int J Circ Theor App,* vol. 42, no. 10, pp. 1016-1032, Oct 2014.

[20] B. Ravelo, "First-order low-pass negative group delay passive topology," *Electronics Letters,* vol. 52, no. 2, pp. 124-126, 2016.

[21] W. Alomar and A. Mortazawi, "Method of generating negative group delay in phase arrays without using lossy circuits," *Proc. IEEE Int. Wireless Symp. (IWS), Beijing, China,* pp. 1-3, Apr. 2013.

[22] G. Chaudhary and Y. Jeong, "Low signal-attenuation negative groupdelay network topologies using coupled lines," *IEEE Trans. Microw. Theory Techn.,* vol. 62, no. 10, pp. 2316-2324, Oct. 2014.

[23] M. Kandic and G. E. Bridgesx, "Asymptotic limits of negative group delay in active resonator-based distributed circuits,," *IEEE Trans. Circuits Syst. I, Reg. Papers,* vol. 58, no. 8, pp. 1727-1735, Aug. 2011.

[24] J. Park, G. Chaudhary, J. Jeong, and Y. Jeong, "Microwave Negative Group Delay Circuit: Filter Synthesis Approach," *Journal of Electromagnetic Engineering and Science,* vol. 16, no. 1, pp. 7-12, Jan 2016.

[25] G. Mathaei, L. Young, and E. M. T. Jone, "Microwave Filters: Impedance Matching Networks and Coupling Structures," vol. Dedham, MA: Artech House, 1964.

[26] H. Choi, K. Song, C. D. Kim, and Y. Jeong "Synthesis of negative group delay time circuit," *Proceedings of IEEE Asia-Pacific Microwave Conference (APMC), Hong Kong,* pp. 1-4, 2008.

[27] G. Chaudhary, J. Jeong, P. Kim, and Y. Jeong, "Negative group delay circuit with improved signal attenuation and multiple pole characteristics," *Journal of Electromagnetic Engineering and Science,* vol. 15, no. 2, pp. 76-81, Apr. 2015.

[28] G. Chaudhary and Y. Jeong, "A Design of Compact Wideband Negative Group Delay Network Using Cross Coupling," *Microwave and Optical Technology Letters,* vol. 56, no. 11, pp. 2495-2497, Nov 2014.

[29] L. J. Chu, "Physical limitations in omni directional antennas," *J. Appl. Phys,* vol. 19, pp. 1163-1175, 1948.

[30] Girdhari C, Yongchae J, Jongsik L, "Microstrip Line Negative Group Delay Filters for Microwave Circuits," *IEEE Transactions on Microwave Theory and Techniques,* vol. 62, no. 2, pp. 234-243, 2014.

[31] O. O. Tade, P. Gardner, and P. S. Hall, "Broadband Matching of Small Antennas Using Negative Impedance Converters.," *Ieee Antennas Prop,* 2012.

[32] E. Ugarte-Munoz, S. Hrabar, D. Segovia-Vargas, and A. Kiricenko, "Stability of Non-Foster Reactive Elements for Use in Active Metamaterials and Antennas," *Ieee Transactions on Antennas and Propagation,* vol. 60, no. 7, pp. 3490-3494, Jul 2012.

[33] S. K. Dhar, M. S. Sharawi, and F. M. Ghannouchi, "An Electrically Small Wideband Antenna with Tunable Non-Foster Matching Network," *Proc Eur Conf Antenn,* 2016.

[34] K. K. Steer, P. J. Kehoe, and T. P. Weldon, "Investigation of an Adaptively-Tuned Digital Non-Foster Approach for Impedance Matching of Electrically-Small Antennas," *Ieee Southeastcon,* 2017.

[35] N. Ivanov, V. Turgaliev, and D. Kholodnyak, "Performance Improvement of an Electrically-Small Loop Antenna Matched with Non-Foster Negative Inductance," *Ieee Mtt S Int Micr,* pp. 344-347, 2017.

[36] T. S. Ming-Chun Tang, Richard W. Ziolkowski, "Design of a planar electrically small huygens source antenna," *International Applied Computational Electromagnetics Society Symposium,* 2017.

[37] A. A. Almahroug, A. P. Feresidis, and P. Gardner, "Antenna Matching Network Using New Class of Non-Foster Reactive Elements," *International Workshop on Electromagnetics: Applications and Student Innovation Competition (Ieee Iwem 2017),* pp. 180-182, 2017.

[38] C. Kalialakis, M. J. Cryan, P. Gardner and P. S. Hall, "FDTD simulation of active integrated antenna," *Electronics Letters,* vol. 33, no. 25, pp. 2091-2092, 4 Dec. 1997.

[39] C. Kalialakis, M. J. Cryan, P. Gardner and P. S. Hall, "FDTD analysis of microstrip configurations incorporating gain blocks," *IEE Colloquium on RF and Microwave Components for Communication Systems(Digest No: 1997/126), Bradford, UK,* pp. 7/1-7/5, 1997.

[40] S. Tanaka, N. Shimomura and K. Ohtake, "Active circulators—The realization of circulators using transistors," *Proceedings of the IEEE,* vol. 53, no. 3, pp. 260-267, March 1965.

[41] M. A. Smith, "GaAs monolithic implementation of active circulators," *IEEE MTT-S International Microwave Symposium Digest, New York, NY, USA,* vol. 2, pp. 1015-1016, 1988.

[42] D. Kother, B. Hopf, T. Sporkmann, I. Wolff and S. Koblowski, "Active CPW MMIC Circulator for the 40 GHZ Band," *24th European Microwave Conference, Cannes, France,* pp. 542-547, 1994.

[43] M. J. Cryan and P. S. Hall, "An integrated active circulator antenna," *IEEE Microwave and Guided Wave Letters,* vol. 7, no. 7, pp. 190-191, July 1997.

[44] C. Kalialakis; M. J. Cryan; P. S. Hall; P. Gardner, "Analysis and design of integrated active circulator antennas " *IEEE Transactions on Microwave Theory and Techniques,* vol. 48, no. 6, pp. 1017-1023, 2000.

[45] Ziad El-Khatib; Leonard MacEachern; Samy A. Mahmoud, "A fully-integrated linearized CMOS bidirectional distributed amplifier as UWB active circulator," *International Conference on Microelectronics,* pp. 106-109, 2008.

[46] S. Wang, C. Lee, and Y. Wu, "Fully Integrated 10-GHz Active Circulator and Quasi-Circulator Using Bridged-T Networks in Standard CMOS " *IEEE Transactions on Very Large Scale Integration (VLSI) Systems,* vol. 24, no. 10, pp. 3184-3192, 2016.

[47] Tissana Kijsanayotin and J. F. Buckwalter, "Millimeter-Wave Dual-Band, Bidirectional Amplifier and Active Circulator in a CMOS SOI Process," *IEEE Transactions on Microwave Theory and Techniques,* vol. 62, no. 12, pp. 3028-3040, 2014.

[48] T. Kawai and S. Toyoda, "20GHz Band Active Circulator Utilizng Fin-Line," *Infrared, Millimeter, and Terahertz Waves (IRMMW-THz), 37th International Conference,* pp. 1-2, 2012.

[49] Ding-Jie Huang, Jing-Lin Kuo and Huei Wang, "A 24-GHz low power and high isolation active quasi-circulator " *Microwave Symposium Digest (MTT), IEEE MTT-S International,* pp. 1-3, 2012.

[50] J. Hsieh, T. Wang and S. Lu, "A 1.5-mW, 2.4 GHz Quasi-Circulator With High Transmitter-to-Receiver Isolation in CMOS Technology," *IEEE Microwave and Wireless Components Letters,* vol. 24, no. 12, pp. 872-874, Dec. 2014.

[51] S. Shin, J. Huang, K. Lin and H. Wang, "A 1.5–9.6 GHz Monolithic Active Quasi-Circulator in 0.18$\mu{\rm m}$CMOS Technology," *IEEE Microwave and Wireless Components Letters,* vol. 18, no. 12, pp. 797-799, Dec. 2008.

[52] S. W. Y. Mung and W. S. Chan, "Novel Active Quasi-Circulator With Phase Compensation Technique," *IEEE Microwave and Wireless Components Letters,* vol. 18, no. 12, pp. 800-802, 2008.

[53] Y. Lo, J. Kiang, and C. Chang, "A 30 GHz Active Quasi-Circulator With Current-Reuse Technique in $0.18~\mu{\rm m}$ CMOS Technology," *IEEE Microwave and Wireless Components Letters,* vol. 20, no. 12, pp. 693-695, Dec. 2010.

[54] Y. Zheng and C. E. Saavedra, "Active quasi-circulator MMIC using OTAs," *IEEE Microw. Wireless Compon. Lett,* vol. 19, no. 4, pp. 218-220, 2009.

[55] D. Ghosh and G. Kumar, "A Broadband Active Quasi Circulator for UHF and L Band Applications," *IEEE Microwave and Wireless Components Letters,* vol. 26, no. 8, pp. 601-603, 2016.

[56] K. Fang and J. F. Buckwalter, "A Tunable 5–7 GHz Distributed Active Quasi-Circulator With 18-dBm Output Power in CMOS SOI," *IEEE Microwave and Wireless Components Letters,* vol. 27, no. 11, pp. 998-1000, Nov. 2017.

[57] Pin-Heng Chen, and Ram M. Narayanan, "Design of Active Circulators Using High-Speed Operational Amplifiers," *IEEE Microwave And Wireless Components Letters,* vol. 20, no. 10, pp. 575-577, October 2010.

[58] S. A. Ayati, D. Mandal, B. Bakkaloglu, and S. Kiaei, "Integrated Quasi-Circulator With RF Leakage Cancellation for Full-Duplex Wireless Transceivers," *IEEE Transactions on Microwave Theory and Techniques,* vol. 66, no. 3, pp. 1421-1430, 2018.

[59] G. Carchon and B. Nanwelaers, "Power and noise limitations of active circulators," *IEEE Transactions on Microwave Theory and Techniques,* vol. 48, no. 2, pp. 316-319, Feb. 2000.

[60] S. W. Y. Mung and W. S. Chan, "Active Three-Way Circulator Using Transistor Feedback Network," *IEEE Microwave and Wireless Components Letters,* vol. 27, no. 5, pp. 476-478, May 2017.

[61] J. R. James and P. S. Hall, "Handbook of microstrip antennas," *Peter Peregrinus Ltd., London,* 1989.

[62] D. M. Pozar, and D. H. Schaubert, "Microstrip Antennas, the Analysis and Design of Microstrip Antennas and Arrays," *IEEE Press, New York,* 1995.

[63] A. P. Feresidis and J. C. Vardaxoglou, "High gain planar antenna using optimised partially reflective surfaces," *IEE Proceedings - Microwaves, Antennas and Propagation,* vol. 148, no. 6, pp. 345-350, 2001.

[64] K. Konstantinidis, A. P. Feresidis, M. J. Lancaster, P. S. Hall, and P. Gardner, "Design of a submillimetre wave Fabry-Perot cavity antenna," in *2013 European Microwave Conference*, 6-10 Oct. 2013 2013, pp. 357-360.

[65] G. V. Trentini, "Partially reflecting sheet arrays," *IRE Transactions on Antennas and Propagation,* vol. 4, no. 4, pp. 666-671, 1956.

[66] J. R. Tames, Kinany, S.J.A., PEEL: P.D., and ANDRASIC, G., "Leaky-wave multiple dichroic beamfomers," *Electron Letters,* vol. 25, pp. 120-121, 1989.

[67] J. R. James and G. Andrasic, "Superimposed Dichroic Microstrip Antenna-Arrays," *Iee Proc-H,* vol. 135, no. 5, pp. 304-312, Oct 1988.

[68] A. J. Robinson, J. C. Vardaxoglou, and R. D. Seager, "Wave Guidance and Radiation from a Hollow Tube Formed from Frequency-Selective Surfaces," *Electronics Letters,* vol. 29, no. 17, pp. 1531-1533, Aug 19 1993.

[69] J.C. Vardaxoglou, A.J. Robinson and R.D. Seager, "Towards a new class of wave guiding structures, light weight horn antennas using passive arrays," *Proceedings of IEEE International Conference on Electromagnetics in Aerospace Applications,Torino, Italy,* pp. 345-346,1993.

[70] R. Mittra, C. H. Chan, and T. Cwik, "Techniques for analyzing frequency selective surfaces-a review," *Proceedings of the IEEE,* vol. 76, no. 12, pp. 1593-1615, 1988.

[71] T. Akalin, J. Danglot, O. Vanbesien, and D. Lippens, "A highly directive dipole antenna embedded in a Fabry-Perot type cavity," *IEEE Microwave and Wireless Components Letters,* vol. 12, no. 2, pp. 48-50, 2002.

[72] N. Guerin, S. Enoch, G. Tayeb, P. Sabouroux, P. Vincent, and H. Legay, "A metallic Fabry-Perot directive antenna," *IEEE Transactions on Antennas and Propagation,* vol. 54, no. 1, pp. 220-224, 2006.

[73] Y. J. Lee, J. Yeo, R. Mittra, and W. S. Park, "Design of a high-directivity electromagnetic bandgap (EBG) resonator antenna using a frequency selective surface (FSS) superstrate," *Microw. Opt. Technol. Lett.,* vol. 43, no. 6, pp. 462-467, Dec. 2004.

[74] Z. Tianxia, D. R. Jackson, J. T. Williams, H. D. Yang, and A. A. Oliner, "2-D periodic leaky-wave antennas-part I: metal patch design," *IEEE Transactions on Antennas and Propagation,* vol. 53, no. 11, pp. 3505-3514, 2005.

[75] Z. Tianxia, D. R. Jackson, and J. T. Williams, "2-D periodic leaky-wave Antennas-part II: slot design," *IEEE Transactions on Antennas and Propagation,* vol. 53, no. 11, pp. 3515-3524, 2005.

[76] A. Oliner, "Leaky-wave antennas," *Antenna Engineering Handbook, R. C. Johnson, Ed., 3rd ed. New York, USA: McGraw-Hill,* 1993.

[77] A. Foroozesh and L. Shafai, "Investigation Into the Effects of the Patch-Type FSS Superstrate on the High-Gain Cavity Resonance Antenna Design," *IEEE Transactions on Antennas and Propagation,* vol. 58, no. 2, pp. 258-270, 2010.

[78] J. Ju, D. Kim, and J. Choi, "Fabry-Perot cavity antenna with lateral metallic walls for WiBro base station applications," *Electronics Letters,* vol. 45, no. 3, pp. 141-142, 2009.

[79] J. R. James, S. J. A. Kinany, P. D. Peel, and G. Andrasic, "Leaky-wave multiple dichroic beamformers," *Electronics Letters,* vol. 25, no. 18, pp. 1209-1211, 1989.

[80] A. P. Feresidis, G. Goussetis, W. Shenhong, and J. C. Vardaxoglou, "Artificial magnetic conductor surfaces and their application to low-profile high-gain planar antennas," *IEEE Transactions on Antennas and Propagation,* vol. 53, no. 1, pp. 209-215, 2005.

[81] S. Wang, A. P. Feresidis, G. Goussetis, and J. C. Vardaxoglou, "High-gain subwavelength resonant cavity antennas based on metamaterial ground planes," *IEE Proceedings - Microwaves, Antennas and Propagation,* vol. 153, no. 1, pp. 1-6, 2006.

[82] J. R. Kelly, T. Kokkinos, and A. P. Feresidis, "Analysis and Design of Sub-Wavelength Resonant Cavity Type 2-D Leaky-Wave Antennas," *IEEE Transactions on Antennas and Propagation,* vol. 56, no. 9, pp. 2817-2825, 2008.

[83] R. Gardelli, M. Albani, and F. Capolino, "Array thinning by using antennas in a Fabry–Perot cavity for gain enhancement," *IEEE Transactions on Antennas and Propagation,* vol. 54, no. 7, pp. 1979-1990, 2006.

[84] D. Sievenpiper Lijun, Zhang, R. F. J. Broas, N. G. Alexopolous and E. Yablonovitch, "High-impedance electromagnetic surfaces with a forbidden frequency band," *IEEE Transactions on Microwave Theory and Techniques,* vol. 47, no. 11, pp. 2059-2074, 1999.

[85] A. P. Feresidis and J. C. Vardaxoglou, "A broadband high-gain resonant cavity antenna with single feed," *First European Conference on Antennas and Propagation*, pp. 1-5, 6-10 Nov. 2006.

[86] L. Moustafa and B. Jecko, "EBG Structure With Wide Defect Band for Broadband Cavity Antenna Applications," *IEEE Antennas and Wireless Propagation Letters,* vol. 7, pp. 693-696, 2008.

[87] Y. Ge, K. P. Esselle, and T. S. Bird, "The Use of Simple Thin Partially Reflective Surfaces With Positive Reflection Phase Gradients to Design Wideband, Low-Profile EBG Resonator Antennas," *IEEE Transactions on Antennas and Propagation,* vol. 60, no. 2, pp. 743-750, 2012.

[88] K. Konstantinidis, A. P. Feresidis, and P. S. Hall, "Multilayer Partially Reflective Surfaces for Broadband Fabry-Perot Cavity Antennas," *IEEE Transactions on Antennas and Propagation,* vol. 62, no. 7, pp. 3474-3481, 2014.

[89] L. Young Ju, Y. Junho, R. Mittra, and P. Wee Sang, "Application of electromagnetic bandgap (EBG) superstrates with controllable defects for a class of patch antennas as spatial angular filters," *IEEE Transactions on Antennas and Propagation,* vol. 53, no. 1, pp. 224-235, 2005.

[90] A. R. Weily, K. P. Esselle, T. S. Bird, and B. C. Sanders, "Dual resonator 1-D EBG antenna with slot array feed for improved radiation bandwidth," *IET Microwaves, Antennas & Propagation,* vol. 1, no. 1, pp. 198-203, 2007.

[91] A. Pirhadi, M. Hakkak, F. Keshmiri, and R. K. Baee, "Design of Compact Dual Band High Directive Electromagnetic Bandgap (EBG) Resonator Antenna Using Artificial Magnetic Conductor," *IEEE Transactions on Antennas and Propagation,* vol. 55, no. 6, pp. 1682-1690, 2007.

[92] A. R. Weily, T. S. Bird, and Y. J. Guo, "A Reconfigurable High-Gain Partially Reflecting Surface Antenna," *IEEE Transactions on Antennas and Propagation,* vol. 56, no. 11, pp. 3382-3390, 2008.

[93] L. Dong Hyun, L. Young Ju, Y. Junho, R. Mittra, and P. Wee Sang, "Novel Thin Dual-band Frequency Selective Surface (FSS) Superstrate for Directivity Enhancement," *IEEE Antennas and Propagation Society International Symposium*, pp. 4183-4186, 9-14 July 2006.

[94] Ahmad T. Almutawa, Alister Hosseini, David R. Jackson and Filippo Capolino, "Leaky-Wave Analysis of Wideband Planar Fabry–Pérot Cavity Antennas Formed by a Thick PRS," *IEEE Transactions on Antennas and Propagation,* vol. 67, no. 8, pp. 5163 - 5175, 2019.

[95] T. Debogović, S. Hrabar, and J. Perruisseau-Carrier, "Broadband Fabry-Pérot radiation based on non-foster cavity boundary," *Electronics Letters,* vol. 49, no. 4, pp. 239-240, 2013.

Chapter 3: Negative Group Delay Network

The negative group delay (NGD) behaviour of a network in transmission mode can be identified by the positive slope of a scattering parameters phase response. It is possible to have NGD behaviour in reflection mode as well. In this work transmission mode NGD networks are used. Non-Foster elements such as a negative inductor or a negative capacitor are useful for achieving impedance matching over a wide bandwidth. The phase characteristics of these elements can be controlled. Non-Foster networks have been developed using NGD networks [1]. The negative group delay is useful for compensating the positive group delay of a transmission line[2]. Impedance matching and signal cancellation using NGD networks is demonstrated in chapters 4 and 5 respectively. The customisable implementation of a NGD network makes it suitable for applications such as portable devices, radar systems and cellular communications. This chapter describes how NGD networks based on filter theory have been designed and tested. One way to identify the NGD behaviour is to observe the transmission S-parameter phase slope. The scattering parameters and the group delay are used to study the behaviour of NGD networks. Some loss is added to the filters to design the NGD networks. These passive non-Foster networks will always have a transmission loss. If necessary an amplifier could be used to compensate the transmission loss of the NGD network. Any positive slope for the transmission phase curve can be achieved over a range of frequency for a trade-off of transmission loss and design complexity.

3.1 Filter Based Negative Group Delay Network Design and Analysis

The NGD network design process using filter theory is detailed in this section. The filter's stopband frequency range and the resistor added to the network will determine the bandwidth

over which the NGD behaviour can be achieved. The proposed NGD networks are experimentally verified using lumped element implementation.

Filter Based NGD Network Design

The well-established filter theory is used as a basis to design the NGD networks. In this approach the NGD network can be designed with precision for the required specifications. The nature of the NGD networks can be better understood by this design procedure and this also provides a way to control the phase and loss characteristics.

- NGD design: with 1st order Filter

In the proposed method the design of the NGD network starts with a band-stop filter. It is observed that the phase response of the band-stop filter can be easily changed to a positive slope phase response by adding sufficient loss by means of a resistor. In the proposed implementation the filter consist of inductors (L) and capacitors (C) connected in parallel and series orientation in series and shunt branches of the network respectively. The number of these L and C resonator blocks per network depends on the order of the filter. To achieve the NGD behaviour a resistor is added in each branch.

For the proposed applications in chapters 4 and 5, a NGD network with a linear positive phase response is advantageous in the optimisation process. It is observed that the Butterworth filter has linear positive phase response compared to other types of filter. The phase responses of NGD networks designed using different types of filters are shown in the next section (Fig 3.5a). Hence the Butterworth band stop filter with added resistors is used to design a NGD network with non-Foster response. When an Elliptic filter is used to design an NGD network, it is easy to achieve negative group delay at different frequency bands. Using this type of filter it is easy to achieve a flat magnitude response for transmission coefficient over a wide bandwidth.

Step 1: Design Band-stop Filter with Required Specification

For ease of analysis a 1st order band-stop Butterworth filter, with 2GHz centre frequency and 400MHz bandwidth has been used as shown in Fig. 3.1. The operating frequency and bandwidth can be selected, however there will be fabrication practicalities depending on the type of implementation.

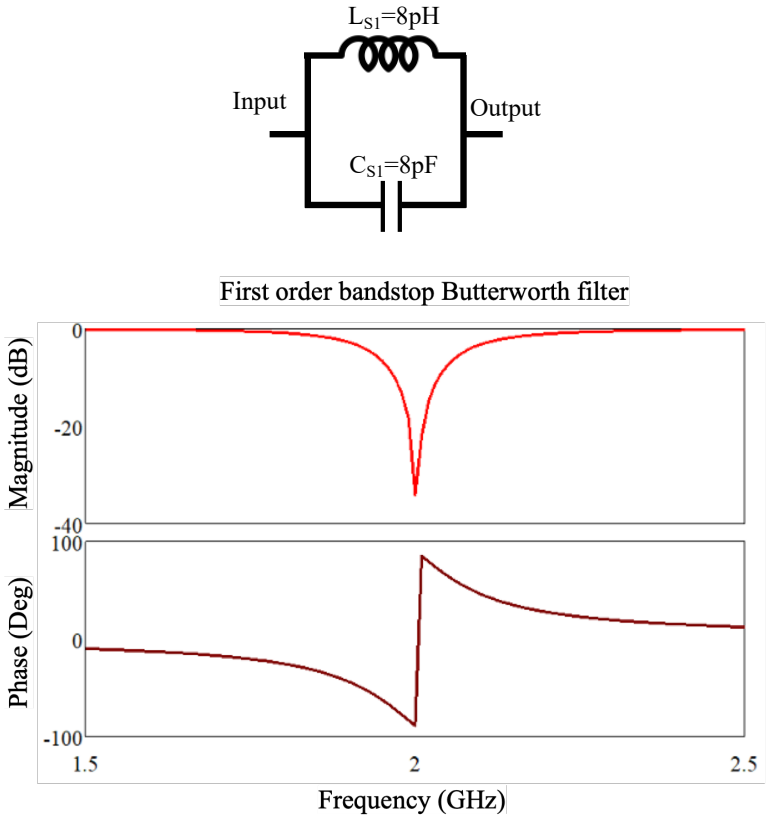

Fig. 3.1 1st order band stop Butterworth filter and transmission mode response

Step 2: Add Sufficient Resistance in Each Branch of the Filter

A resistor is added in parallel to L and C as shown in Fig. 3.2. In the proposed design process the resistor is optimised to achieve the required transmission coefficient phase and magnitude characteristics. Though it is obvious that the added resistors will contribute to the transmission loss, the relation between these two is not directly proportional. Moreover the relation between

these two quantities becomes more complex when higher order filters are used. With the availability of sophisticated computer aided design software such as AWR Microwave Office and CST Microwave Studio the optimisation of the resistor values is easy and helpful in matching (chapter 4) and signal cancellation (chapter 5) applications as it will be shown in these chapters. However, Equ. 2.5 and 2.6 can be used to determine the resistor values for a required group delay as presented in Chapter 2 from the literature [3].

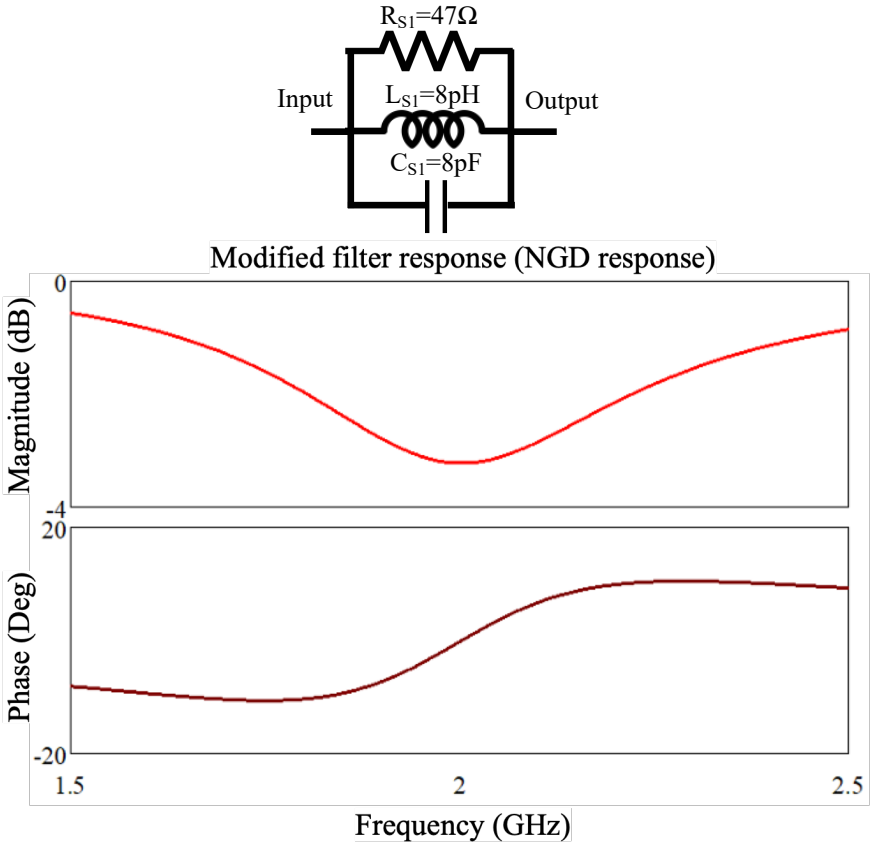

Fig. 3.2 Filter converted into NGD network and filter based NGD response

For the NGD network, the transmission coefficient magnitude and positive phase slope are functions of the filter order, filter type and the resistors value. The following Fig. 3.3 shows the variation in NGD network transmission coefficient phase and magnitude responses with different resistor values. In this case loss and group delay values are increasing with the resistor value.

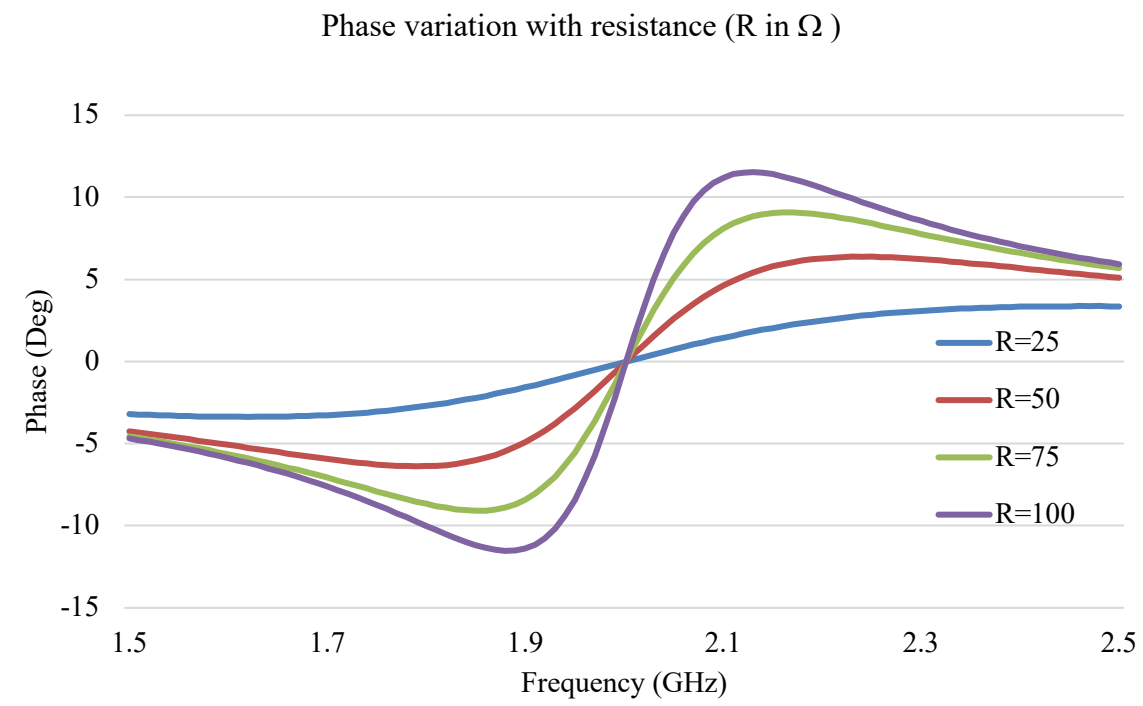

Fig. 3.3 (a) Filter based NGD network phase characteristics with changing resistor value

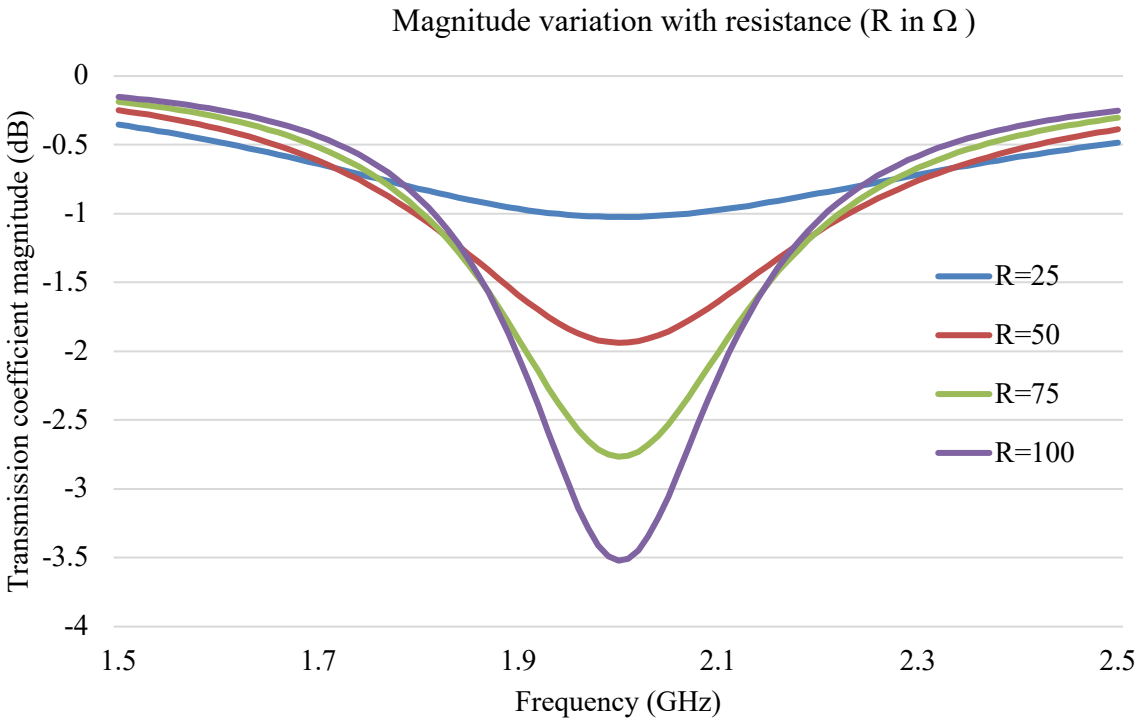

Fig. 3.3 (b) Filter based NGD network transmission coefficient magnitude characteristics with changing resistor value

The resistor values of the NGD network will determine the slope of the phase curve and the bandwidth over which the positive phase slope can be obtained as shown in Fig. 3.4. In case of Fig.3.4 (a) bandwidth is defined as the frequency band over which phase response of the NGD network has a positive slope.

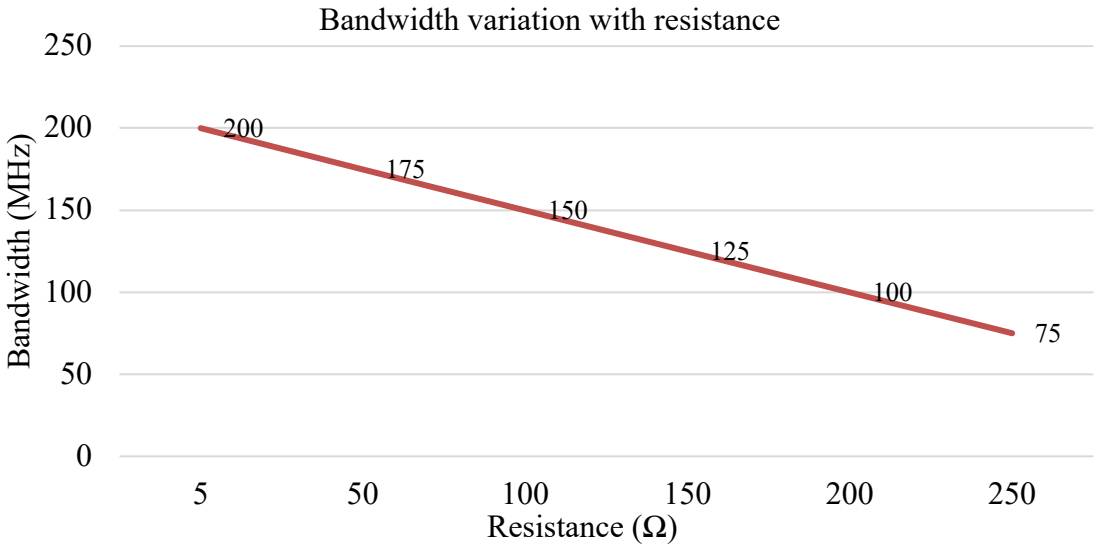

Fig. 3.4 (a) Impact of resistor values on NGD network bandwidth.

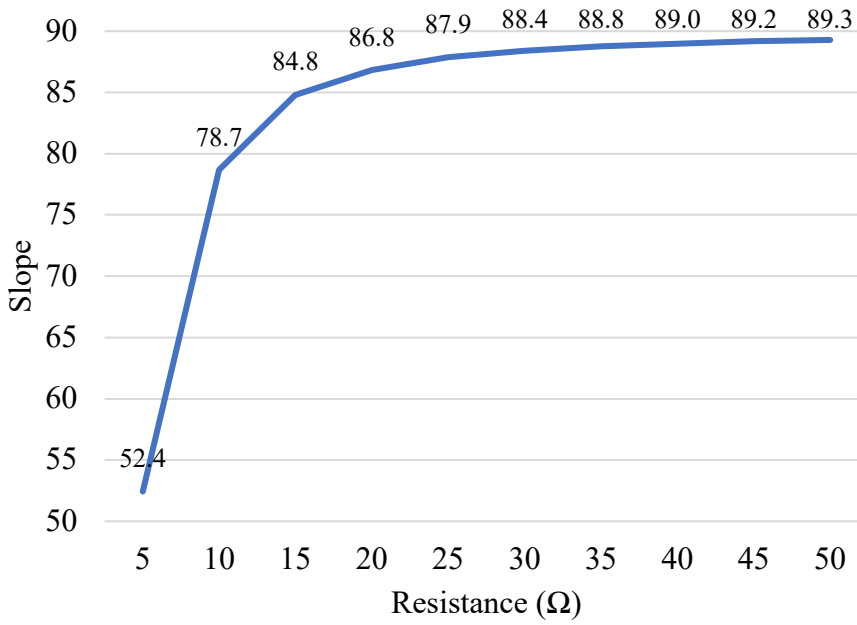

Fig. 3.4 (b) Impact of resistor values on NGD network phase curve slope.

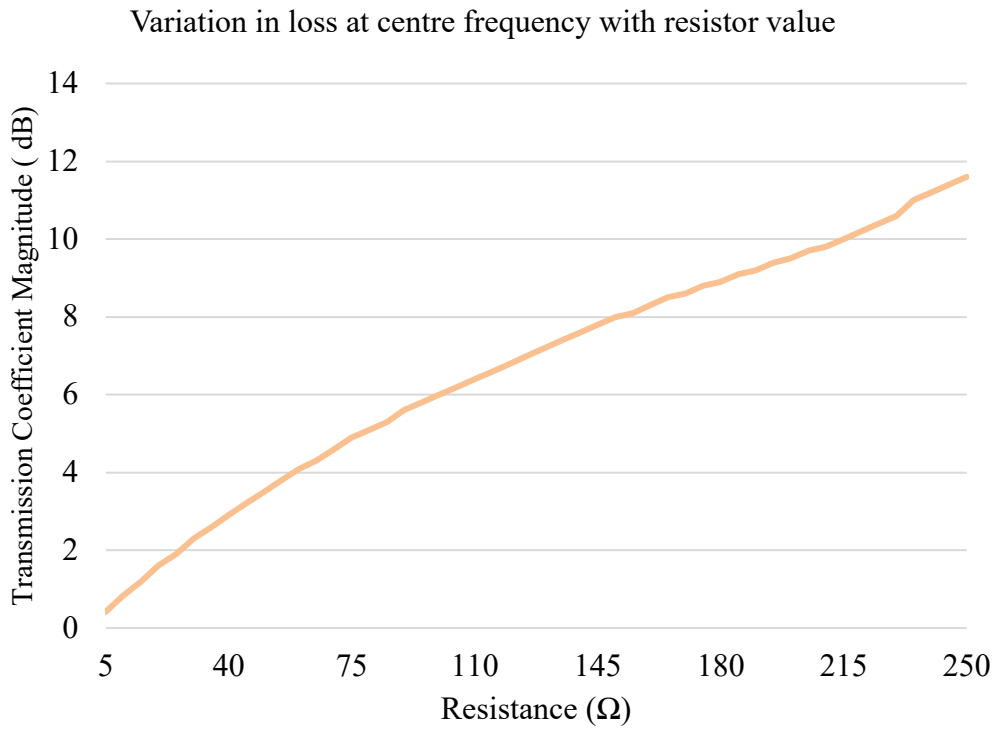

Fig. 3.4 (c) Impact of resistor values on NGD network transmission coefficient magnitude characteristics.

- **NGD design: with 4th order filter**

Design flexibility and more NGD can be achieved with higher order designs. The variation in the NGD network response is further analysed with higher order design. A 4th order filter based NGD analysis is presented in this section. A NGD network with non-Foster behaviour over a wide bandwidth is designed by the proposed process and it is shown in Fig. 3.5. For the design of the NGD network the following filter specifications are used: A 4th order Butterworth band-stop filter of centre frequency 2GHz and pass bandwidth 0.7GHz with 1dB and 10dB of pass-band, stop-band attenuations respectively. The following two port network is used in transmission mode, for the transmission coefficient S-parameter (S21), port 1 is indicated as input port and port 2 is indicated as output port in the following Fig. 3.5 (b).

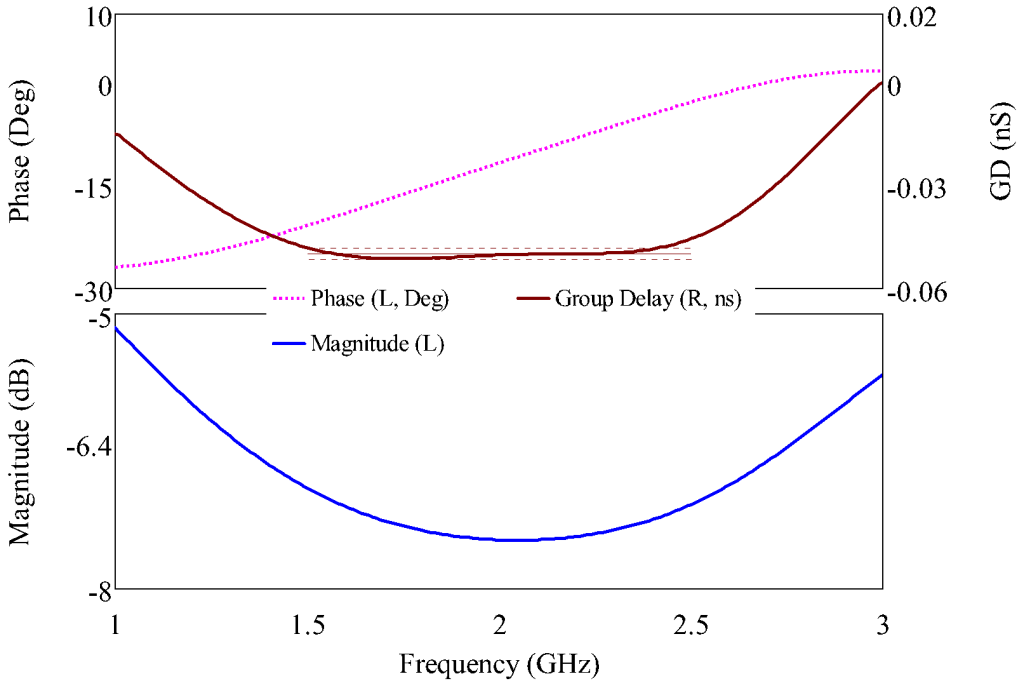

(a). NGD network transmission coefficient group delay, phase and magnitude curves.

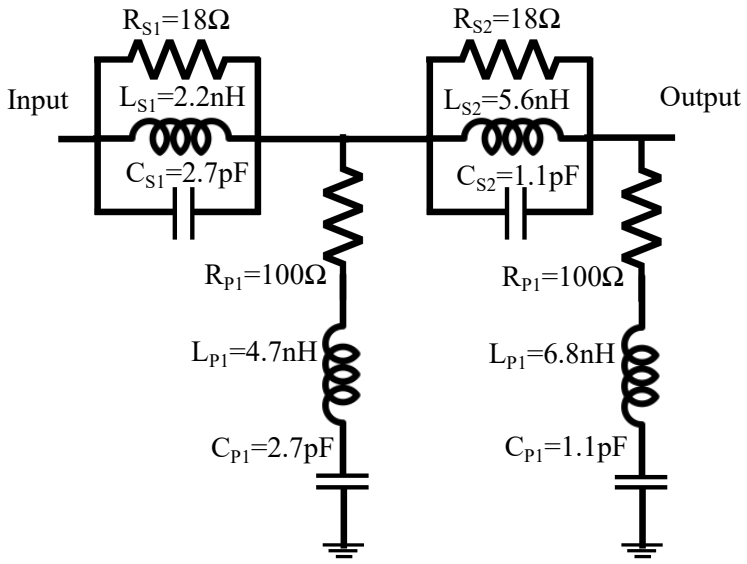

(b). NGD circuit.

Fig. 3.5 NGD network designed using fourth order Butterworth filter.

The series branch resistor 18 Ω and shunt branch resistor 100 Ω are obtained by the optimisation process. For optimisation a goal function is set to achieve -0.05 ns of group delay over 1.5 to 2.5 GHz. For both the resonators in series and in parallel resistor Rs and Rp are used

respectively. The Rs and Rp are variables in this optimisation process. In the AWR microwave office the "Discrete local search" optimiser is used with the following specifications: maximum iterations = 500; number grid levels = 1; allow increase (0-1) = 1; cost function is 1.802e-18 for initial resistor values of 1Ω. After optimisation, cost function is 1.577e-24. The design in Fig 3.5 is presented to demonstrate the simplicity of the proposed design approach in achieving the required characteristics for the NGD network with the help of filter design theory.

Different types of filters result in different NGD behaviour. Fig. 3.6(a) shows the phase response of a NGD network designed using different types of 4^{th} order filters. Bessel, Butterworth, Chebyshev 1, Chebyshev 2 and Elliptic filters are used. These filters differ in the flatness of transmission coefficient magnitude response and transition from pass band to stop band. The presence of ripples is another difference in character of these filters. A CST microwave studio filter synthesiser is used to design these 5 types of 4^{th} order filters. Following specifications are used: Frequency 2 GHz; Stop bandwidth 500 MHz; Stop band attenuation 10dB; Pass band attenuation 1dB. A 50 Ω resistor is added to each resonator of these circuits to introduce loss and to obtain the NGD behaviour. The transmission coefficient magnitude characteristics of the network vary with the type of filter used in the design as shown in Fig. 3.6(b). For the proposed applications in Chapters 4 and 5, the Butterworth filter type is used because of its linear phase response compared to other filter types. The maximum transmission loss, slope of the phase response and the bandwidth over which NGD could be achieved are determined by the filter order. With an increase in the filter order the transmission loss and complexity of the network increases. These high losses necessitate the use of a compensating amplifier. However, a low-loss NGD network can be used in some applications depending on the loss-tolerance. The type and order of the filter should be selected based on the bandwidth over which the positive phase response is needed and the acceptable transmission loss.

The variation in transmission coefficient phase and magnitude characteristics with the filter order is shown in Fig. 3.7. For the same filter specifications and resistor values the NGD network characteristics change considerably with the order.

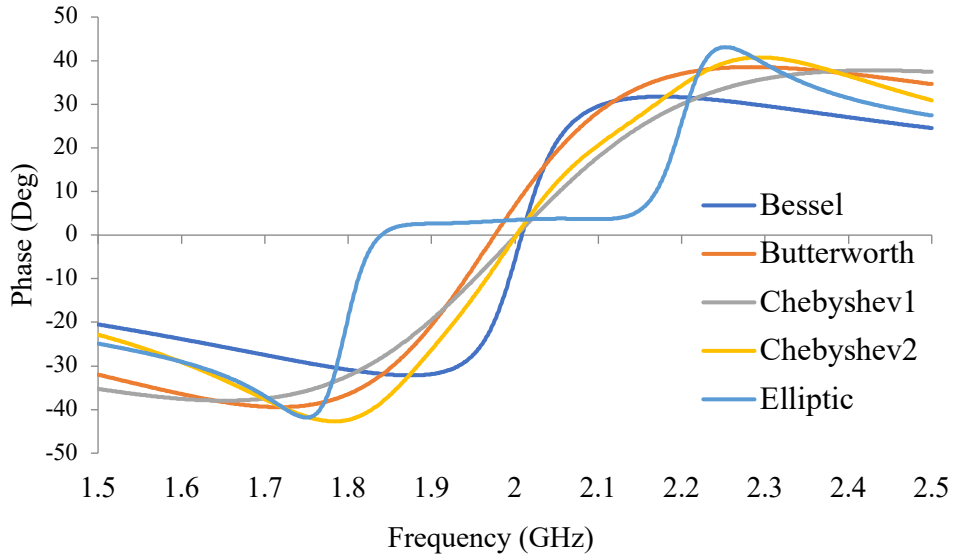

(a). Filters phase response with NGD behaviour

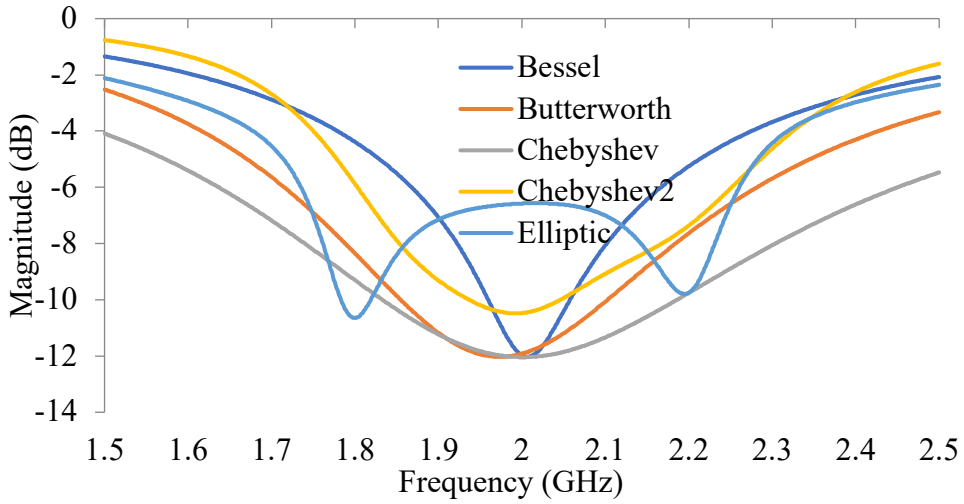

(b). Variation in the S21 Magnitude due to added resistors

Fig. 3.6 NGD network characteristics designed using 4th order filters with 0.2GHz bandwidth stop band and 10 dB stop band attenuation. In each shunt and series resonator branch of the filter a 50Ω resistor is added to form the NGD network.

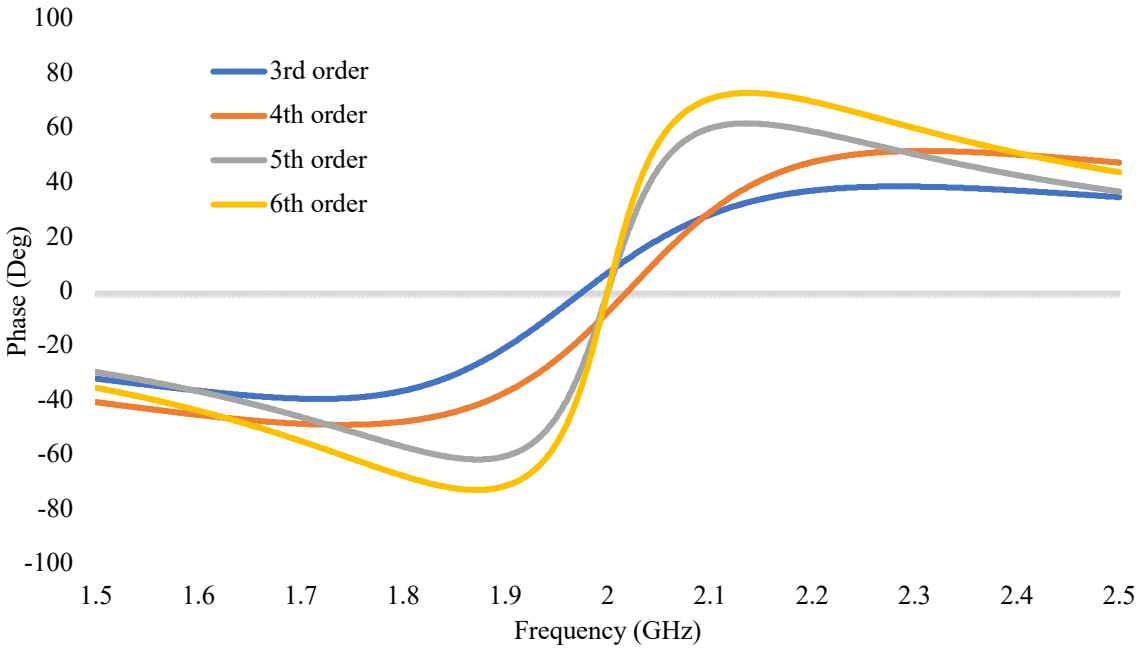

(a). Butterworth filter based NGD network phase response

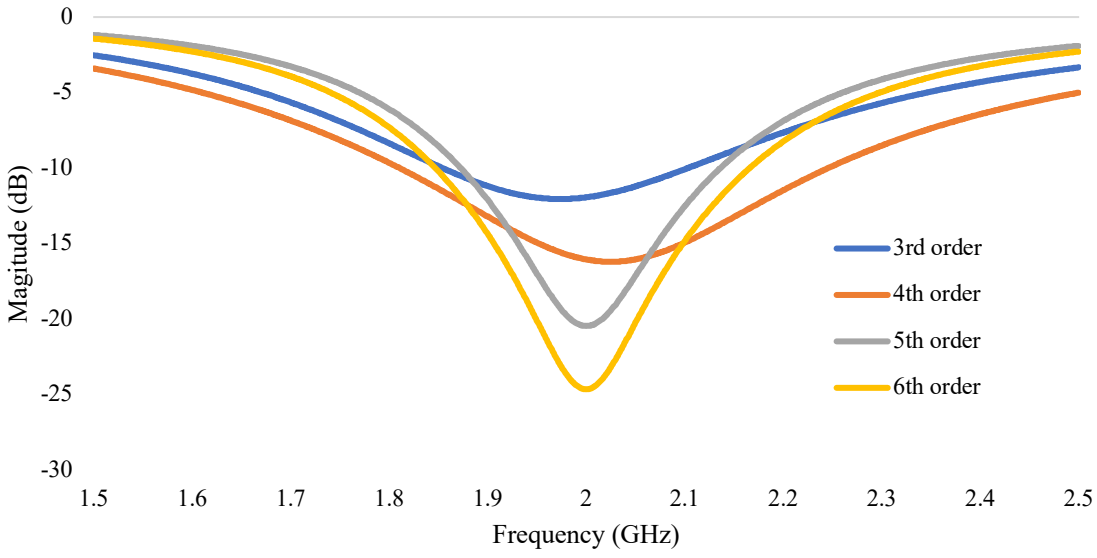

(b). Variation in S21 magnitude with the order of the filter

Fig. 3.7. NGD network transmission coefficient phase and magnitude responses with different filter orders.

With more resistors in the network in series (R_S) and parallel (R_P) branches there will be more design flexibility in terms of phase response slope and transmission coefficient magnitude. Fig. 3.8 shows change in phase and magnitude curves with decreasing R_S and increasing R_P. This is just one case study; other combinations of Rs and Rp are possible.

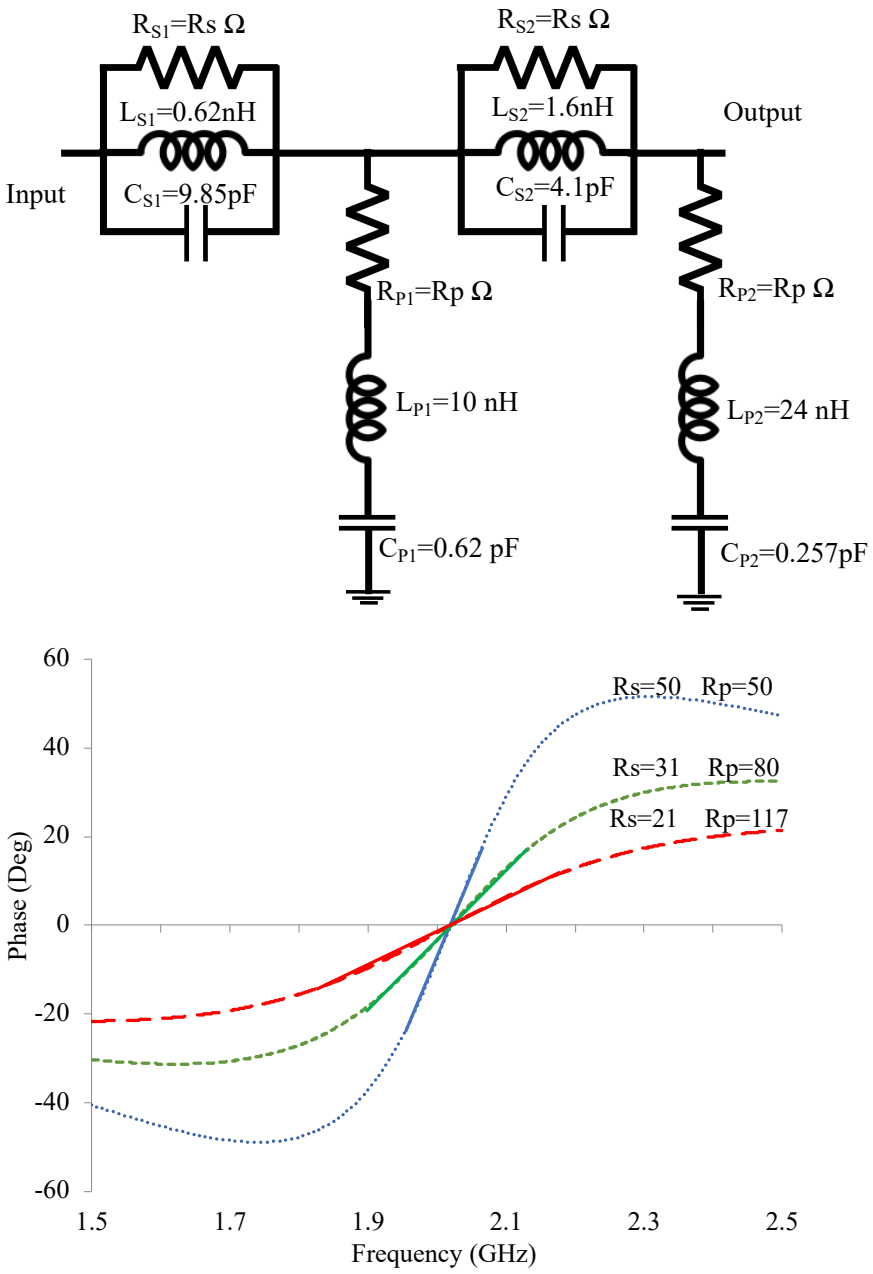

Fig. 3.8. Butterworth filter based NGD network: change in linear phase bandwidth with Rp and Rs. With more resistors in the network more design flexibility can be achieved.

The NGD network phase and transmission loss characteristics could be optimised using the resistors in the network. The lossy passive NGD networks can be used in signal cancellation. A loss compensated higher order network offers more design flexibility. Even achieving different slopes for phase response over different portions of the frequency bands within the operational bandwidth is possible with higher order networks. The huge variety of filter implementations gives the possibility of different NGD network implementations. In any particular implementation of the filter if loss can be added there is a possibility for achieving the NGD behaviour. This will be further discussed in Chapter 6 using frequency selective surfaces.

3.2 Filter Based NGD Network Experimental Results

A fifth order Butterworth band-stop filter is used to develop the NGD network prototype. In the filter design, in each branch a resistor is added in order to achieve NGD behaviour. By optimising these resistor values in the network, the NGD characteristics are controlled. The reactive effects of any network/structure/junction can be represented as a two port equivalent network with idealised elements. These elements can be related to actual components/dimensions through S and Z parameters [1, 4]. To establish the fact that the NGD network acts as a non-Foster network, the equivalent T-network (this is explained in detail in Chapter 4 section 2) is designed for the proposed NGD network and it is shown in Fig. 3.9. The ideal series inductor and shunt capacitor of the T-network (this gives same behaviour as the proposed network) can be determined using the following equations [4].

$$L = \frac{imag(Z_{11} - Z_{12})}{2\pi f} \tag{3.1}$$

$$C = \frac{1}{2\pi f * imag(Z_{12})} \tag{3.2}$$

Where f – frequency of operation

For obtaining the L and C values of the T-network for the prototype NGD network, reciprocity condition is enforced i.e., $Z_{11}=Z_{22}$, and $Z_{12}=Z_{21}$. The Z-parameters are obtained from the S-parameters of the proposed NGD network.

The NGD network is designed in AWR-MS using Modelithics library elements for RLC components. For the experimental prototype a Rogers RS5880 substrate of 1.57mm height is used. For the experimental prototype surface mount RLC components are used. The resistors of 0603 package and ±0.5% tolerance from KOA Speer Electronics [5], the inductors of 0402 package and ± 3% tolerance from Coilcroft [6] and the capacitors of 0402 package and ±0.05% tolerance from ATC [7] are used. 50Ω PCB SMA connectors are used for the input and output ports of the network. The ZVA-67 network analyser [8] is used to measure the scattering parameters of the fabricated prototype. The network is designed to operate in transmission mode as a NGD network. A positive slope for the transmission phase curve is observed in the simulation and measured results.

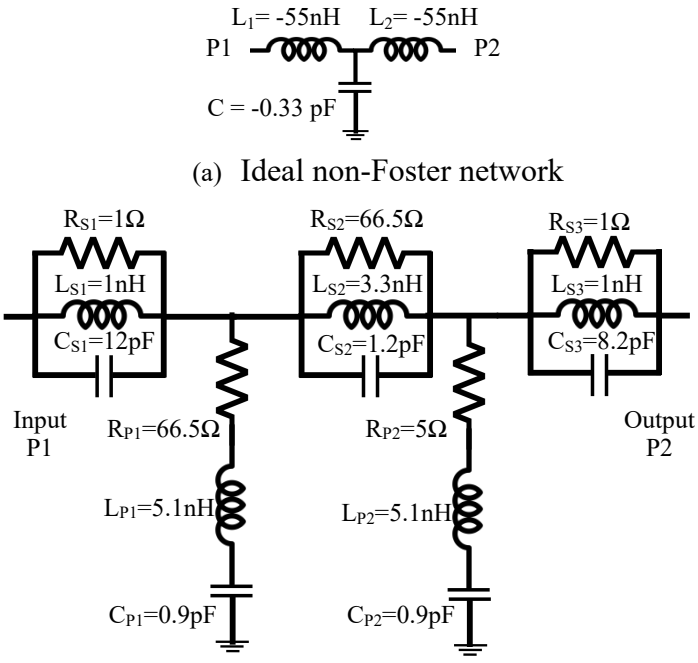

(a) Ideal non-Foster network

(b) Experimental network element values.

Fig. 3.9 Filter based NGD network prototype and its equivalent non-Foster circuit.

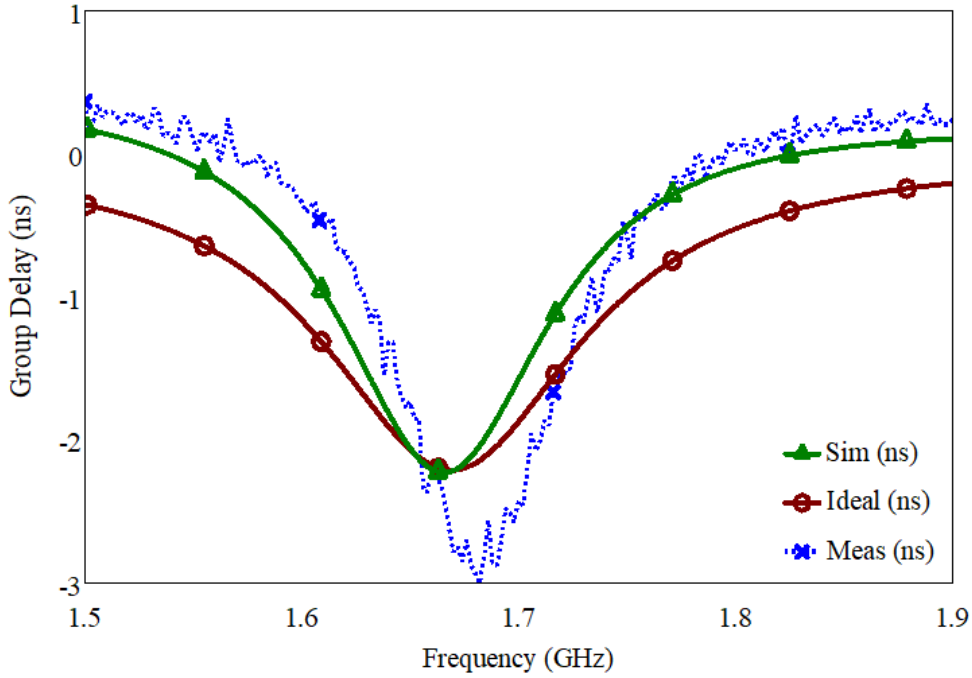

Fig. 3.10 Comparison of group delay of the NGD network and ideal non-Foster network.

The comparison of experimental and simulation NGD network transmission phase and magnitude characteristics are shown in Fig. 3.10 and Fig. 3.11. The NGD behaviour is well demonstrated both in the simulation and experimental models.

A slight difference is observed in the simulated and measured results. The tolerance of surface mount components used for the prototype and the soldering are contributing to these differences. Inaccuracies in modelling the parasitic capacitance and inductance effects introduced due to the PCB layout and SMA connectors is another factor leading to the mismatch in these results.

The ideal non-Foster equivalent network has zero transmission loss at 1.7GHz frequency, whereas the NGD network has around 20dB loss as shown in Fig. 3.11. Loss compensated NGD network transmission loss characteristics will be similar to that of the ideal equivalent network. Using an amplifier to compensate the NGD network loss will make the transmission magnitude characteristics of both circuits similar.

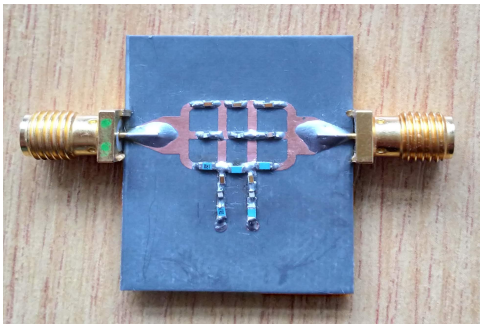

(a) Fabricated prototype of NGD network

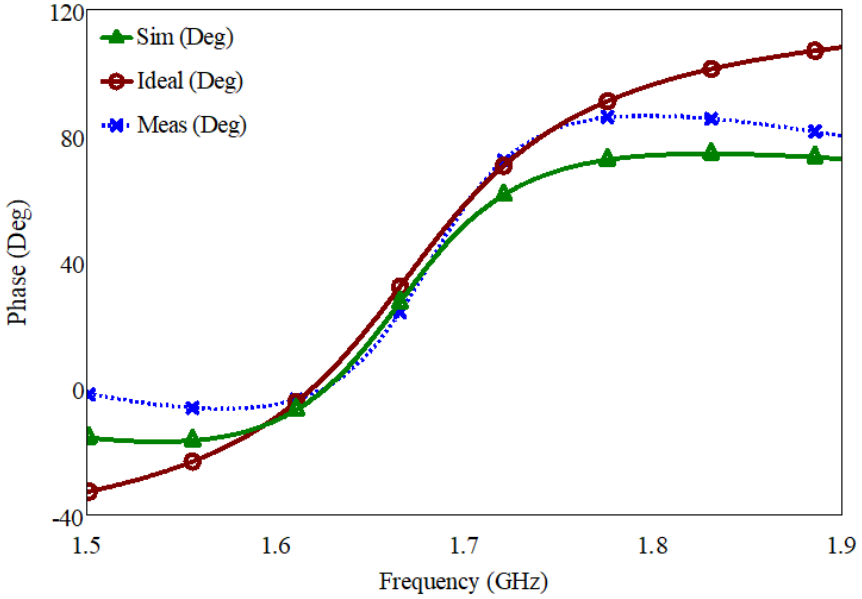

(b) The NGD network phase response comparison

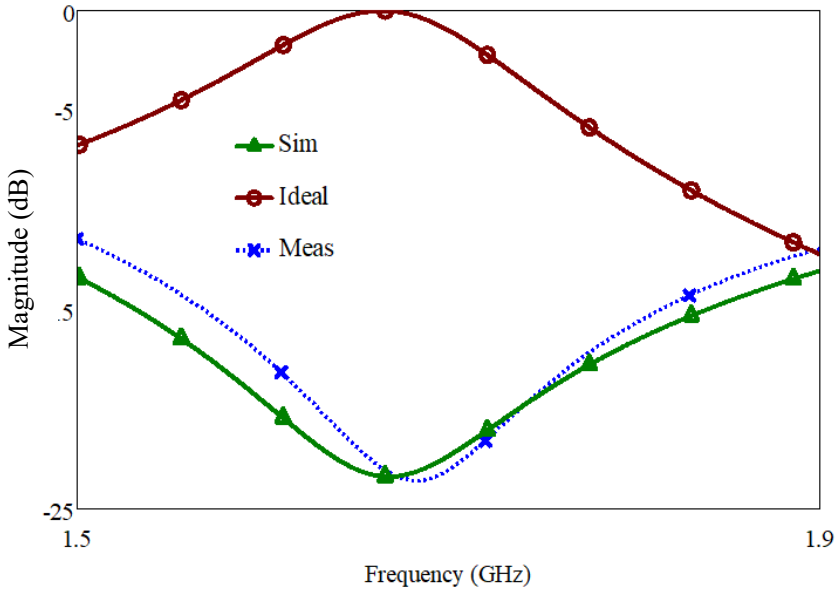

(c) The NGD network transmission coefficient magnitude characteristics

Fig. 3.11 Filter based NGD network prototype characteristics

3.3 NGD Network Implementation Using MMIC Technology

To demonstrate that the proposed concept can be developed for highly integrated applications, the NGD network is also designed in MMIC technology as shown in Fig. 3.12. The design is simulated using AWR Project Development Kit(PDK). This is an example PDK and helps to run the MMIC simulation using AWR Design Environment without the need of any specific foundry.

For both the designs shown in Fig. 3.12 and 3.15 a circular microstrip inductor with strip bridge is used in the simulation. The specifications of this inductor are given: conductor width is 10μm, conductor spacing length is 5μm, angle of bridge departure is 0^0, width of bridge strip conductor is 10μm, height of bridge dielectric is 2μm, length of bridge extension beyond inductor is 0, relative dielectric constant (permittivity) of the substrate layer between two metal layers that are forming a bridge is 1, loss tangent of bridge metal is 0, thickness of bridge strip is 1μm, bridge metal bulk resistivity (normalised to gold) is 1 Ω, number of turns (NT) and inside radius of innermost turn (R). The values of NT and R are given in the respective circuit diagrams.

A thin film capacitor is used and the conducting plate widths are adjusted to get the required values as shown in Fig. 3.12. For the tunable MMIC NGD network design a Varactor diode is used as a capacitor as shown in Fig. 3.15.

A thin film resistor is used for the design in Fig. 3.12. A MOSFET is used for the tunable NGD design as shown in Fig. 3.15, the width (W) and the number of fingers (NG) are varied to get the required resistance value.

The circuit in Fig. 3.12(a) and the model in (b) have different element values. The ideal elements in the AWR MS software are used for the lumped element implementation. In both the implementations inductors and capacitors are achieved to resonate at 1.7 GHz frequency. The substrate details and the parasitic effects are not included in the lumped element network. By

using the parameter sweep the elements of the lumped network are optimised to match the results of the MMIC implementation as shown in Fig. 3.13.

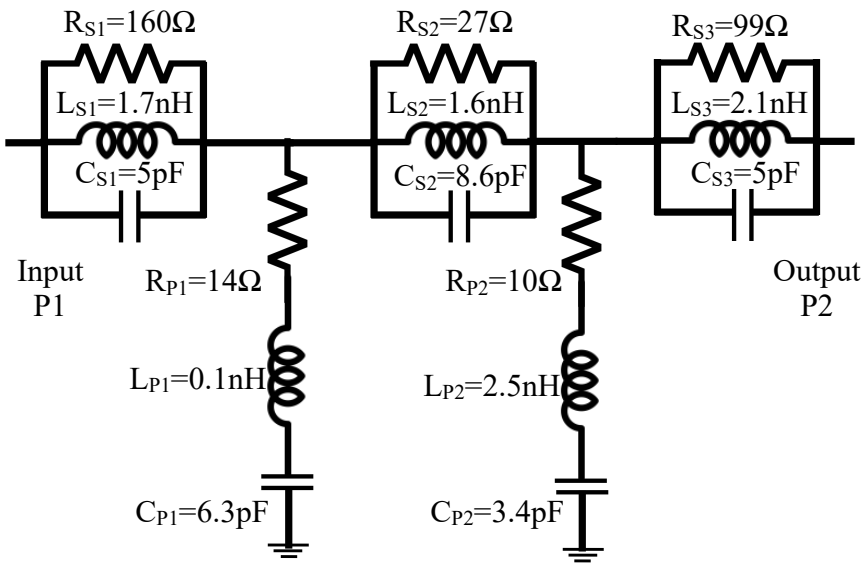

(a). NGD network using ideal lumped elements.

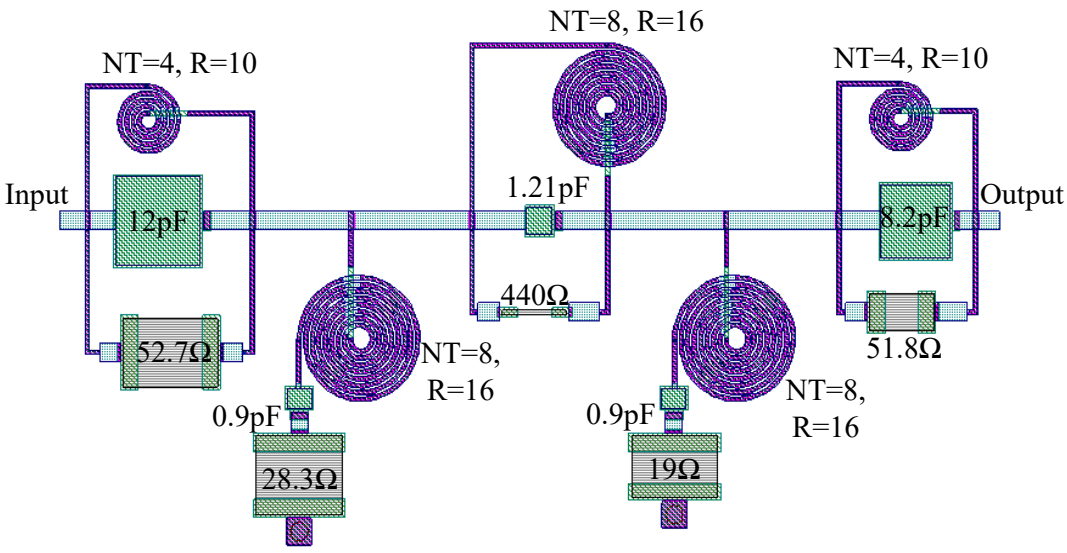

(b). NGD network implemented using MMIC technology.

Fig. 3.12 The NGD network implemented in MMIC technology

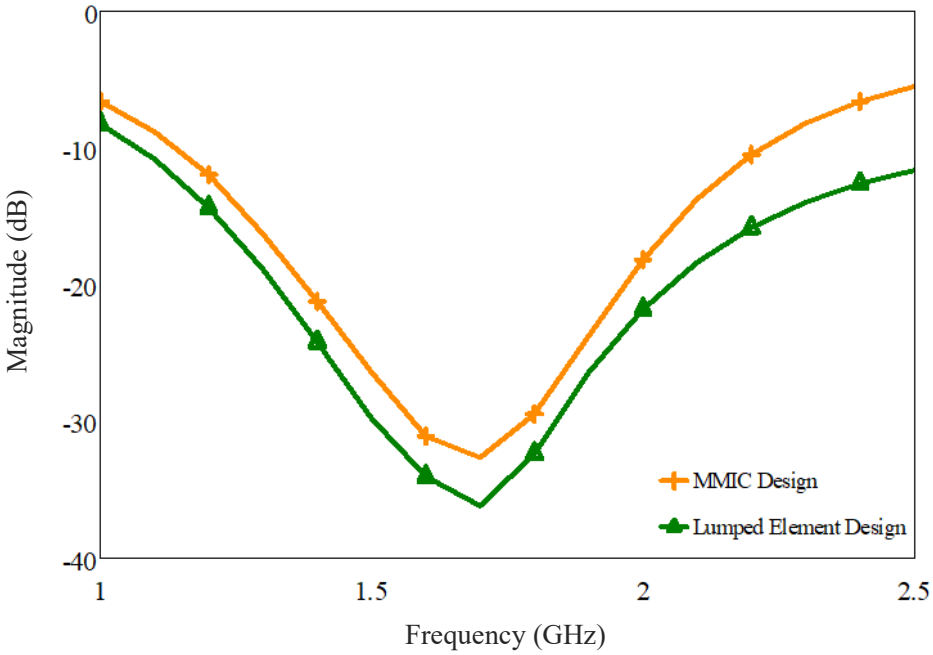

(a). Transmission loss curves of NGD network

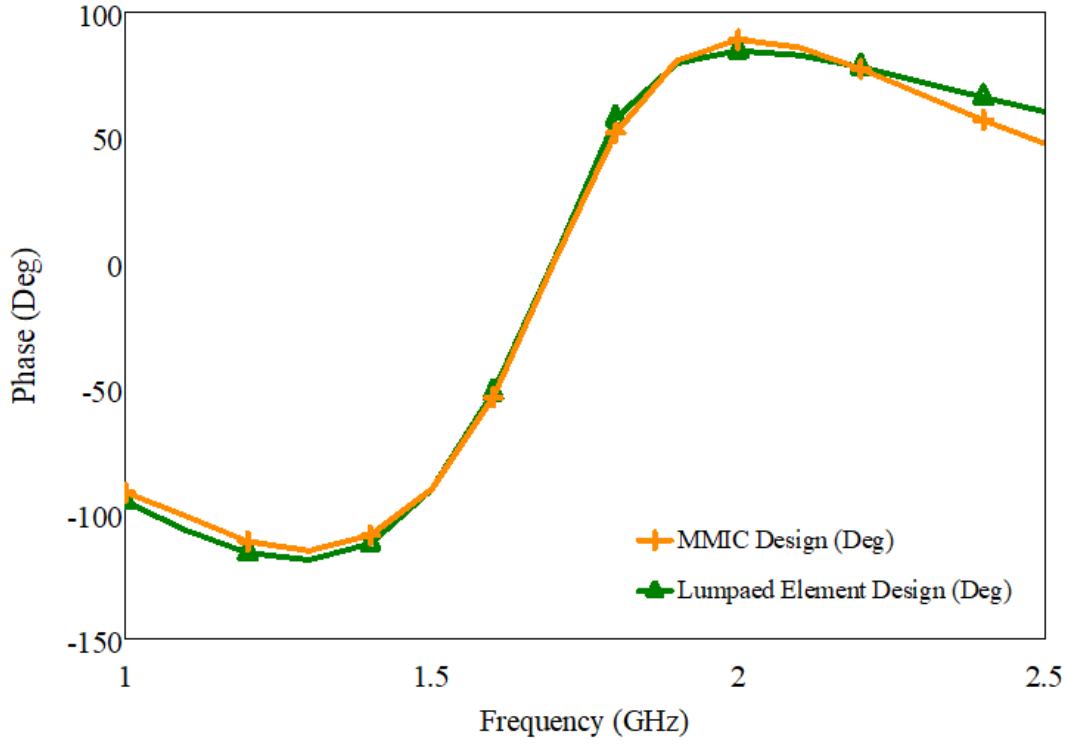

(b). Phase response of NGD network

Fig. 3.13 Comparison of NGD network characteristics in lumped element and MMIC implementations.

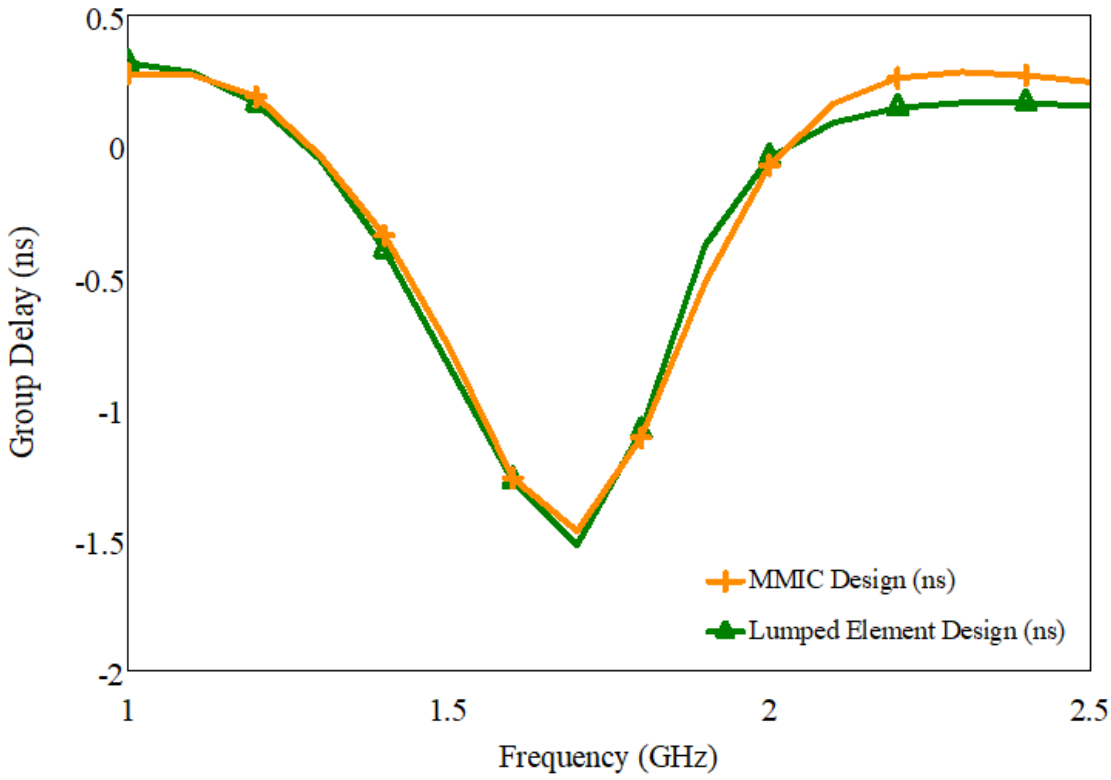

Fig. 3.14 Comparison of MMIC NGD network group delay characteristics with equivalent lumped element implementation.

The NGD network characteristics are shown in Fig. 3.13 and 3.14. This possibility of NGD network implementation in MMIC technology helps in designing networks for low profile applications.

3.4 Tunable NGD Network Implementation in MMIC Technology

The tunability of the NGD network is also verified by replacing the capacitor and resistor with a Varactor diode and a MOSFET respectively in the series branches of the network. Fig. 3.15 shows the MMIC design and corresponding lumped element network for one set of Varactor and MOSFET bias voltages. The group delay response of these two networks is shown in Fig. 3.16. The bias voltages of the series Varactor diode and the series MOSFET are varied in order to observe the tuning of the NGD behaviour. For Varactor diode and MOSFET, data models are used with bias voltages and corresponds capacitance and resistance values respectively.

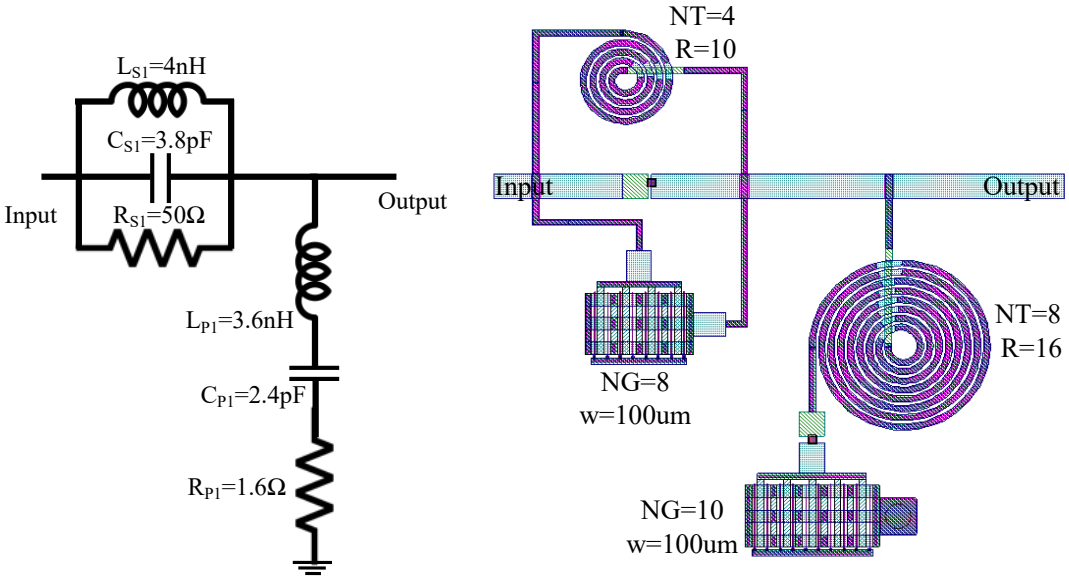

(a). Lumped element network (b) NGD network in MMIC implementation.

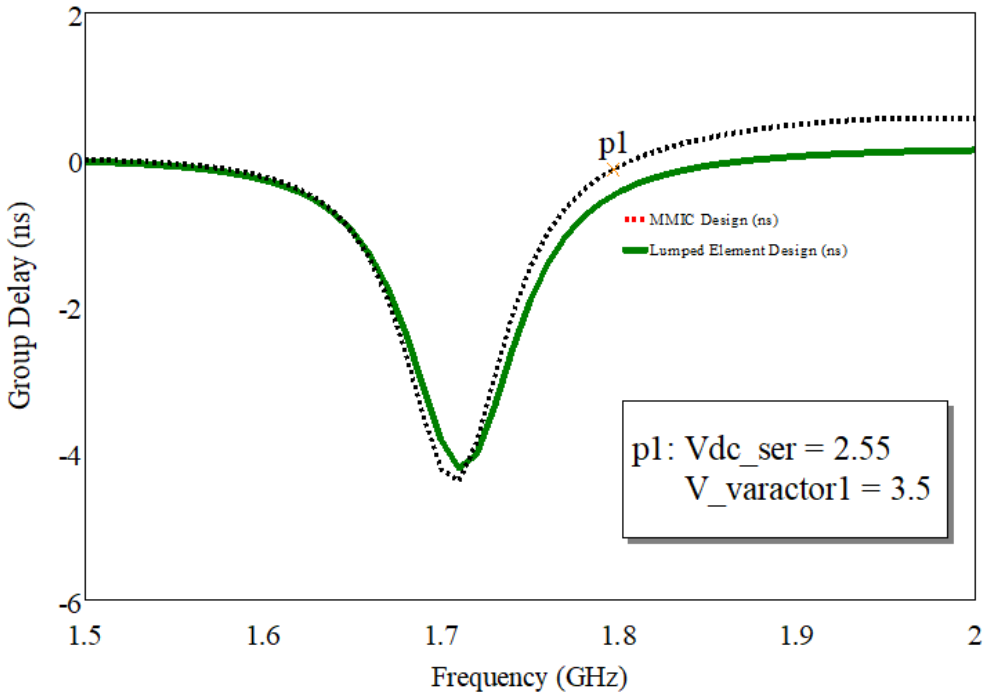

(c). Comparison of group delay characteristics in two implementations.

Fig. 3.15 Tunable NGD network implementation in MMIC technology

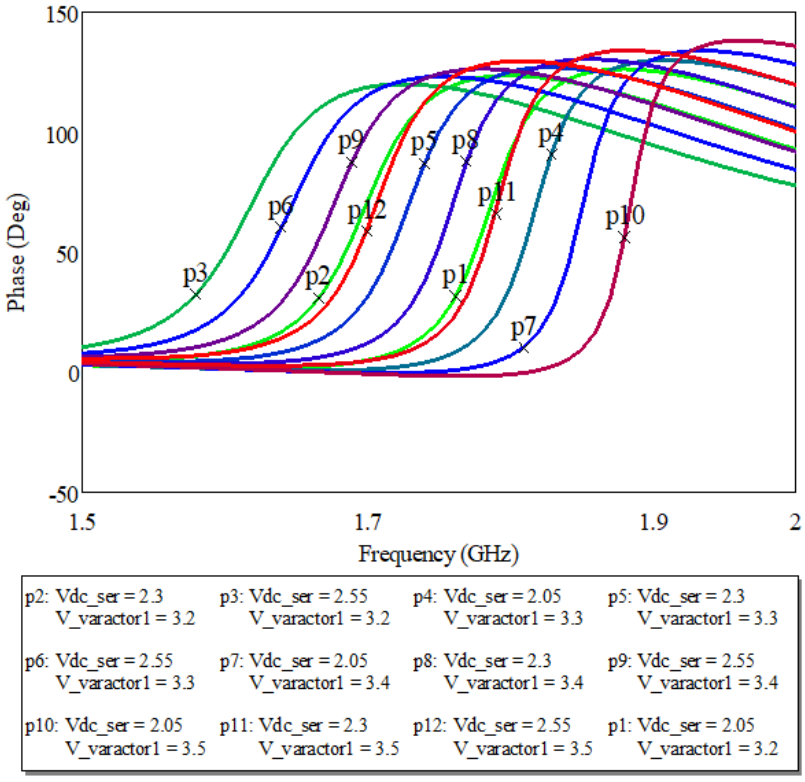

(a) The phase characteristics over tuning range

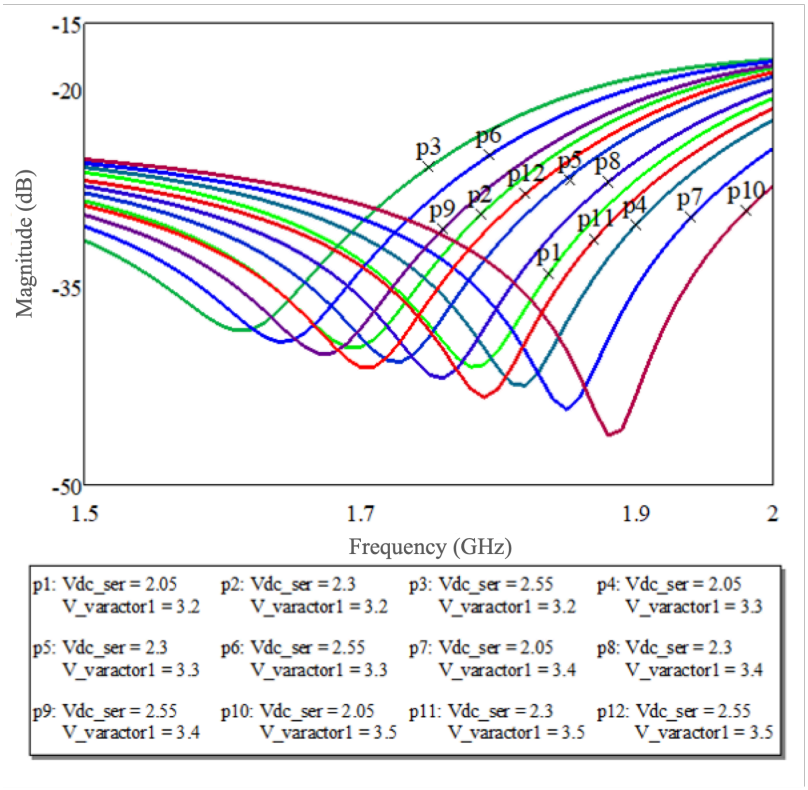

(b) The magnitude characteristics over the tuning range

Fig. 3.16 Tunable NGD network transmission coefficient phase and magnitude responses

The variation of the MOSFET bias voltage results in the variation of the resistance and the variation of the Varactor diode potential results in the variation of the capacitance. Fig. 3.16 and 3.17 show the tuning of the NGD network transmission coefficient phase, magnitude and group delay responses.

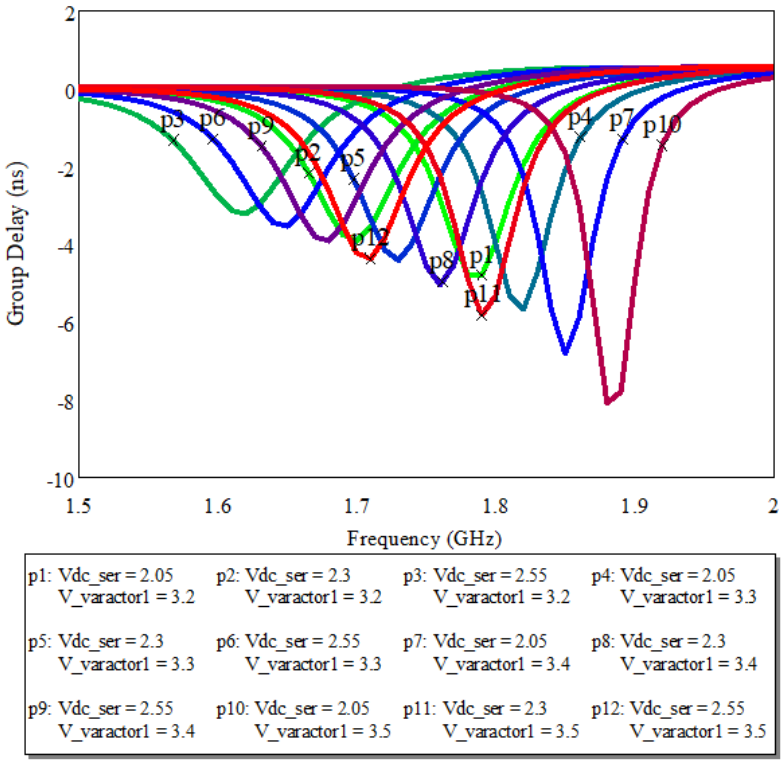

Fig. 3.17 Tunable group delay characteristics of the MMIC NGD network

List of References

[1] H. Mirzaei and G. V. Eleftheriades, "Realizing Non-Foster Reactive Elements Using Negative-Group-Delay Networks," IEEE Transactions on Microwave Theory and Techniques, vol. 61, no. 12, pp. 4322-4332, 2013.

[2] T. Thatapudi, P. Gardner, and A. Feresidis, "Engineered group delay transmission lines based on novel negative group delay networks," in Loughborough Antennas & Propagation Conference (LAPC 2017), 13-14 Nov. 2017 2017, pp. 1-2.

[3] G. Chaudhary, Y. Jeong, and J. Lim, "Microstrip Line Negative Group Delay Filters for Microwave Circuits," IEEE Transactions on Microwave Theory and Techniques, vol. 62, no. 2, pp. 234-243, 2014.

[4] D. M. Pozar, "Microwave and RF Design of Wireless System," John Wiley & Sons, INC, New York, 2001.

[5] https://www.digikey.co.uk/en/product-highlight/k/koa/rs73-thick-film-resistor-d.

[6] https://www.coilcraft.com/en-us/products/rf/ceramic-core-chip-inductors/0402-(1005)/0402hp/.

[7] https://www.digikey.co.uk/products/en/capacitors/ceramic-capacitors/60?k=atc&k=&pkeyword=atc&sv=0&pv16=39158&sf=1&FV=-8%7C60&quantity=&ColumnSort=0&page=1&pageSize=25.

[8] https://www.rohde-schwarz.com/ph/product/zva-productstartpage_63493-9660.html.

Chapter 4 Electrically Small Antenna Using Negative Group Delay Network

An antenna is a necessary element in wireless communication system. Most often in conventional design methods, an antenna resonates at the frequency where the physical length is equal to a quarter of the operating wavelength. Designing an antenna for low profile applications, such as mobile phones, handheld devices and radar systems is always challenging. An electrically small antenna (ESA) is ideal for applications where a small footprint is needed. The ESA is defined as an antenna operating at λ wavelength with its length smaller than $\lambda/2\pi$. The performance parameters of the ESA degrade with reductions in the physical dimension. The design challenges and performance trade-offs of the ESAs are discussed by Wheeler [1] and Chu [2]. Most of the electrically small antennas suffer from high quality factor due to their small input impedance and high reactive part. Achieving a high gain-bandwidth product and improvement of efficiency are always challenging in the case of an ESA.

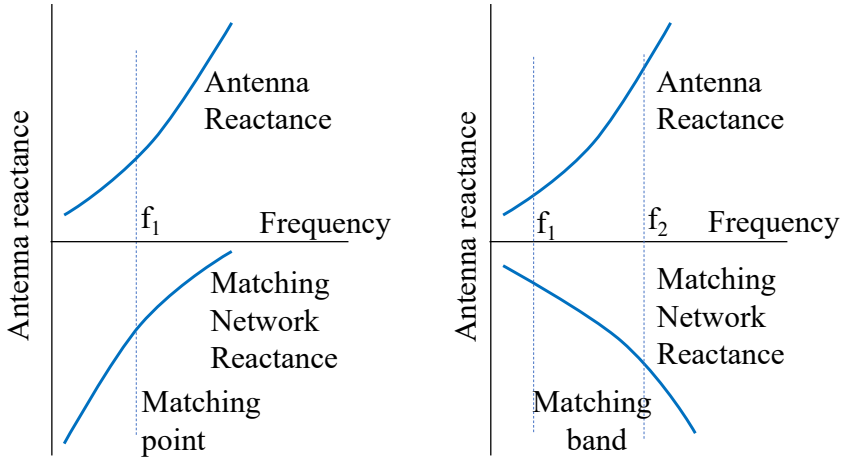

(a) Passive LC based matching (b) Negative element based matching

Fig. 4.1 Comparison of antenna matching in different approaches.

In designing the ESA the principle objective is to achieve resonance at frequencies far lower than the resonance frequencies associated with the physical length of the antenna, while maintaining efficiency. In conventional matching methods either an inductor is used to compensate capacitive reactance, or a capacitor is used to compensate the inductive part of impedance, at a single frequency as shown in Fig. 4.1(a). A non-Foster element which exhibits NGD behaviour and acts as a negative reactive element. Using an ideal negative reactive element, matching can be achieved over a wide bandwidth by counteracting the reactive part of an antenna's impedance. By using the NGD network, which will act as a negative reactance over a wide bandwidth, the ESA can be designed by achieving impedance matching at the desired frequency as shown in Fig. 4.1(b).

4.1. NGD Network Based Electrically Small Antennas

A wideband ESA designed using a NGD-based impedance matching network is presented. Using the NGD network the impedance characteristics of a radiating element can be altered. With the optimisable elements of the NGD network, impedance matching can be achieved at the required frequencies.

The characteristics of NGD networks can be better understood when they are designed using filter theory. The detailed analysis and design of NGD networks using filter theory is presented in chapter 3. Some of the observations are useful to reproduce here. The phase and transmission loss characteristics of the NGD circuit are functions of resistor values in the network and the order of the filter. The inevitable transmission loss of these networks needs to be compensated. In order to benefit from the higher order networks, amplifiers should be used to compensate the higher losses. Optimal circuit design and the right type of amplifier are needed, to avoid feedback instability.

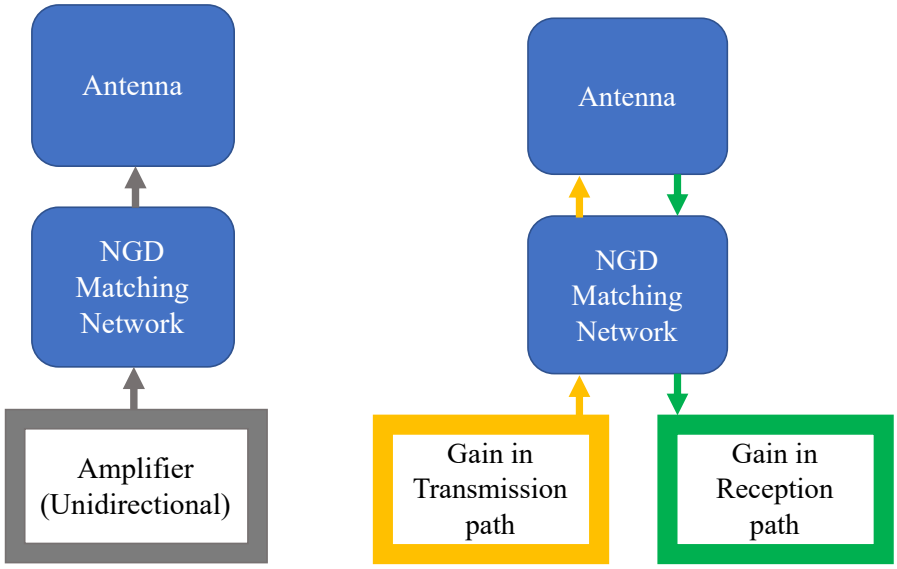

(a) One way communication (b) Duplex communication

Fig. 4.2 Compensation of NGD matching network loss in two different possibilities

Using a uni-directional amplifier to compensate the matching NGD network losses will limit the use of the antenna to only one mode, either for transmission or for reception as shown in Fig.4.2(a). Bi-directional amplifiers can be used, but they are at high risk of instability.

In this work an ESA is connected to an active circulator. The circulator is designed with sufficient gains in transmission and reception paths to compensate the loss of the NGD matching network as shown in Fig. 4.2 (b). Further design details and analysis are presented in chapter 5.

A monopole antenna is matched using the NGD network to design an ESA and the prototype is fabricated to experimentally verify the concept. The design details of the electrically small monopole using the NGD matching network are presented in the next section. The NGD network is also used as a matching circuit for a patch antenna and for a wire dipole antenna to validate the suitability of the proposed concept for different types of antennas.

4.2. Design of an Electrically Small Antenna

An ESA is designed using a printed monopole in the first case study. Other types of antenna are also used in the next case studies, to justify the scope of the NGD network as a matching network in order to design the wideband ESA.

Case #1 Electrically Small Antenna: Monopole

A printed monopole 43mm in length is used as a radiator. The aim is to design an electrically small monopole at 1.08GHz where the length of the monopole is $0.98\lambda/2\pi$. Fig. 4.3 shows the prototype and the return loss characteristics of the electrically small monopole [3].

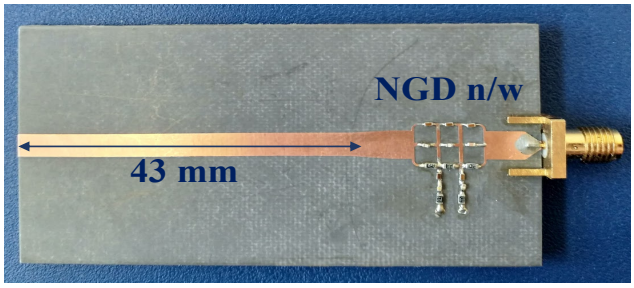

(a) Electrically small monopole prototype.

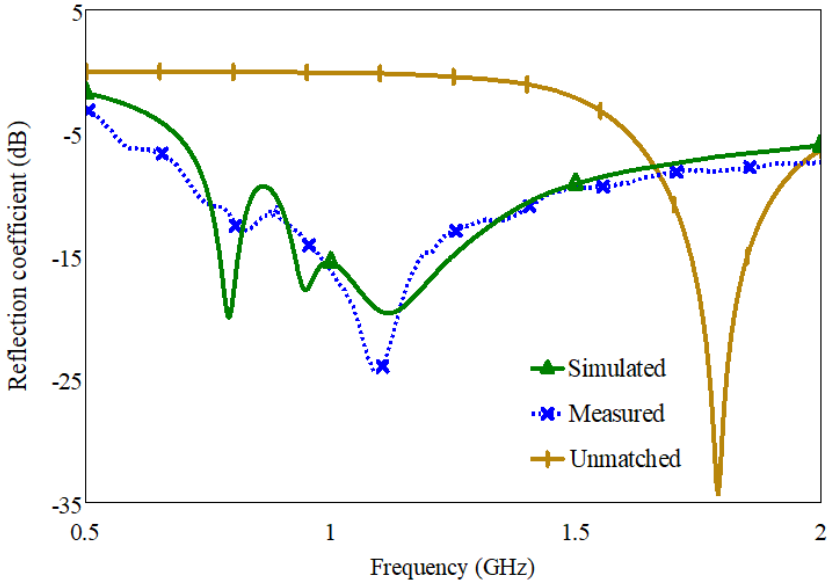

(b) Reflection coefficient characteristics of an electrically small monopole

Fig. 4.3 NGD network based electrically small monopole antenna. Unmatched monopole reflection coefficient (simulated result) is also presented for comparison purpose.

A transmission mode NGD network is used for impedance matching of this electrically small monopole. As explained in chapter 3, the design of a NGD network starts with the selection of a band-stop filter with the right order, with added resistors in each section of the network. The phase and transmission characteristics of the NGD network can be optimised using the resistors. A lumped element implementation is used in this design, the values of inductors and capacitors of the network are determined based on the resonance frequency. The optimisation process is used to determine the resistor values to achieve the impedance matching for the monopole at the desired frequency. A 5th order Butterworth filter is used for designing the NGD based matching network with the topology shown in Fig. 4.4.

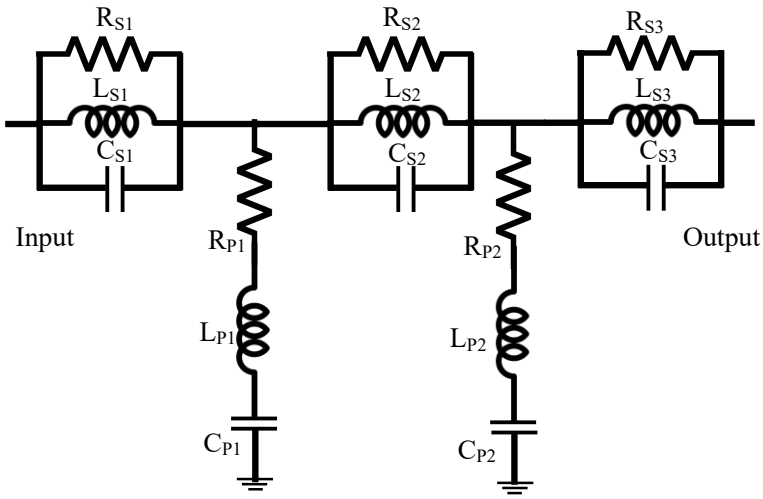

Fig. 4.4 The lumped element topology of the proposed matching NGD network

The following are the network RLC element values: (resistance in Ω, inductance in nH, capacitance in pF) R_{S1}=5.9, L_{S1}=1, C_{S1}=12, R_{S2}=143, L_{S2}=3.3, C_{S2}=1.2, R_{S3}=5.1, L_{S3}=1, C_{S3}=8.2, R_{P1}=1K, L_{P1}=5.1, C_{P1}=0.9, R_{P2}=82.3, L_{P2}=5.1 and C_{P2}=0.9. For fabrication of the experimental prototype a Rogers RT5880 substrate of a dielectric constant (ε_r) 2.2 and a height of 1.57mm is used. The equivalent non-Foster ideal network and its reactive elements are shown in Fig. 4.5(a). The behaviour of the network resembles that of the proposed NGD network. The series inductor and shunt capacitor are obtained using Z-parameters of proposed NGD network.

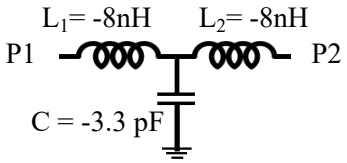

(a) The equivalent non-Foster ideal network

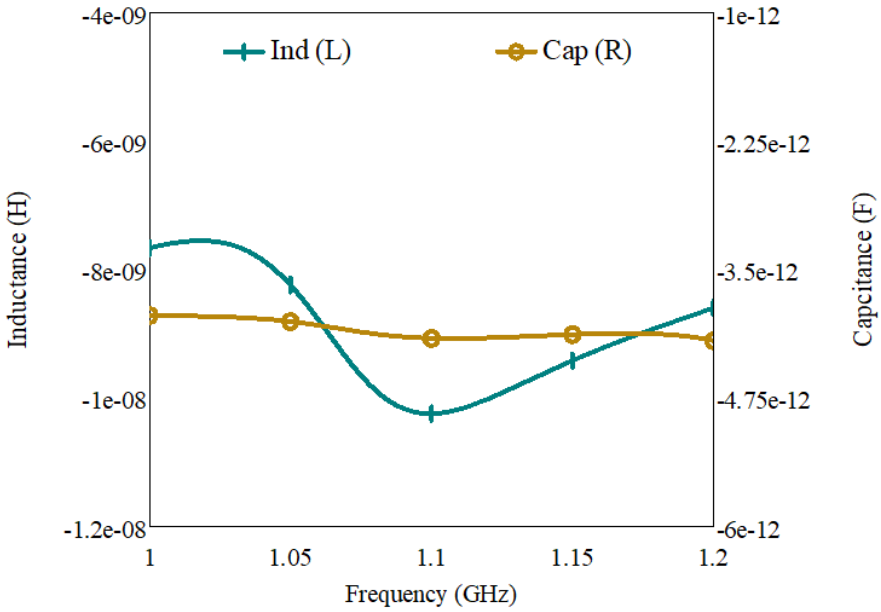

(b) The capacitance and inductance curves of the ideal non-Foster network.

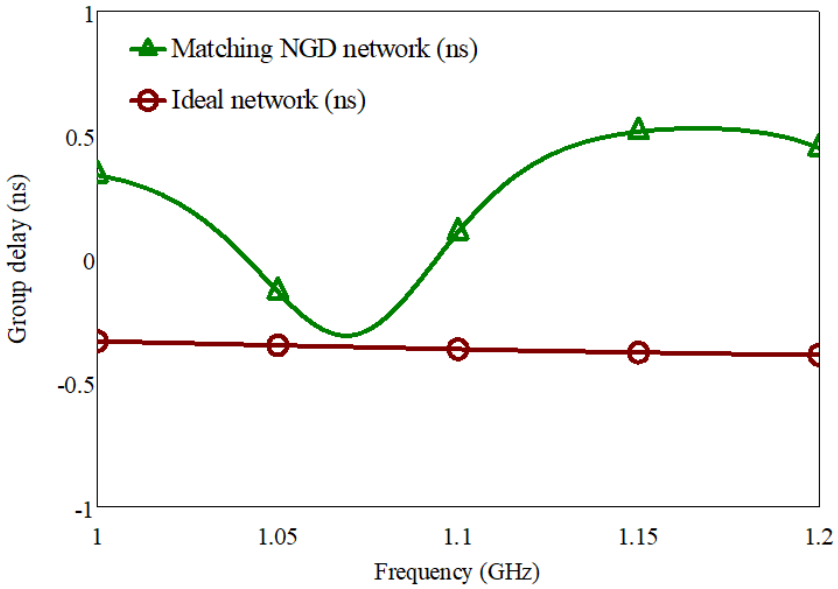

(c). Group delay characteristics of the proposed and ideal non-Foster networks

Fig. 4.5 The equivalent ideal non-Foster network elements and comparison of its group delay characteristics with those of the NGD network.

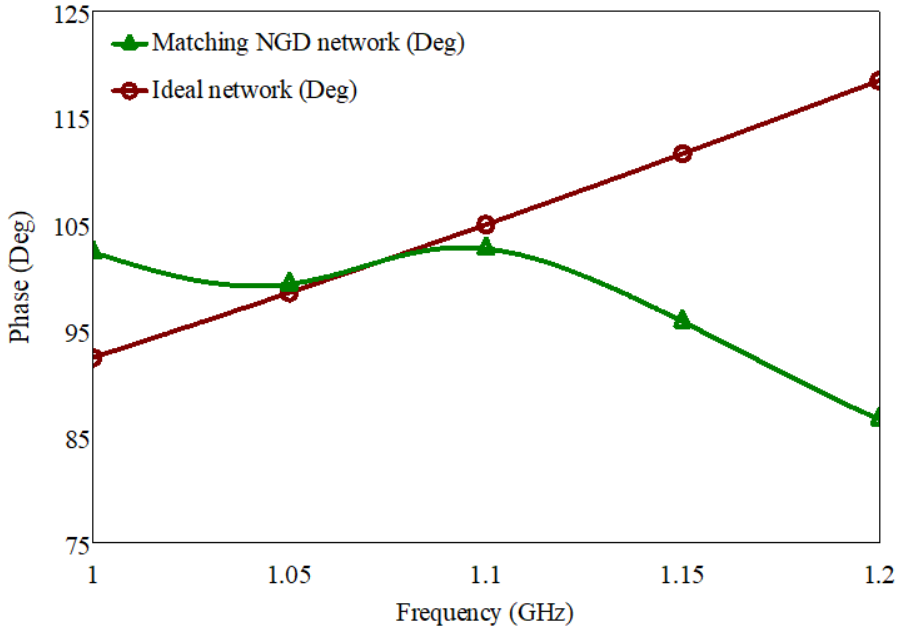

(a) Phase characteristics of the matching NGD network

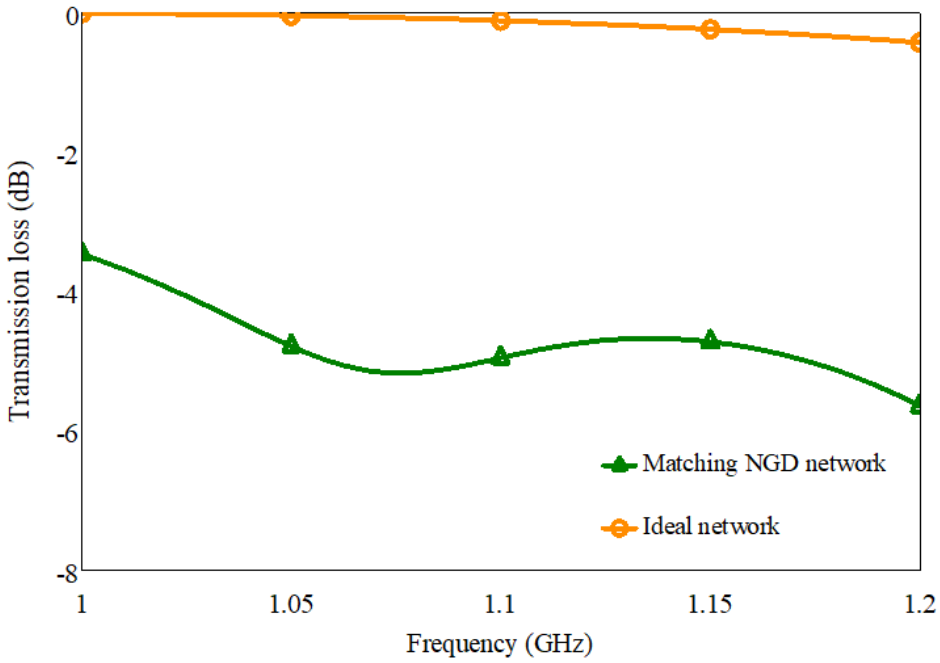

(b) Transmission loss characteristics of the NGD network

Fig. 4.6 Comparison of characteristics of the proposed NGD matching network with the ideal equivalent network.

The transmission mode inductive and capactitive reactance curves of the ideal non-Foster equivalent network is shown in Fig.4.5(b). These curves are obtained using the inductor and

capacitor equations presented in Chapter 3, Equ. 3.1 and 3.2. The ideal non-Foster network with negative capacitance and negative inductance will act as a negative reactive element and compensate the reactance of the antenna to achieve impedance matching over a range of frequencies. In the same manner the negative reactive behaviour of the proposed NGD network contributed towards the matching of the monopole at 1.08GHz centre frequency. Fig. 4.6 shows the phase and magnitude responses of the transmission coefficient for the proposed NGD network and the ideal non-Foster network. A loss compensated NGD network will have a magnitude response similar to the ideal non-Foster network. The radiation patterns of the ESA at 1.08GHz are shown in Fig. 4.7. The E-plane pattern demonstrated a omnidirectional radiation performance of the ESA. If a loss compensated NGD matching network had been used, the efficiency of this prototype antenna would have been better. Due to the presence of NGD network loss this antenna efficiency can be very low. However, the prototype clearly demonstrated the concept of antenna impedance matching using a NGD network. These losses can be compensated by using an amplifier, but this will limit the use of the antenna to either transmission or reception mode. In chapter 5, an ESA design using NGD network suitable for duplex operation is presented. The matching NGD network loss is compensated by using an active circulator.

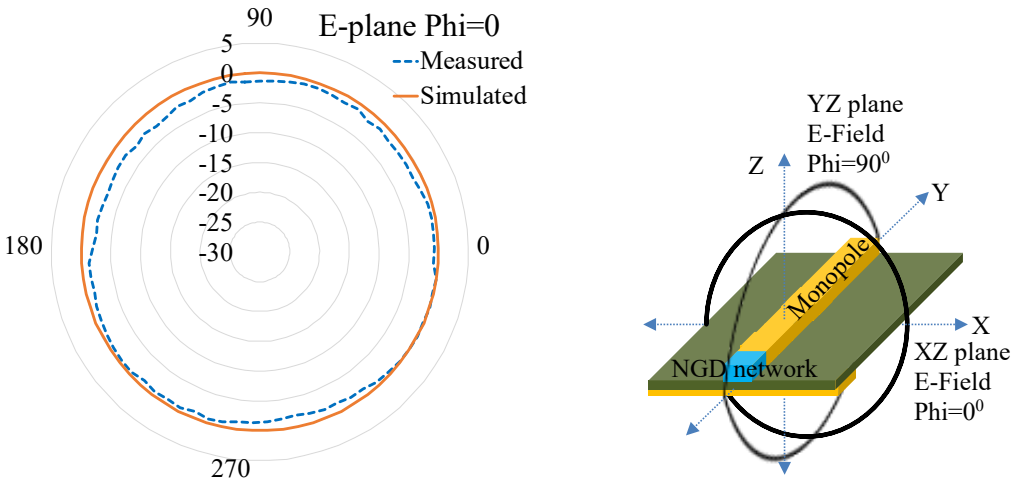

Fig. 4.7 ESA radiation patterns in E field patterns at 1.08GHz.

Case #2 Electrically Small Antenna: Dipole, Patch

A dipole and a patch are also used to investigate the benefits of the NGD network as a matching circuit. The RLC values of the NGD network and the corresponding ESA dimensions are given below. The inductor and capacitor values of the NGD network can be obtained by using filter design by insertion loss method. A filter synthesiser will generate LC values for a given resonance frequency, stop bandwidth and stop-band attenuation values. By using a parameter sweep, resistor values are obtained for the NGD network. The reflection coefficient of the patch antenna attached with NGD impedance matching network is the goal function. For these networks the topology is same as that shown in Fig. 4.4. The electrically small dipole operating at 0.7GHz is only of length $0.95\lambda/2\pi$. A perfect electric conductor is used to design a thin wire dipole of length 74 mm in CST microwave studio. The dipole's S-parameter touchstone file is imported into AWR microwave office. The lumped element NGD network is used as a matching network to feed this dipole. As shown in Fig. 4.8 (blue curve) the dipole is impedance matched at 0.7 GHz. The NGD network has the following element values: (with units Frequency ~ GHz, R ~ Ω, L ~ nH, C ~ pF) R_{S1}=100, L_{S1}=1.6, C_{S1}=30, R_{S2}=50, L_{S2}=6.6, C_{S2}=2.4, R_{S3}=14, L_{S3}=1.4, C_{S3}=10, R_{P1}=1, L_{P1}=3.3, C_{P1}=1.8, R_{P2}=21, L_{P2}=0.5 and C_{P2}=1.8. The

electrically small patch operating at 0.7 GHz has a 40X55 mm^2 footprint. This patch is simulated in AWR EM environment using AXIEM simulator. The patch is designed on a 1.53 mm thick substrate with a dielectric constant of 3.3. A copper patch of 0.035mm thickness on this substrate is simulated in EM environment. In the AWR software this EM structure is embedded as a subsystem into the circuit simulator. The lumped element NGD network is used as a feeding network to impedance match the patch at 0.7 GHz as shown in Fig. 4.8 (red curve). The NGD network elements are R_{S1}=178, L_{S1}=1.5, C_{S1}=38.5, R_{S2}=21, L_{S2}=4, C_{S2}=0.7, R_{S3}=15, L_{S3}=0.9, C_{S3}=11.5, R_{P1}=1, L_{P1}=10.2, C_{P1}=1.8, R_{P2}=1, L_{P2}=8.7 and C_{P2}=1.8.

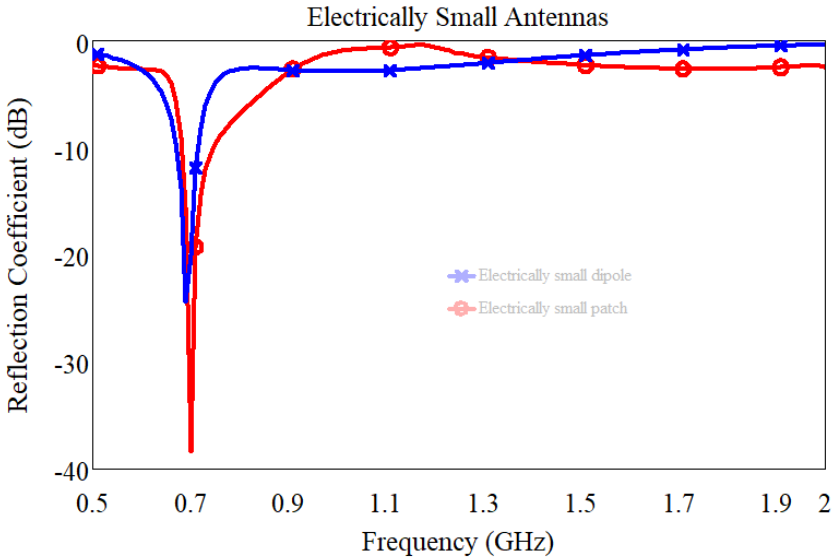

Fig. 4.8 Reflection coefficient of electrically small dipole and patch designed using NGD based impedance matching.

4.3. Analysis of NGD Network Based Matching

Case #1 Wide Bandwidth Matching

The NGD network is used to achieve wide bandwidth matching for a printed monopole. The return loss is more than 10dB over 1.5 to 2.5 GHz bandwidth, as shown in Fig. 4.9. A dual resonance is observed due to the use of a higher order filter for designing NGD matching network. The combination of multiple resonators in a higher order filter based NGD design has created a second resonance. The unmatched monopole has only 4% of bandwidth with return loss less than 20dB at 2GHz. To verify that the NGD network is not just a lossy element like an attenuator, the monopole is fed through a 2.45dB (this is same as the NGD network loss) attenuator. The NGD network matched monopole return loss characteristics are different to those of the attenuator matched. It is evident that the NGD network is not just a lossy element but is able to impedance match the antenna at the required frequency band; whereas the attenuator caused more signal loss instead of impedance matching the antenna. The loss compensated NGD network offers the best antenna matching benefits. The return loss and impedance characteristics are presented in the following Fig.4.9. The NGD network and the RLC elements are as follows: (resistance in Ω, inductance in nH, capacitance in pF) R_{S1}=13, L_{S1}=0.36, C_{S1}=12, R_{S2}=53, L_{S2}=3.3, C_{S2}=1.2, R_{S3}=31, L_{S3}=0.5, C_{S3}=8.2, R_{P1}=200, L_{P1}=5.1, C_{P1}=0.9μF, R_{P2}=34, L_{P2}=5.1 and C_{P2}=0.9μF.

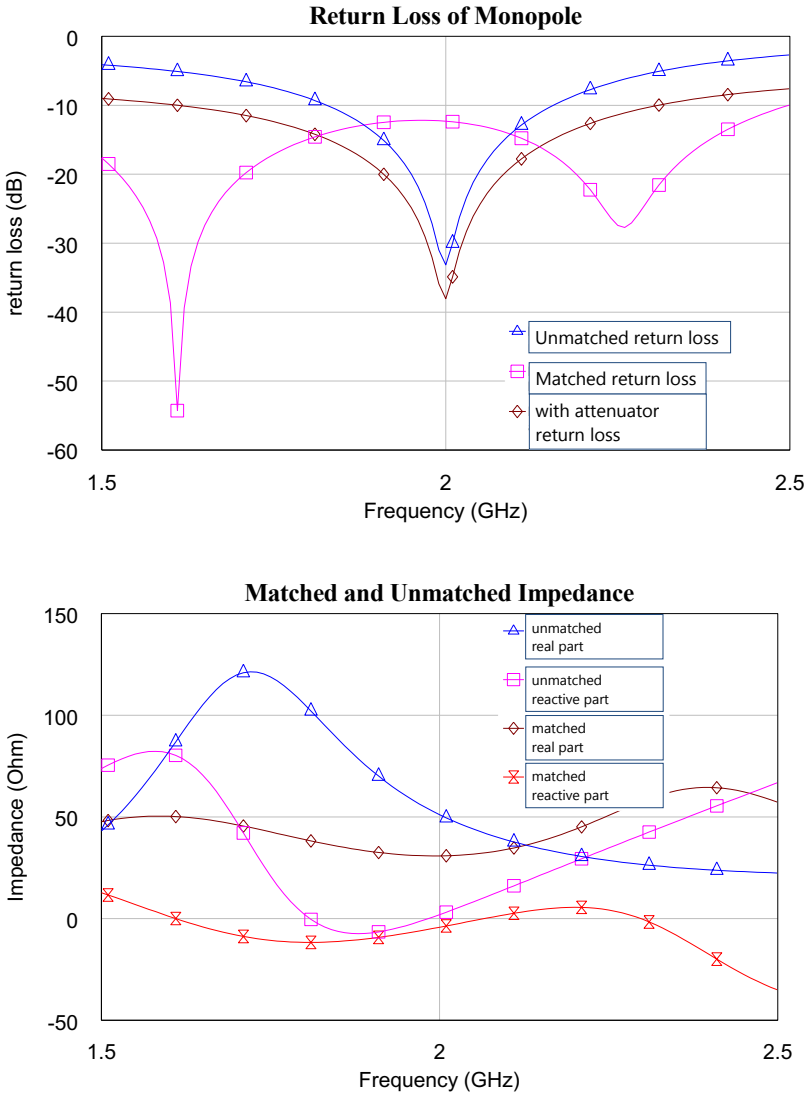

Fig. 4.9 The impact on impedance characteristics of a monopole due to NGD network and attenuator.

Case #2 Matching at Lower Frequencies

The NGD network in this case is used to achieve impedance matching over a wide bandwidth at frequencies far lower than the actual resonance frequency which corresponds to the physical length of the antenna. A monopole of 0.85λ/2π length is impedance matched to operate around 1.08GHz with a 35% bandwidth. Over this band a 20dB return loss is observed. The antenna can also be seen operating around 1.18GHz with a 60% bandwidth with a 10dB return loss as shown in Fig. 4.10. The 5th order topology which is shown in Fig.4.4 is used to implement the

NGD network and the RLC elements are as follows: (resistance in Ω, inductance in nH, capacitance in pF) R_{S1}=14, L_{S1}=0.5, C_{S1}=12, R_{S2}=101, L_{S2}=3.3, C_{S2}=1.2, R_{S3}=10, L_{S3}=0.5, C_{S3}=8.2, R_{P1}=40, L_{P1}=5.1, C_{P1}=0.9μF, R_{P2}=40, L_{P2}=5.1 and C_{P2}=0.9μF.

In conventional design, for the monopole to resonate at 1.08 GHz it should be 69.5mm (λ/4) long. However, a 37.5mm (0.85 λ/2π) long monopole is impedance matched using a NGD network to operate at 1.08GHz as shown in Fig. 4.10. The monopole return loss in three different cases is shown in Fig.4.10: unmatched; matched with NGD network; and matched with an attenuator. This is to justify the role of the NGD network as an negative reactive element in effective impedance matching, also to prove that NGD network is not just acting as a lossy element. A NGD network has 8 dB transmission loss, so an 8 dB attenuator is used to feed the same monopole. It is evident that the impact of the NGD network is far different to that of an attenuator. The attenuator is only causing more signal loss; whereas the loss of the NGD network can be compensated and better matching benefits can be achieved.

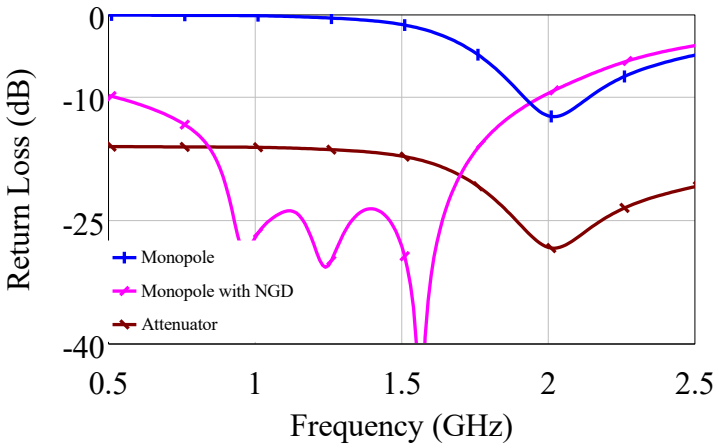

Fig. 4.10 Monopole return loss characteristics in three cases: unmatched; matched with a NGD network; and matched with an attenuator.

Analysis of NGD Network Noise Figure:

The NGD network is designed by adding resistance to the filter design; these added losses introduce noise in the transmission mode. In this case it is observed that the noise figure is proportional to the transmission loss characteristics as shown in Fig. 4.11. The noise figure can be optimised for a trade-off of the group delay value and bandwidth over which a positive phase slope can be achieved. Depending on the application it is better to use low noise amplifiers for the NGD network loss compensation.

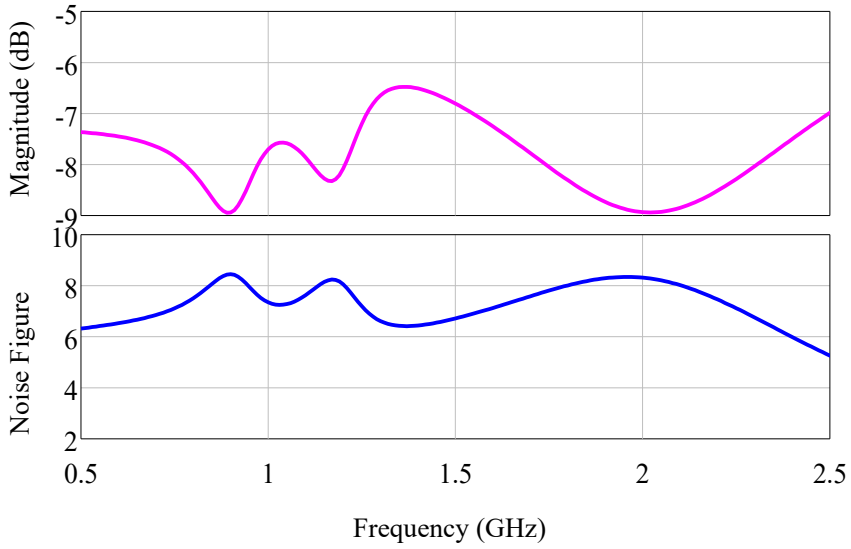

Fig. 4.11 Comparison of noise figure with the transmission coefficient magnitude characteristics

4.4. Dual Band Impedance Matching

An Elliptic band-stop filter based dual band NGD network is shown in Fig. 4.12. The series and shunt resistors are added to a 3rd order Elliptic filter resonating at 2GHz. This design exhibits NGD behaviour at two different frequency bands.

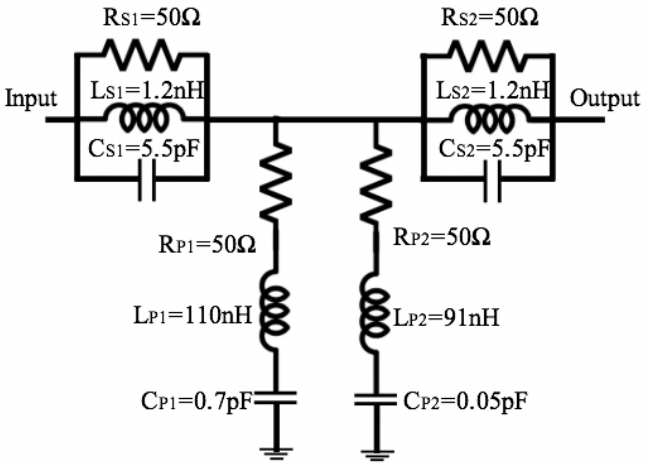

(a) Dual Band NGD Network

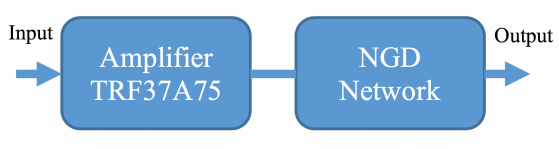

(b) Loss compensated dual band NGD network model

Fig. 4.12 The Elliptic band-stop filter based NGD network.

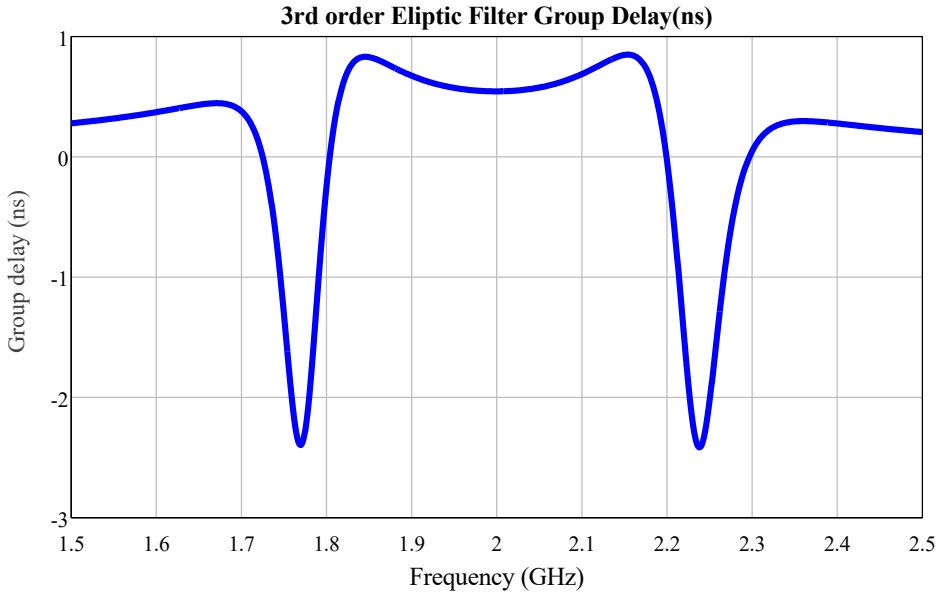

Fig. 4.13 Dual band NGD network group delay response

A group delay of -2.5ns is observed at 1.77GHz and at 2.23GHz as shown in Fig. 4.13. The loss at the respective frequencies is around 10dB as shown in Fig. 4.14. The transmission loss is an implication of employing the resistors in the filter design in order to achieve the NGD characteristics, which can be compensated by using an amplifier as shown in Fig. 4.12 (b). The

NGD network can be optimised in a trade-off between loss and the group delay. The order of the filter is a primary factor in deciding the maximum and minimum transmission loss. A stable amplifier, in this case TRF37A75 (with 12dB average gain) is used to compensate the loss of the NGD network. For this network the resistors can be further optimised in order to achieve the required NGD without the loss as shown in Fig. 4.15(a).

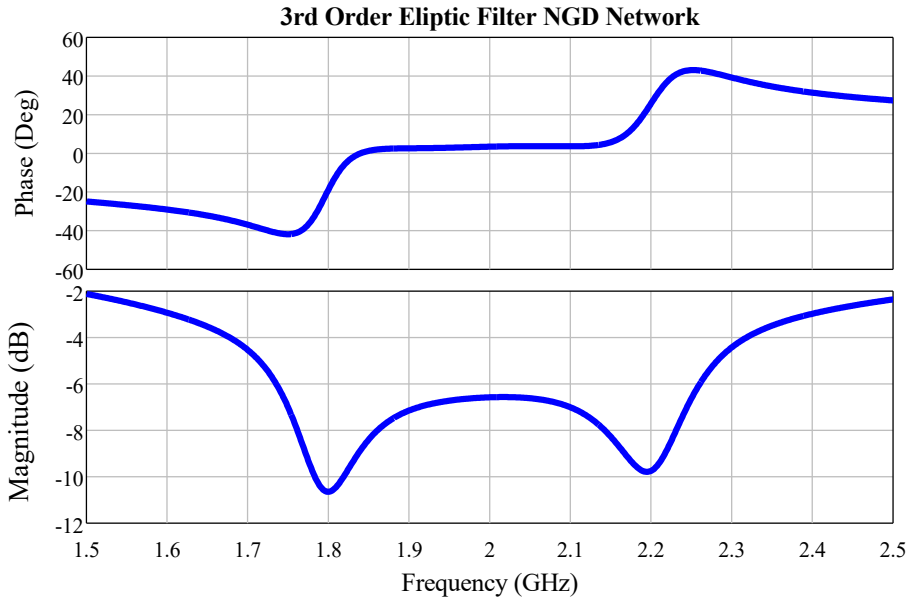

Fig. 4.14 Dual band NGD network transmission coefficient phase and magnitude characteristics

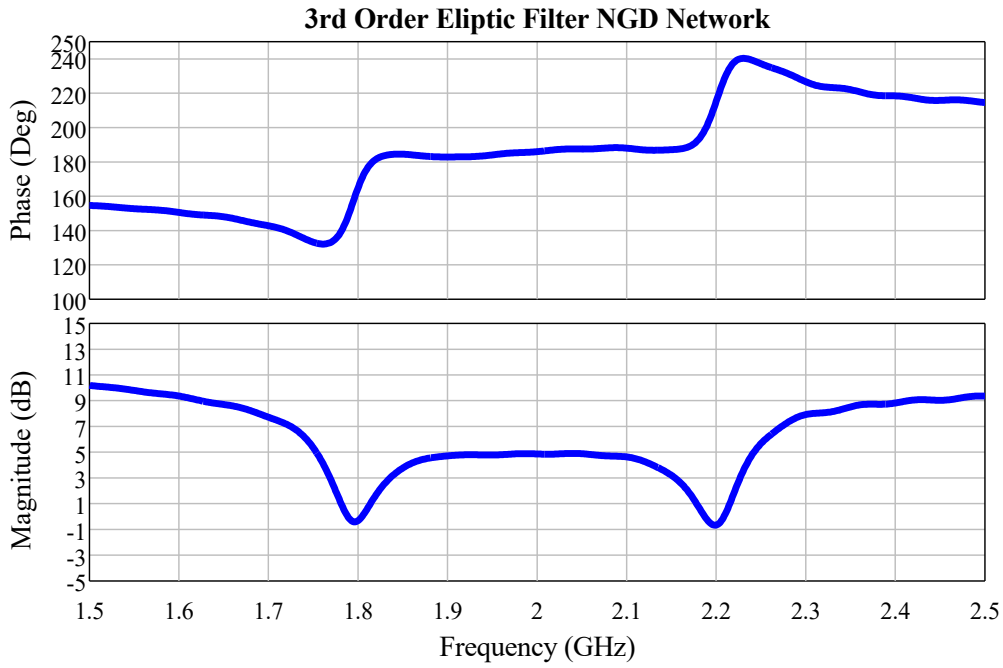

(a) The transmission coefficient phase and magnitude characteristics of a dual band ESA (The loss of the NGD network is compensated by an 12 dB amplifier - TRF37A75)

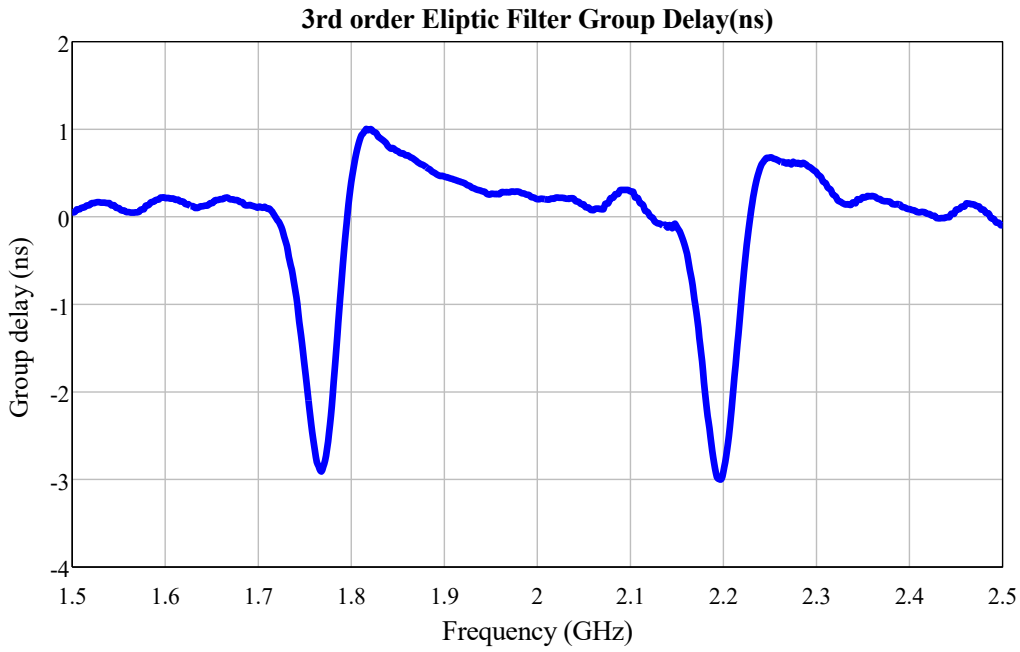

(b) Group delay characteristics of a loss compensated NGD network

Fig. 4.15 Dual Band NGD Network with an amplifier TRF37A75

After the use of an amplifier at the feeding port of the NGD network, a group delay of -3ns is observed at 1.77GHz and 2.2GHz. The amplifier phase characteristics caused a small shift in

the second resonance frequency. The resistors in Fig. 4.12 (a) in this case have been optimised to achieve the NGD behaviour, as follows: R_{S1}=35Ω; R_{S2}=70Ω ; R_{P1}=30Ω; R_{P2}=27Ω. Depending on the application, even a passive NGD network alone can effectively work as an impedance matching network, provided that the low insertion loss of a few dB's is acceptable in the application. A loss compensated dual band NGD network can be used as an impedance matching network for the dual band antenna. In practical designs the optimisation of the resistor values of the NGD network with an attached antenna would give the best matching.

4.5. Conclusions: NGD Network Based Matching

With these possibilities the NGD networks are proved to be very effective in designing an ESA. Unlike inductor or capacitor based matching, NGD networks are suitable for achieving wide band matching. However the losses of the NGD network must be compensated. These losses are compensated by using an active circulator as discussed in chapter 5. The gains in the transmission path and the reception path would provide the necessary loss compensation, enabling the ESA to be used for duplex communication over a wide bandwidth.

List of References

[1] H. A. Wheeler, "Fundamental limitations of small antennas," *Proceedings of IRE,* vol. 35, pp. 1479–1484, 1947.

[2] L. J. Chu, "Physical limitations in omni directional antennas," *J. Appl. Phys,* vol. 19, pp. 1163-1175, 1948.

[3] T. Thatapudi, P. Gardner, and A. Feresidis, "The antenna impedance matching circuit using negative group delay network: Design and analysis," in *Antennas and Propagation Conference 2019 (APC-2019)*, 11-12 Nov. 2019, pp. 1-4.

Chapter 5 Negative Group Delay Network Based Active Circulator With An Integrated Electrically Small Antenna

The circulator is a duplexer in a wireless communication system, which is a non-reciprocal multiport structure. The circulator facilitates an electrical isolation between the high power transmitter and low power receiver systems, while employing a single antenna for duplex wireless communication. The frequency bandwidth over which electrical isolation can be achieved, while maintaining low insertion loss among ports, is always a design challenge. Integrating an antenna to the active circulator is another challenge. Most of the designs presented in literature assume a 50 Ω load at the antenna port and expect the antenna to have 50 Ω input impedance over the operating bandwidth. Usually, antennas will have impedance characteristics that are a function of frequency, hence the design of a circulator with an integrated antenna is challenging. In fact, integrating an antenna with the circulator would make the design of an experimental prototype over a wide bandwidth more challenging, this therefore needs to be addressed. If active elements are involved in the design, then the stability of the overall system is another issue that needs to be addressed. The design challenges and design approaches in relation to active circulators are discussed in chapter 2.

A hybrid active circulator with an integrated antenna, designed in ring configuration with gain blocks, proved to be effective in establishing the signal cancellation conditions required to achieve isolation between the transmitter and the receiver [1]. In order to achieve signal cancellation, an anti-clockwise (ACW) path is introduced to counteract with the clockwise (CW) path signal at the receiver junction. With the right microstrip line lengths and gain values, an equal amplitude and opposite phase can be achieved for ACW & CW signals at the receiver junction resulting in successful signal cancellation. However, with this configuration the isolation can only be achieved over a very narrow bandwidth, typically a few MHz.

In the proposed active circulator design negative group delay (NGD) networks are used to achieve isolation over a wide bandwidth. The NGD networks can be used to engineer the phase characteristics of a signal. By introducing the NGD network at the end of the AWC & CW paths the phase and amplitude of the signal arriving at the receiver junction can be controlled over a wide bandwidth. In the proposed design NGD networks are implemented using passive lumped elements i.e. resistors, inductors and capacitors (RLC). The detailed filter based NGD network design procedure is presented in chapter 3.

An electrically small monopole is subsequently integrated with the active circulator. This electrically small antenna (ESA) is designed using a NGD matching network. In transmission mode the loss of the matching NGD network is compensated by the gain in the transmitter to antenna path. Similarly in reception mode the loss is compensated by the gain in the antenna to receiver path. This enables duplex operation over a wide bandwidth. The proposed model of an active circulator integrated with an ESA operating over a wide bandwidth is shown in Fig. 5.1.

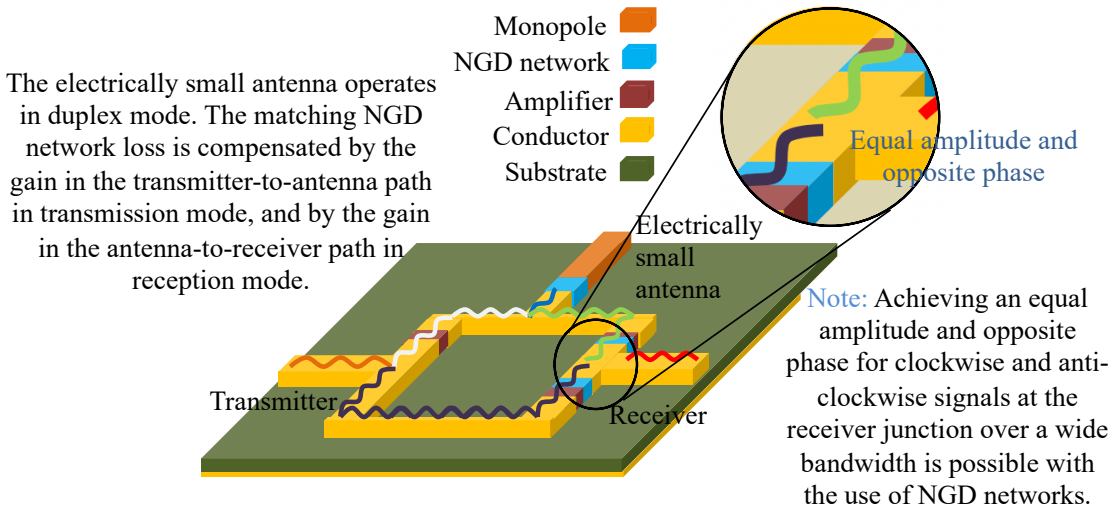

Fig. 5.1 The operating principle of the proposed active circulator

5.1. Signal Cancellation Over A Wide Bandwidth Using Negative Group Delay Network

The phase and amplitude of a signal varies with the distance along a microstrip line. At a three way junction, signal cancellation can be achieved by maintaining equal amplitude and opposite phase for the two inward travelling signals. In most cases gain blocks are needed to achieve equal magnitude for both signals. This scenario works for signal cancellation only over a very narrow frequency bandwidth. The signals travelling into the junction will have different phase and amplitude according to their respective frequency of operation. Therefore the physical structure designed to achieve perfect signal cancellation at one frequency will not generally work at other frequencies.

5.1.1. NGD Based Wide Bandwidth Signal Cancellation

In order to achieve cancellation between two signals $x(\omega t),\ y(\omega t)$ over bandwidth $\omega_1\ to\ \omega_2$ the signals should be 180^0 out of phase and equal in amplitude. If any two periodic waveforms are taken for analysis, equation (5.1) represents the scenario where two signals are combined at the junction.

Let two signals

$$x(\omega t) = A_x \sin\theta_x \ = A_x \frac{1}{2j}\left\{e^{j(\omega t+\varphi_x)} - \ e^{-j(\omega t+\varphi_x)}\right\}$$
$$y(\omega t) = \ A_y \sin\theta_y = A_y \frac{1}{2j}\left\{e^{j(\omega t+\varphi_y)} - \ e^{-j(\omega t+\varphi_y)}\right\}$$

$for\ x(\omega t) + y(\omega t) = 0$ over a wide bandwidth, the following are the signal cancellation conditions

$$x(\omega t) + y(\omega t)|_{\omega=\omega_1\ to\ \omega_2} = \begin{Bmatrix} A_x \frac{1}{2j}\left\{e^{j(\omega t+\varphi_x)} - \ e^{-j(\omega t+\varphi_x)}\right\} \\ + A_y \frac{1}{2j}\left\{e^{j(\omega t+\varphi_y)} - \ e^{-j(\omega t+\varphi_y)}\right\} \end{Bmatrix} \quad (5.1)$$

For $\omega = \omega_1\ to\ \omega_2$

$$\varphi_x = \varphi_y + \pi \tag{5.2}$$

$$A_x = A_y \tag{5.3}$$

A NGD network is employed to achieve the conditions in Equ. 5.2 and 5.3 over a wide bandwidth. Keeping microstrip line parameters, amplifier gains and LC values of NGD network unchanged, just by varying the resistor values of the NGD network, a wide bandwidth signal cancellation can be achieved.

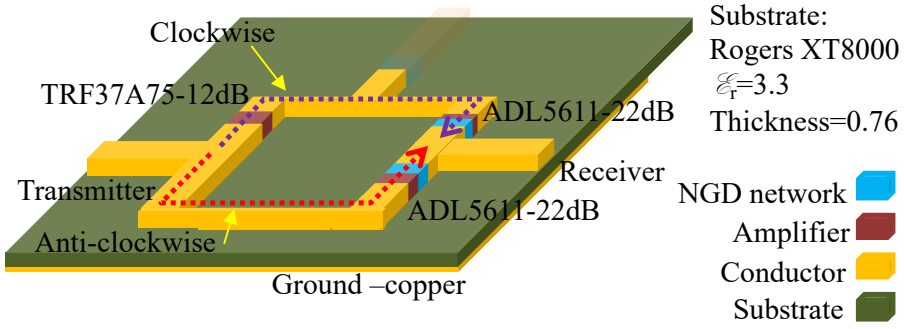

Fig. 5.2 The model is used to verify the signal cancellation over a wide bandwidth.

To verify signal cancellation over a wide bandwidth using NGD networks a circulator of ring configuration is used as shown in Fig. 5.2. The NGD networks are employed in CW and ACW paths to achieve wide bandwidth signal cancellation at the receiver junction. This ring configuration is used later to achieve full active circulator operation. Between the transmitter and the receiver CW and ACW paths are created and NGD networks are employed in both paths. To achieve signal cancellation at the receiver junction, the opposite phase and equal amplitude condition is established. In ring configuration the microstrip line lengths are optimised and amplifiers with the right gains are used in order to achieve an equal amplitude and opposite phase condition at the receiver junction. An electrical isolation between transmitter and receiver over a wide bandwidth is achieved by using the NGD networks to alter the CW and ACW signal phase and magnitude responses. The surface mount lumped element are used for the NGD network. These NGD networks are designed following the filter based design discussed in

chapter 3. For NGD network the LC values will be obtained by using filter design by insertion loss method. In this case, CST microwave studio filter synthesiser is used with the following specifications: A 5th order Butterworth with resonance frequency 2 GHz, a stop bandwidth of 25%, and stop band attenuation of 10 dB. These values of inductor and capacitor have to be adjusted to take into account the parasitic effects of circuit layout. The next step is to place the NGD network at the end of the clockwise and anticlockwise paths with parameterised resistor values in AWR microwave office software. The resistor values are varied until the required level of signal cancellation is achieved at this junction. Also the return loss of the three ports of the ring configuration is another parameter that should be observed during this process. The following are the CW path NGD network RLC element values: (resistance in Ω, inductance in nH, capacitance in pF) R_{S1}=160, L_{S1}=0.36, C_{S1}=12, R_{S2}=290, L_{S2}=3.3, C_{S2}=1.2, R_{S3}=3, L_{S3}=0.51, C_{S3}=8.2, R_{P1}=210, L_{P1}=8.2, C_{P1}=0.47, R_{P2}=115, L_{P2}=11 and C_{P2}=0.36. The following are the ACW path NGD network RLC element values: (resistance in Ω, inductance in nH, capacitance in pF) R_{S1}=12, L_{S1}=0.36, C_{S1}=12, R_{S2}=88, L_{S2}=3.3, C_{S2}=1.2, R_{S3}=97, L_{S3}=0.51, C_{S3}=8.2, R_{P1}=14, L_{P1}=8.2, C_{P1}=0.47, R_{P2}=165, L_{P2}=11 and C_{P2}=0.36.

While using the AWR-MS software to run the simulations, for accurate modelling of the components Modelithics library is used. The 0603 package KOA resistors, 0402 package ATC capacitors, and 0402 package Coilcroft inductors are used for this model. All these are surface mount components. Measured S-parameter files are used in place of the amplifiers for this design. A TRF37A75 amplifier of 12dB gain is used in the path between the transmitter and the antenna. In the CW and ACW paths ADL5611 amplifiers of 22dB are used. Microstrip lines in the ring configuration are designed for 50Ω impedance.

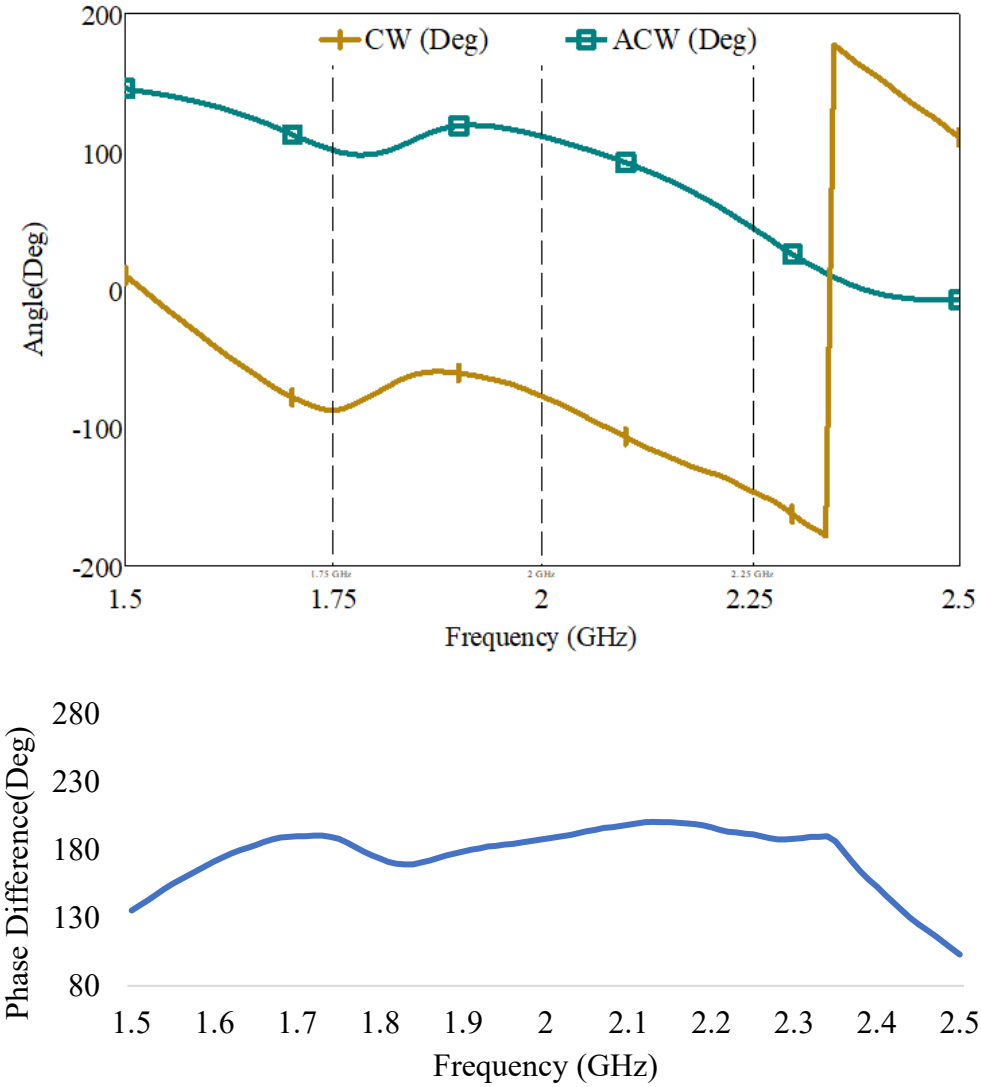

Fig. 5.3 The opposite phase condition to achieve signal cancellation

(For the clockwise and anti-clockwise signals 180° opposite phase is achieved over 1.75 to 2.25 GHz bandwidth.)

As shown in Fig. 5.3 the clockwise and anti-clockwise signals are nearly 180^0 anti-phase over 1.75 to 2.25 GHz bandwidth. Unlike in the conventional methods where this is only possible at a single frequency or over a very narrow bandwidth, when using NGD networks an approximate 180^0 phase difference between these two signals is achieved over a range of frequencies. The bandwidth over which signal cancellation can be achieved using this approach is limited by the stop-bandwidth of the filter that is used to design the NGD network (as discussed in chapter 3).

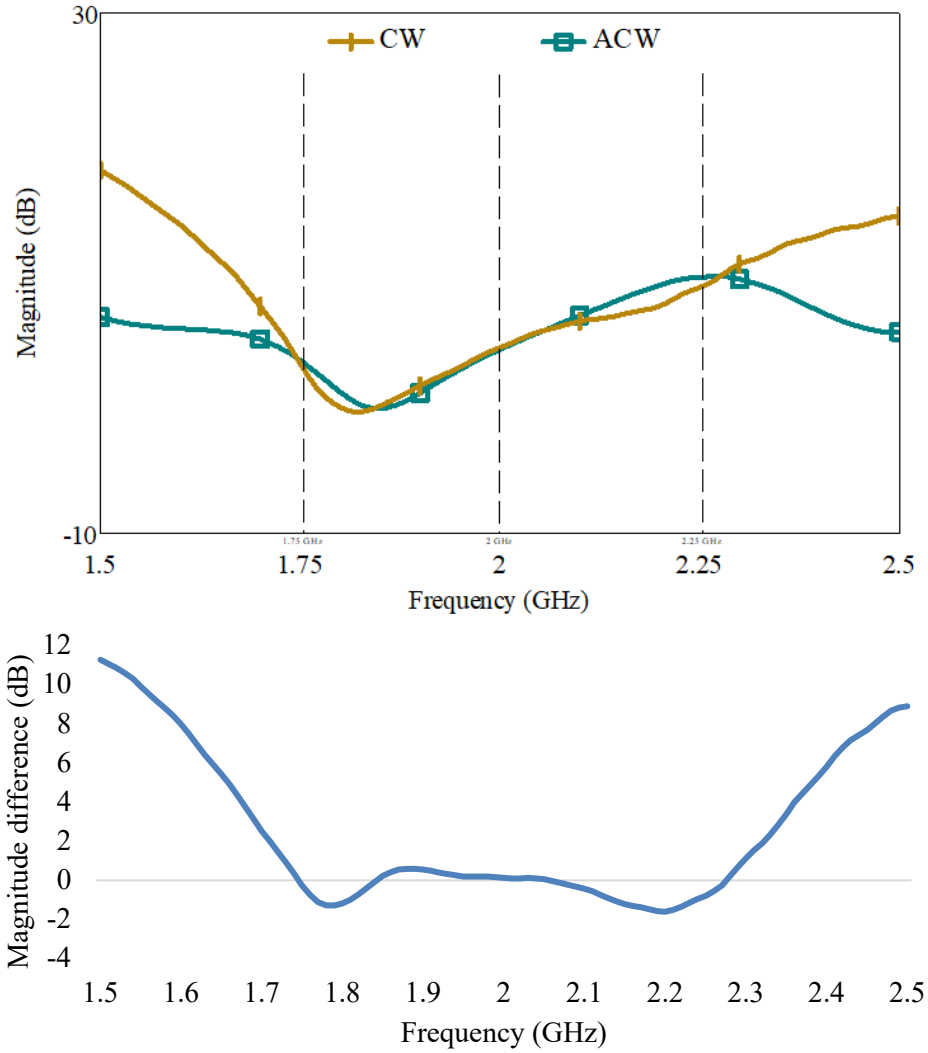

Fig. 5.4 The magnitude conditions necessary to achieve signal cancellation

(For the clockwise and anti-clockwise signals a nearly equal amplitude is achieved over 1.75 to 2.25 GHz bandwidth.)

The loss of the NGD networks along with the amplifier gain has been adjusted such that an equal amplitude is achieved for CW and ACW signals as shown in Fig.5.4. As a result of the wide bandwidth signal cancellation an isolation between the transmitter and receiver is achieved. As shown in Fig. 5.5 an average isolation of 17dB is achieved over 1.75 to 2.25 GHz bandwidth. The NGD networks are proved to be very effective in achieving wide bandwidth signal cancellation. Network complexity and the availability of the right gain blocks are the factors that need addressing when designing wideband models.

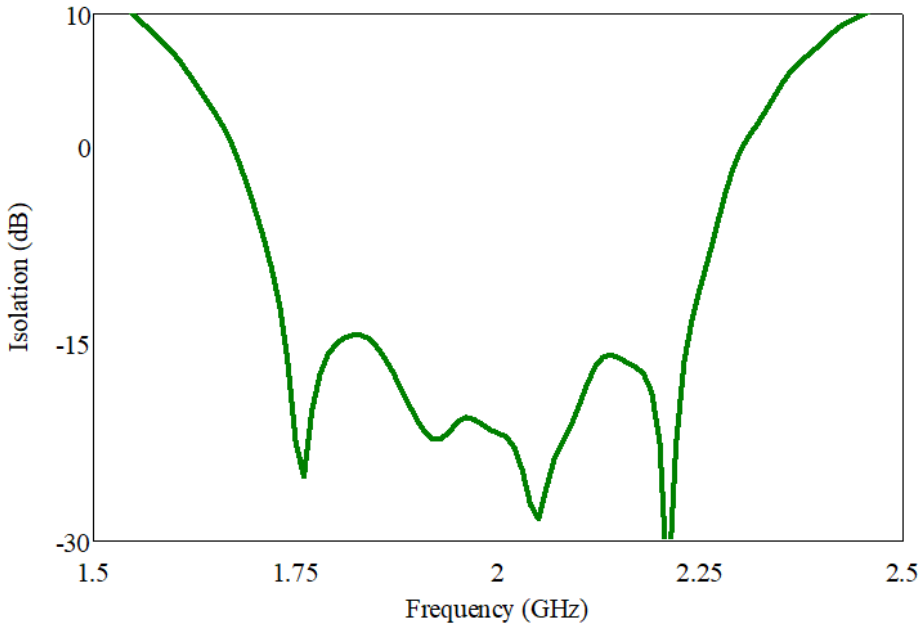

Fig. 5.5 As a result of wide bandwidth signal cancellation an isolation is achieved between transmitter and receiver (S21).

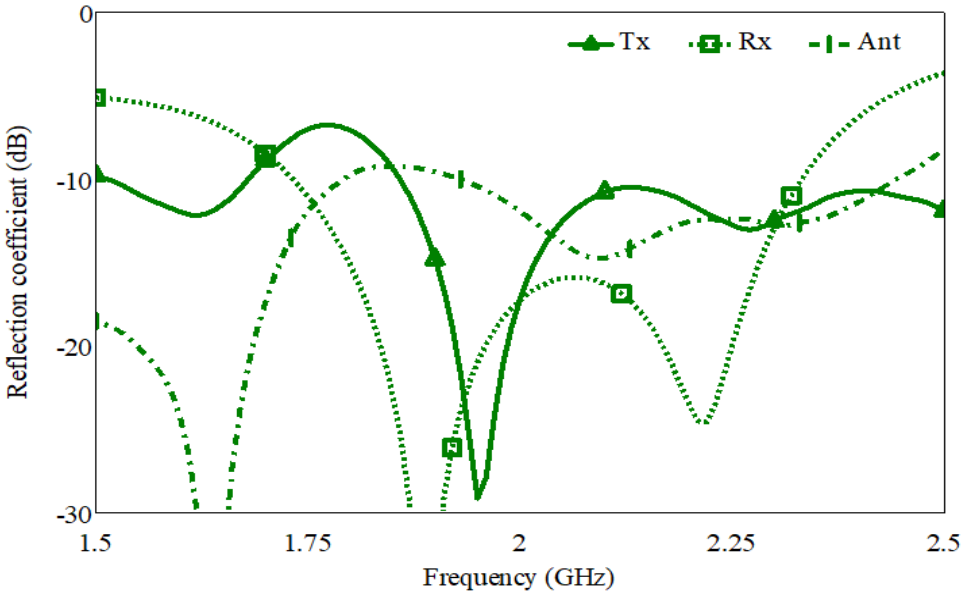

Fig. 5.6 Reflection coefficients of transmitter (S11), receiver (S22) and antenna (S33) ports of the active circulator.

The reflection coefficients of the 3 ports of the ring configuration are shown in Fig. 5.6. The optimisable resistor values of the NGD network are key in this design approach to balance the performance parameters of the design. This also enables the use of off the shelf amplifiers.

5.2. A Wide Bandwidth Active Circulator With An Integrated Electrically Small Antenna Using Negative Group Delay Network

In this section an active circulator with an integrated electrically small monopole is presented. The design approach using NGD networks is shown in Fig. 5.7. The proposed method is suitable in different implementations. All the design blocks are compatible with MMIC technology, so the proposed concept is suitable for designing active circulators for low profile applications.

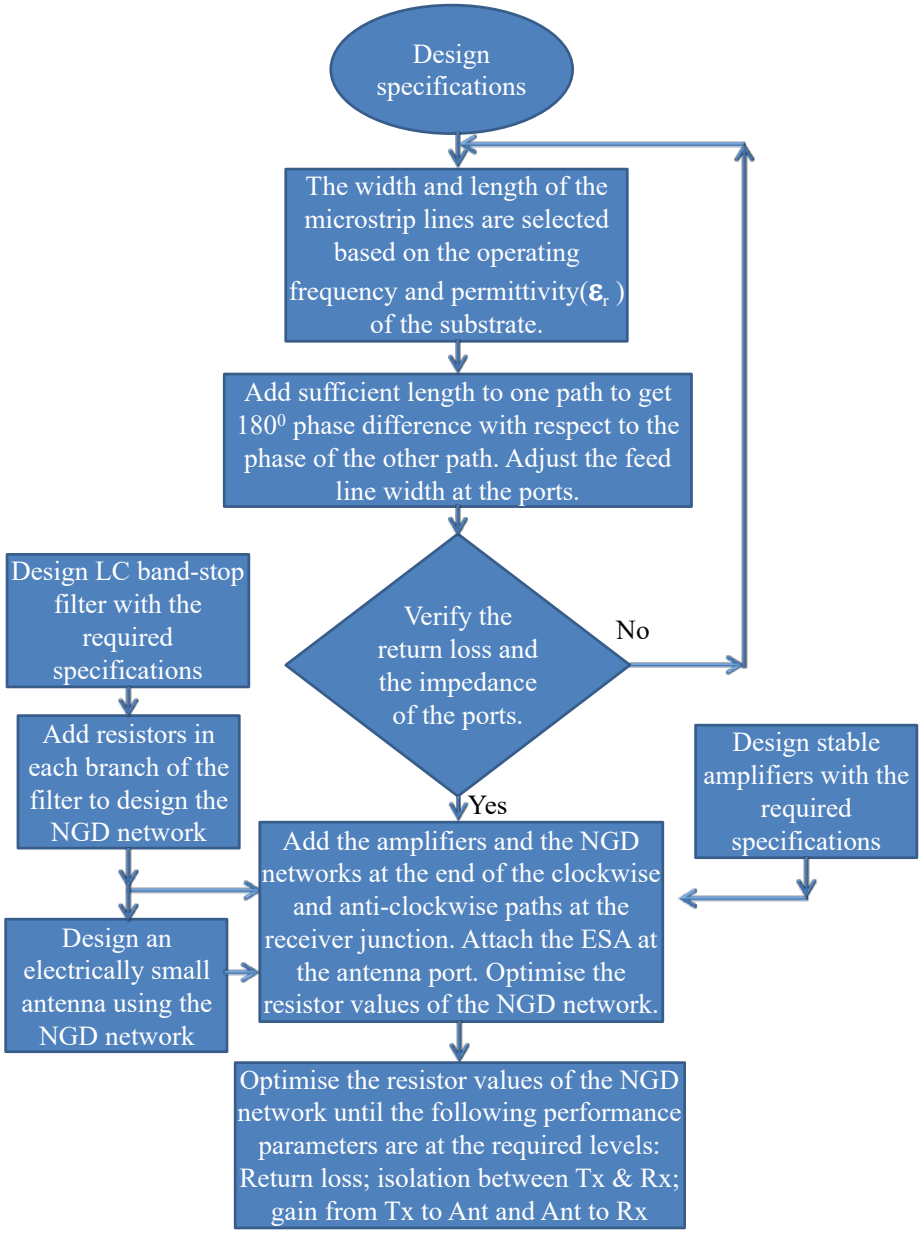

Fig. 5.7 The proposed design approach of an active circulator with an integrated electrically small antenna using NGD network

The proposed design has desirable values over 1.69 - 1.93 GHz bandwidth for the following of parameters:

- Matching NGD network – NGD behaviour (positive phase slope)
- Matching NGD network – return loss
- Matching NGD network – negative group delay
- Electrically small antenna – return loss
- Active circulator – return loss
- Active circulator – insertion characteristics (Tx-Aa & Aa-Rx gains)
- Active circulator – isolation (Tx to Rx isolation)

As shown in Fig 5.7 the NGD network design starts with LC band-stop filter. To minimise any distortion problems it is recommended to have a filter with a linear transmission phase response, in this case the Butterworth filter type is used. The order of the filter should be selected based on the bandwidth required, usually with higher order filters a flat group delay behaviour can be achieved over a wider bandwidth. Having a higher order filter also gives more flexibility in the optimisation or in the parameter sweep. However, a higher order circuit will have more complexity and the footprint of the design will be affected. These networks with many passive elements are one of the sources for noise. Particularly the noise profile should be considered if the NGD network is in the receiver path. Higher order circuits tend to produce higher losses. Availability of an amplifier with sufficient gain in the required operating frequency is another factor to be considered. Also based on the method of implementation parasitic effects and tolerances will have significant impact on the prototype performance. The resistors values for NGD networks should be obtained in order to get desired responses for all the above parameters.

Either for optimisation or parameter sweep the above list will be goal parameters for finding the resistor values.

5.2.1. Electrically Small Monopole

A 20mm monopole is used in this design, the length is arbitrarily selected to verify the concept. The unmatched monopole reflection coefficient is shown in Fig.5.8. Rogers XT8000 with 3.3 permittivity is used as a substrate for this printed monopole design.

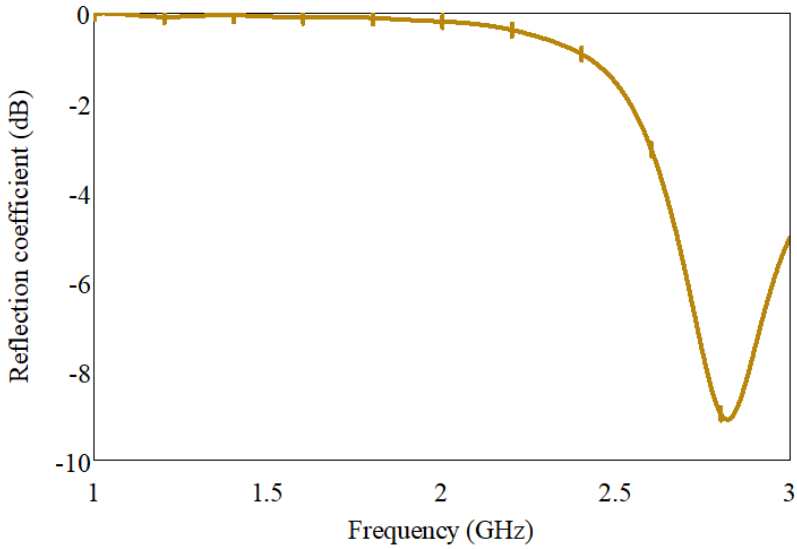

Fig. 5.8 Reflection coefficient of an unmatched monopole of 20mm length

A LC based matching network is used to match this monopole at 1.7GHz and it is observed that the impedance matching is possible only over a very narrow bandwidth as shown in Fig. 5.9. When a NGD network is used for matching the monopole a wider bandwidth is achieved as shown in Fig. 5. 10.

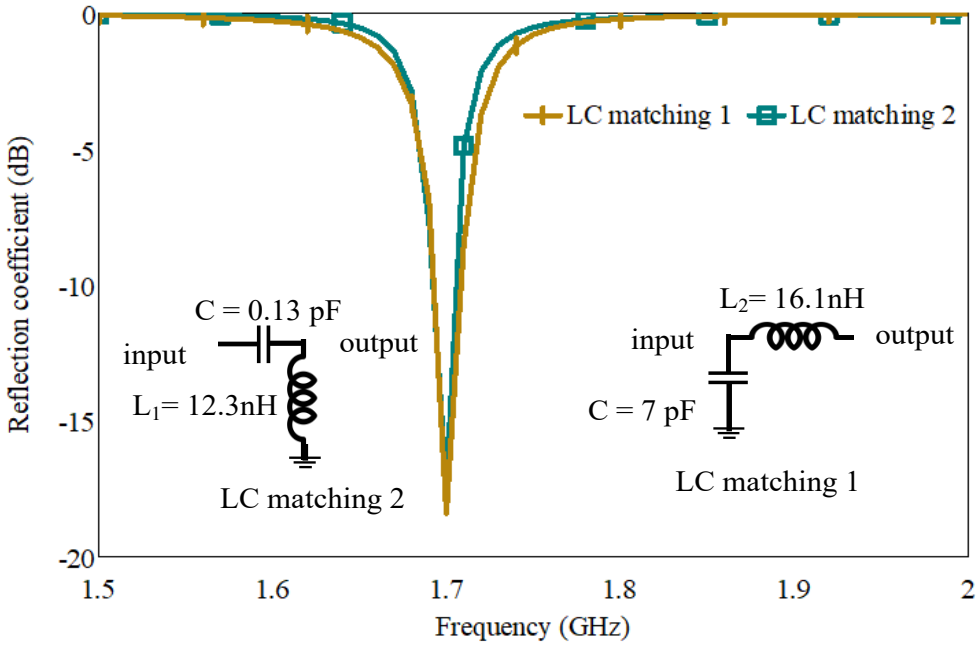

Fig. 5.9 Monopole impedance matching using LC networks

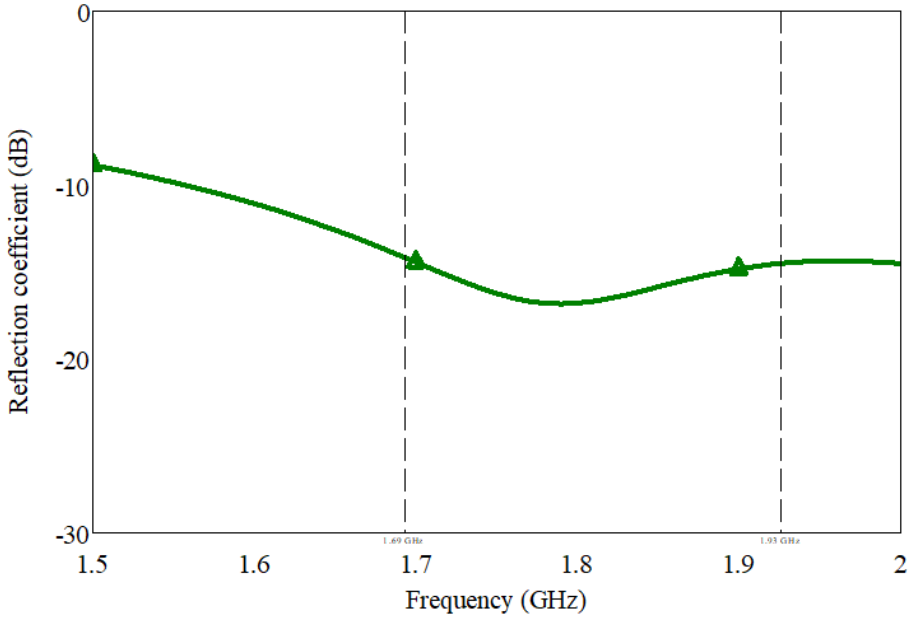

Fig. 5.10 Reflection coefficient of an electrically small monopole matched using NGD network

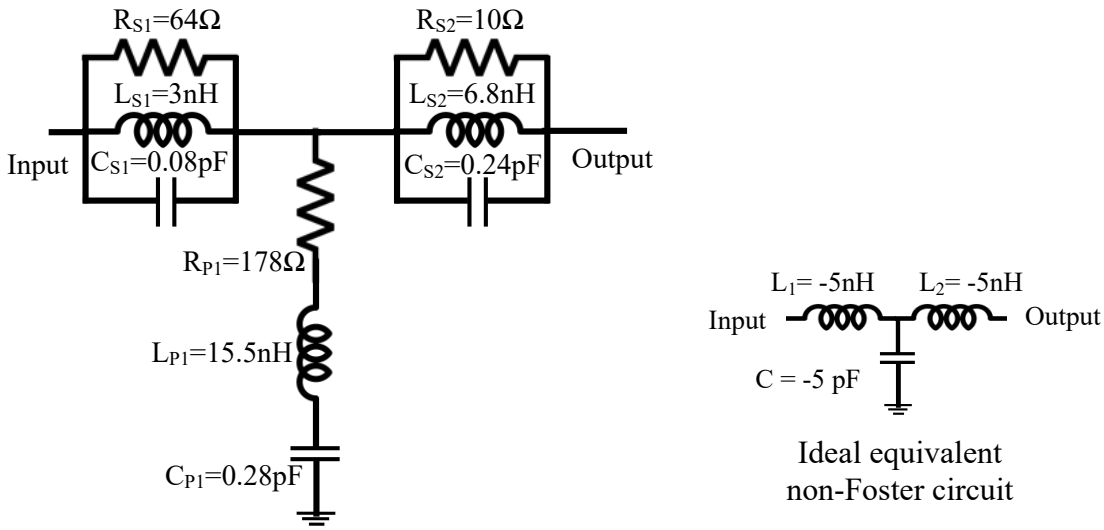

Fig. 5.11 The matching NGD network topology, elements and its equivalent ideal non-Foster network.

The matching NGD network is designed using the filter based approach which is presented in chapter 3. The inductor (L) and capacitor (C) values are selected to design a 3rd order Butterworth band-stop filter at 1.8GHz centre frequency and around two hundred MHz bandwidth. Due to the added microstrip layout for the surface mount lumped elements, there is a slight shift in the operating frequency. The resistors are added to design the matching NGD network as shown in Fig 5.11. The parameter sweep is used to find out the values of resistors which will give desirable return loss, positive phase slope and transmission loss. Using this network the monopole is matched over the desired frequency range.

This NGD network acts as a negative reactance element. To verify this phenomenon an ideal non-Foster equivalent network is designed as shown in Fig. 5.11. The ideal series inductor and shunt capacitor values for the equivalent network are taken from the curves shown in Fig. 5.11. The curves show the variation of the reactance with frequency and these are obtained using the equivalent T-network design procedure given in [2, 3]. The procedure to obtain an equivalent ideal T-network is presented in Chapter 4 section 2.

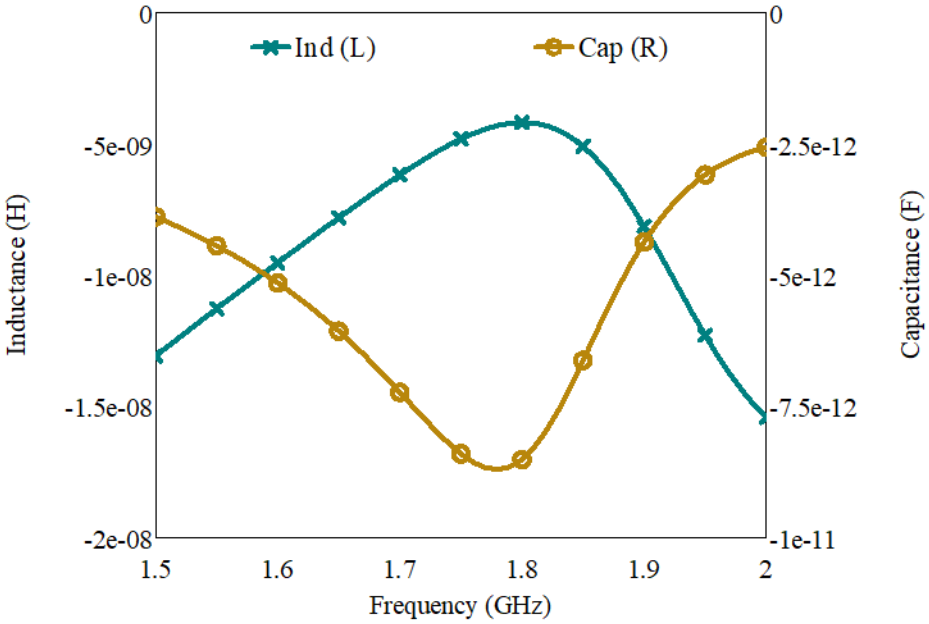

(a) The shunt capacitance and series inductance of ideal equivalent non-Foster network

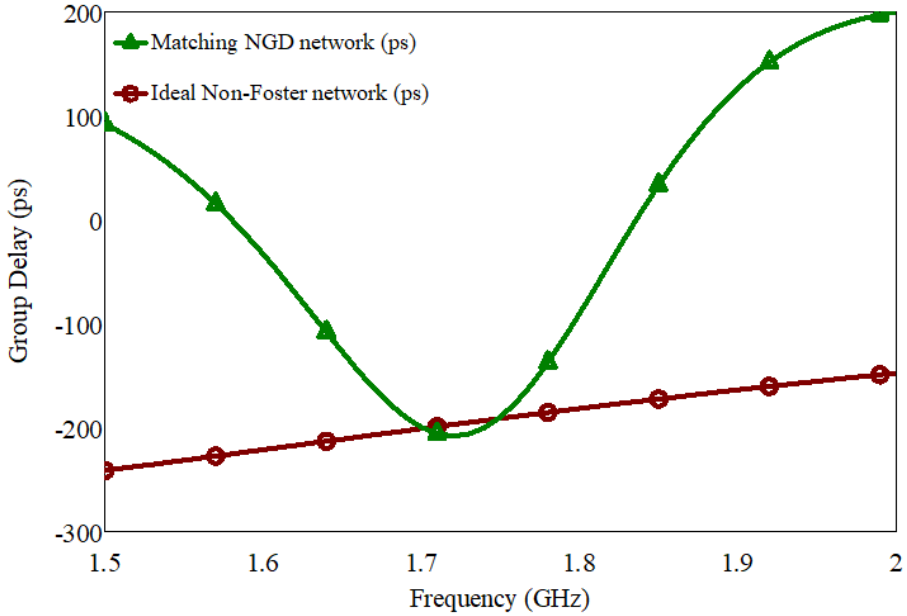

(b) Group delay response of the ideal and NGD networks

Fig. 5.12 Ideal non-Foster and matching NGD network group delay characteristics.

The series inductor of -5nH and shunt capacitor of -5pF are the ideal elements of the equivalent non-Foster network. Both the ideal and NGD networks are reciprocal. The comparison of the group delay response of the ideal and NGD networks is shown in Fig. 5.12(b).

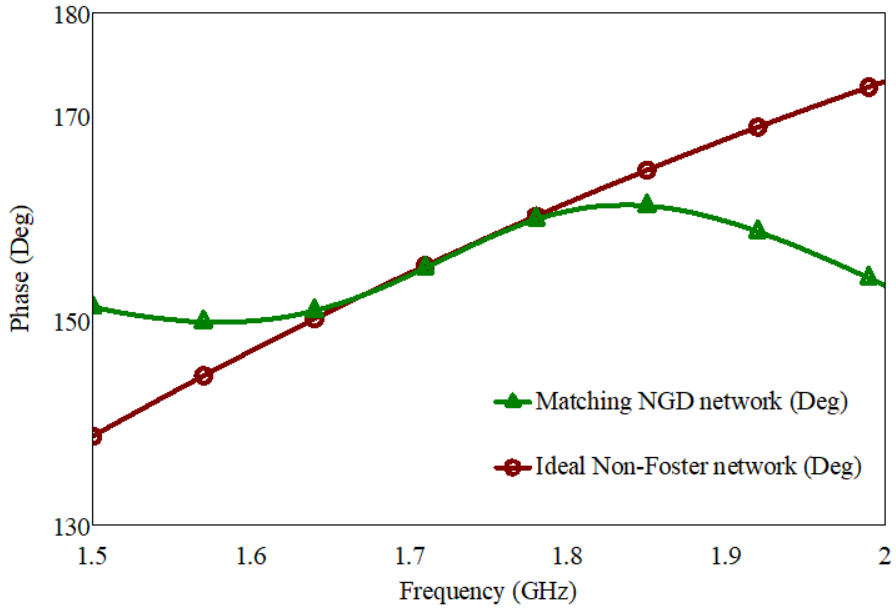

(a) Phase response of Ideal and NGD networks

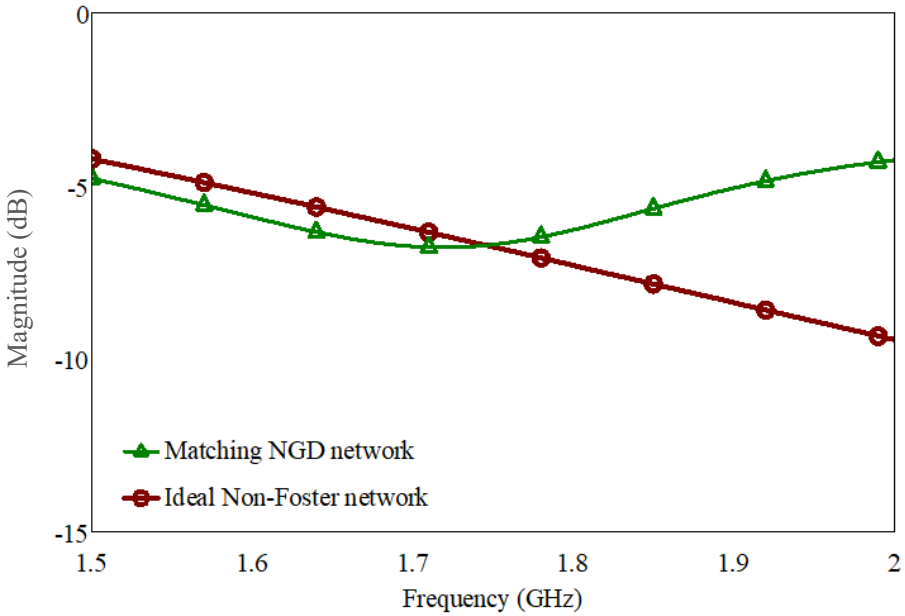

(b) Magnitude response of ideal and NGD networks

Fig. 5.13 Ideal non-Foster and matching NGD network transmission coefficient phase and magnitude characteristics.

The phase and loss characteristics of the NGD network and the ideal T-network are shown in Fig. 5.13. The negative reactive behaviour of the NGD network is the key to achieving wideband impedance matching. An average transmission loss of 4.5dB is introduced due to the added resistors. These also add an extra noise figure in the antenna to receiver path.

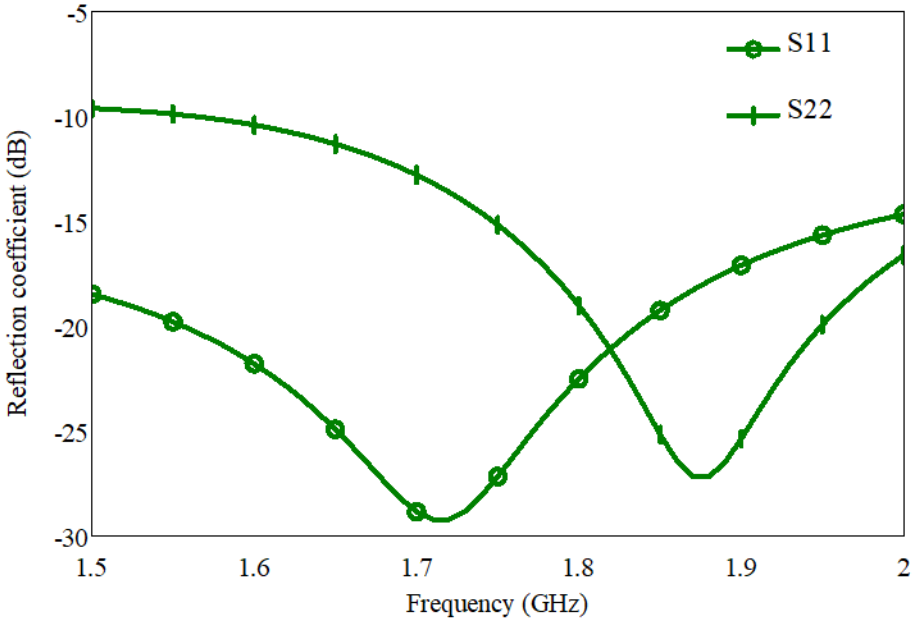

Fig. 5.14 Matching NGD network reflection coefficient characteristics.

The reflection coefficient characteristics of the matching NGD network are shown in Fig 5.14. The matching of the monopole is achieved by the NGD network over the 1.69 to 1.93 GHz bandwidth. An average transmission loss of 4.5dB is observed for the NGD network. To be able to maintain duplex operation the loss of this matching network will be compensated by an active circulator. In the following section an active circulator is designed with gains in transmission and reception paths approximately equal to the loss of the matching NGD network.

5.2.2. An Active Circulator with An Integrated Electrically Small Antenna

An active circulator design, operating over 1.69 to 1.93 GHz bandwidth, with an integrated electrically small monopole is shown in Fig. 5.15. This quasi-active circulator works on the signal cancellation phenomena. The active circulator model consists of two ADL5611 amplifiers along with the NGD networks at the receiver junction, one pair in CW and the other in ACW paths from the transmitter. These networks and amplifiers facilitate the phase and amplitude adjustments needed for signal cancellation to achieve isolation between the transmitter and the receiver.

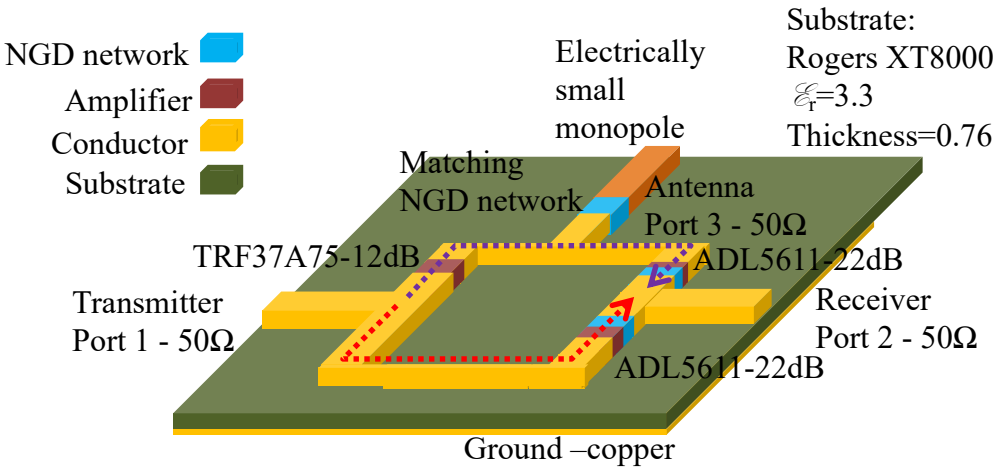

Fig. 5.15 An active circulator integrated with a monopole

A TRF37A75 amplifier of 12dB gain is used in the path from the transmitter to the antenna in order to provide enough gain to compensate the matching NGD network loss in transmission mode. The de-embedded amplifier s-parameter files are used for the AWR-MS simulation. The amplifiers used in the design are acting as gain blocks. Along with an amplifier the NGD network will achieve required phase and amplitude for clockwise and anti-clockwise signals at the receiver junction to establish signal cancellation. This design approach allows freedom to use any amplifier with the required gain, transmission phase and good stability.

The filter based NGD networks are implemented using lumped resistor, inductor and capacitor elements and the values are given Table 5.1. In designing the NGD network the first step is to design a 5^{th} order Butterworth band-stop filter with stop bandwidth of 250MHz, where the inductor and capacitor values for the NGD network will be determined. As discussed in chapter 3, a Butterworth filter based NGD network is preferable in the optimisation process due to its linear phase response. As the order of the filter increases the flexibility in the design and optimisation also increase. However, the possible higher transmission loss of the NGD network should be addressed. In this design ADL5611 amplifiers of 22dB gain are used and the NGD network resistor values are optimised such that the transmission loss of the NGD network is

smaller than the amplifier gain, while achieving the signal cancellation over a wide bandwidth. The variation in the impedance of the ESA with frequency will also be taken into account during the optimisation of the NGD network resistor values. Therefore the proposed approach is very effective in customising the design as required for applications. The AWR-MS software is used to run the simulations. For accurate modelling of the components Modelithics library is used. The 0603 package KOA resistors, 0402 package ATC capacitors and 0402 package Coilcroft inductors are used for this model.

Table: 5.1 The resistor, inductor and capacitor lumped element values for NGD networks (Units : R - Ω, L - nH, C - pF)

	Elements of NGD networks for an active circulator integrated with an electrically small monopole	
	Clockwise	Anti-clockwise
R_{S1}	32	5
L_{S1}	0.36	0.36
C_{S1}	12	12
R_{S2}	50	17
L_{S2}	3.3	3.3
C_{S2}	1.2	1.2
R_{S3}	13	18
L_{S3}	0.51	0.51
C_{S3}	8.2	8.2
R_{P1}	65	281
L_{P1}	8.2	8.2
C_{P1}	0.47	0.47
R_{P2}	40	32
L_{P2}	11	11
C_{P2}	0.36	0.36

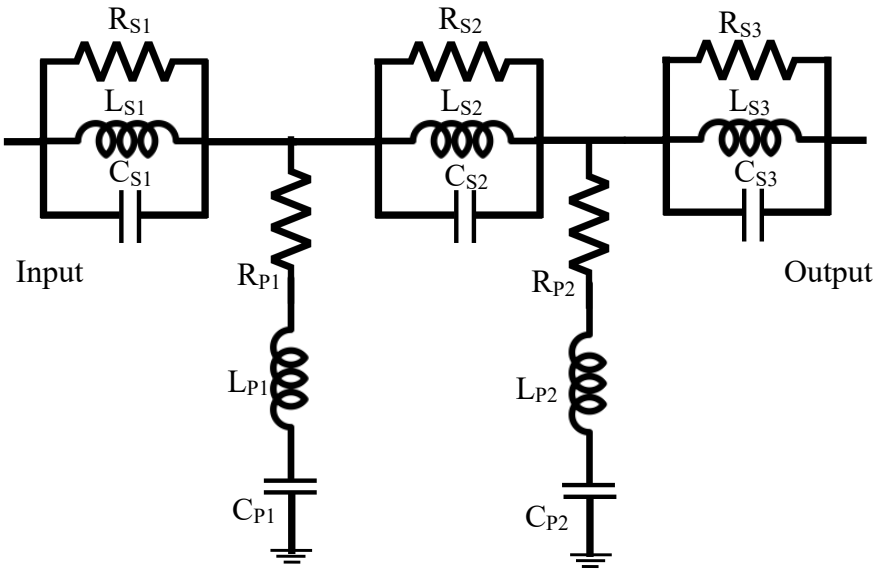

(a) The 5th order topology used for NGD networks

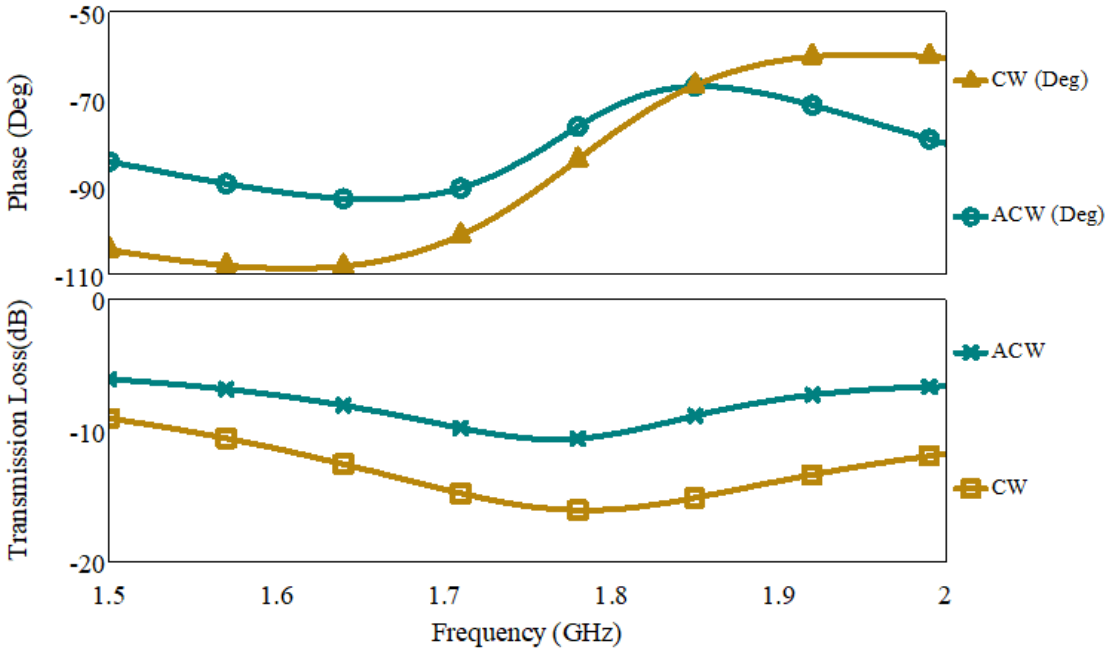

(b) Clockwise (CW) and Anti-clockwise (ACW) NGD network characteristics

Fig. 5.16 The topology used for NGD networks and the characteristics

The phase and transmission loss characteristics of the NGD networks in CW and ACW paths along with the corresponding network topology are shown in Fig. 5.16. With the added layout for surface mount elements a slight shift in frequency is noticed.

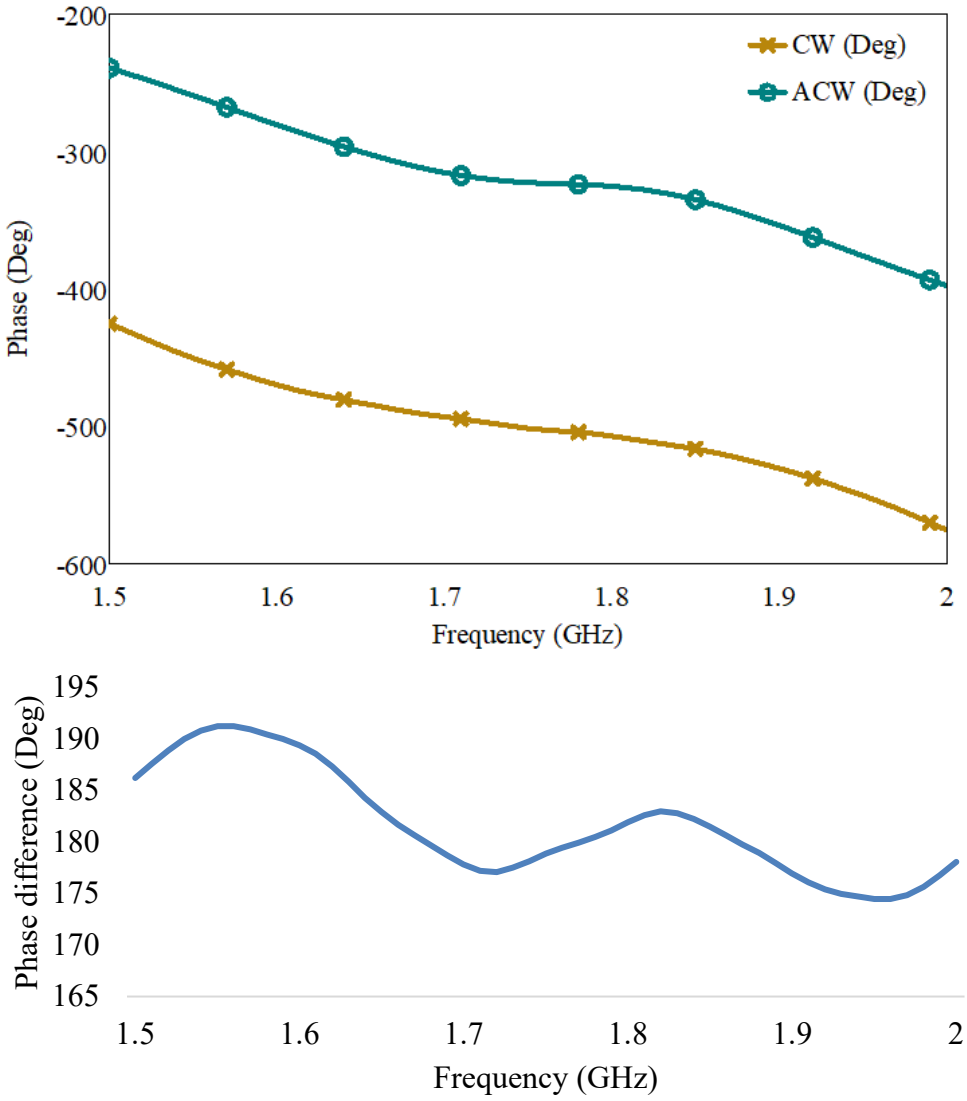

Fig. 5.17 180º phase difference for signal cancellation

The signal cancellation method is used to achieve electrical isolation between the transmitter and the receiver. Over the bandwidth of interest an equal amplitude and opposite phase for CW and ACW signals are achieved by using the NGD network. As shown in Fig. 5.17 the phase of the signals arriving at the receiver junction are opposite. A 180º phase difference between CW and ACW signals is expected in an ideal case. When there is 180º phase difference isolation is maximum. For an isolation over a wide bandwidth, there will be a compromise between bandwidth and isolation value.

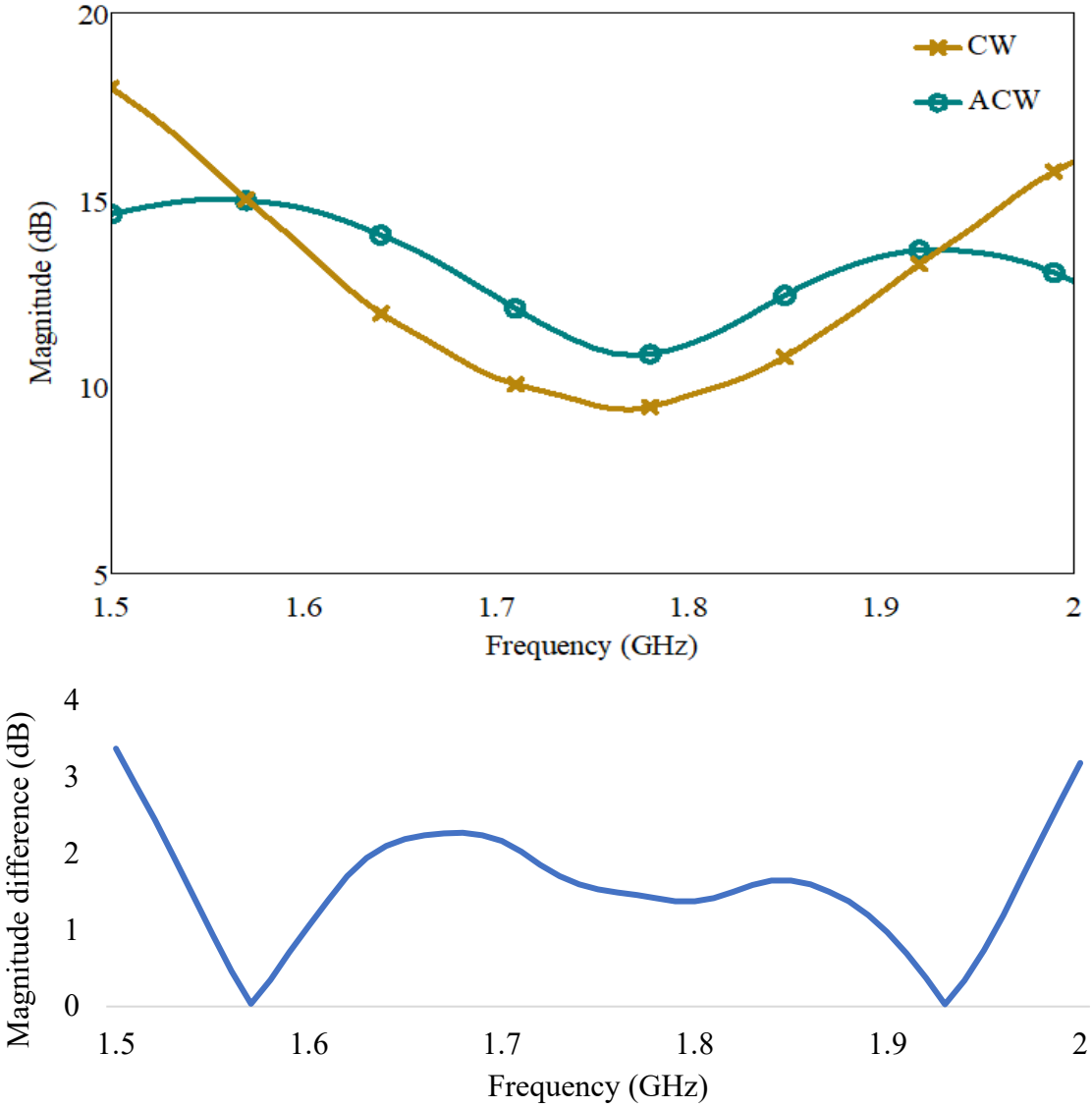

Fig. 5.18 Equal Amplitude for signal cancellation

As shown in Fig. 5.18 approximately equal amplitude is achieved for both the signals, contributing to signal cancellation over a wide bandwidth.

The effect of the amplitude and phase differences of CW and ACW signals in achieving signal cancellation are shown in Fig. 5.19, as a case study. The isolation will be maximum when CW and ACW have equal amplitude and opposite phase. In this case only isolation is observed not all the parameters of the circulator. The combination of equal amplitude and opposite phase at

1.84 GHz for CW and ACW signals is crucial to achieve the isolation. In optimising the NGD network resistor values there is a need to balance the bandwidth and isolation.

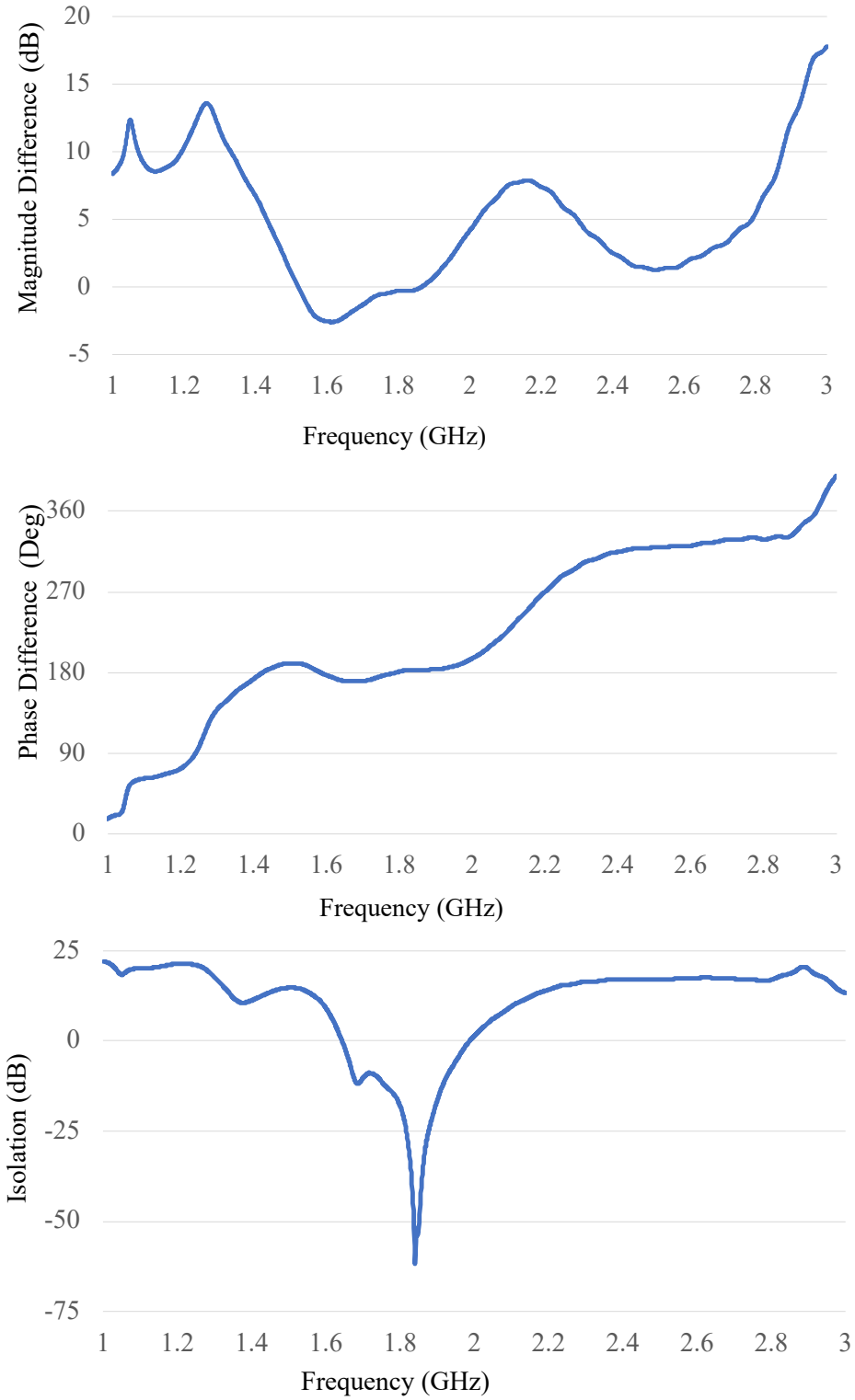

Fig. 5.19 180º phase difference and equal amplitude for high isolation.

To prove the proposed concept an isolation around 20dB is taken as a required value. For the CW and ACW signals the phase is neither exactly opposite nor the amplitude exactly equal over the operating bandwidth but they are sufficiently close to achieve the required isolation. The NGD network resistors could be optimised to improve the isolation for a trade-off of bandwidth or more insertion losses among the transmitter, antenna and receiver ports.

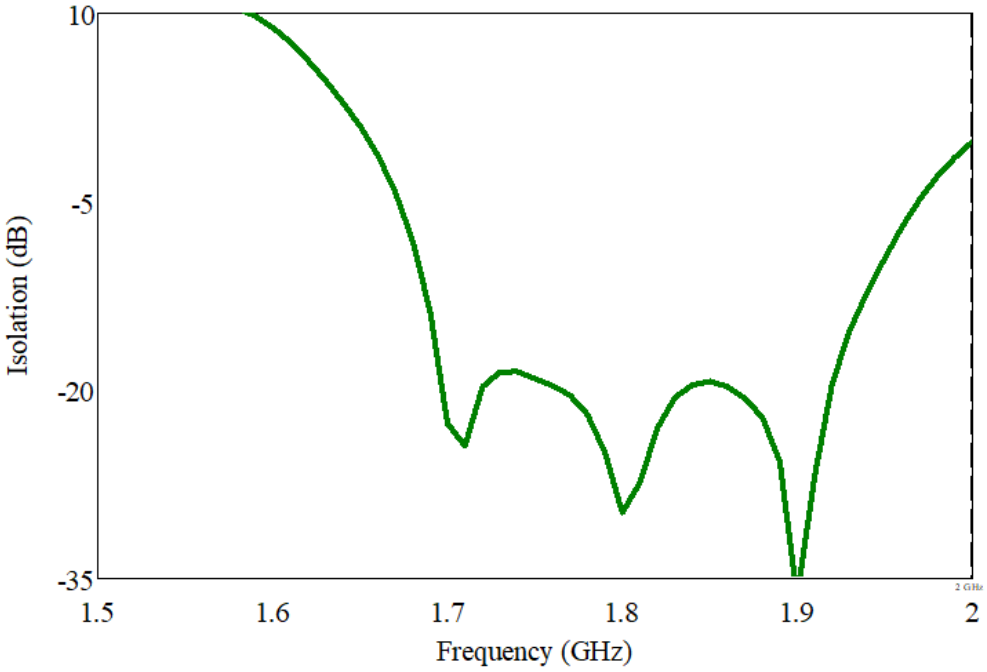

Fig. 5.20 The isolation between the transmitter and the receiver

An isolation of around 20dB over 200MHz bandwidth is observed, as shown in Fig. 5.20. The proposed method allows optimisation of the resistor values of the NGD network to be able to design a wide bandwidth active circulator with an integrated antenna. By employing the NGD network in an hybrid ring active circulator which is reported in [1], isolation is achieved over a bandwidth of 200 MHz. Without the use of NGD network the similar model only achieved isolation over 7 MHz bandwidth.

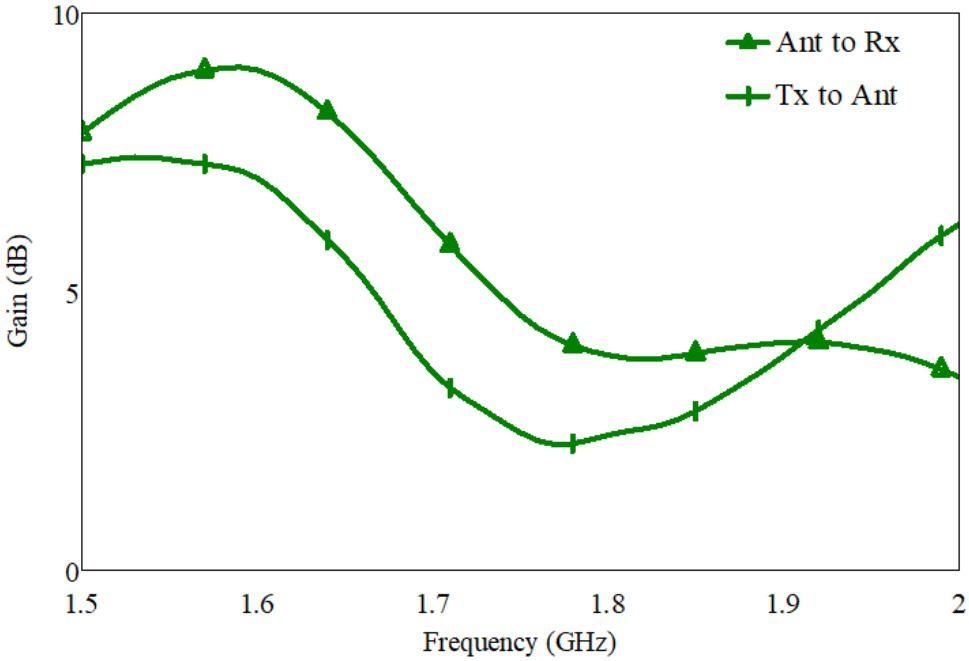

Fig. 5.21 The gain in the transmitter-antenna and antenna-receiver paths

As shown in Fig. 5.21, an average gain of 4dB and 6dB is observed between the two pairs of ports i.e. transmitter-antenna and antenna-receiver respectively. The matching NGD network used to design the ESA has an average 5dB transmission loss. As expected the active circulator gains are sufficient to compensate the matching NGD network losses both in transmission and reception mode, enabling the duplex operation. It is observed that there is a trade-off between these transmission gains and the bandwidth over which isolation can be achieved. Selecting the right filter order for the NGD network and the right amplifier gain and optimisation of the NGD network resistor values will enable the design of an active circulator with the required performance parameters over the required bandwidth. The design process of NGD network is discussed in Section 5.1.1 and Section 5.2.

The reflection coefficients of the proposed active circulator ports are shown in Fig. 5.22. Over the operating bandwidth all three ports have reflection coefficient values less than -10dB. The quarter-wavelength impedance transformer is used at the ports to achieve the 50 Ω port

impedance. The length and width of the feeding microstrip lines should be adjusted for good impedance matching at these ports. For the circulator at the antenna port the reflection coefficient is plotted before the ESA is integrated in Fig. 5.22. The radiation pattern of the ESA is shown in Fig. 5.23. There is a need for further study to improve the radiation performance parameters of the ESA.

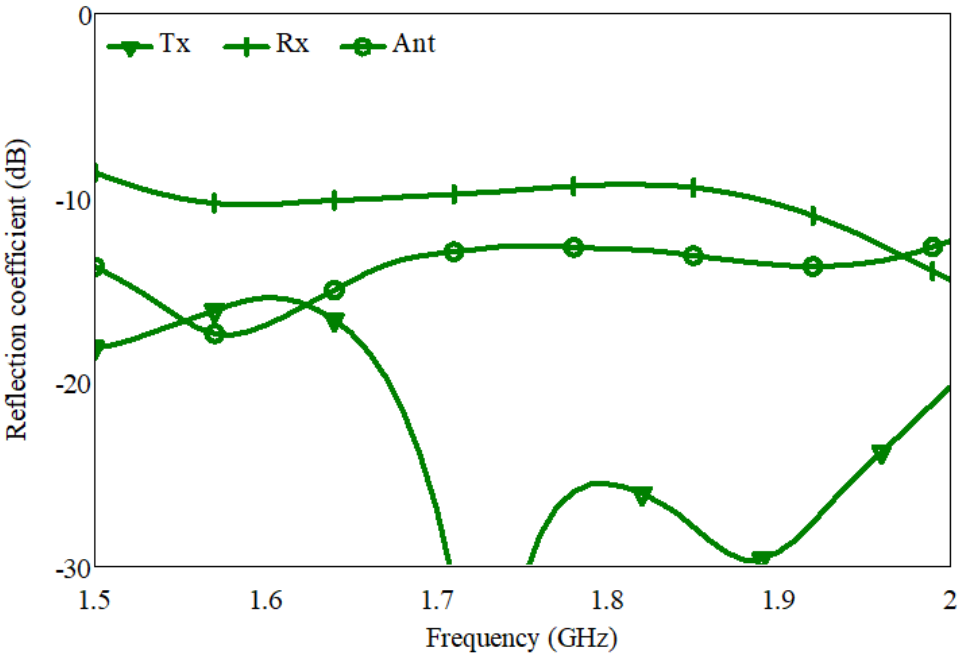

Fig. 5.22 Reflection coefficient characteristics of the three ports of the proposed active circulator.

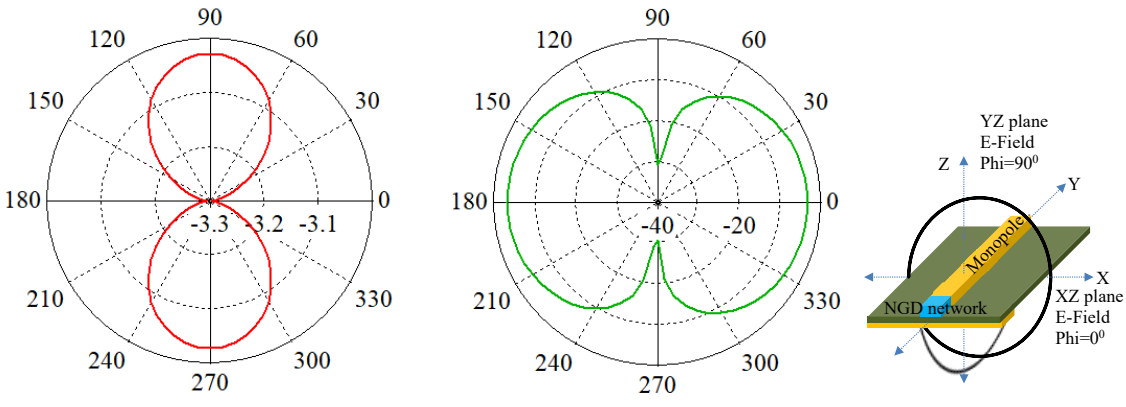

E-Field (Phi-0^{O}) E-Field (Phi-90^{O})

Fig. 5.23 Radiation patterns of an electrically small antenna.

5.3. A Wide Bandwidth Active Circulator Prototype

In the previous section an active circulator integrated with an electrically small monopole is presented. Due to the phase and amplitude sensitivity of the design, fabrication of such a model in an academic setting is challenging. To prove the proposed concept a segmented active circulator model is fabricated. This segmented version of the active circulator is fabricated for two important reasons: 1). To highlight the advantage of the proposed method which enables the use of stable amplifier modules as gain blocks in the active circulator design. 2). The tolerances of surface mount component values, inaccuracies in microstrip line dimensions and inaccuracies of the amplifier bias voltages can be addressed to some extent in the experimental model. The segmented version of an active circulator prototype along with the amplifier module specifications and the measurement setup is presented in Fig. 5.24.

The design approach for simulating and fabricating a segmented active circulator is shown in Fig. 5.24(c). AWR-MS circuit simulator is used to design the circulator using the proposed concept. To maintain accuracy in the dimensions all the microstrip line segments are fabricated and measured. The measured S-parameter files of microstrip lines and amplifiers are used in the simulation in the respective places. As a next step amplifiers and fabricated microstrip line segments are joined using SMA adaptors to form a ring configuration without the NGD networks at the receiver junction. This forms a 4 port structure and in the measurement a 4-port S-parameter file is generated. In this way any phase and loss resulting from extra lengths are taken into account. As a final step the NGD networks at the receiver junction are optimised to achieve the desired active quasi circulator operation. In light of the facilities available in house and to maintain reasonable microstrip line widths a Rogers RT5880 substrate with 2.2 permittivity is used for the prototype.

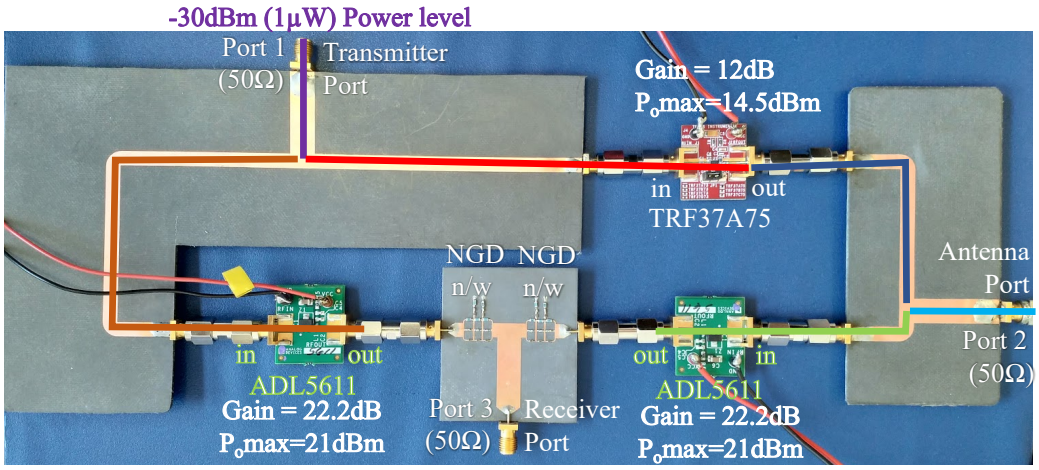

(a) Active circulator prototype

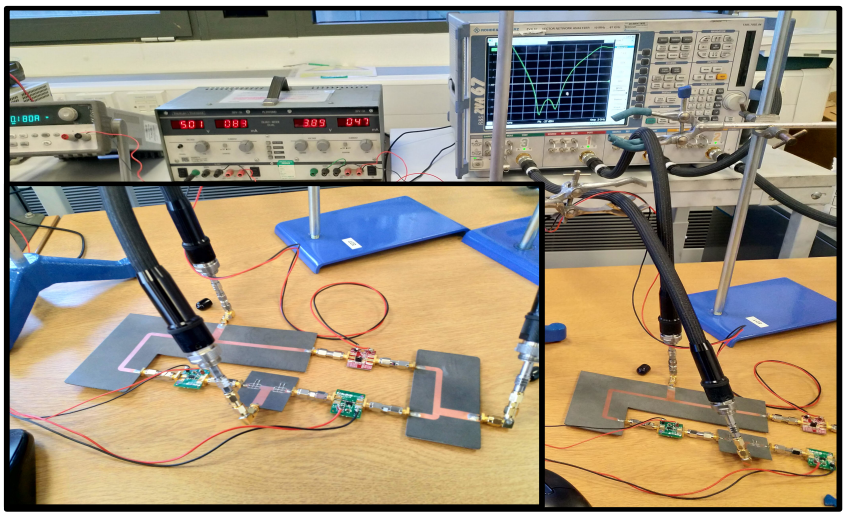

(b) Measurement setup

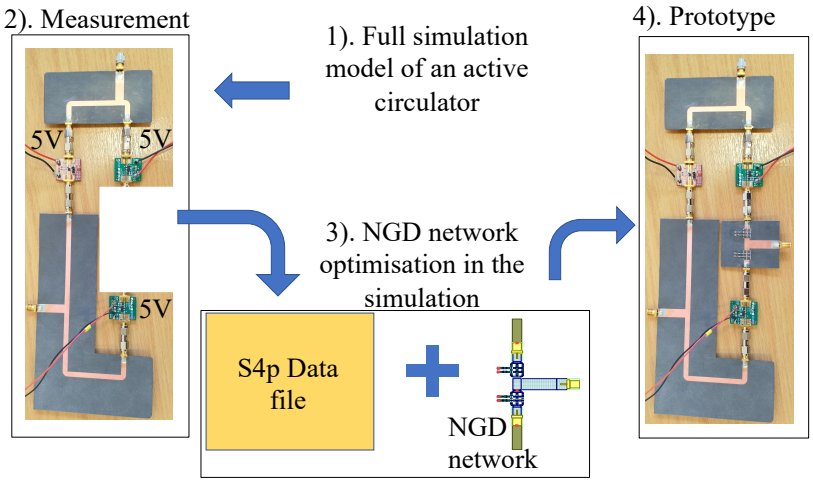

(c) The design procedure of the prototype (Rogers 5880 substrate)

Fig. 5.24 The prototype of an active circulator

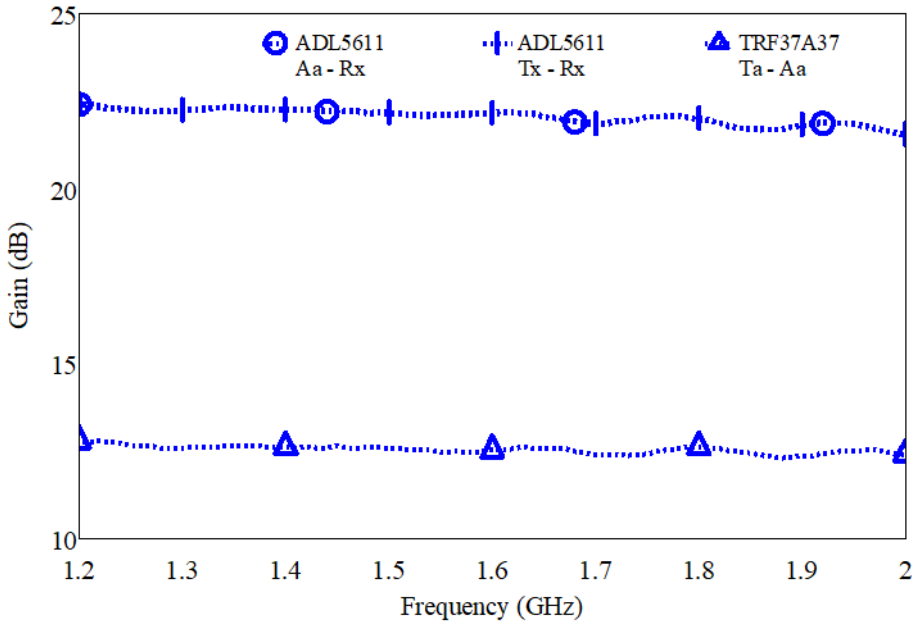

(a) The measured gain characteristics of three amplifiers

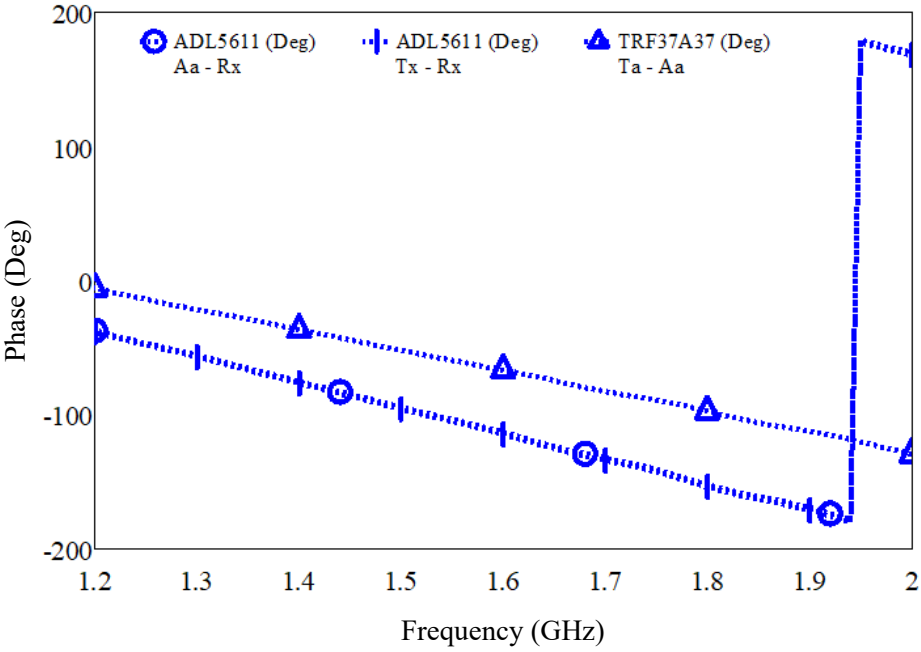

(b) Measured transmission phase characteristics of three amplifiers

Fig. 5.25 The characteristics of the three amplifiers used for the active circulator.

The transmission gain and loss characteristics of the three amplifiers employed in the active circulator design are shown in Fig. 5.25. Two ADL5611 and one TRF37A75 are used in their respective places as shown in Fig. 5.24(a).

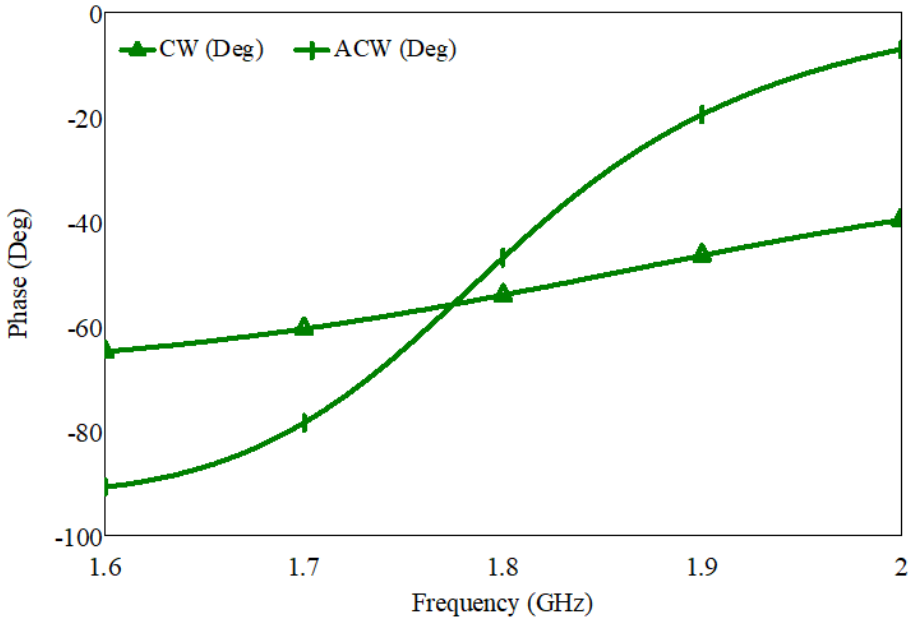

(a) Phase characteristics of NGD networks in CW and ACW paths

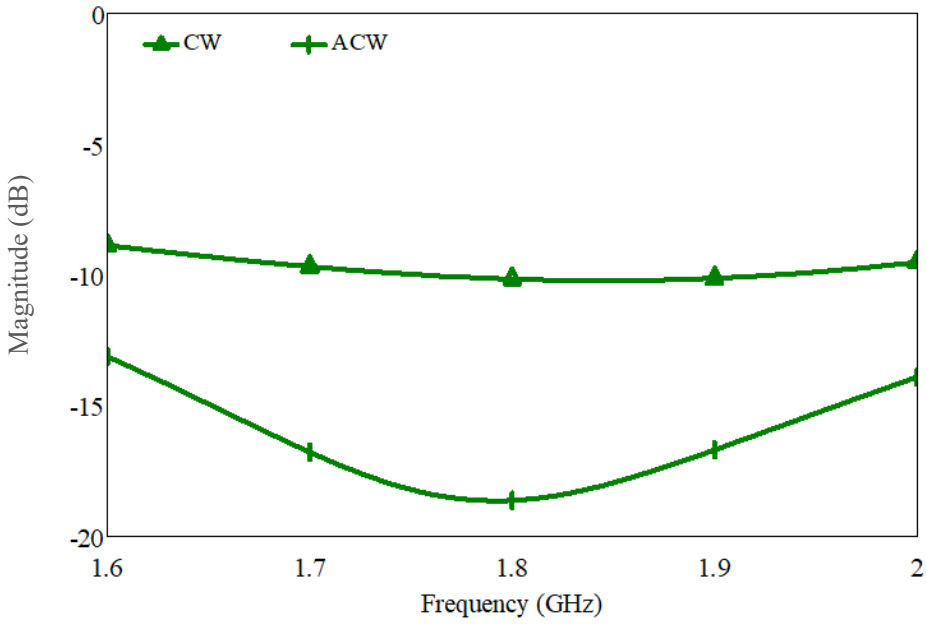

(b) Loss characteristics of NGD networks in CW and ACW paths

Fig. 5.26 The transmission coefficient phase and magnitude characteristics of NGD networks employed in clockwise and anti-clockwise paths (simulation).

The NGD characteristics of the two networks used in CW and ACW paths are shown in Fig. 5. 26. Different phase curve slopes and losses can be observed. The CW and ACW paths have

different lengths and different amounts of attenuations, hence the respective NGD networks are optimised such that the signal cancellation condition is established over a wide bandwidth.

Table: 5.2 The resistor, inductor and capacitor lumped element values for NGD networks. The topology shown in Fig.5.16(a) is used to implement these networks.
(Units : R - Ω, L - nH, C - pF)

Elements	Clock wise	Anti-clock wise
R_{S1}	500	500
L_{S1}	1	1
C_{S1}	12	12
R_{S2}	90	59
L_{S2}	3.3	3.3
C_{S2}	1.2	1.2
R_{S3}	5	970
L_{S3}	1	1
C_{S3}	8.2	8.2
R_{P1}	77	81
L_{P1}	5.1	5.1
C_{P1}	0.9	0.9
R_{P2}	600	13
L_{P2}	5.1	5.1
C_{P2}	0.9	0.9

The lumped element values of the NGD networks are shown in Table 5.2 above. A 5^{th} order Butterworth filter with added resistors is used to design the NGD networks. The 5^{th} order topology offers 5 resistors as the optimisation parameters and it is advantageous to have more optimisable parameters. Also the amplifiers have enough gain to compensate the transmission

loss of the NGD network. The order of the filter for the design of the NGD network should be selected to balance the flexibility in the optimisation process and transmission loss compensation.

A. Isolation between transmitter and receiver

The isolation characteristics are shown in Fig. 5.27. Though the transmitter and receiver are physically connected, they are electrically isolated. The -20dB measured isolation over 200MHz (14% bandwidth at 1.5GHz) bandwidth is achieved. The advantage of using NGD networks is clearly demonstrated when the results are compared with a similar design without a NGD network (which reported a bandwidth of 7MHz [1]).

It is observed that the isolation could be further improved by optimising the resistor values for a trade-off of insertion loss in the paths of transmitter~antenna, antenna~receiver and operating bandwidth. To improve the bandwidth a higher order filter with wider stop bandwidth should be selected for NGD network design. Amplifiers with higher gains are also needed to avoid the insertion losses.

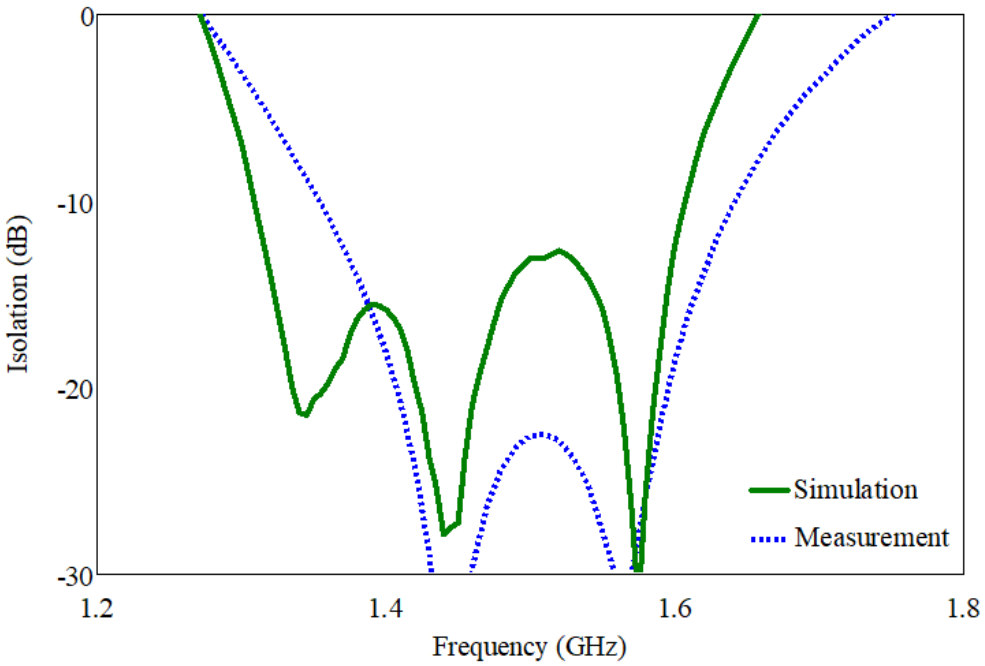

Fig. 5.27 Isolation between transmitter and receiver

It is observed that the isolation characteristics in measurement and simulation have disagreement. Due to the phase and amplitude sensitivity of the design, to build a prototype, the active circulator was designed in segments. In simulation by integrating the segments the desirable results were obtained. However, in the fabricated prototype there are various factors which caused the uncertainty. For the fabricated prototype surface mount components with a tolerance ranging from 0.1% to 5% are used. This will have an effect on the behaviour of the NGD network. The PCB layout and Via has parasitic effects. There is some degree of inaccuracy in modelling the SMA connector and SMA adaptors which are used to join the segments. The inability to guarantee the exact reproduction of the amplifier bias used for simulation in the measurement is another factor. At the operating frequency an extra length of 1 mm will result in a phase change of 4^0. All these factors affected the performance of the prototype to some extent.

B. Reflection coefficient characteristics of the three ports

The reflection coefficient characteristics of the transmitter port, receiver port and antenna port are shown in Fig. 5.28. The transmitter port and antenna port have good reflection coefficient characteristics. The reflection coefficient of the receiver port is around 5dB. At the receiver junction, where the CW and ACW paths are joining the resultant impedance is 25Ω. The quarter wavelength transformation from 25Ω to 50Ω used at the receiver junction and the NGD network optimisation are having an impact on the impedance characteristics of the receiver port. It is observed that the ports impedance matching can be improved by optimising the length and width of the quarter wavelength feeding microstrip lines.

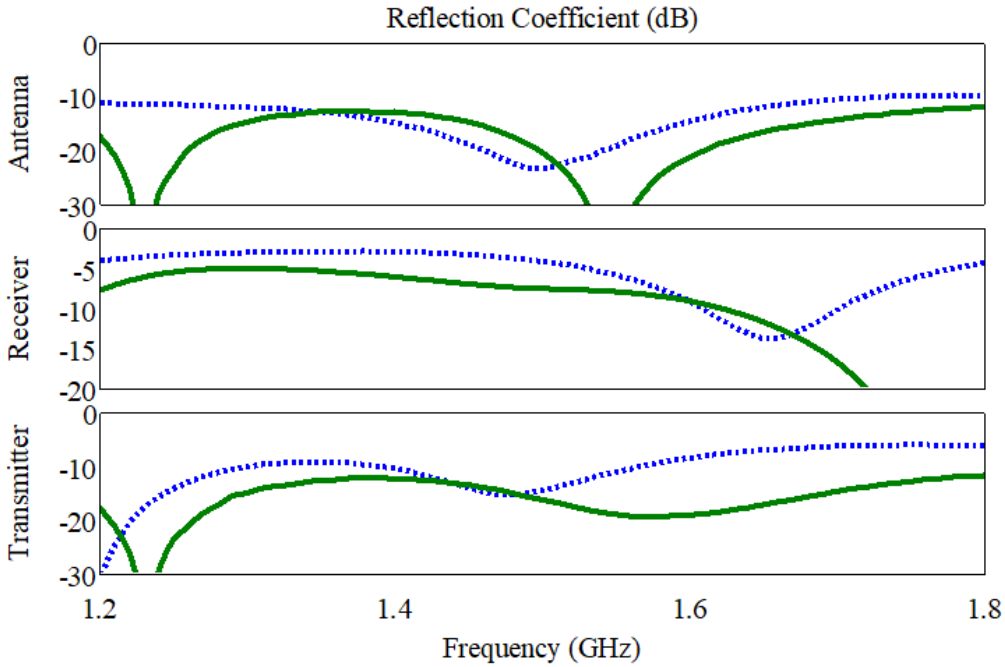

Fig. 5.28 Port reflection coefficient characteristics

C. Gains among the three ports

The gain characteristics between transmitter and antenna and antenna and receiver are shown in Fig. 5.29. In simulation these are around 5dB. An insertion loss from the transmitter to the antenna is observed in the measurement. The fabrication challenges of the printed microstrip lines and tolerances of the lumped elements used in the prototype changed the phase condition needed for signal cancellation. By changing the bias voltage of the amplifiers signal cancellation has been achieved and consequently insertion loss is also introduced between ports. According to the simulation model, it is clear that despite the losses in the NGD networks, amplifiers in the respective paths between the antenna and the receiver are able to offer lossless transmission of the signal from the antenna to the receiver. The proposed concept uses circuits that are compatible with MMIC technology. By implementing the NGD network based active circulator in MMIC technology more accurate design and better results can be achieved.

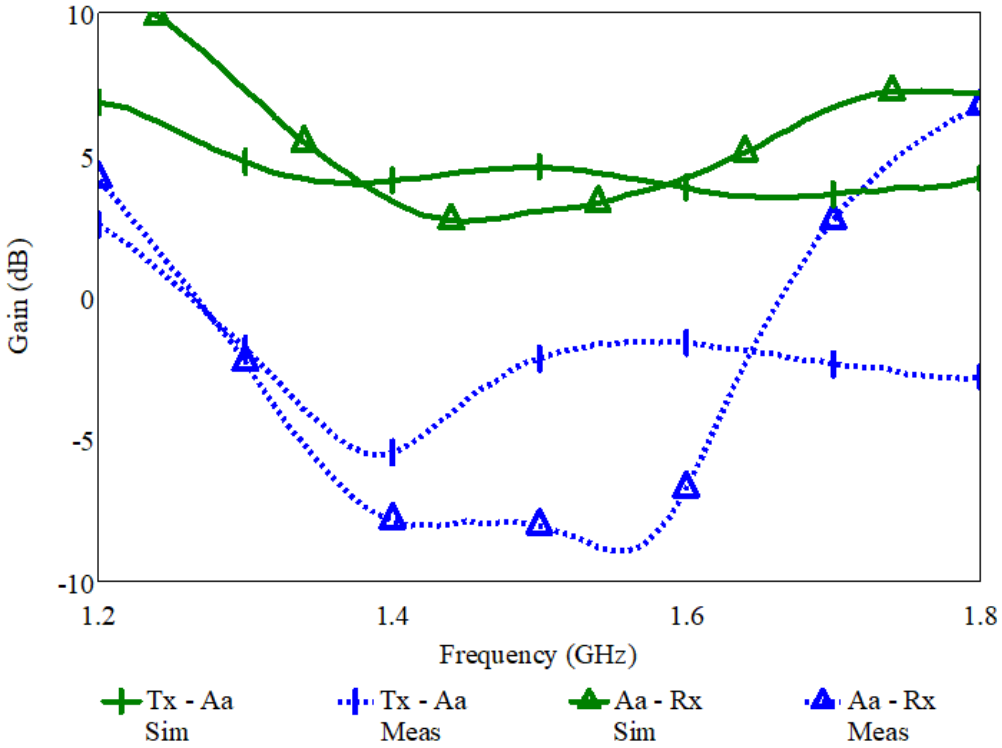

Fig. 5.29 Prototype gain characteristics.

D. Noise figure between antenna and receiver

The noise figure at the receiver is required to be as low as possible to maintain a good signal to noise ratio. The lumped element NGD networks are employed for signal cancellation in the CW and ACW paths from the transmitter to the receiver. An additional thermal noise is introduced by the NGD networks in the paths that lead to the receiver port. However it is evident from Fig. 5.30 that the noise figure is below 5dB between the antenna and the receiver in the operating bandwidth. In this case the noise figure of the NGD network which is in the CW path between the antenna and the receiver ports is shown. In the simulation the amplifier has no noise data in its S-parameter file. Therefore, the noise figure introduced by the NGD network alone is clearly demonstrated.

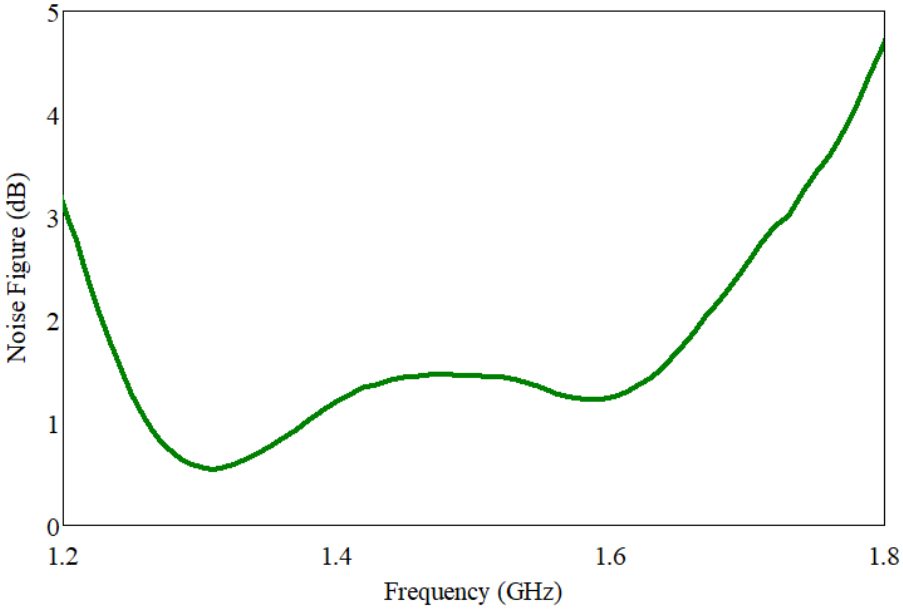

Fig. 5.30 Noise characteristics at receiver port

The NGD network elements can be optimised for a reduced noise figure at the receiver for a trade-off of operational bandwidth. Another source of noise in these paths is the amplifier. With the availability of low noise amplifiers the noise figure can be reduced for the amplifier circuit. Moreover, the proposed design approach enables the use of an amplifier that has the best performance parameters. In the experimental modal ADL5611 amplifier with only 2dB noise figure is used. The performance parameters of the proposed models are given in Table 5.3.

More fabricated samples and their measurement details are discussed in Appendix A. Also a study on active circulator characteristics with varying amplifier bias is presented for the model given in Fig. 5 24. For these prototypes, the experimental results indicate that gains and isolation over a wide bandwidth is possible but not both at same time due to the surface mount component tolerances, parasitic effects, amplifier biasing inaccuracies, modelling of SMA connectors and adaptors, and soldering imperfections. Moreover, the fabrication challenges are further explored. It is evident that the NGD network based approach has enhanced the bandwidth of hybrid ring

active circulator. It has also offered design flexibility in using "off the shelf" stable amplifiers, offering a possibility to address stability issues.

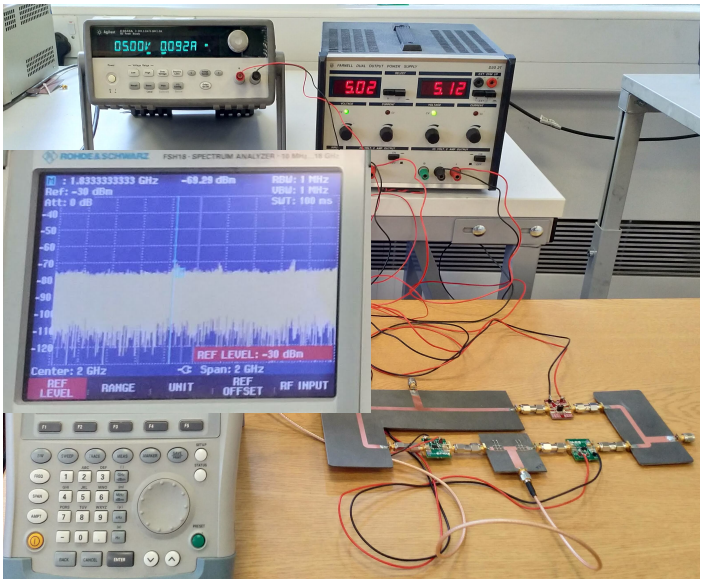

(a) Stability analysis using spectrum analyser at antenna port

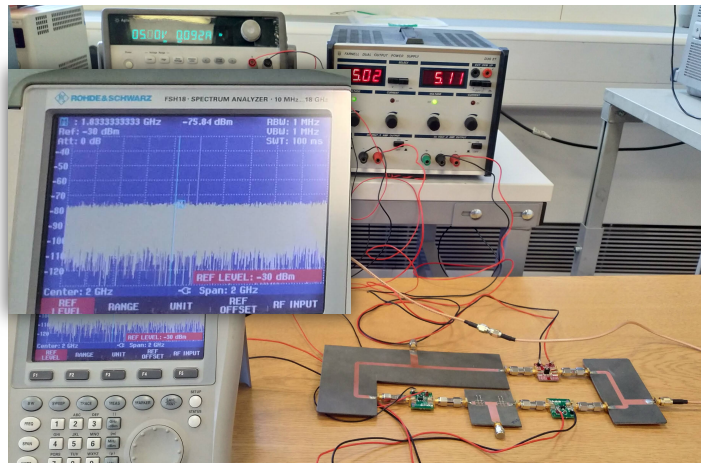

(b) Stability analysis using spectrum analyser at receiver port

Fig. 5.31 Stability analysis of the prototype

The stability of the fabricated active circulator prototype is verified using the spectrum analyser. The unilateral amplifiers have created a unidirectional signal path between any two ports. The reverse isolation of these amplifiers is sufficient enough to block any loop formation in the ring

configuration of the circulator. As shown in Fig. 5.31 the fabricated circulator is stable in transmission and reception modes.

Table 5.3 Comparison of proposed active circulator performance parameters

* TRF37A75 amplifier output IP3, ^ TRF35A75 amplifier output 1dB compression point

	[1]	Quasi active circulator Simulation	Quasi active circulator Measured	Quasi active circulator integrated with monopole
BW (GHz, %)	3.745	1.4 ~ 1.6 (14) (Fig. 5.27)	1.4 ~ 1.6 (14) (Fig. 5.27)	1.69 ~ 1.93 (16) (Fig. 5.20)
Tx- Rx Iso (dB)	27	12 (Fig. 5.27)	20 (Fig. 5.27)	19 (Fig. 5.20)
Tx-ANT average gain (dB)	10	5 (Fig. 5.29)	-3 (Fig. 5.29)	4.5 (Fig. 5.21)
ANT-Rx average gain (dB)	4	5 (Fig. 5.29)	-7 (Fig. 5.29)	6 (Fig. 5.21)
Peak P_{sat} (dBm)	n/a	<18	<18	<18
Tx-ANT $IIP3/IP_{1dB}$ (dBm)	n/a	32.5*/19^	32.5*/19^	32.5*/19^
ANT- Rx NF (dB)	n/a	<5	n/a	<5
Technology	Hybrid	Hybrid	Hybrid	Hybrid

Observations:

The design in [1] is a hybrid ring circulator with an integrated antenna but without NGD networks. The use of the NGD network in the hybrid ring active circulator configuration improved the operating bandwidth from 7 MHz to 200 MHz. Duplex communication over a wide bandwidth is achieved by integrating an ESA with an active circulator. The losses of the matching NGD network that is used for designing the ESA are compensated by the gains of the active circulator. The ability to optimise the resistor values of the NGD network in this design approach has improved the overall design flexibility. In author's knowledge this is first of its kind.

List of References

[1] C. Kalialakis, M. J. Cryan, P. S. Hall and P. Gardner, "Analysis and design of integrated active circulator antennas " *IEEE Transactions on Microwave Theory and Techniques,* vol. 48, no. 6, pp. 1017-1023, 2000.

[2] D. M. Pozar, "Microwave and RF Design of Wireless System," *John Wiley & Sons, INC, New York,* 2001.

[3] H. Mirzaei and G. V. Eleftheriades, "Realizing Non-Foster Reactive Elements Using Negative-Group-Delay Networks," *IEEE Transactions on Microwave Theory and Techniques,* vol. 61, no. 12, pp. 4322-4332, 2013.

Chapter 6 NGD Based Wideband Fabry-Perot Cavity Antenna With Reduced Beam Squint

Directional antennas are essential in satellite communication, radar applications and in point-to-point communication systems. Array antennas are the conventional designs used in these applications for high directional radiation performance. Depending on the type of elements used array antennas can be complicated, bulky and feeding can be challenging. The Fabry-Perot cavity antennas are low profile structures with good directional properties[1, 2] as discussed in chapter 2. However beam squint is a problem that needs addressing in these antennas. In this chapter the procedure of introducing negative group delay (NGD) behaviour in one of the layers of the cavity antenna to reduce the beam squint is presented.

Fabry-Perot Cavity antennas exhibit highly directional properties. Wide bandwidth cavity antennas can be designed. Although the radiation properties such as directivity and gain are high over this bandwidth the main lobe direction will shift with frequency. The following Fig. 6.1 shows the proposed cavity antenna model with a NGD based surface to reduce beam squint.

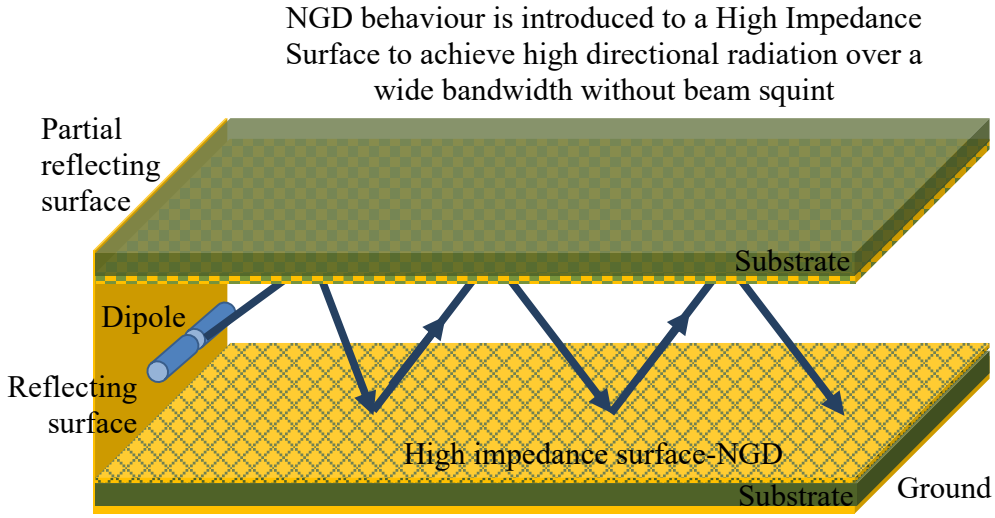

Fig. 6.1 Proposed Fabry-Perot cavity antenna

A Fabry-Perot cavity antenna consists of a reflecting surface and a partially reflecting surface joined at one end by a reflecting metallic wall. A dipole is used as a primary source of radiation near the reflecting metallic wall. As the radiation energy proceeds forwards towards the open end multiple reflections will take place in the cavity. Some energy will leak through the partially reflective upper surface resulting in radiation perpendicular to this surface. When a certain phase condition is established between the two surfaces of the cavity, the energy that is undergoing multiple reflections in the cavity will contribute to a highly directional radiation in boresight. The following Eq. 6.1 is the phase condition that needs to be satisfied in order to have highly directional boresight radiation[3-5].

$$\emptyset_{\mathrm{PRS}} + \emptyset_{\mathrm{HIS}} - \frac{4\pi}{\lambda} \mathrm{h} \cos\theta = -2\pi \mathrm{N} \qquad (6.1)$$

$$\emptyset_{\mathrm{PRS}} - \text{Partial Reflective Surface Phase}$$

$$\emptyset_{\mathrm{HIS}} - \text{High Impedance Surface Phase}$$

$$\mathrm{h} - \text{height of cavity}$$

$$\theta - \text{main lobe direction with respect to normal of PRS surface}$$

$$\mathrm{N} = 0,1,2 \ldots$$

As shown in Fig. 6.2 (this figure is same as Fig. 2.2, reproduced here for convenience) various modifications to the cavity structure are reported in literature in order to improve the radiation properties and bandwidth and to reduce the size. Various changes are made to the bottom surface to improve the operational bandwidth of the cavity antenna. A multilayer partially reflective surface can give a wider operational bandwidth, but the structure will be bulky. In addition as the phase characteristics of the cavity surfaces change with frequency, the main lobe direction also changes. Therefore even though a highly directional wide bandwidth cavity antenna design is possible, it still suffers from beam squint.

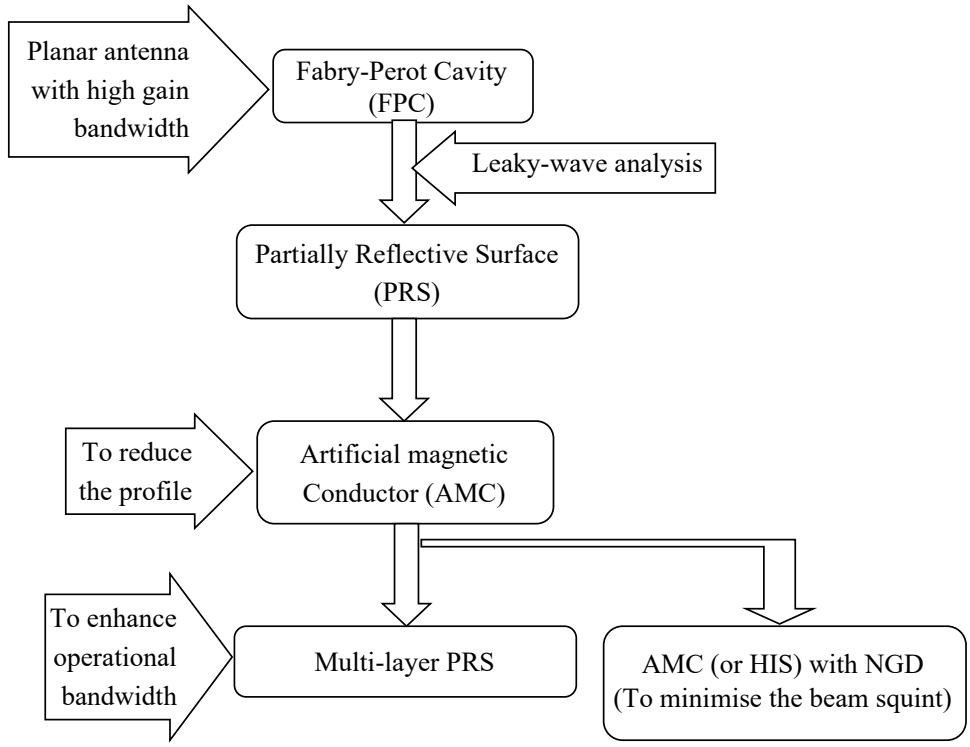

Fig. 6.2 Development of Fabry-Perot Cavity antenna

The objective is to design a high impedance structure with NGD behaviour such that the phase condition can be established over a wide bandwidth. This will result in highly directional radiation properties over a wide bandwidth with reduced beam squint as shown in Fig. 6.3. This method offers a low profile solution.

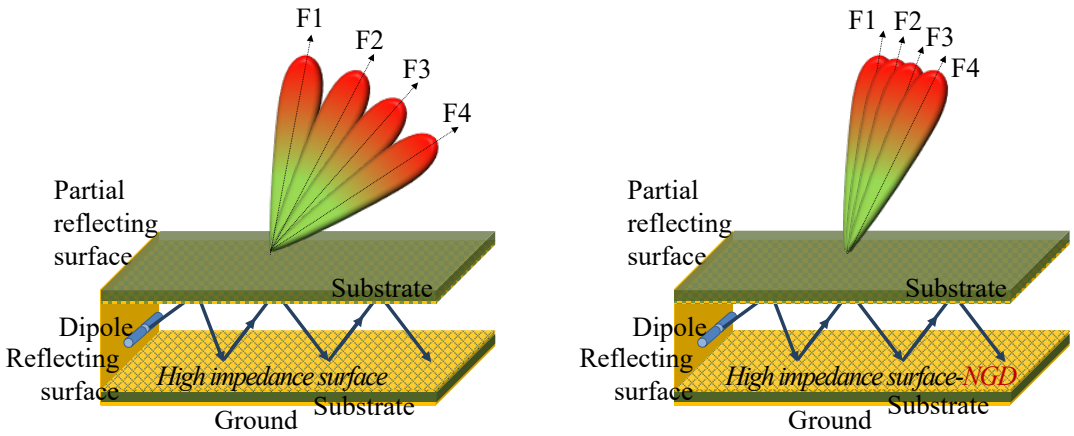

Fig. 6.3 Proposed Fabry-Perot cavity antenna with NGD based HIS to reduce the beam squint

6.1. Fabry-Perot Cavity Antenna: PRS and Ground Plane

The cavity antenna is designed with a partial reflective surface (PRS) and metal ground plane to operate at 10GHz. The PRS is designed by a square conductor patch of length 13.10mm printed on a substrate of 2.2 permittivity and 0.79mm thickness, with 14mm periodicity in both X and Y direction as shown in Fig. 6.4(a). A metal ground plane and PRS are used to form the cavity with a height of 13.89mm to satisfy the phase condition given in Eq. 6.1. The unit cell simulation results are used to observe the phase and loss characteristics of each surface, as shown in Fig. 6.4-6.5, and the full wave model of the cavity antenna is shown in Fig. 6.6. Over the bandwidth 11.2 to 11.6 GHz the main lobe has a beam squint of 2.75^0 per 100MHz.

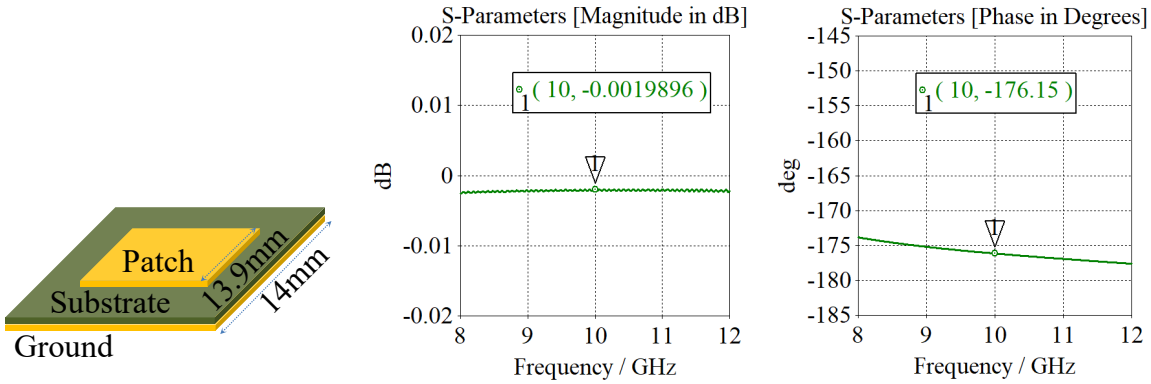

(a) PRS unit cell (b) Magnitude response (c) Phase response

Fig. 6.4 Partial reflective surface characteristics

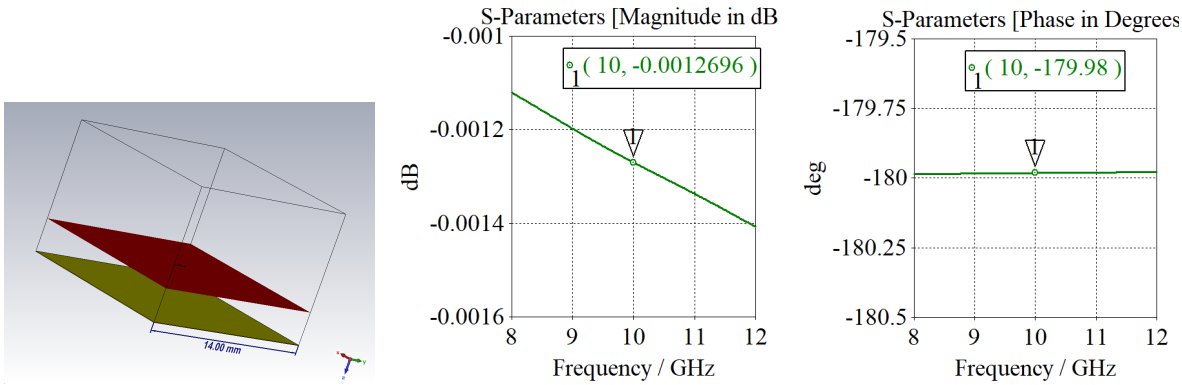

(a) Metal ground unit cell (b) Magnitude response (c) Phase response

Fig. 6.5 Metal ground surface characteristics

At 11.4GHz a maximum directivity of 22.2dBi and a gain of 15.8dB are observed as shown in Fig. 6.7.

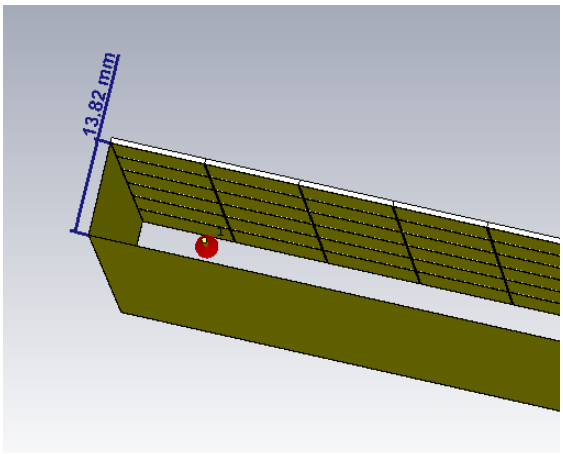

(a) PRS - Metal ground cavity antenna

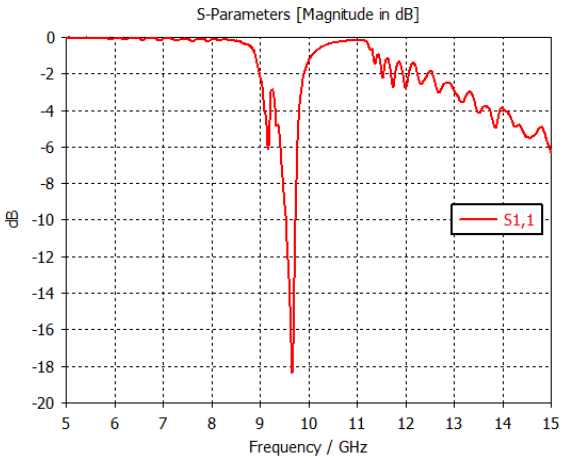

(b) Return loss of cavity antenna

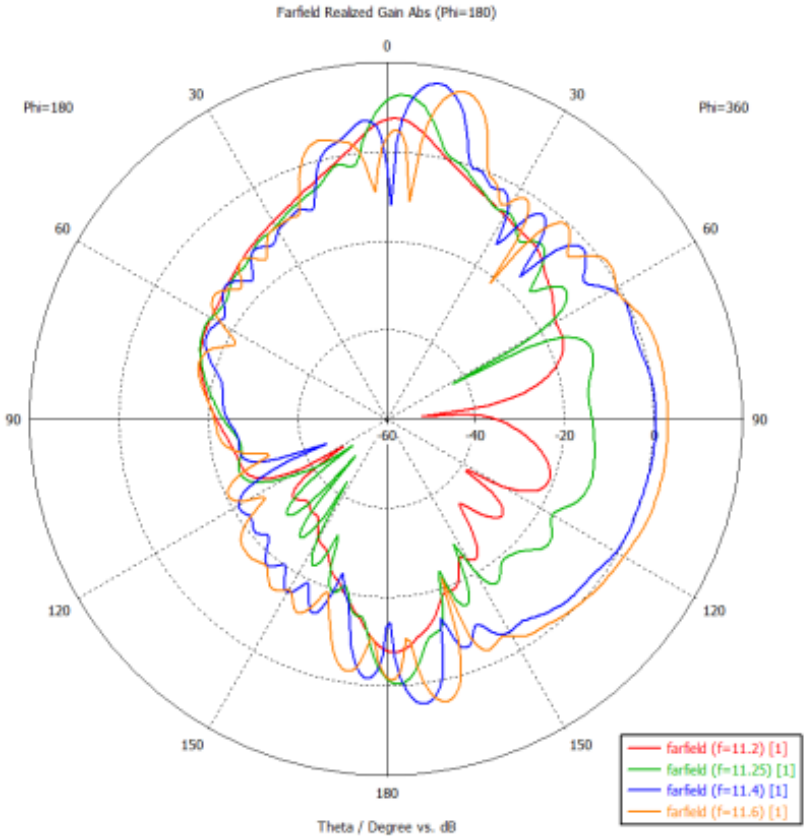

(c) Radiation pattern of cavity antenna

Fig. 6.6 PRS- Metal ground cavity antenna radiation properties

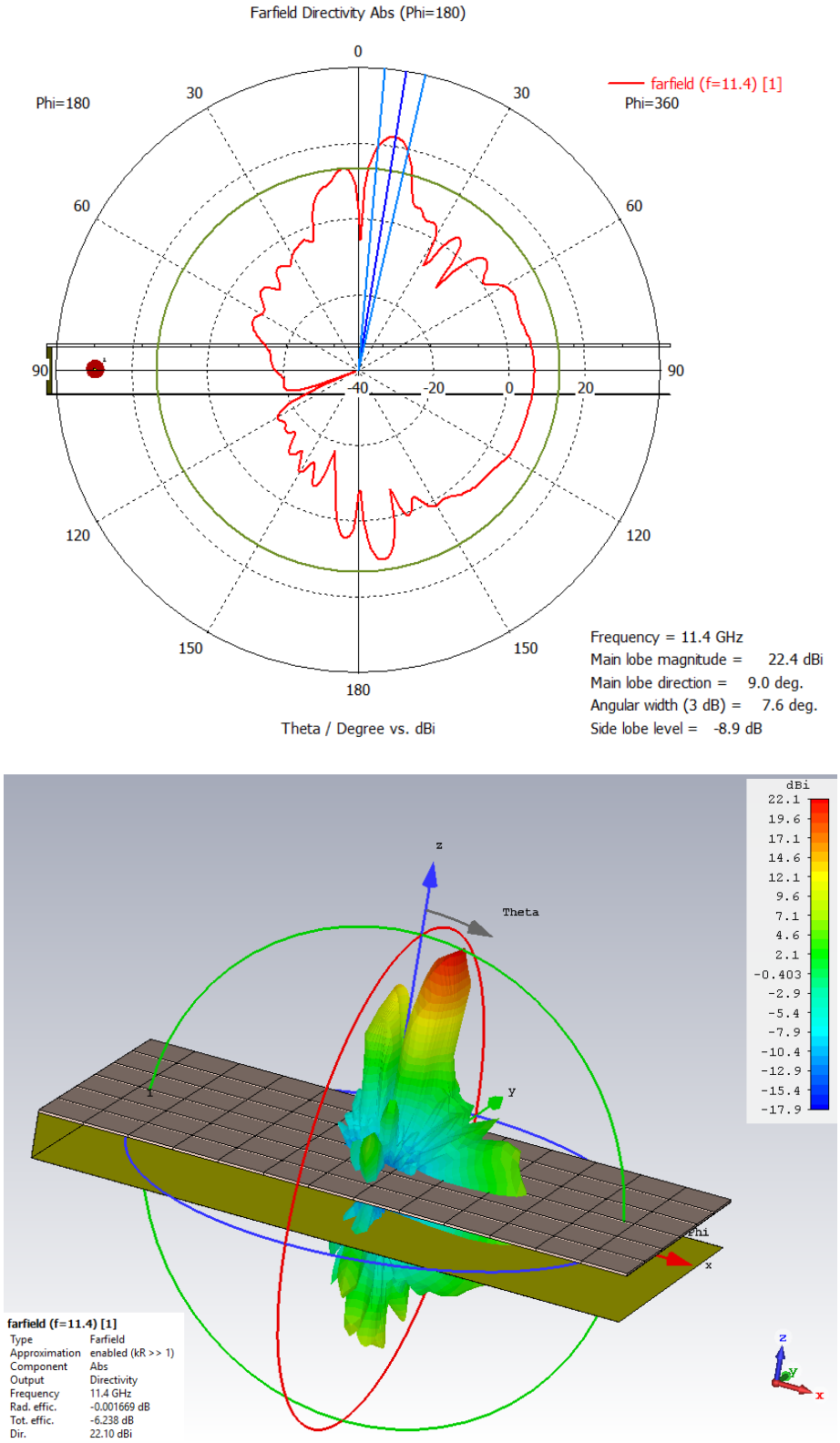

Fig. 6.7 (a) Radiation pattern of PRS – Metal ground cavity antenna

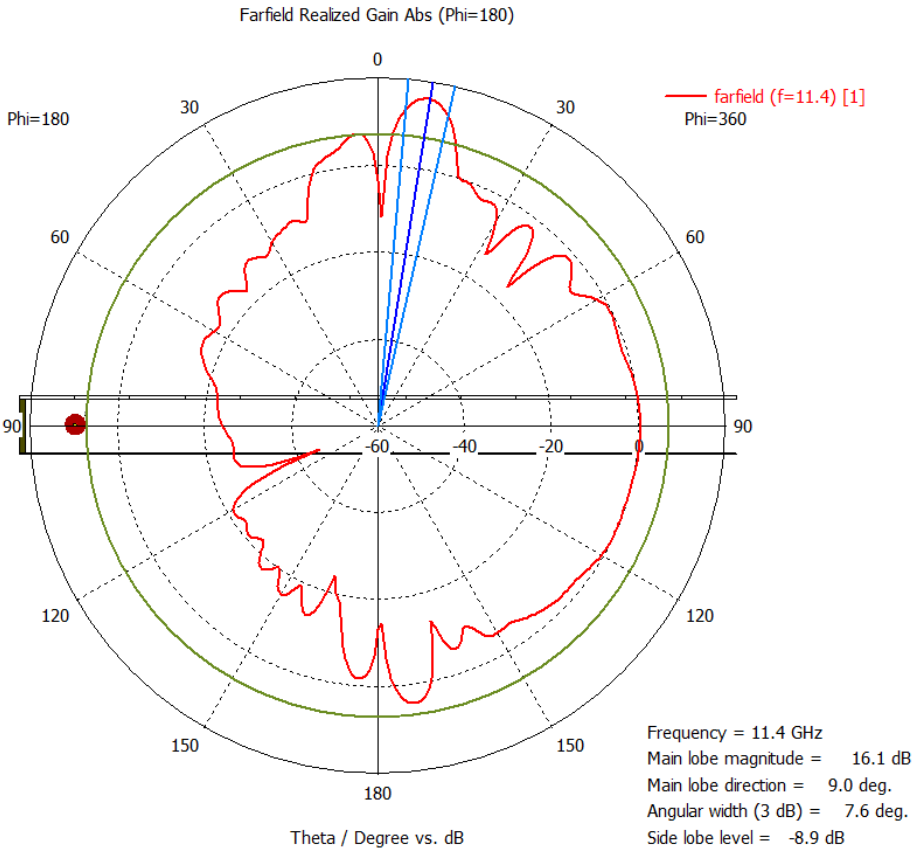

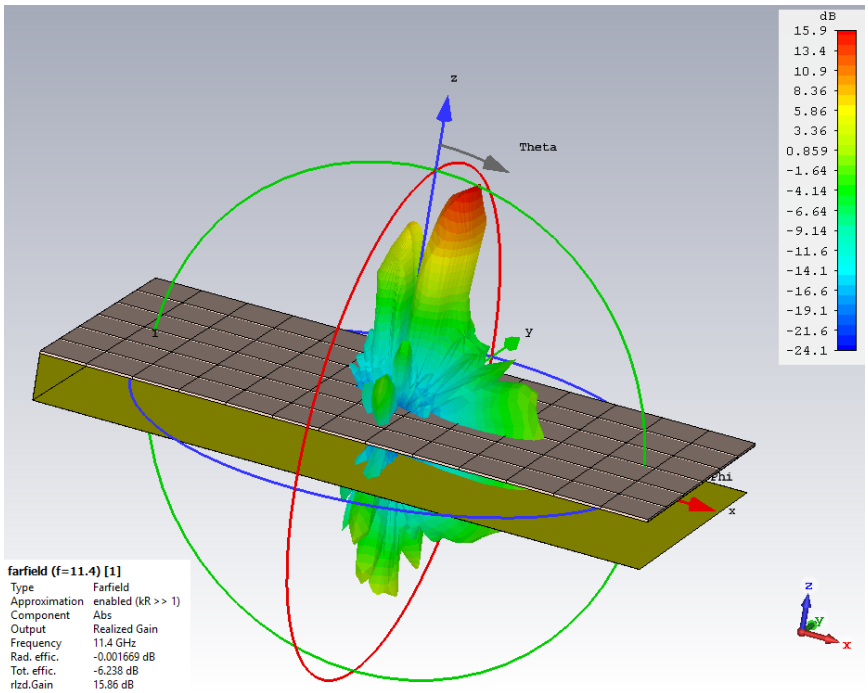

Fig. 6.7 (b) Radiation pattern of PRS – Metal ground cavity antenna

6.2. Fabry-Perot Cavity Antenna: PRS and High Impedance Surface

The High Impedance Surface(HIS) is designed by a square conductor patch of length 8.82 mm printed on a substrate of 2.2 permittivity and 0.79mm thickness, with 14mm periodicity in both X and Y direction. With the HIS and PRS, that is designed in section 6.1, the cavity is formed with a height of 13.03mm to satisfy the phase condition given in Eq. 6.1. The unit cell simulation results are used to observe the phase and loss characteristics of the HIS, as shown in Fig. 6.8, and the full wave model of the cavity antenna is shown in Fig. 6.9. Over the bandwidth 9.8 to 10.2 GHz the main lobe has a beam squint of 6^0 per 100MHz. At 10GHz a maximum directivity of 20dBi and a gain of 17.6 dBi are observed as shown in Fig. 6.10.

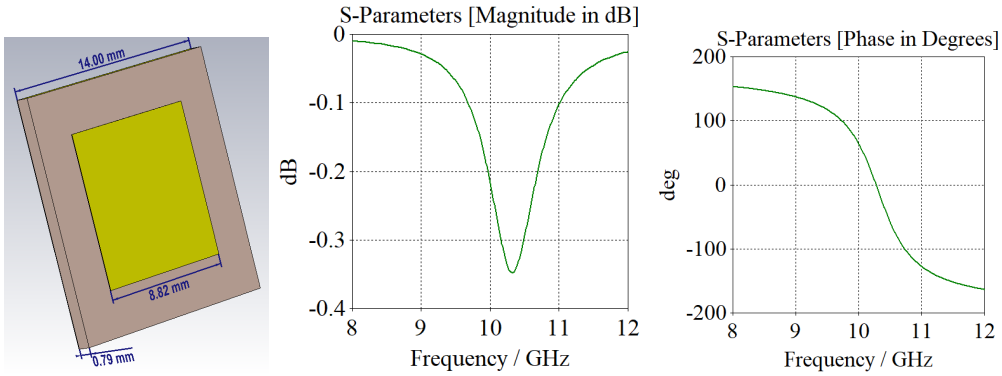

(a) HIS unit cell (b) Magnitude response (c) Phase response

Fig. 6.8 High Impedance surface characteristics

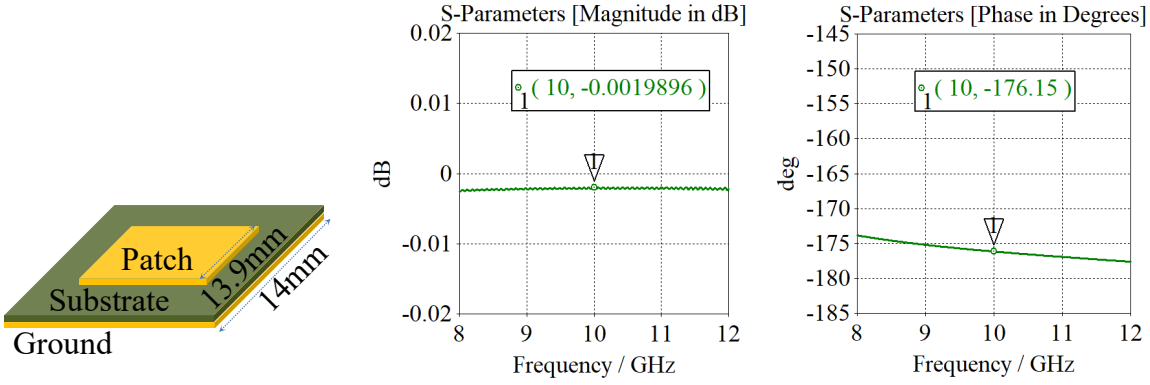

(b) PRS unit cell (b) Magnitude response (c) Phase response

Fig. 6.4 Partial reflective surface characteristics

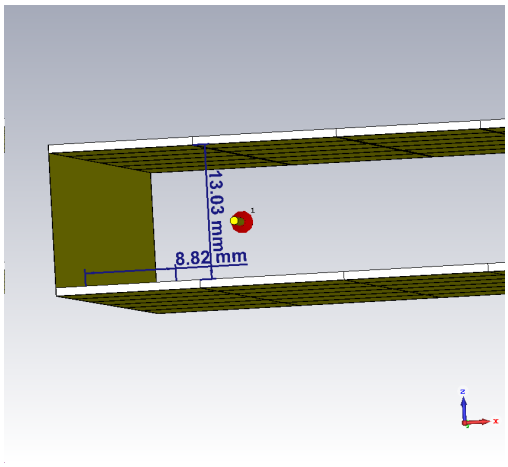

(a) PRS - HIS cavity antenna

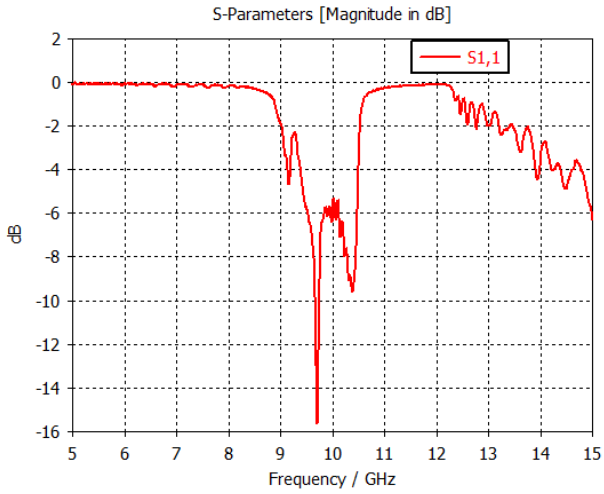

(b) Return loss of cavity antenna

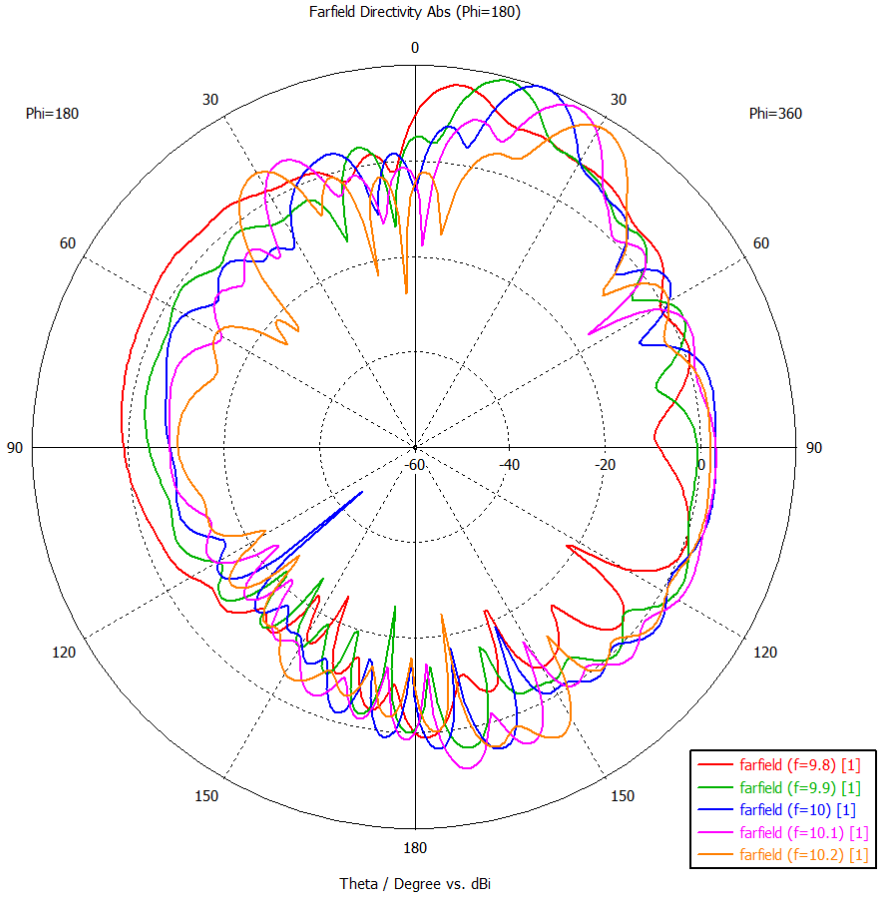

(c) Radiation pattern

Fig. 6.9 PRS- HIS cavity antenna

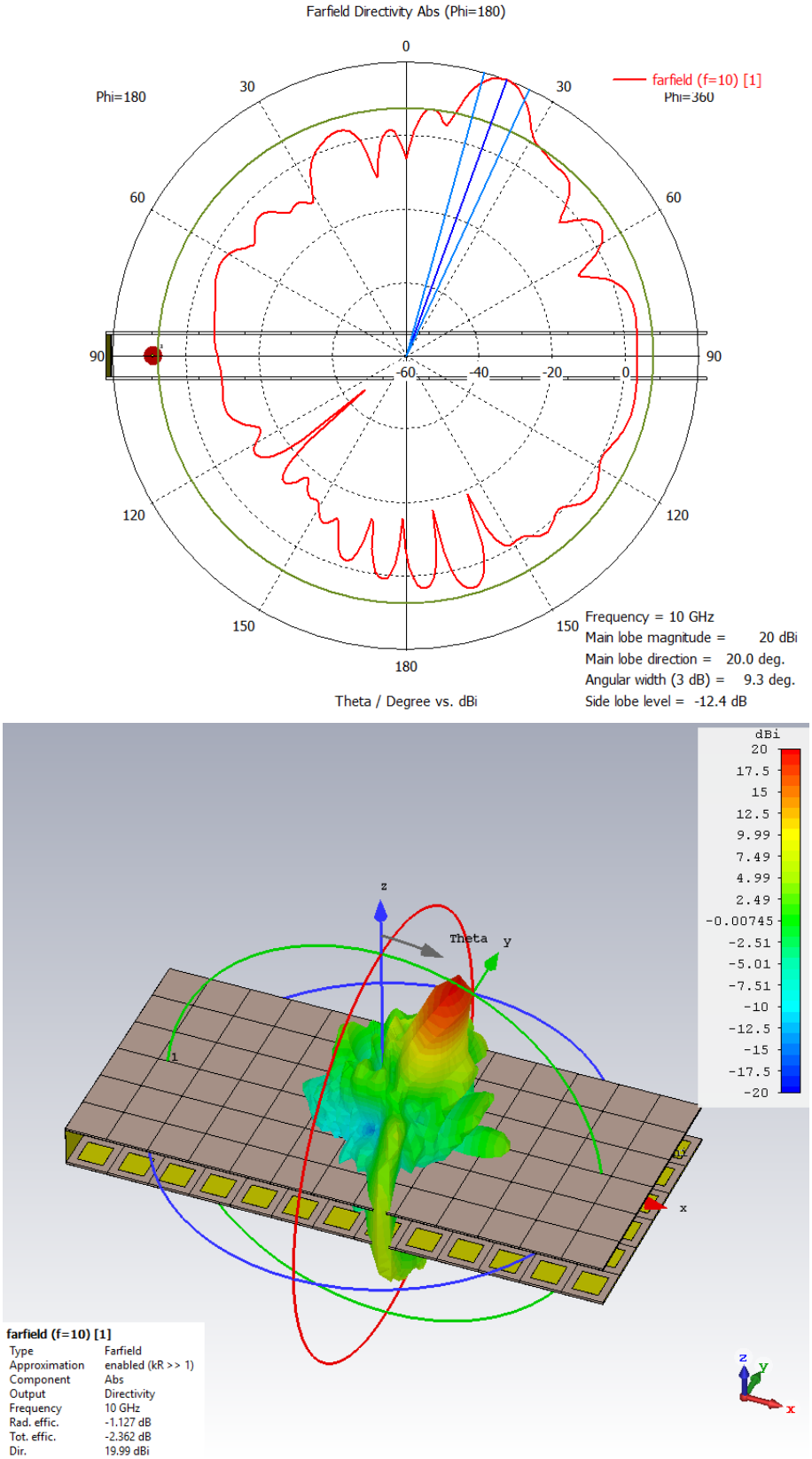

Fig. 6.10 (a) Radiation pattern of PRS – HIS cavity antenna

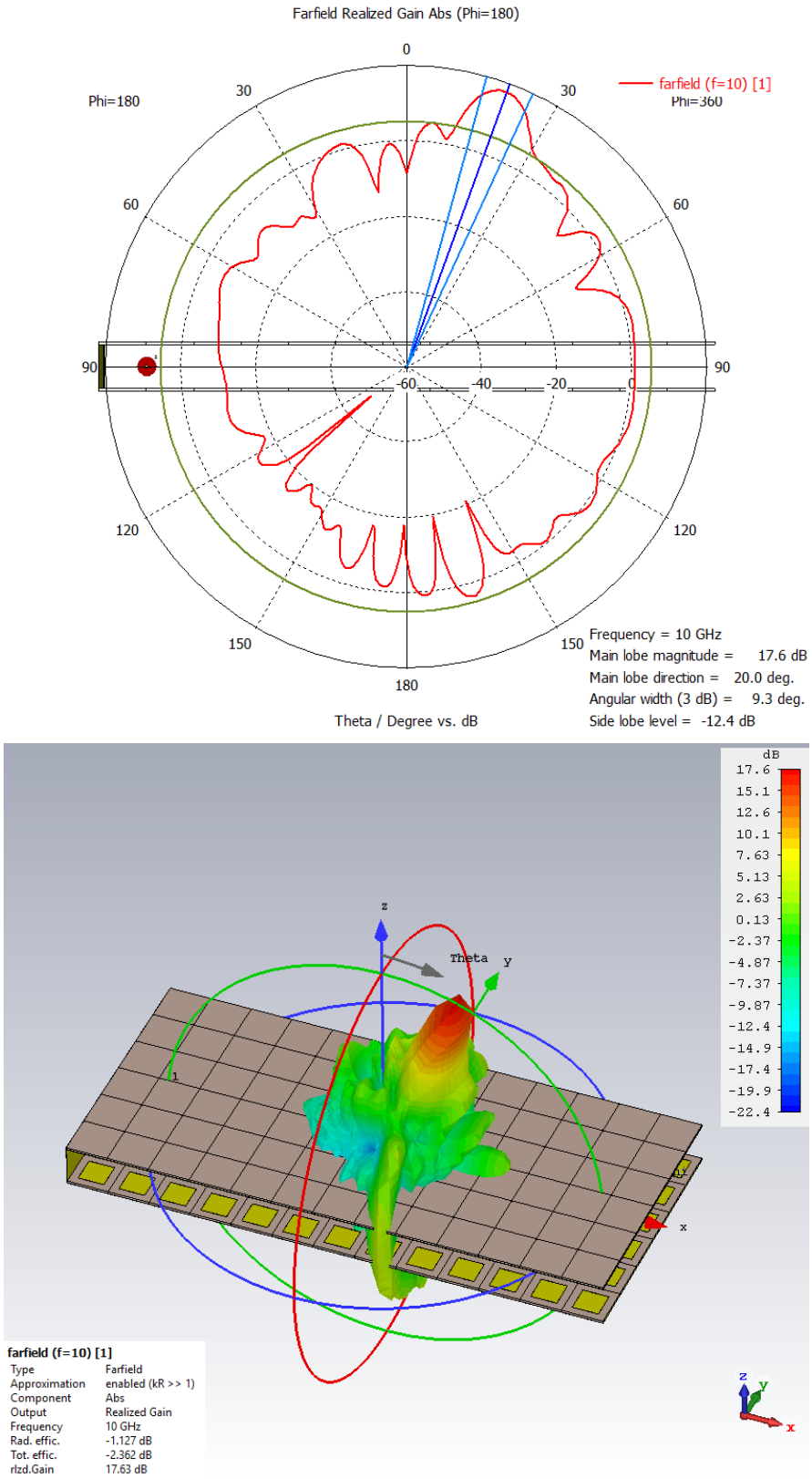

Fig. 6.10 (b) Radiation pattern of PRS – HIS cavity antenna

6.3. Fabry-Perot Cavity Antenna: PRS and HIS with Negative Group Delay Behaviour

NGD behaviour is introduced to the High Impedance Surface (HIS) by replacing the conductive patch with a lossy metal of 11.2Ω sheet resistance. In CST software a layer of unit cell is parameterised to get different sheet resistances. The sheet resistance and the dimension of the unit cell should be optimised, such that the phase response of the NGD based HIS satisfies Eq. 6.1 over 9.8 to 10.2 GHz bandwidth, as shown in Fig. 6.11. The theoretical and simulation phase responses of the NGD-HIS over the required bandwidth, to satisfy Eq. 6.1, are compared in Table. 6.1.

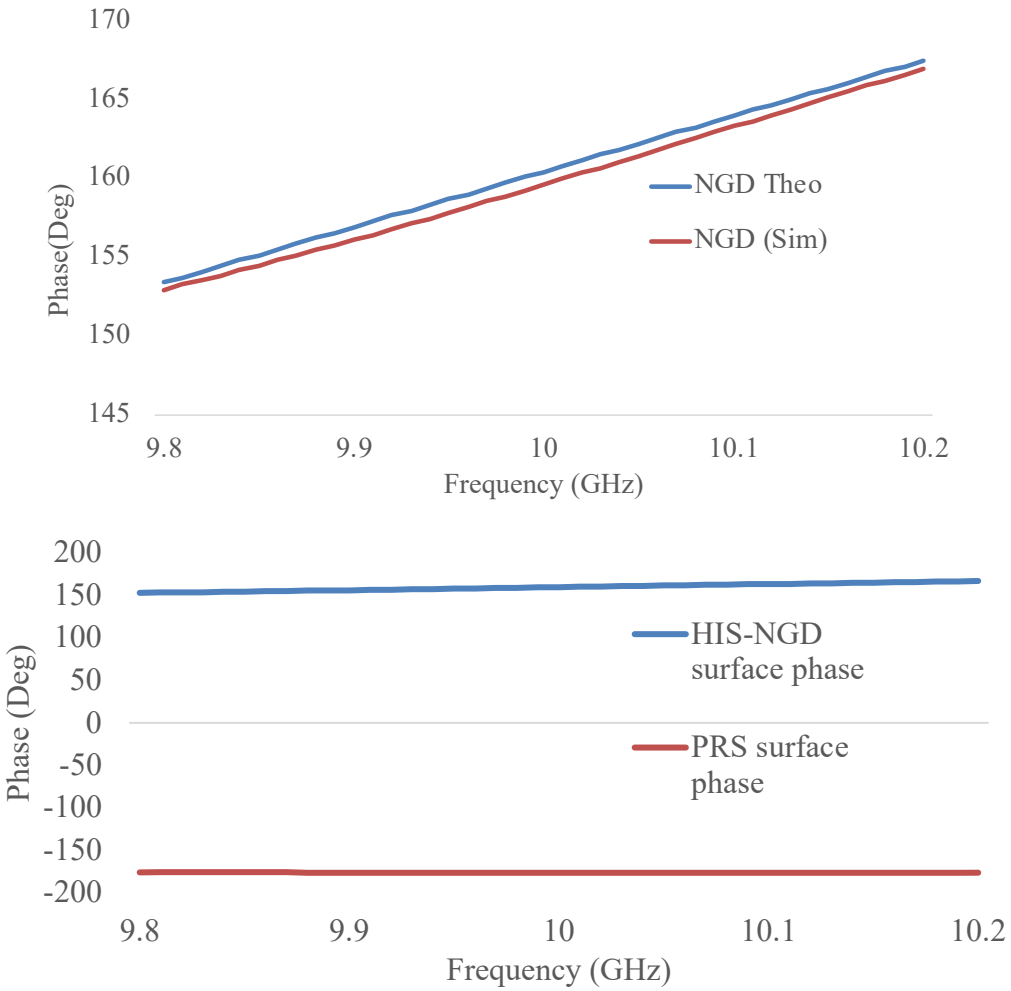

Fig. 6.11 Theoretical and simulation phase response comparison for HIS with NGD

Table 6.1 Comparison of theoretical and simulation phase responses of NGD-HIS

			Theoretical	Simulation
Frequency (GHz)	Wavelength λ (mm)	$Ø_{PRS}$ (Deg)	$Ø_{HIS}$ (Deg)	$Ø_{HIS}$ (Deg)
9.8	30.61224	-175.982	153.3812	152.96
9.81	30.58104	-175.99	153.7335	153.254
9.82	30.5499	-175.998	154.0858	153.553
9.83	30.51882	-176.007	154.439	153.857
9.84	30.4878	-176.016	154.7923	154.166
9.85	30.45685	-176.025	155.1456	154.479
9.86	30.42596	-176.034	155.4989	154.796
9.87	30.39514	-176.043	155.8522	155.117
9.88	30.36437	-176.051	156.2045	155.443
9.89	30.33367	-176.06	156.5578	155.772
9.9	30.30303	-176.068	156.91	156.105
9.91	30.27245	-176.076	157.2623	156.442
9.92	30.24194	-176.085	157.6156	156.782
9.93	30.21148	-176.094	157.9689	157.125
9.94	30.18109	-176.103	158.3222	157.472
9.95	30.15075	-176.111	158.6745	157.821
9.96	30.12048	-176.119	159.0267	158.173
9.97	30.09027	-176.127	159.379	158.528
9.98	30.06012	-176.136	159.7323	158.886
9.99	30.03003	-176.144	160.0846	159.245
10	30	-176.153	160.4379	159.607
10.01	29.97003	-176.162	160.7912	159.97
10.02	29.94012	-176.171	161.1445	160.335
10.03	29.91027	-176.179	161.4967	160.701
10.04	29.88048	-176.187	161.849	161.069
10.05	29.85075	-176.195	162.2013	161.438
10.06	29.82107	-176.203	162.5536	161.807
10.07	29.79146	-176.212	162.9069	162.178
10.08	29.7619	-176.22	163.2592	162.548
10.09	29.73241	-176.229	163.6125	162.919
10.1	29.70297	-176.237	163.9647	163.29
10.11	29.67359	-176.244	164.316	163.661
10.12	29.64427	-176.252	164.6683	164.031
10.13	29.615	-176.261	165.0216	164.401
10.14	29.5858	-176.269	165.3739	164.77
10.15	29.55665	-176.278	165.7272	165.138
10.16	29.52756	-176.286	166.0794	165.505
10.17	29.49853	-176.294	166.4317	165.871
10.18	29.46955	-176.302	166.784	166.235
10.19	29.44063	-176.309	167.1353	166.597
10.2	29.41176	-176.317	167.4876	166.958

A high impedance surface with NGD behaviour is created by replacing the conductor patch with a lossy metal layer in the unit cell simulation as shown in Fig. 6.12. In the simulation a layer with sheet resistance R is used as a lossy metal. As the sheet resistance R changes the phase and transmission loss characteristics of the surface also change, as shown in Fig. 6.13. With the particular value of sheet resistance R the HIS phase slope can be achieved to satisfy Equ. 6.1 over a wideband. For all these frequencies the main lobe direction in Equ. 6.1 is set to same values so the cavity antenna will work with high directional properties over a wideband with reduced beam squint.

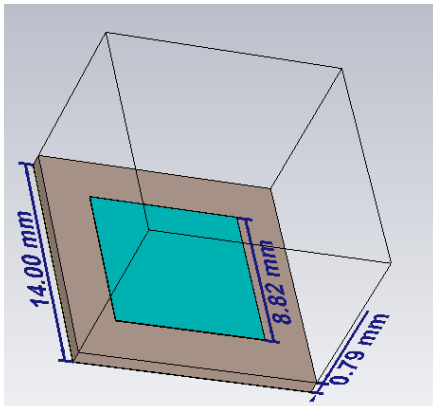

(a) Unit cell with lossy conducting layer

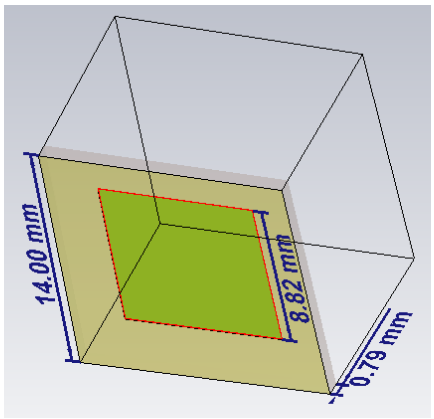

(b) unit cell with conductor

Fig 6.12 The proposed unit cell for high impedance surface with negative group delay characteristics

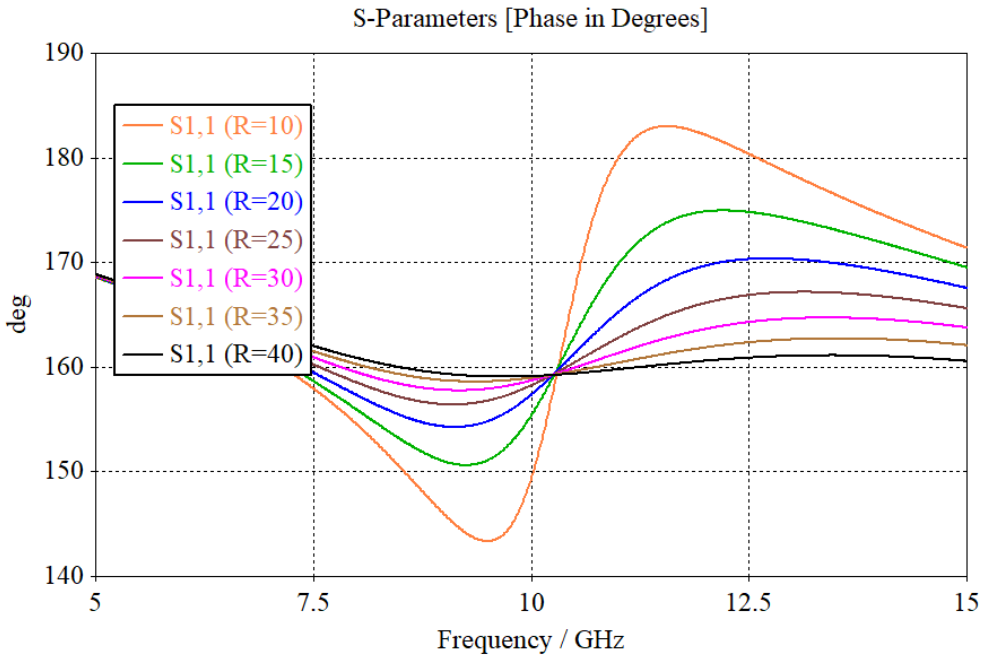

(a) Phase characteristics

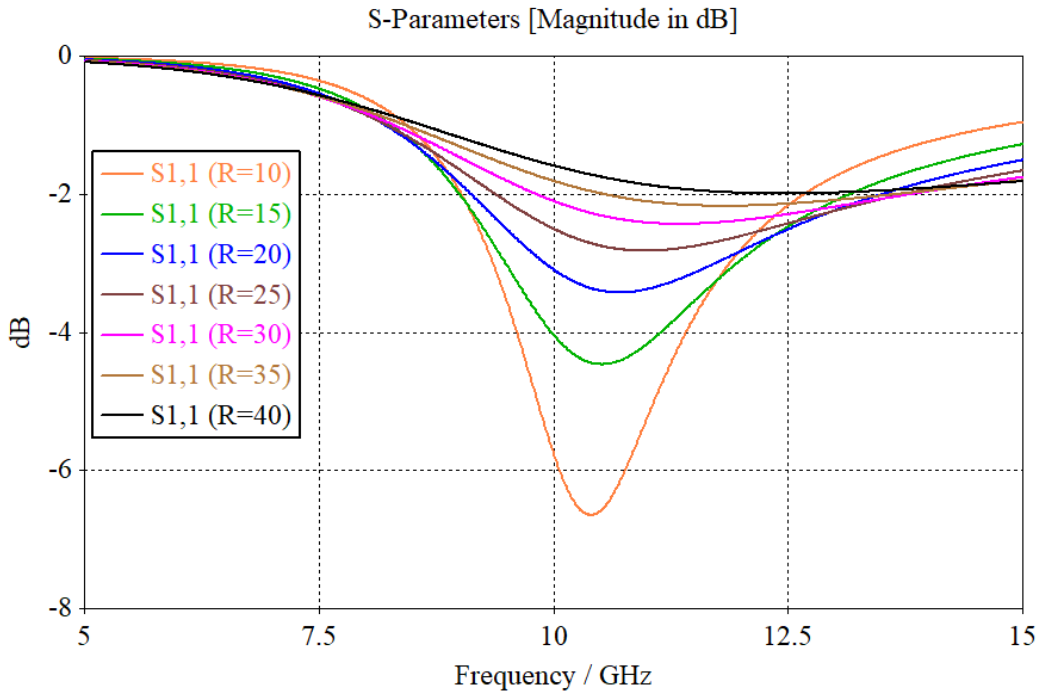

(b) Magnitude characteristics

Fig. 6.13 The transmission coefficient phase and magnitude characteristics of high impedance surface with negative group delay behaviour.

HIS with NGD Behaviour Unit Cell:

A square lossy metal patch of length 9 mm, printed on a substrate of 2.2 permittivity and 0.79mm thickness, with 13.1mm periodicity in both X and Y direction, is used for unit cell simulations. With the NGD-HIS and PRS, that is designed in section 6.1, the cavity is formed with a height of 14.77mm to satisfy the phase condition given in Eq. 6.1. The unit cell simulation results are used to observe the phase and loss characteristics of the NGD-HIS, as shown in Fig. 6.14, and the full wave model of the cavity antenna is shown in Fig. 6.15. Over the bandwidth 9.5 to 11 GHz, the main lobe has a beam squint of 0.2^0 per 100MHz. At 9.8GHz a maximum directivity of 11.6 dBi and a gain of -3.19 dBi are observed as shown in Fig. 6.16.

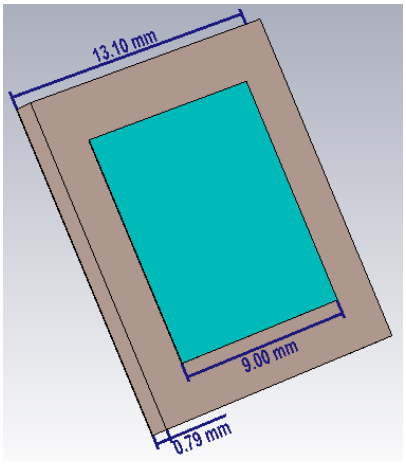

(a) NGD-HIS unit cell

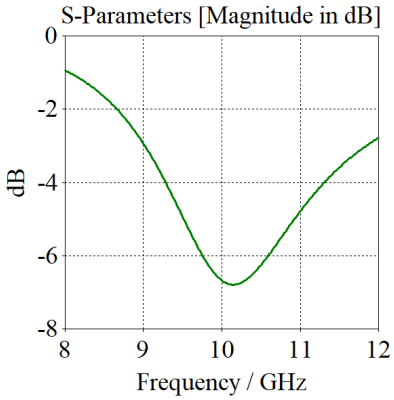

(b) Magnitude response

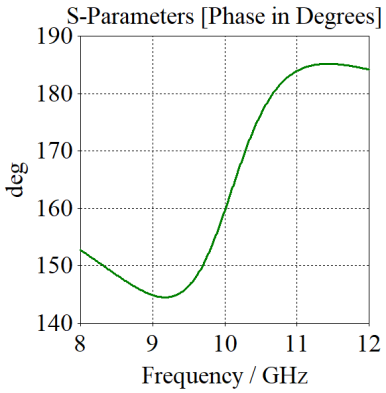

(c) Phase response

Fig. 6.14 NGD-High Impedance surface characteristics

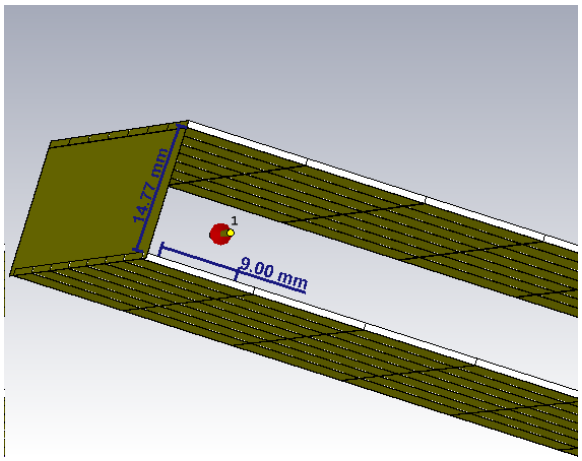

(a) PRS – NGD-HIS cavity antenna

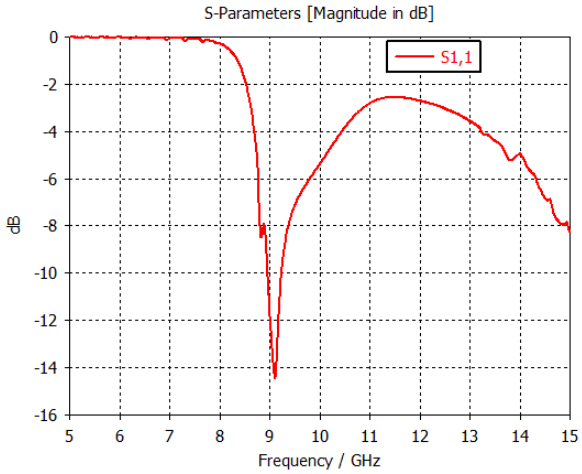

(b) Return loss of cavity antenna

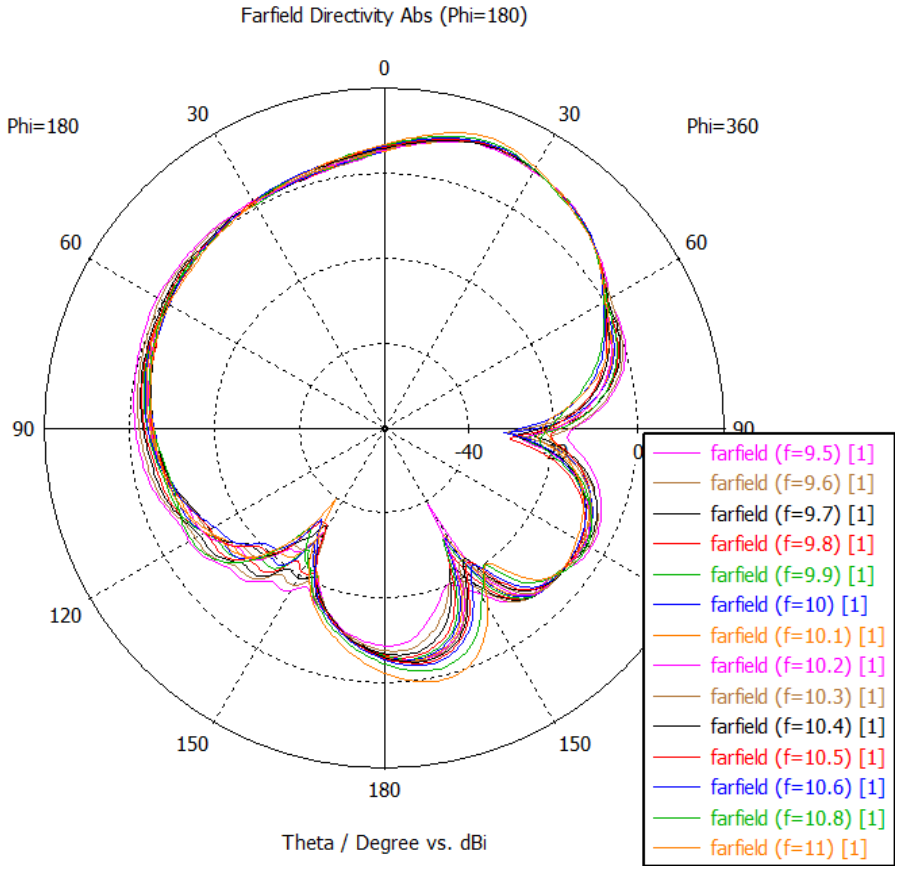

(c) Radiation patterns

Fig. 6.15 PRS- NGD-HIS cavity antenna

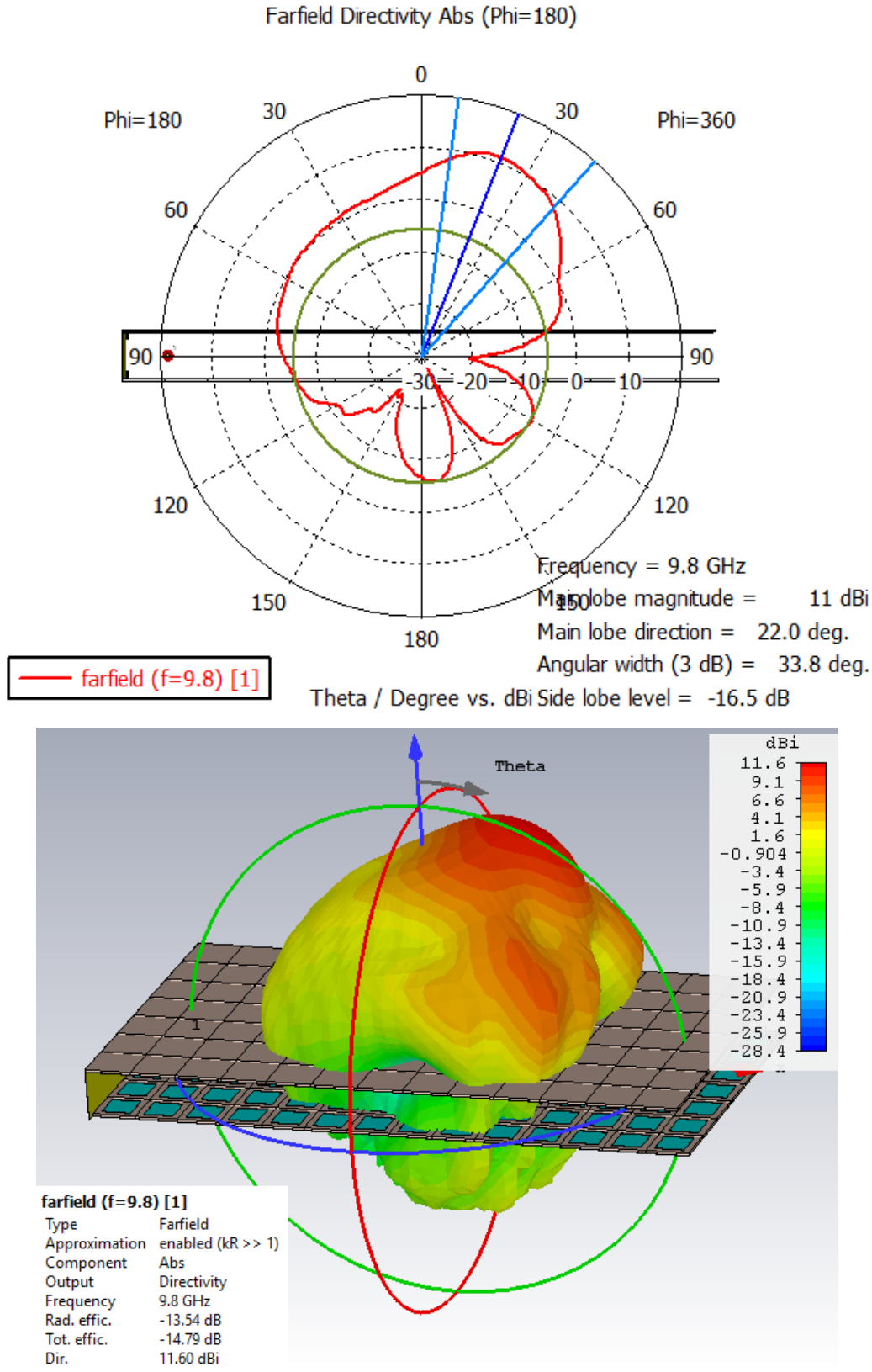

Fig. 6.16(a) Radiation pattern of PRS – NGD-HIS cavity antenna

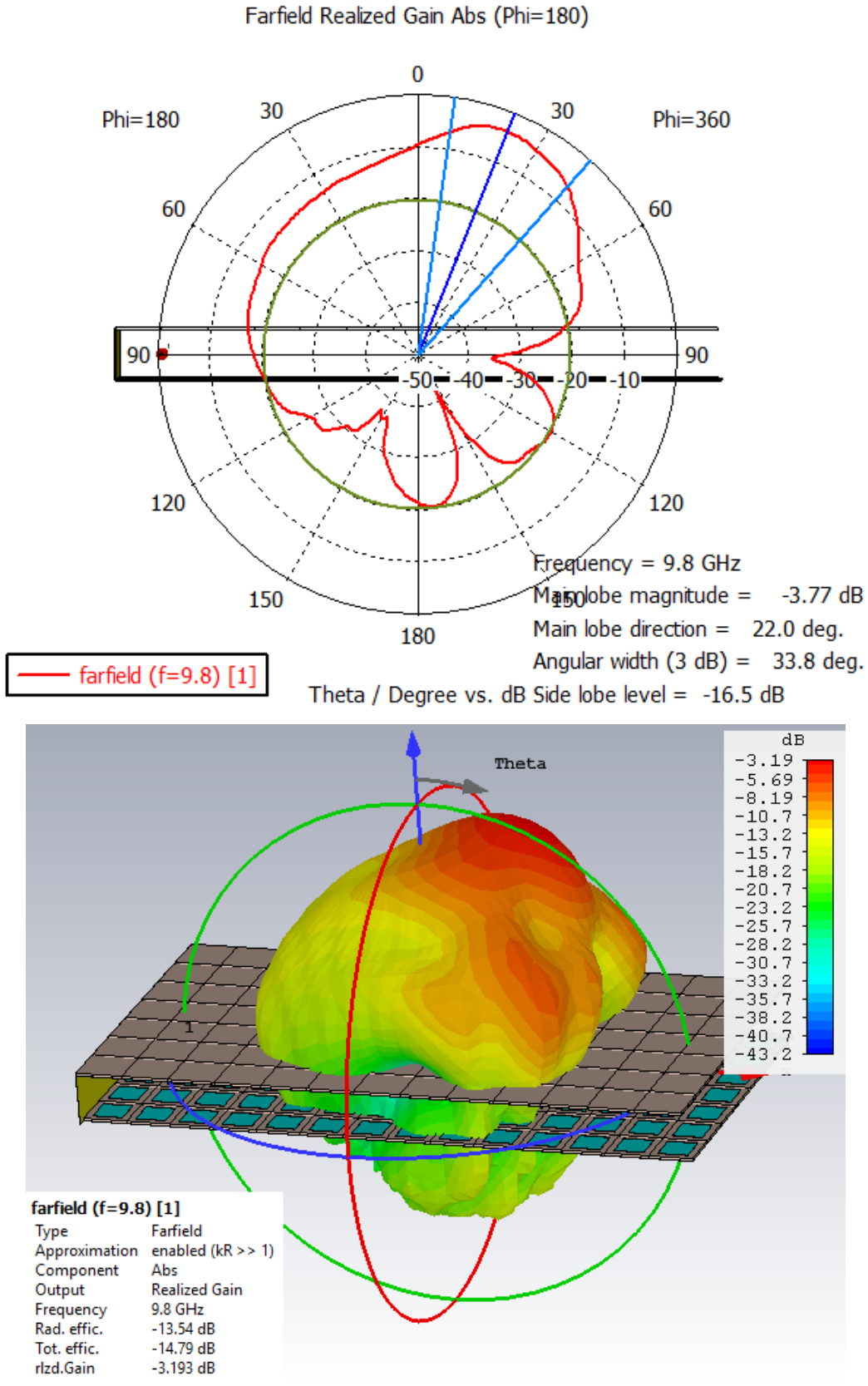

Fig. 6.16 (b) Radiation pattern of PRS – NGD-HIS cavity antenna

The NGD based cavity antenna has operation over a wide bandwidth with 0.2^0 beam squint per 100 MHz. It is observed that the loss introduced in the HIS to get the NGD behaviour has degraded the directivity and gain. The absorption of the HIS along the direction of signal propagation from dipole to the end of the cavity has increased due to the lossy patches. By introducing amplification between the patches of the NGD-HIS, radiation performance can be improved. In the next section loss compensated cavity antenna models are presented.

6.4. Fabry-Perot Cavity Antenna: PRS And Loss Compensated NGD-HIS Models

The signal degradation has increased due to the loss introduced in the HIS to achieve NGD behaviour. The amplifier blocks are employed between patches of HIS along the E-filed direction, i.e. parallel to the length of the dipole.

A HMC633LC4 unidirectional amplifier block of 27dB gain is embedded between the square lossy metal patches of length 9 mm, printed on a substrate of 2.2 permittivity and 0.79mm thickness, with 13.1mm periodicity in both X and Y direction. With the loss compensated NGD-HIS and PRS, that is designed in section 6.1, the cavity is formed with a height of 16.87mm to satisfy the phase condition given in Eq. 6.1. The unit cell simulation results are used to observe the phase and loss characteristics of the NGD-HIS, as shown in Fig. 6.17, and the full wave model of the cavity antenna is shown in Fig. 6.18. Over the bandwidth 10 to 10.75 GHz the main lobe has a beam squint of 1.3^0 per 100MHz. This beam squint can be further reduced by optimising the phase response of the HIS to satisfy Eq. 6.1, by taking the amplifier phase characteristics into account. At 10.6GHz a maximum directivity of 18.8dBi and a gain of 5.64dB are observed as shown in Fig. 6.19. The performance parameters of the loss compensated cavity antenna are significantly improved, compared to the lossy model in section 6.3. It is certainly evident that the loss compensated NGD based cavity antenna will enable the design of a highly directional cavity antenna over a wide bandwidth with minimum beam squint.

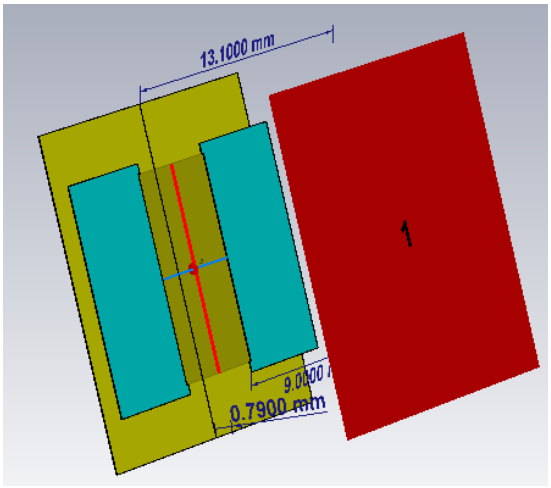

(a) Loss compensated NGD-HIS unit cell

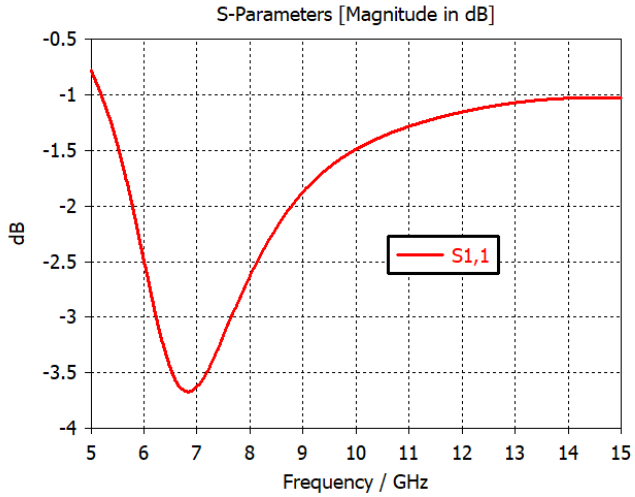

(b) Magnitude response

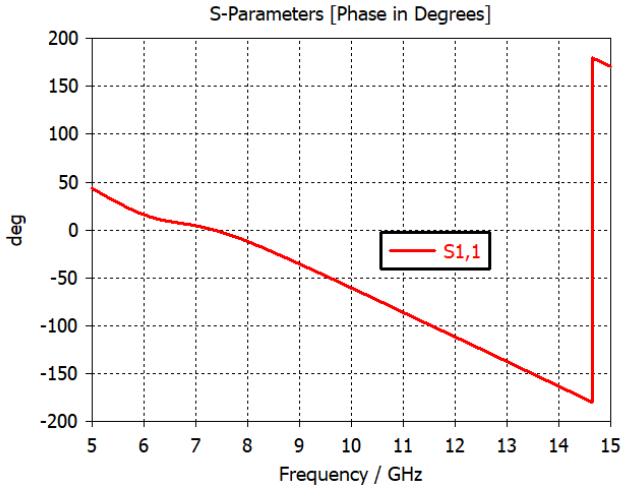

(c) Phase response

Fig. 6.17 Loss compensated NGD-High impedance surface characteristics

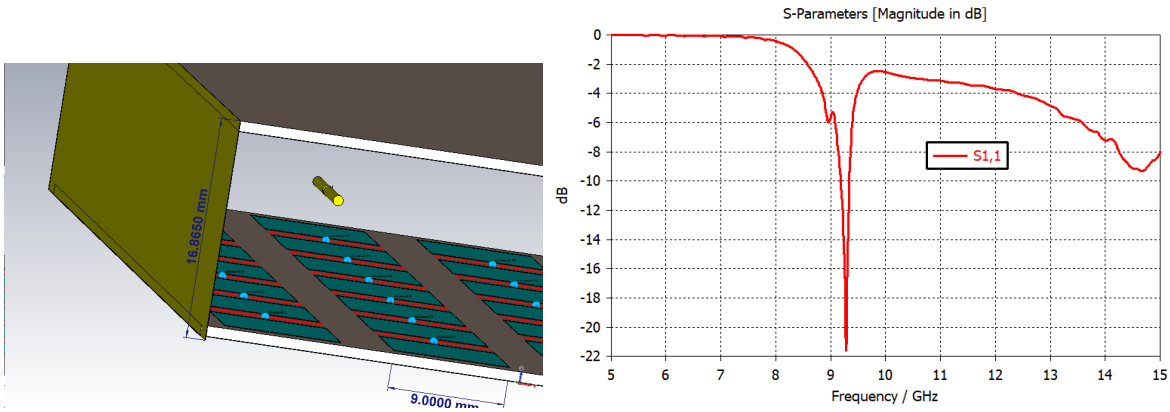

(a) PRS – Loss compensated NGD-HIS cavity antenna (b) Return loss of cavity antenna

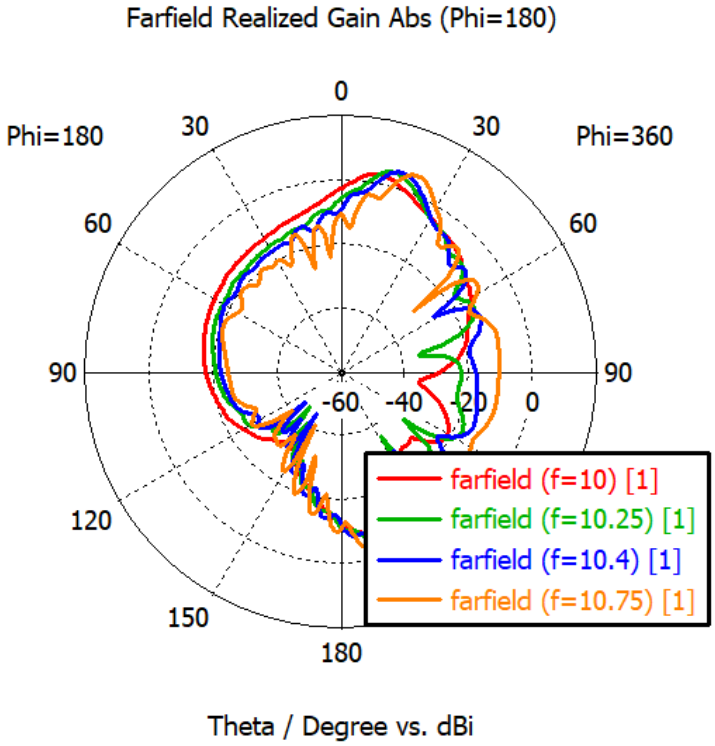

(c) Radiation pattern of the cavity antenna

Fig. 6.18 PRS- Loss compensated NGD-HIS cavity antenna

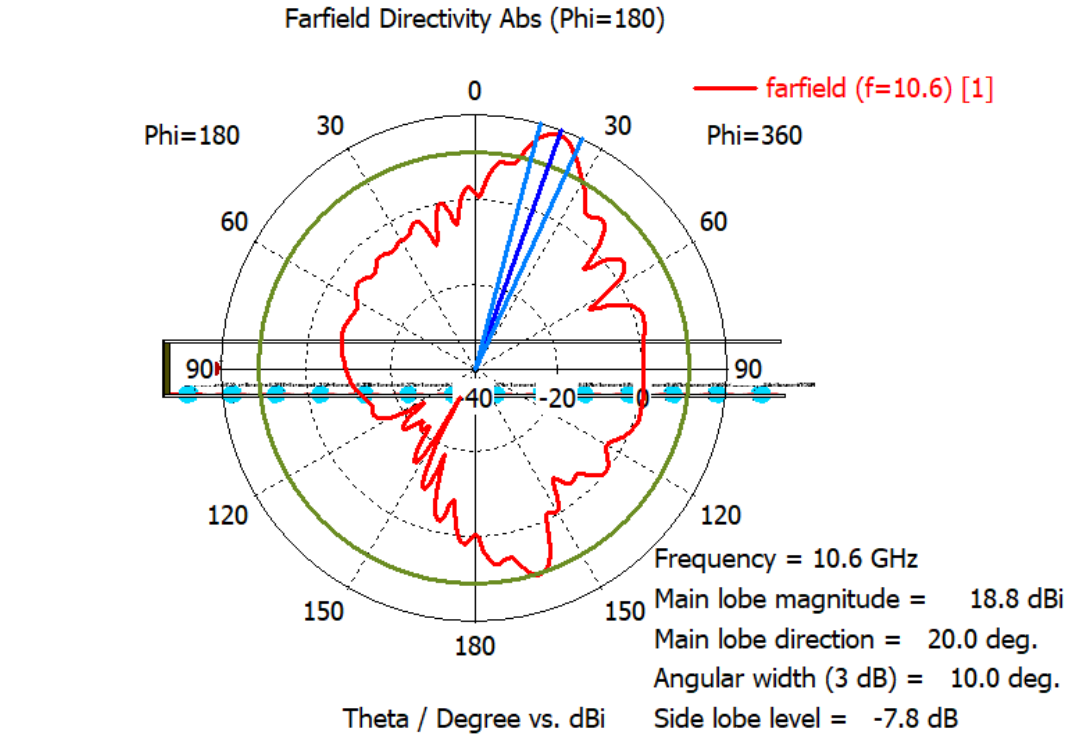

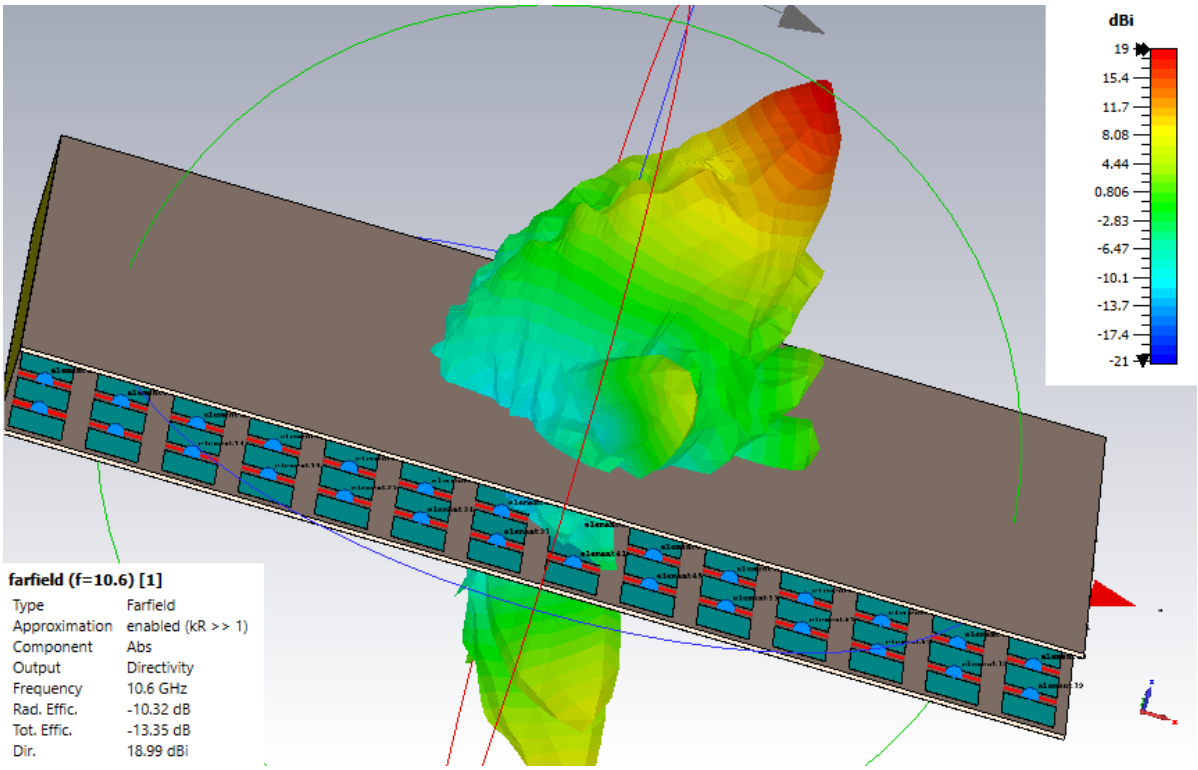

Fig. 6.19 (a) Radiation properties (Directivity) of PRS – Loss compensated NGD-HIS cavity antenna

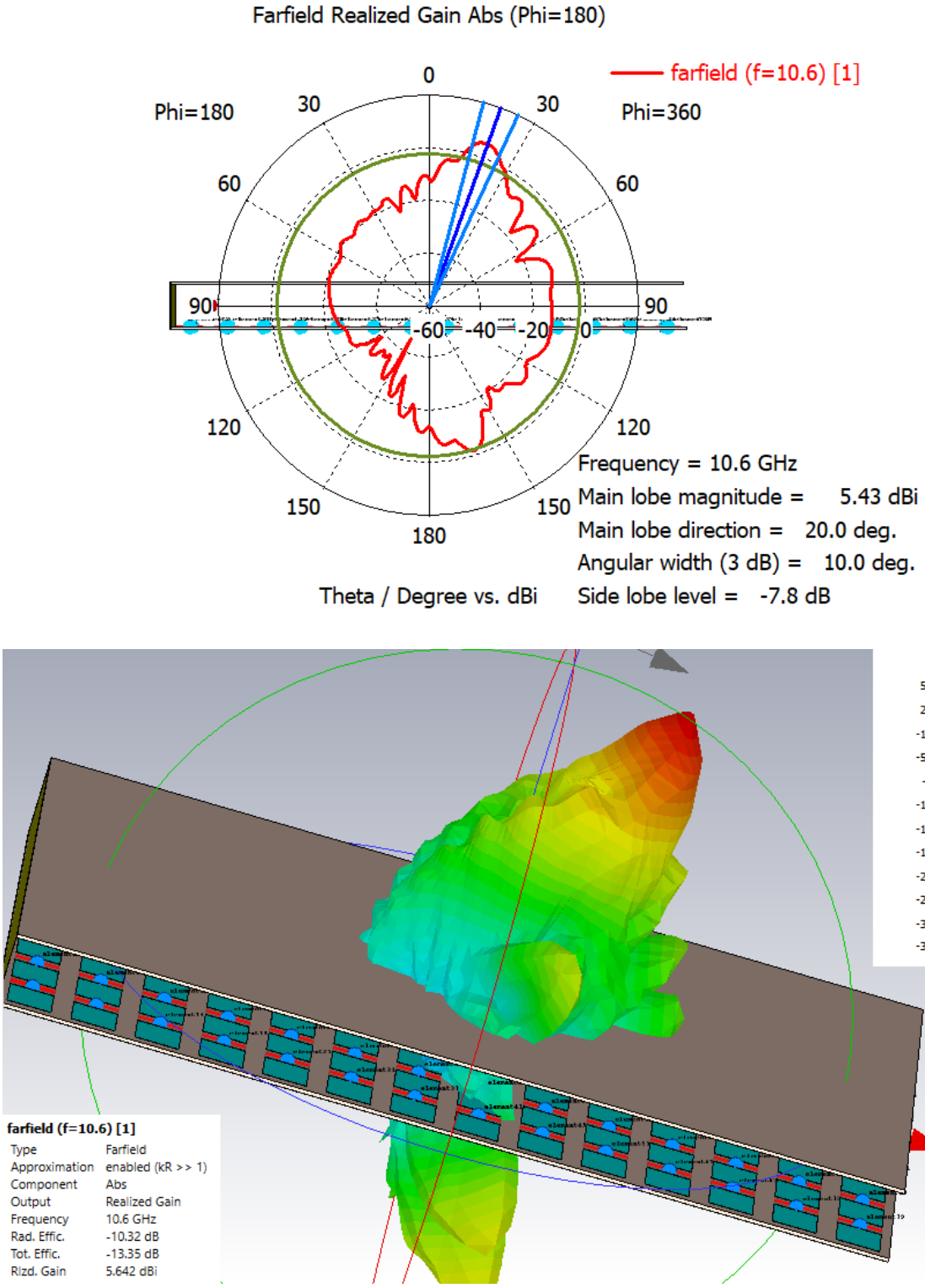

Fig. 6.19 (b) Radiation properties (Gain) of PRS – Loss compensated NGD-HIS cavity antenna

Loss Compensation Using Ideal Bi-directional Amplifier

To confirm the possibility of further improvement in the radiation properties of the NGD based cavity antenna, an ideal 50dB amplifier block is embedded between the square lossy metal patches of length 9 mm, printed on a substrate of 2.2 permittivity and 0.79mm thickness, with 13.1mm periodicity in both X and Y direction. Over the bandwidth 10 to 10.75 GHz, the main lobe has a beam squint of 1.3^0 per 100MHz. At 10GHz a maximum directivity of 20.4dBi and a gain of 14.2dB are observed as shown in Fig. 6.20 and Fig. 6.21.

In the loss compensated model a biasing circuit for the amplifier has to be included to study its impact on the radiation properties of the proposed cavity antenna. Although there will be some degree of impact on the radiation properties of the cavity antenna due to the biasing network of the amplifiers, it has been proved that the HIS with NGD behaviour can reduce beam squint.

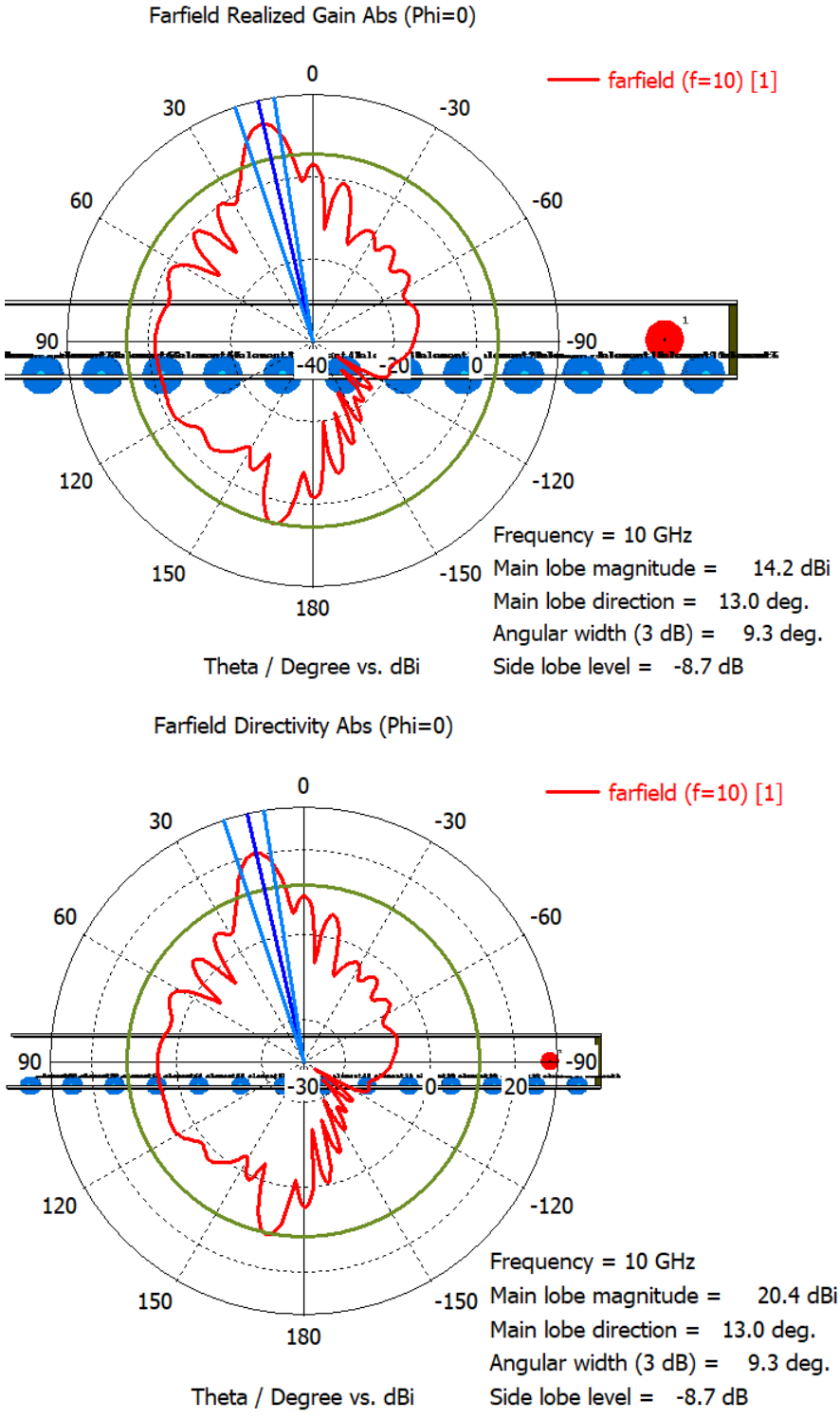

Fig. 6.20 Radiation properties of NGD based cavity antenna with ideal bidirectional gain blocks for loss compensation.

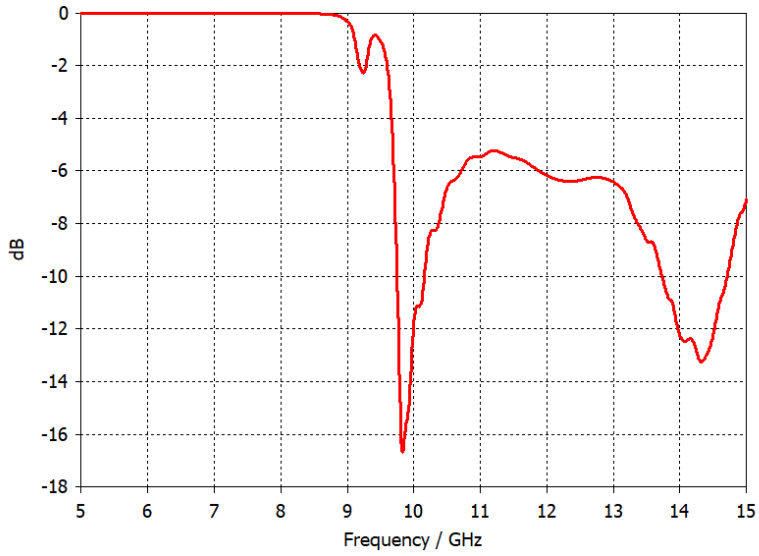

(a) Return loss of full wave cavity antenna model

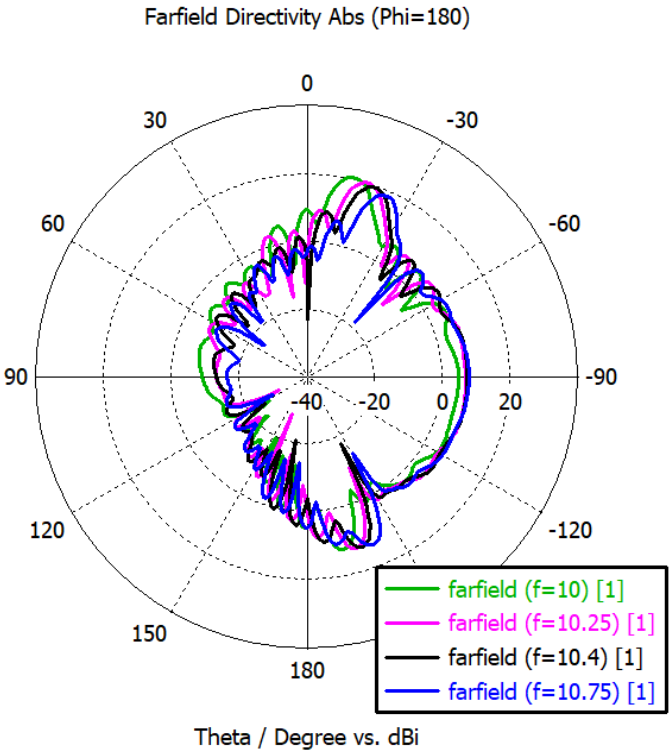

(b)Radiation pattern at different frequencies

Fig. 6.21 Radiation pattern of NGD based cavity antenna with ideal bidirectional gain blocks for loss compensation.

With the possible implementation of NGD behaviour in the HIS of the cavity, highly directional radiation properties over a wide bandwidth with less beam squint has been achieved. The following Table 6.2 summarises and gives a comparison of the directional properties in the various scenarios discussed in this chapter.

Table: 6.2 Comparison of the directional properties of a cavity antenna in various scenarios

	Ground PRS Cavity Antenna	**HIS PRS Cavity Antenna**	**NGD-HIS PRS Cavity Antenna**	**NGD-HIS PRS Cavity Antenna With Amplifier**	**NGD-HIS PRS Cavity Bi-Dir Ideal Amplifier**
Frequency (GHz)	11.2 ~ 11.6	9.8 ~ 10.2	9.5 ~ 11	10 ~ 10.75	10 ~ 10.75
BW(GHz)	0.4GHz	0.4GHz	1.5GHz	0.75GHz	0.75GHz
Main lobe	2^{O}-13^{O}	7^{O}-31^{O}	21^{O}-24^{O}	11^{O}-21^{O}	13^{O}-24^{O}
Beam squint	11^{O}	24^{O}	3^{O}	10^{O}	11^{O}
per 100MHz	2.75^{O}	6^{O}	0.2^{O}	1.3^{O}	1.3^{O}
Directivity MAX	22.1dBi @11.4GHz	20dBi @10GHz	11.6dBi @9.8GHz	19dBi @10.6GHz	20.4dBi @10GHz
Gain MAX	15.8dBi @11.4GHz	17.6dBi @10GHz	-3.19dBi @9.8GHz	5.64dBi @10.6GHz	14.2dBi @10GHz

A novel concept based on negative group delay phenomena to reduce the beam squint in the cavity antenna is proposed in this thesis. A full-wave simulation based analysis has been made to show that the proposed antenna concept has sufficient level of gain and directivity with an advantage of reduced beam squint. Material such as graphene could be used to implement the resistive layer in this proposed work in order to implement the negative group delay behaviour in Frequency Selective Surfaces. However, achieving an exact resistance value for this sheet will become a design challenge. With the availability of MMIC amplifiers it is possible to

design loss compensated cavity antennas. The way the amplification is achieved with respect to the electric field vector direction in the cavity will have an effect on the radiation properties. The biasing network of amplifiers will also have an effect on the overall performance of the cavity antenna.

List of References

[1] A. P. Feresidis and J. C. Vardaxoglou, "High gain planar antenna using optimised partially reflective surfaces," *IEE Proceedings - Microwaves, Antennas and Propagation,* vol. 148, no. 6, pp. 345-350, 2001.

[2] K. Konstantinidis, A. P. Feresidis, M. J. Lancaster, P. S. Hall, and P. Gardner, "Design of a submillimetre wave Fabry-Perot cavity antenna," *European Microwave Conference*, 6-10 Oct. 2013, pp. 357-360.

[3] G. V. Trentini, "Partially reflecting sheet arrays," *IRE Transactions on Antennas and Propagation,* vol. 4, no. 4, pp. 666-671, 1956.

[4] J. R. James, S. J. A. Kinany, P. D. Peel, and G. Andrasic, "Leaky-wave multiple dichroic beamformers," *Electronics Letters,* vol. 25, no. 18, pp. 1209-1211, 1989.

[5] A. P. Feresidis, G. Goussetis, W. Shenhong and J. C. Vardaxoglou, "Artificial magnetic conductor surfaces and their application to low-profile high-gain planar antennas," *IEEE Transactions on Antennas and Propagation,* vol. 53, no. 1, pp. 209-215, 2005.

Chapter 7 Conclusion and Future Work

7.1. Conclusion

A novel negative group delay (NGD) based technique to improve the performance of an antenna is presented in this thesis. A printed electrically small antenna (ESA) and a Fabry-Perot cavity antenna are designed using the NGD concept. An ESA integrated with an active circulator for simultaneous signal transmission and reception (duplex operation) operating at 1.8GHz over 14% bandwidth is presented. In addition a loss compensated Fabry-Perot cavity antenna is shown to exhibit 1.3^0 per 100MHz beam squint over 0.75GHz with improved directivity and gain of 19dBi and 5.6dB respectively.

The NGD based design approach has been proven to be effective in designing low profile antennas operating over a wide bandwidth with enhanced radiation performance. It is demonstrated that the NGD concept is easy to implement as a lumped element network and as a Frequency Selective Surface. It is observed that the NGD network with the desired characteristics can be designed by using a filter of right type and order.

The advantages of NGD matching networks over conventional matching networks for antennas have been demonstrated. For example the active matching networks suffer from stability issues and most often such designs are limited to unidirectional operation. By using LC based passive networks, matching can be achieved only over a very narrow bandwidth. However, the passive NGD network offers wide bandwidth impedance matching for an antenna. Also using NGD networks matching can be achieved at frequencies far lower than the quarter wavelength resonance frequency associated with the physical length of the antenna. Hence this approach is proved to be effective in the design of an ESA. The inevitable transmission loss of the NGD

based matching network is compensated using an active circulator. This enabled the ESA to be used in duplex mode.

In the design of an active circulator transistors can either be used as the core element of the design or as an amplifier. In the first case, the reverse isolation of a transistor can be used to achieve isolation between the transmitter and receiver ports of the circulator. In this case the functionality of the circulator will be greatly affected by any variation in the bias voltage of the transistor. In such designs it will be more challenging to manage the overall stability and circulator operation. In the second case, transistors can be used to design an amplifier, which will act as a gain block to control the magnitude of signals to achieve signal cancellation in a ring configuration. In the ring configuration there will be less design flexibility when only amplifiers are used. Both the microstrip lines and amplifiers have frequency dependent transmission characteristics. This will result in signal cancellation over a very narrow bandwidth. With the use of a NGD network the magnitude and phase of clockwise (CW) and anti-clockwise (ACW) signals can be controlled, so that signal cancellation can be achieved over a wide bandwidth. The use of NGD networks offered more design flexibility in the choice of amplifiers for the active circulator. The proposed design approach enables the use of off-the-shelf stable amplifiers as gain blocks, improving the stability of the overall system. This novel approach can be used to design active antennas integrated to circulators for different applications and can be implemented in different technologies.

Due to the phase sensitivity of the design, ESA and active circulator prototypes are fabricated separately. The proposed concepts are experimentally verified by designing and testing an ESA operating at 1.08GHz($0.98\lambda/2\pi$) of 50% bandwidth with a physical length of 43mm. A quasi-active circulator operating at 1.5GHz with 200MHz (14%) bandwidth offering 20dB isolation between transmitter and receiver is also fabricated and tested. Between any pair of ports the

average gain in the CW direction is 5dB and the isolation in the ACW direction is greater than 20dB. The noise figure is less than 5dB from the antenna to the receiver. Using the proposed method the bandwidth of the circulator is improved compared to similar designs reported in the literature.

A novel Fabry-Perot cavity antenna designed with a partially reflective surface (PRS) and a high impedance negative group delay surface is presented. The effectiveness of the high impedance surface (HIS) with NGD behaviour in reducing the beam squint is demonstrated. The HIS with NGD characteristics enabled the establishment of the resonance phase condition over a 0.75GHz bandwidth resulting in a wideband cavity antenna with reduced beam squint. The signal absorption along the HIS and the possible loss compensation techniques are also discussed. A lossy design has only 0.2^0 per 100MHz beam squint over 1.5GHz bandwidth with degraded directivity and gain.

Though the proposed method is proved to be effective in antenna impedance matching there is a need of improvement in efficiency. Also if this method is used for matching a receiver antenna, the NGD network will contribute noise that might affect the signal to noise ratio. In the case of an active circulator, hybrid implementation is observed to be very phase sensitive. However, a fully integrated MMIC implementation helps to avoid unwanted parasitic effects and component tolerances. These factors will lead to differences between fabricated and simulated models. Having successfully proved the concept the author is now convinced that implementing the proposed concept in MMIC technology will give a better prototype.

In this thesis the possibility of using negative group delay concept to minimise the beam squint is successfully verified using full wave simulation. However, the availability of materials to get the required resistance value for layers should be studied further. This could be a limitation for

this concept. Embedding an amplifier and biasing circuit for loss compensation is another aspect that should be addressed both in view of complexity and cost.

Despite the limitations and challenges discussed above the NGD based technique is stable and offered design flexibility in all the above scenarios. The possibilities of using the NGD concept in antenna impedance matching and signal cancellation are verified. The way the NGD network and amplifiers are used has helped to improve the stability. The NGD network based design has offered flexibility to use “off the shelf” stable amplifiers, this will help to address the stability issues in an active circulator. This design approach is suitable for a wide range of the frequency spectrum, for different antenna types and for different implementations.

7.2. Future Work

The proposed designs can be fabricated and tested in an industrial setting. The author used in-house facilities to fabricate prototypes. When a prototype is made in a industry facility the design and fabrication processes are more established. Also availability of sophisticated equipment ensures the accuracy of the feature size in the design. The enhanced fabrication standards guarantees the repeatability. It is possible some of the mismatches between the simulation and measurement results can be minimised by making prototypes from industry standard facilities. Various possible future works are discussed below.

Matching: The maximum bandwidth over which matching can be obtained using NGD networks can be further studied. A dual band matching using Elliptic filter based NGD network can be further explored.

There is a trade-off between the bandwidth of the ESA and the loss that requires compensation when a NGD network is used. This will have a further impact on the efficiency of the ESA, therefore the efficiency of an ESA is another performance parameter that needs improvement.

Active circulator: The proposed active circulator integrated with an ESA can be implemented in MMIC technology. A fully integrated design would give more accurate results. The following Fig. 7.1 shows the work accomplished in this thesis and the possible future works that can be done in relation to circulators.

A further study could be carried out to investigate the suitability of the proposed concept for different types of antenna. A further experimental study on the noise figure would also be useful. The power handling capabilities could be experimentally verified further to set the limitations.

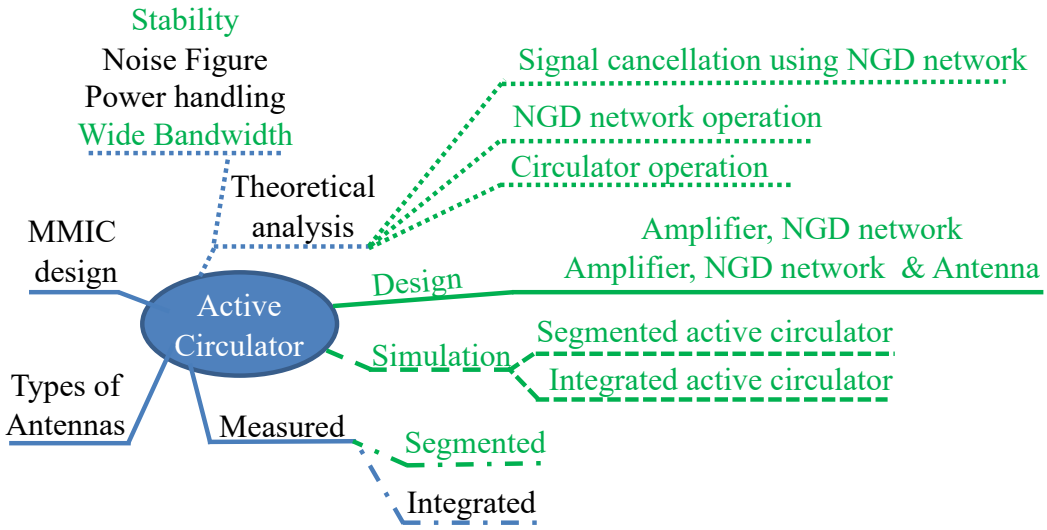

Fig. 7.1 Various tasks related to the active circulator and possible future work

(Tasks shown in green are accomplished in this thesis. Tasks shown in blue are possible further work related to circulators using the NGD concept)

Cavity antenna: The performance of the proposed Fabry-Perot cavity antenna needs to be experimentally verified. The degradation of energy in the cavity due to the lossy HIS has been limited by using amplifiers between the patches. However, the effects of embedding the amplifier either within a unit cell or between unit cells should be studied. In addition the impact of amplifier biasing circuit on the overall antenna performance should be studied.

Appendix A

Active Circulator Experimental Results of Different Prototypes

The isolation and antenna to receiver gain characteristics are studied with varying bias voltage of three amplifier (amplifiers are embedded in the paths: TA- Tx to antenna; AR- Antenna to Rx; and TR- Tx to Rx) for the model shown in Fig. 5.24, page-111. As shown in Fig. A.1, it is has been observed that the accurate reproduction of bias condition used in the simulation is necessary to get perfect working experimental model.

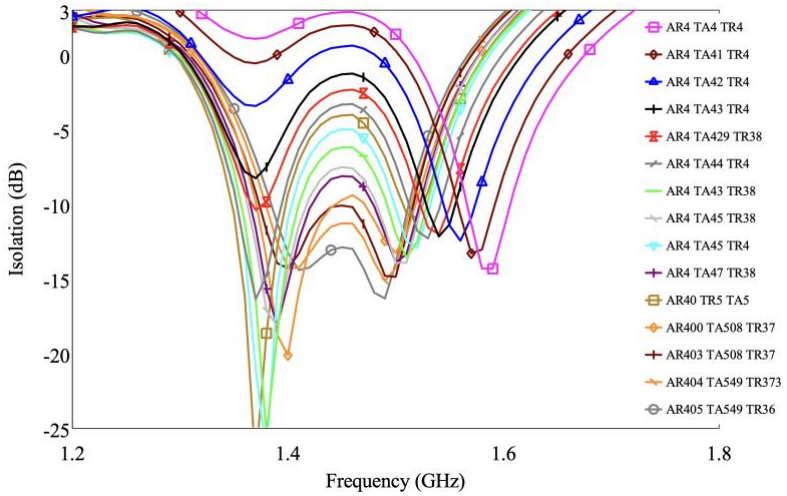

(a). Change in isolation characteristics with varying amplifier bias.

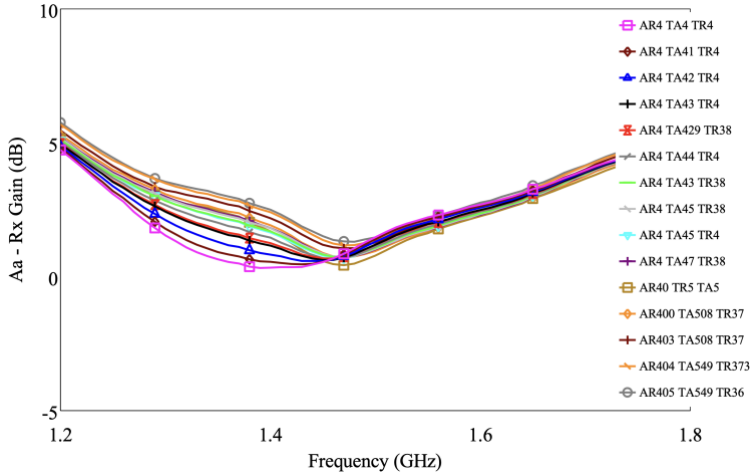

(b). Change in gain characteristics with varying amplifier bias.

Fig. A.1 The active circulator isolation and gain characteristics variation with changing amplifier bias voltage.

In addition to the prototype experimental results presented in chapter 5, in this section two more prototypes are presented. A quasi-active circulator model is fabricated and tested. A Rogers RT5880 substrate is used for these prototypes. In the ring configuration between the transmitter and antenna ports a TRF37A75 amplifier is used. Two ADL5611 amplifiers are also used: one between the antenna and the receiver ports in the clockwise direction and the other between the transmitter and the receiver in the anti-clockwise direction.

Active Circulator Prototype 2

In the following Fig. A.2 the measurement setup of prototype 2 is presented. In simulation this design exhibited 20dB isolation over a 200MHz bandwidth.

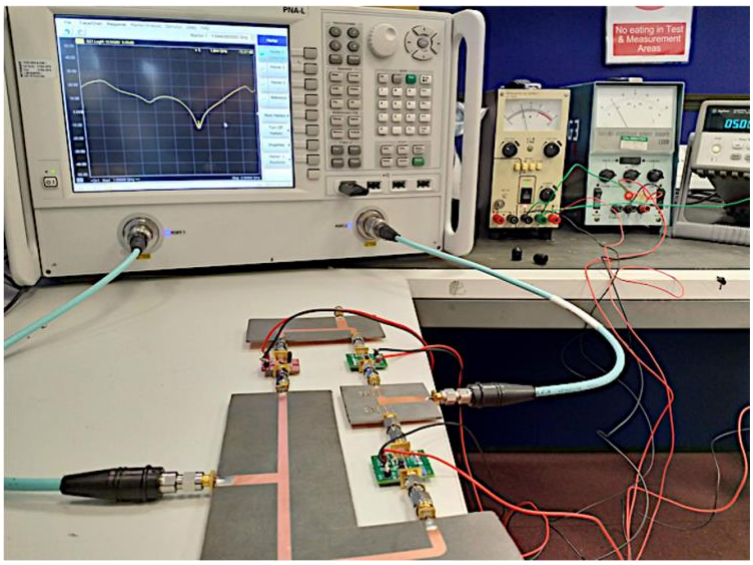

Fig. A.2 The prototype 2 of an active circulator

The gains in the transmitter to antenna path and the antenna to receiver path are on average 5dB. The lumped element values of the NGD networks are shown in Table A.1 below. A 5th order Butterworth filter with added resistors is used to design the NGD networks. The surface mount components, namely KOA 0603 resistors, ATC 0402 capacitors and Coilcroft 0402 inductors

are used in the fabrication of the NGD network. The Keysight N5232B PNA-L (0-20GHz) Microwave Network Analyzer is used to measure the scattering parameters of the active circulator.

Table: A.1 The resistor, inductor and capacitor lumped element values for NGD networks. The topology shown in Fig.5.16(a) is used to implement these networks.

(Units : R - Ω, L - nH, C - pF)

Elements	Clockwise	Anti-clockwise
R_{S1}	60.4	200
L_{S1}	1	1
C_{S1}	12	12
R_{S2}	180	60.4
L_{S2}	3.3	3.3
C_{S2}	1.2	1.2
R_{S3}	60.4	60.4
L_{S3}	1	1
C_{S3}	8.2	8.2
R_{P1}	97.6	75
L_{P1}	5.1	5.1
C_{P1}	0.9	0.9
R_{P2}	84.5	30
L_{P2}	5.1	5.1
C_{P2}	0.9	0.9

The reflection coefficient characteristics of the port of the active circulator are shown in Fig. A.3. A good agreement is observed between the simulation and experimental results over 1.32 to 1.42 GHz band.

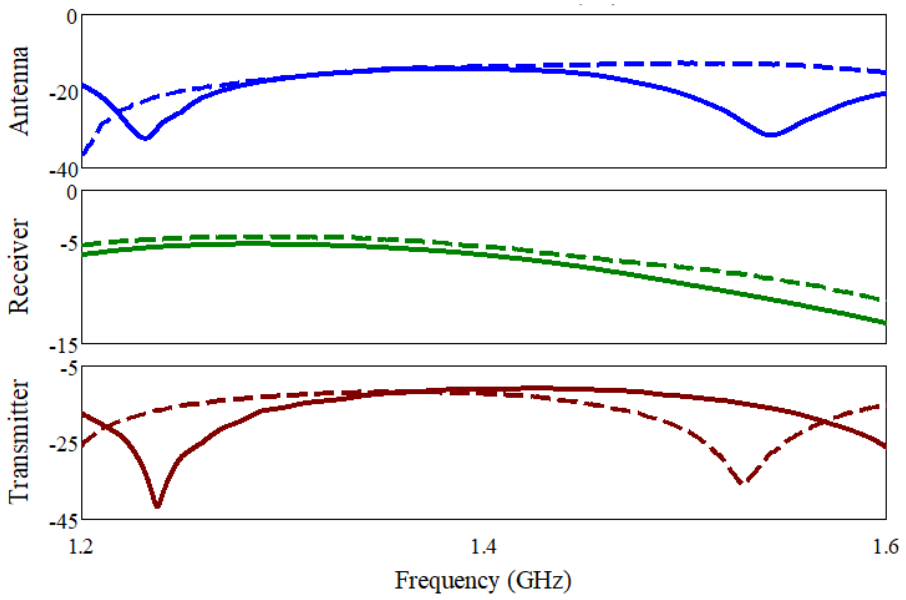

Fig. A.3 Port reflection coefficient (dB) characteristics

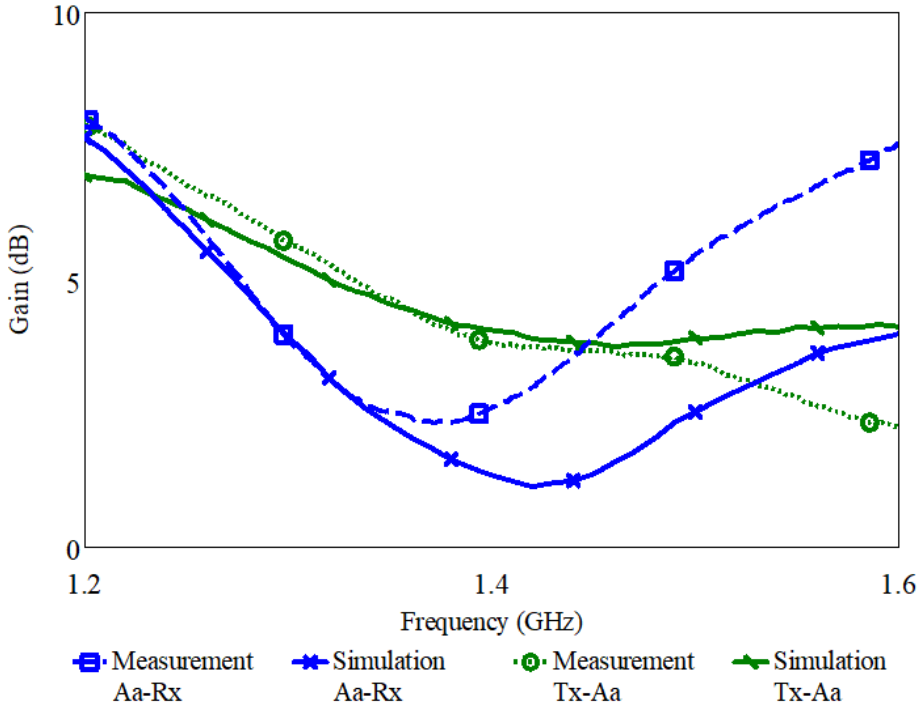

Fig. A.4 Prototype gain characteristics.

An average gain of 5dB is observed in the path from the transmitter to the antenna. The simulation and measured results have good agreement. Similarly an average gain of 2.5dB is

observed in the path from the antenna to the receiver. There is a disagreement between the simulation and measured results however. This is due to adjusting the ADL5611 amplifier bias that is in the path from the antenna to the receiver. This is all shown above in Figure A.4.

As discussed in chapter 5 due to the sensitivity of the design to length and tolerances of the surface mount components, for 5V DC bias voltage signal cancellation is not achieved. By adjusting the bias voltages of the ADL5611 amplifiers isolation is observed over a narrow band. The following Fig. A.5 shows the isolation characteristics between the receiver and the transmitter. In simulation an average isolation of 30dB is achieved over 1.32 to 1.42GHz band.

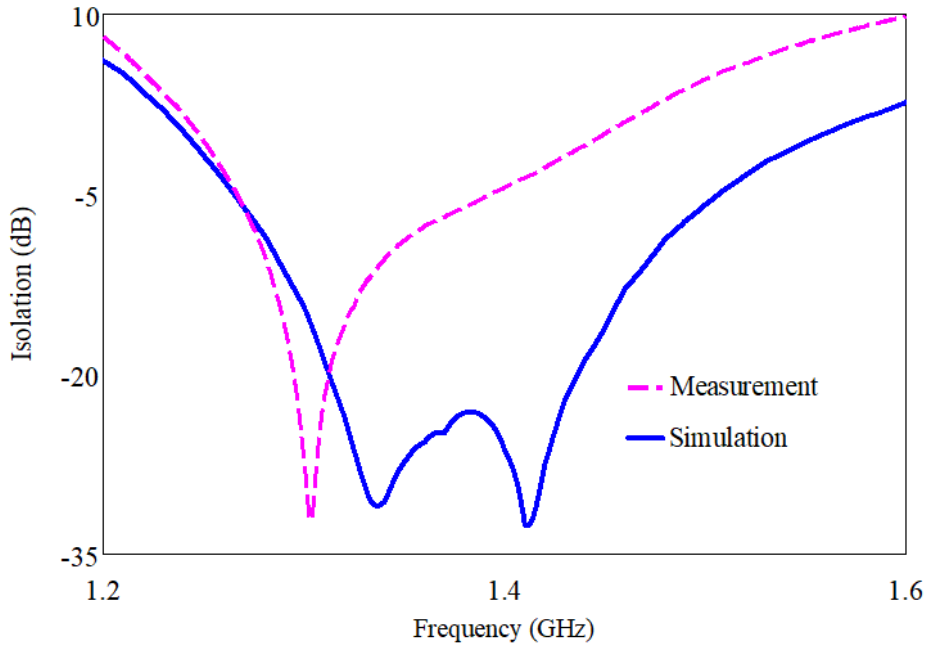

Fig. A.5 Isolation between the transmitter and the receiver of prototype 2

Active Circulator Prototype 3

Another active circulator prototype is presented in the following Fig. A.6. A similar design approach is used as discussed in chapter 5. The prototype is fabricated on a Rogers RT5880 substrate. The surface mount components, namely Koa 0603 resistors, ATC 0402 capacitors and Coilcroft 0402 inductors are used in the fabrication of the NGD network. The Keysight N5232B

PNA-L (0-20 GHz) Microwave Network Analyzer is used to measure the scattering parameters of this active circulator.

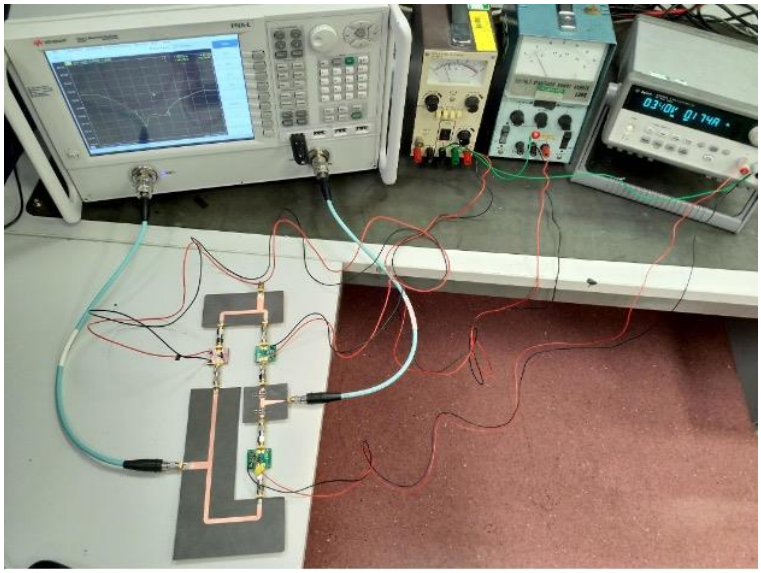

(a) Measurement setup of an active circulator prototype 3

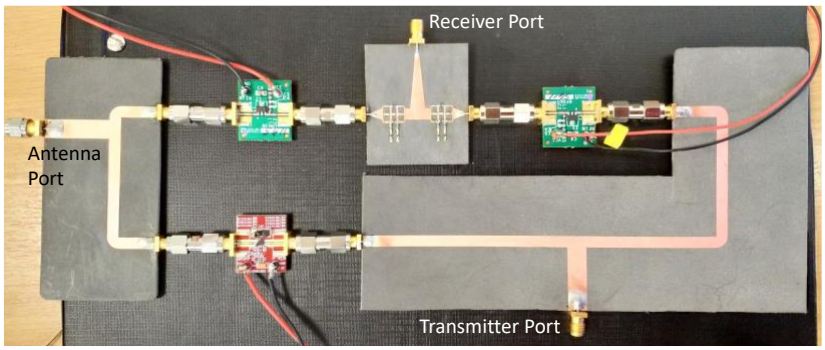

(b) Active circulator prototype 3

Fig. A.6 The prototype 3 of an NGD based active circulator

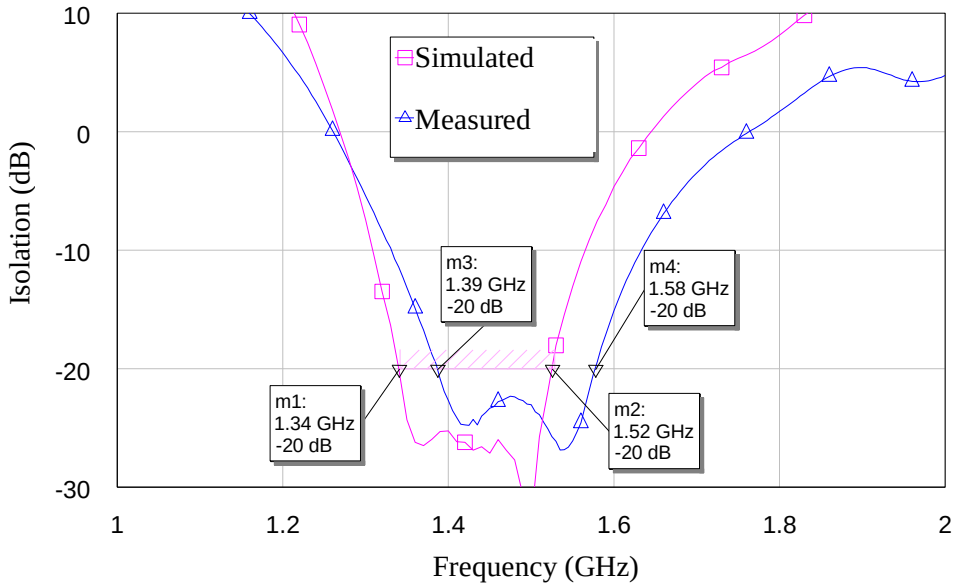

Fig. A.7 The isolation characteristics of an active circulator prototype 3

As shown in Fig. A.7 a similar response of isolation between the transmitter and the receiver is achieved in simulation and in measurement. However a shift in frequency is observed. This is because of the adjustment of the bias voltage and tolerances of the surface mount elements used in the fabrication. As has been mentioned in previous sections and in chapter 5 in the fabricated prototype a few factors such as the tolerance of the RLC elements and the soldering inaccuracies are creating extra phase and magnitude differences. For compensating these changes in phase and magnitude of the CW and ACW signal the DC bias voltage of amplifiers in the respective paths are adjusted.

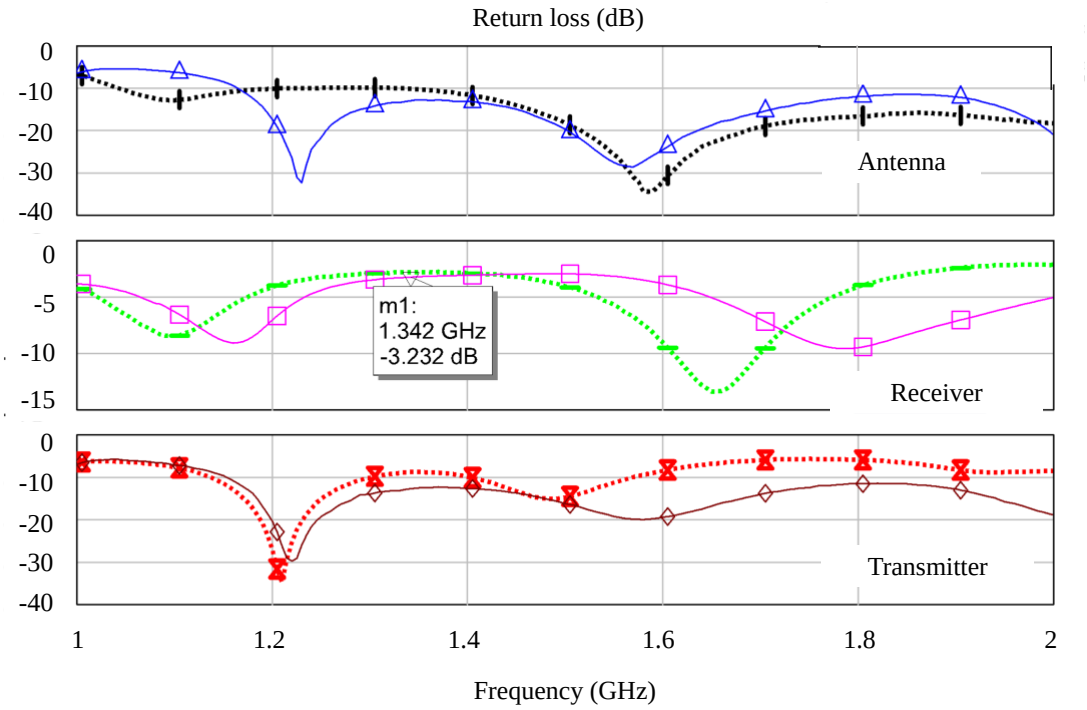

Fig. A.8 The return loss characteristics of three ports of an active circulator

The return loss characteristics of the three ports of the circulator are shown in Fig. A.8. The measured and simulated port return loss characteristics are nearly the same within the operating bandwidth(the shaded range of frequency band). The receiver return loss characteristics need further improvement and this can be achieved by optimising the width and length of the receiver port feed line.

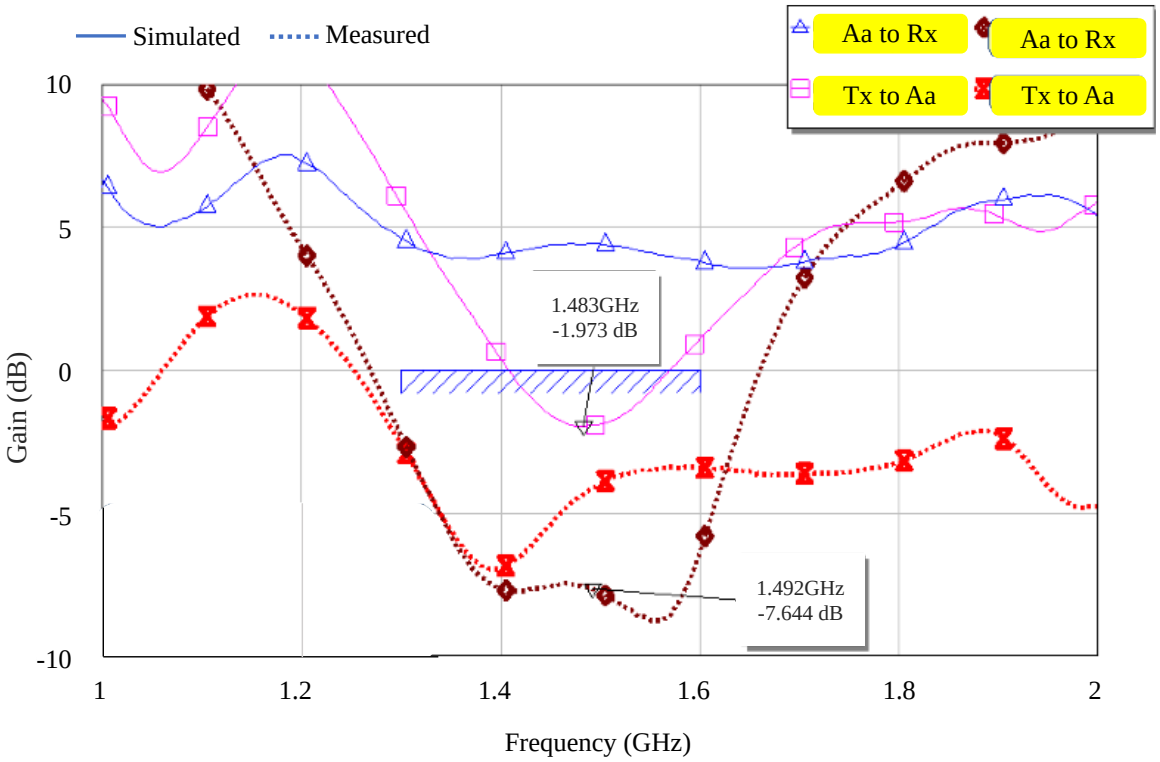

Fig. A.9 The gain characteristics of an active circulator from antenna to receiver and transmitter to antenna.

In Fig. A.9 the gain characteristics in the CW path from the transmitter to the antenna and in the AWC path from the antenna to the receiver are shown. In the AWR microwave office circuit simulation gains in these paths are obtained for a 5V bias condition for the amplifiers. Whereas during the measurement the bias voltage of amplifiers is adjusted. This is to compensate the phase and magnitude changes resulting from the tolerance and soldering inaccuracies. As a result of this modified bias voltage an insertion loss is introduced in these paths.